Uncertainty quantification for complex structures: Statics and dynamics.

Pascual, Blanca

Uncertainty Quantification for Complex Structures: Statics and Dynamics

Swansea University
Prifysgol Abertawe

Blanca Pascual

Submitted to Swansea University in fulfilment of the requirements
for the degree of Doctor of Philosophy

Swansea University
College of Engineering

May, 2012

ProQuest LLC.
789 East Eisenhower Parkway
P.O. Box 1346
Ann Arbor, MI 48106 – 1346

Abstract

The effect of uncertainty on complex engineering structures is investigated. These structures are generally modelled using partial differential equations. On the one hand, uncertainty can affect the parameters of the equation, for example through tolerance in measurements, leading to parametric uncertainty. On the other hand, non-parametric uncertainty can arise from errors in the numerical resolution of the model or in the model itself. Both of these uncertainties have been propagated in order to assess the confidence in the response.

The propagation of parametric uncertainty to the response has been studied with the Spectral Stochastic Finite Element Method (SSFEM). SSFEM is computationally expensive, as it requires the solution of a system of size several times that of the deterministic system. A method is proposed to reduce the size of this system for the elliptic problem. Several methods to obtain a polynomial expansion of the eigenvalues and eigenvectors in terms of the random parameters are investigated and compared. Dynamic response statistics due to parametric uncertainty is also considered. Analytical methods are proposed to study non-parametric uncertainty for dynamic systems. Systems affected by both kinds of uncertainty are also studied. Analytical expressions for the first two moments of the response are obtained for the case where both uncertainties affect the same domain. The case where each type of uncertainty affects a different subdomain is solved using a mixture of SSFEM and direct simulation.

In summary, this thesis proposed novel efficient methods to propagate parametric uncertainty in elliptic problems, the random eigenvalue problem and dynamic problems. Analytical expressions to retrieve the statistics of systems affected by non-parametric uncertainty are obtained for dynamic systems, and for elliptic problems affected by both types of uncertainties.

Declaration

This work has not previously been accepted in substance for any degree and is not being concurrently submitted in candidature for any degree.

Signed ..... (candidate)
Date .....20/06/2012.....

STATEMENT 1

This thesis is the result of my own investigation, except where otherwise stated. Where correction services have been used, the extend and nature of the correction is clearly market in a footnote(s).
Other sources are acknowledged by footnotes giving explicit references. A bibliography is appended.

Signed ..... (candidate)
Date .....20/06/2012.....

STATEMENT 2

I hereby give consent for my thesis, if accepted, to be available for photocopying and for inter-library load, and for the title and summary to be made available to outsider organizations.

Signed ..... (candidate)
Date .....20.06.2012.....

Contents

Acknowledgements

I am very grateful to Swansea University for granting me a full research studentship and providing an environment propitious for my research.

I would also like to thank my supervisor Prof. Sondipon Adhikari for his technical guidance throughout the period of my research work in Swansea.

Finally, I'd like to acknowledge my appreciation for the help I have received from my parents and my sister, for their patience, unconditional support, encouragements and guidance.

List of Figures

List of Tables

Nomenclature

$(\mathcal{X}_E, \mathbb{X}_E, m_{EX})$ evidence space for $\mathbf{x}$, with $\mathcal{X}_E$ the set of possible values,$\mathbb{X}_E$ a set of subsets of $\mathcal{X}_E$, m_{EX} the basic probability assignment

$(\Omega, \mathcal{F})$, κ measurable space and measure, respectively

$(\Omega, \mathcal{F}, P)$ probability space where Ω is the sample space, $\mathcal{F}$ is the σ-algebra of events and P is the probability measure

$\mathbf{B}^{(e)}$, $\mathbf{N}^{(e)}$ $\mathbf{D}$ matrix relating the strain components to nodal displacement, matrix of shape functions and constitutive matrix

$\mathbf{c}_0$, $\mathbf{c}_{1i}$, $\mathbf{c}_{2igk}$ Matrices obtained from the mean of, respectively, two polynomial chaoses, two polynomial chaoses and one random variable ξ_i and two polynomial chaoses and two random variables ξ_i and ξ_g

$\mathbf{d}_0$, $\mathbf{d}_{1i}$, $\mathbf{d}_{2ig}$, $\mathbf{d}_{3igh}$ Vectors obtained from the mean of, respectively, on polynomial chaos, one polynomial chaos and one random variable ξ_i, one polynomial chaos and two random variables ξ_i and ξ_g, and one polynomial chaos and three random variables ξ_i, ξ_g and ξ_h

$\mathbf{e}_{0i}$, $\mathbf{g}_{lm}$ Matrices obtained from the mean of, respectively, three and four polynomial chaoses

$\mathbf{I}_p$ Identity matrix of size $p \times p$

$\mathbf{K}_0$, $\mathbf{K}_i$, $\mathbf{u}$, $\mathbf{f}$ deterministic system matrix, matrices appearing in the KL expansion, response and forcing term of a discretized elliptic PDE

$\mathbf{M}$, $\mathbf{K}$, $\mathbf{C}$, $\mathbf{U}(t)$, $\mathbf{F}(t)$ system mass, stiffness and damping matrices, the response vector and the forcing vector in time domain appearing in the dynamic problem

$\mathbf{M}_0$, $\mathbf{M}_i$ deterministic mass matrix, matrices appearing in the KL expansion of the mass matrix

$\mathbf{\Sigma_{XX}}$ covariance matrix of vector of random variables $\mathbf{X}$

$\mathbf{u}$, $\mathbf{f}$, ω response and forcing vector in frequency domain, and frequency

$\boldsymbol{\zeta}$, $\boldsymbol{\Omega}$ diagonal matrices of damping ratios and of natural frequencies

$\mathcal{S}(f_X)$, γ_i entropy of a random variable X and Lagrange multiplier appearing in the entropy maximisation process

δ_G dispersion parameter of a random matrix $\mathbf{G}$

$\mathrm{E}[X^i]$, σ i-th moment and standard deviation of the random variable X. The first moment is also referred to as mean.

$\|\mathbf{G}\|_{\mathrm{F}}$ Frobenius norm of matrix $\mathbf{G}$

Γ_i i-th function basis of the stochastic spectral method. These basis functions are orthogonal with respect to the pdf of the random variables $\{\xi_1, \ldots, \xi_M\}$. A particular case of Γ_i are the polynomial chaoses.

$\Gamma_n(a)$, $\mathrm{etr}(\mathbf{A})$ multivariate gamma function and $e^{\mathrm{Trace}(\mathbf{A})}$, both appearing in the pdf of the Wishart matrix distribution

$\lambda^{(j)}$, $\mathbf{v}^{(j)}$ eigenvalues and eigenvectors of the generalized eigenvalue problem

$\mathcal{D}, \mathcal{D}_e$ N_i spatial domain, element domain and shape functions associated with each element (defined on $\mathcal{D}_e$)

$\mathcal{V}$ a subset of $\mathcal{X}_E$

$\mathrm{N}_n(\Delta)$, $s_n(z)$ normalized counting measure of a squared matrix $\mathbf{H}$ of size $n \times n$ on the interval Δ, and Stieltjes transform of $\mathrm{N}_n(\Delta)$

$\mathcal{K}_m$ Krylov subspace, the subspace spanned by the vectors of the Krylov sequence

$\mathrm{R}(\mathbf{r}_1, \mathbf{r}_2)$, b autocorrelation function of $H(\mathbf{r}, \varpi)$ and correlation length of the random field

ν_i, $\varphi_i(\mathbf{r})$, ξ_i eigenvalues, eigenvectors and random variables of the Karhunen-Loève expansion of a random field $H(r, \varpi)$

$\subset$, $\in$, $\notin$ simbols to indicate a subset, is an element of, and is not an element of.

ϖ, A_i elements of Ω and of $\mathcal{F}$ respectively

Var $[X]$ Variance of the random variable X

$a(\mathbf{r}, \varpi)$, $u(\mathbf{r}, \varpi)\, p(\mathbf{r})$ material random field, primary variable and source variable in an elliptic PDE

a^+, a^-, $a\, c$ Parameters appearing in the Marčenko-Pastur distribution

$bel_X(\mathcal{V})$ belief of subset $\mathcal{V}$

$d(x_i, x_j)$ distance between two intervals in interval analysis

$H(\mathbf{r}, \varpi)$ random field, with $\mathbf{r}$ related to the geometry and ϖ to the probability space

$N(\mathbf{0_{p\times n}}, \mathbf{I_p} \otimes \mathbf{\Sigma})$ Multivariate normal distribution of size $p \times n$ with uncorrelated columns and correlation matrix $\mathbf{\Sigma}$ for its rows.

$Pl_X(\mathcal{V})$ plausibility of subset $\mathcal{V}$

R_i, R_0, a, b, m In a congruential generator, term of the serie, multiplier, seed, increment and modulus used to obtain the serie

S, S_f, μ_{S_f} universe set, fuzzy subset and membership function used in fuzzy set theory

$S_{\bar{\alpha}}$, $\alpha S_{\bar{\alpha}}$ the weak α-cut or α level set and the fuzzy subset

$W_n(p, \mathbf{\Sigma})$ Wishart matrix of dimension n with parameters p and $\mathbf{\Sigma}$

X, F_X, f_X random variable and distribution and density function of the random variable X

$x_i \in [\bar{x}_i - \epsilon_i, \bar{x}_i + \epsilon_i]$ parameter defined over an interval in interval analysis

EOLE Expansion Optimal Linear Estimation method

FEM Finite Element Method

FETI finite element tearing and interconnect

FRF frequency response function

KL Karhunen-Loève

MCS Monte Carlo Simulation

OSE Orthogonal Series Expansion

PC Polynomial chaos

PDE Partial differential equation

pdf, CDF probability density function or density function, cumulative distribution function or distribution

RPC Reduced polynomial chaos

RQPEv Rayleigh quotient using first-order perturbation of eigenvectors

RSCCM reduced spectral constrained coefficients method

RSIPM reduced spectral inverse power method

RSPM reduced spectral power method

SCCM spectral constrained coefficients method

SDOF, MDOF single-degree-of-freedom, multiple-degrees-of-freedom

SEA statistical energy analysis

SSFEM Spectral Stochastic Finite Element Method

Chapter 1

Introduction

1.1 Uncertainty analysis

The development of both numerical methods (e.g. the Finite Element method) and computational hardware makes it possible to solve deterministic high-resolution models of physical problems (e.g. fluid mechanics or structural mechanics), represented by algebraic nonlinear systems of equations with thousands of degrees of freedom. However, spatial resolution is not enough to determine the credibility of a numerical model. A correct representation of the physical model as well as its parameters is also crucial, and both are affected by uncertainty. This uncertainty is due to several reasons (Oberkampf et al., 2002, Der-Kiureghian and Ditlevsen, 2009), the first one is that any measurement has a limited precision. The second one is that measurements of apparently identical systems will lead to different measurements of the parameters, as, for example, the modulus of elasticity of two different samples of the same alloy, due to unaccountable effects in the production of the samples. The third one is related to errors in the mathematical model of the system considered.

As a result of having uncertain parameters, the degree of confidence in a particular equation's predictions has to be assessed. This is specially true in fields of study such as reliability, where the probability of failure of a structure is calculated. Another important field affected by uncertainty is sensitivity analysis, where knowing the effect of the variation of a parameter on the response can aid in decision making. Also, knowing the effect of uncertainty in the parameters of a model can help to quantify the degree of confidence of the model, as in cases like model updating or model validation (Friswell and Mottershead, 1995). In particular, uncertainties arising from measurements of system

eigenvalues and eigenvectors can be used to assess the uncertainty of system parameters derived with the inverse problem (Khodaparast et al., 2008, 2011). Finally, quantifying the effects of different sources of uncertainty on a given response can help to determine the sources of uncertainty that are not important.

Examples of practical cases where these considerations are relevant can be elliptic partial differential equations (Babuska et al., 2005), random vibrations (Lin, 1967), seismic activity (Desceliers et al., 2004), oil reservoir management (Lim, 2005), or composite materials (Chen et al., 2006).

The uncertainty analysis of a model follows two basic steps. Firstly, identifying and characterizing this uncertainty. This approach leads to modelling the governing partial differential equations within the framework of stochastic equations. Secondly, estimation of the uncertainty in the response of the system induced by the propagation of uncertainty from the system parameters, that is, uncertainty propagation.

The first kind of uncertainties studied were the uncertainties introduced by random forces applied to the structure (Lin, 1967). Then followed the study of uncertainties introduced by material properties (e.g. Young's modulus, mass density, Poisson's ratio, damping coefficient) or geometric parameters and modelled by random variables and random fields. A third kind of uncertainty, known as epistemic/model uncertainty has been introduced during the last decade. This kind of uncertainty does not explicitly depend on the system parameters as it is expected to account for unquantified errors associated with the equation of motion, the damping model or the model of structural joints. The method is also used for errors associated with the numerical methods, as discretization of displacement fields, truncation and roundoff errors, tolerances in the optimization and iterative algorithms or step-sizes in the time-integration methods. As a results, the system matrices can be modelled as multivariate distributions.

The propagation of uncertainty can be addressed in two ways: through simulation techniques and non-simulation techniques. Simulation techniques imply solving the deterministic system for a given number of parameter combinations and can therefore be computationally very expensive. These samples can be used to obtain a surrogate model of the system, i.e. an equation relating the uncertain parameters to the response, whose expression is simpler to evaluate than the original equation. Non-simulation techniques can be based on perturbation methods, which imply that the results are only valid for small variations of the uncertain parameters. Otherwise, they can be based on

spectral methods, which imply solving a system of equations of size several times the size of the deterministic system.

1.2 Numerical methods for mechanical systems

The relationship between the response and the forcing of a system is generally given by a partial differential equation (PDE), defined on a domain and subjected to boundary and initial conditions. The response to the PDE can be approximated with different numerical methods. Amongst them the Finite Element method (FEM) (Zienkiewicz and Taylor, 1991) is most widely used in practice. This method discretizes the domain of the equation into elements, and shape functions are defined within each element. These shape functions can be equal to one at one node of the element and zero for all the other nodes. The solution is then approximated by an expansion in all the resulting shape functions, and a variational method is applied to obtain the coefficients of the expansion. As a result, the coefficients of the expansion are an approximation to the solution of the PDE at the selected nodes.

The systems for which uncertainty propagation is studied in this work are linear systems (e.g. elliptic PDEs), eigenvalue problem and dynamic problem. The elliptic PDE is given by

$$-\nabla.[a(\mathbf{r})\nabla u(\mathbf{r})] = p(\mathbf{r}); \quad \mathbf{r} \text{ in } \mathcal{D} \tag{1.1}$$

with the associated Dirichlet condition

$$u(\mathbf{r}) = 0; \quad \mathbf{r} \text{ on } \partial\mathcal{D} \tag{1.2}$$

The domain $\mathcal{D}$ is divided into elements, e.g. rectangular or triangular elements. The response within each element is approximated with

$$u(\mathbf{r}) \approx \sum_{i=1}^{n_{nodes}} u(\mathbf{r}_i)N_i(\mathbf{r}) = \mathbf{u}^T\mathbf{N}^{(e)} \tag{1.3}$$

where n_{nodes} is the number of nodes in an element, $u(\mathbf{r}_i)$ is the response for the node with coordinate $\mathbf{r}_i$ of the elements and $\mathbf{N}^{(e)} = [N_1, \ldots, N_n]$ is the vector of shape functions, e.g. Lagrange polynomials, defined on a given element. Introducing this expansion for all the elements in the weak form of the elliptic equation (Reddy, 1993),

an algebraic linear system is obtained

$$\mathbf{Ku} = \mathbf{f} \tag{1.4}$$

$$\mathbf{K}^e = \int_{\mathcal{D}_e} a(\mathbf{r})\mathbf{B}^{(e)\,T}(\mathbf{r})\mathbf{B}^{(e)}(\mathbf{r})\,d\mathbf{r} \tag{1.5}$$

$$\mathbf{f}^{(e)} = \int_{\mathcal{D}_e} p(\mathbf{r})\mathbf{N}^{(e)}(\mathbf{r})\,d\mathbf{r} \tag{1.6}$$

where $\mathbf{B}^{(e)} = d\mathbf{N}^{(e)}/d\mathbf{r}$ is the matrix relating the strain components to nodal displacements and $\mathbf{K}^e$ and $\mathbf{f}^{(e)}$ are the stiffness matrix and forcing vector of an element. The global stiffness matrix $\mathbf{K}$ and forcing vector $\mathbf{f}$ are obtained after assembling the element stiffness matrices and forcing vectors and applying boundary conditions. In a more general case, the element stiffness matrix can be given by

$$\mathbf{K}^e = \int_{\mathcal{D}_e} \mathbf{B}^{(e)\,T}(\mathbf{r})\mathbf{D}\mathbf{B}^{(e)}(\mathbf{r})\,d\mathbf{r} \tag{1.7}$$

where $\mathbf{D}$ is the constitutive matrix.

For a dynamic problem, applying the FE method to the partial differential equation leads to the equation

$$\mathbf{M}\ddot{\mathbf{U}}(t) + \mathbf{C}\dot{\mathbf{U}}(t) + \mathbf{K}\mathbf{U}(t) = \mathbf{f} \tag{1.8}$$

where $\mathbf{U}$ is the response, t is the time variable, the element mass matrix is given by

$$\mathbf{M}^e = \int_{\mathcal{D}_e} \rho\mathbf{N}^{(e)\,T}(\mathbf{r})\mathbf{N}^{(e)}(\mathbf{r})\,d\mathbf{r}, \tag{1.9}$$

and the global mass matrix is assembled from the element mass matrices using the same procedure used for the stiffness matrix. The damping matrix is assumed to be proportional, i.e. $\mathbf{C} = a_M\mathbf{M} + a_K\mathbf{K}$. The dynamic response of the system from Equation (1.8) can be given by modal analysis (see, e.g. Meirovitch, 1967). When we consider uncertainty these matrices become random. In the following sections we review different models of uncertainty.

1.3 Characterization of system uncertainties

Uncertainty can be classified in "irreducible" and "reducible" (Oberkampf et al., 2002, Der-Kiureghian and Ditlevsen, 2009). "Irreducible" or aleatory uncertainties arise from

the presence of natural uncertainty (e.g. weather conditions), for which a probabilistic description of uncertainties is available. "Reducible" or epistemic uncertainty can be lowered through improvements in the measurement instrumentation or in the model formulation, and a probabilistic description of the uncertainty is not available. Aleatory uncertainty is generally studied through a probabilistic approach while epistemic uncertainty has been studied with the probabilistic approach, evidence theory, interval analysis and fuzzy set theory. Different approaches have been applied to the same system, as , for example, the case of uncertainty propagation in linear aeroelastic stability (Khodaparast et al., 2010). In this dissertation, only probabilistic approach is perused, but a brief description of all the different approaches is given in this section.

1.3.1 Probabilistic approach

The most widely used approach to deal with uncertainty is the probabilistic approach (see, e.g., Bauer, 1996, Papoulis and Pillai, 2002, Grigoriu, 2002, Red-Horse and Ghanem, 2009). In this approach probabilities are associated to events. For this, a probability space $(\Omega, \mathcal{F}, P)$ is defined. In an experiment, Ω is the set of elementary events or sample space, containing all the possible outcomes of the experiment, where each element of Ω is denoted by ϖ. $\mathcal{F}$ is the σ-algebra of events: collection of possible events or subsets of Ω that are relevant to a particular experiment, a particular element of $\mathcal{F}$ is denoted by A_i. It is noted that the union, intersection and complement of elements of $\mathcal{F}$ are also in $\mathcal{F}$, and $\Omega \in \mathcal{F}$. The pair $(\Omega, \mathcal{F})$ is called a measurable space. A measure κ is a function associating a real positive number to each element of $\mathcal{F}$, $\kappa : \mathcal{F} \rightarrow [0, \infty)$, and is countably additive, i.e., $\kappa(\bigcup_{i=1}^{\infty} A_i) = \sum_{i=1}^{\infty} \kappa(A_i)$. A probability measure or probability P is a measure such that $P(\Omega) = 1$, and each element $A_i \in \mathcal{F}$ has a well-defined probability $P(A_i) \in [0, 1]$.

The probability space allows to define random variables and random fields, used to model the system random parameters. Consider two measurable spaces $(\Omega, \mathcal{F})$ and $(\Psi, \mathcal{G})$. A measurable function X from $(\Omega, \mathcal{F})$ to $(\Psi, \mathcal{G})$ is defined by

$$X^{-1}(B) = \{A : X(A) \in B\} \in \mathcal{F}, \forall B \in \mathcal{G} \tag{1.10}$$

The measurable function X is a random variable if, for a probability measure P on

$(\Omega, \mathcal{F})$

$$Q(B) = P(X^{-1}(B)),\ B \in \mathcal{G} \tag{1.11}$$

is a probability measure on $(\Psi, \mathcal{G})$. Generally, we will consider $(\Psi, \mathcal{G}) = (\mathbb{R}, \mathcal{B})$, with $\mathbb{R}$ the set of real numbers, and $\mathcal{B}$ the Borel σ-field, generated by the intervals in $\mathbb{R}$. In this case, $Q(B)$ is referred to as the distribution of X, denoted by $F_X(x) = P(X \leq x)$ and with derivative $f_X = dF_X/dx$, referred to as the density function of X.

The variation of randomness over the physical space can be discrete or continuous. A discrete variation can be modelled with a set of random variables, that is, a random vector. Generally, this variation of randomness is assumed continuous and is modelled through the use of random fields. A random field $H(\mathbf{r}, \varpi)$ is a collection of random variables indexed by $\mathbf{r}$, a space coordinate of the system geometry. That is, for a given $\mathbf{r}_0$, $H(\mathbf{r}_0, \varpi)$ is a random variable and for a given outcome A_i, $H(\mathbf{r}, A_i)$ is a realization of the field. Details about the modelling process of the random field will be given in the next two sections.

1.3.2 Possibilistic approaches

Both reducible and irreducible uncertainties have been studied using a probabilistic approach. Other methods have also been developed:

- Evidence theory or Dempster-Shafer theory (Helton et al., 2006) provides a less structured representation of uncertainty than probability theory but is still closely related to it. Consider the set of q parameters affected by uncertainty $\mathbf{x} = \{x_1, \ldots, x_q\}$ with x_i, $i = 1, \ldots, q$. An evidence space for $\mathbf{x}$, $(\mathcal{X}_E, \mathbb{X}_E, m_{EX})$ is defined with $\mathcal{X}_E$ the set of possible values of $\mathbf{x}$, $\mathbb{X}_E$ the set of subsets of $\mathcal{X}_E$ and m_{EX} a function satisfying $m_{EX}(\mathcal{V}) > 0$ if $\mathcal{V} \subset \mathcal{X}_E$ and $\mathcal{V} \in \mathbb{X}_E$, $m_{EX}(\mathcal{V}) = 0$ if $\mathcal{V} \subset \mathcal{X}_E$ and $\mathcal{V} \notin \mathbb{X}_E$, and $\sum_{\mathcal{V} \in \mathbb{X}_E} m_{EX}(\mathcal{V}) = 1$. Evidence theory has two measures of uncertainty: belief and plausibility defined respectively by $bel_X(\mathcal{V}) = \sum_{\mathcal{U} \in \mathcal{V}} m_{EX}(\mathcal{U})$ and $Pl_X(\mathcal{V}) = \sum_{\mathcal{U} \cap \mathcal{V} \neq \emptyset} m_{EX}(\mathcal{U})$. That is, belief provides a measure of the information that has to be assigned to a set while plausibility provides a measure of the amount of information that could possibly be assigned to a set. These definitions allow to measure the amount of information that can be assigned to a set but cannot be assigned specifically to any subset of that set.

- Interval analysis (Alefeld and Herzberger, 1983, Chen and Pham, 2000) addresses data uncertainty arising from imprecise measurements or due to the existence of alternative methods to estimate model parameters. The uncertain parameters of the model are assumed to be bounded, e.g. the parameter $x_i \in [\bar{x}_i - \epsilon_i, \bar{x}_i + \epsilon_i]$, with this interval being called the interval of confidence of x_i. Then, the method is used to estimate bounds of the model response based on these parameters bounds, i.e. $x_i + x_j \in [\bar{x}_i + \bar{x}_j - \epsilon_i - \epsilon_j,\ \bar{x}_i + \bar{x}_j + \epsilon_i + \epsilon_j]$. Several properties related to the intervals of confidence of two parameters can be defined, such as equality, intersection, union, inequality, inclusion, width, absolute value, midpoint and symmetry. The operations defined for interval arithmetics are addition, substraction, reciprocal, multiplication and division. All these operations are defined in a conservative way, so as to obtain the largest interval when they are applied. The addition and multiplication operations of intervals are commutative and associative but not distributive. Also, a distance between two intervals is defined $d(x_i, x_j) = \max\{|\bar{x}_i - \bar{x}_j - \epsilon_i + \epsilon_j|,\ |\bar{x}_i - \bar{x}_j + \epsilon_i - \epsilon_j|\}$, thus inducing a metric into the family of intervals, so that the concepts of convergence and continuity are defined and used as usual. Following these operations, the real-variable and real-valued functions can be extended to interval-variable and interval-value functions, and interval matrices can also be defined.

- Fuzzy set theory (Chen and Pham, 2000, Moens and Vandepitte, 2005, Moens and Hanss, 2011) was developed to handle the concept of partial truth. In classic set theory an element belongs or not to a given set, condition mathematically expressed by defining a characteristic function by $\mathbf{X}_S(s) = 1$ if $s \in S$, and $\mathbf{X}_S(s) = 0$ if $s \notin S$. A membership function is a generalization of $\mathbf{X}_S(s)$ given by a continuous positive function defined on $[0, 1]$, indicating that an element partially belongs to a given set. Another difference from classical set theory is that a member of a fuzzy set may assume several and sometimes conflicting membership values, that is, measures of complementary sets do not add one or cancel out. The membership function differs from the probability density function (pdf) in that the area under the curve is given by a positive real number instead of being equal to one. If S_f is a fuzzy subset defined in a universe set S together with the membership function μ_{S_f}, two fuzzy subsets can be defined: the weak α-cut

or α level set $S_{\bar{\alpha}} = \{s \in S_f | \mu_{S_f}(s) \geq \alpha\}$, $\alpha \in (0,1]$, and the fuzzy subset $\alpha S_{\bar{\alpha}} = \{s \in S_f | \mu_{\alpha S_{\bar{\alpha}}}(s) = \min\{\alpha, \mathbf{X}_{S_{\bar{\alpha}}}(s)\}\}$. This last subset is related to S_f through $S_f = \bigcup_{\alpha \in (0,1]} \alpha S_{\bar{\alpha}}$. This relationship is known as the *Resolution Principle*, and allows to described a fuzzy subset using only α-cuts. If a fuzzy subset S_f is transformed $F : S \to Y$, the result $Y_f = F(S_f)$ is also a fuzzy subset and its membership function can be retrieved from the membership function of S_f. A fuzzy number is a fuzzy subset with convex membership function (convex fuzzy subset) whose maximum is one and whose α-cut is a closed interval. Fuzzy numbers are used to model parameters, while the membership function of the response is obtained through α cuts.

1.4 Parametric uncertainty

Several sources of uncertainty affect model parameters, such as measurement errors, uncertainties in the model or uncertainties inherent to a physical system. All of them can be characterised using a probabilistic approach. That is, all of them can be represented using random variables or random fields. Random variables can be used to model system parameters when the parameter does not vary with the position in the geometry, while random fields are used to represent distributed parameters. In this section, methods for the discretization of random fields are reviewed. We firstly introduce some basic elements of functional analysis needed for the study of stochastic calculus (Sudret and Der-Kiureghian, 2000, Grigoriu, 2002, Red-Horse and Ghanem, 2009).

It has already been said that a random variable is a measurable function inducing a mapping $X : (\Omega, \mathcal{F}) \to (\mathbb{R}, \mathcal{B})$. The i-th moment and standard deviation of the random variable X can be defined as

$$\mathrm{E}\left[X^i\right] = \int_\Omega X^i(\varpi) P(d\varpi) = \int X^i \, dP \quad \text{and} \quad \sigma = \sqrt{\mathrm{E}[X^2] - (\mathrm{E}[X])^2} \tag{1.12}$$

The space $\mathcal{L}^i(\Omega, \mathcal{F}, P)$ is the collection of real valued random variables X defined on $(\Omega, \mathcal{F}, P)$ such that $\mathrm{E}[|X|^i] < \infty$ for $i < \infty$. In particular, the space $\mathcal{L}^2(\Omega, \mathcal{F}, P)$ is a Hilbert space where the inner product between two random variables $X, Y : (\Omega, \mathcal{F}, P) \to \mathbb{R}$ is defined by $< X, Y >= \mathrm{E}[XY]$, and $||X||_{\mathcal{L}^2} = (\mathrm{E}[|X|^2])^{1/2}$ is the $\mathcal{L}^2$-norm.

Consider the random variables X and X_n defined on $\mathcal{L}^2(\Omega, \mathcal{F}, P)$. The mean square

convergence, probability convergence and the almost sure convergence of the sequence X_n to X are defined respectively by (Xiu, 2010)

$$X_n \xrightarrow{m.s} X \quad \text{if} \quad \lim_{n\to\infty} \mathrm{E}[|X_n - X|^2] = 0 \tag{1.13}$$

$$X_n \xrightarrow{pr} X \quad \text{if} \quad \lim_{n\to\infty} P(|X_n - X| > \varepsilon) = 0, \, \forall \varepsilon > 0 \tag{1.14}$$

$$X_n \xrightarrow{a.s} X \quad \text{if} \quad \lim_{n\to\infty} X_n(\varpi) = X(\varpi), \, \forall \varpi \in \Omega \tag{1.15}$$

and both almost sure and mean square convergence imply probability convergence.

A random field $H(\mathbf{r}, \varpi)$ can be considered as a curve in the probability space $\mathcal{L}^2(\Omega, \mathcal{F}, P)$, where $\mathbf{r}$ is a space coordinate. We will only consider continuous random fields. An homogeneous random field is such that

$$H(\mathbf{r}_0, \varpi) \overset{d}{=} H(\mathbf{r}_0 + \mathbf{t}, \varpi) \tag{1.16}$$

with $\mathbf{t}$ a space shift. That is, the probability density functions of the random variables $H(\mathbf{r}_0, \varpi)$ and $H(\mathbf{r}_0 + \mathbf{t}, \varpi)$ coincide. When dealing with random fields, it is desirable to approximate it by a different random field $\hat{H}$ using a finite set of random variables, and this process is referred to as a discretization of the random field. Several methods are available to perform the discretization process, namely, point discretization, average discretization and series expansion methods (Li and Der-Kiureghian, 1993b, Matthies et al., 1997, Ditlevsen and Madsen, 1996, Sudret and Der-Kiureghian, 2000, Stefanou, 2009).

1.4.1 Point discretization methods

Discretization methods based on point discretization use a set of random variables $\{X_i\}$ given by estimations of the random field $H(\mathbf{r}, \varpi)$ at some given points $\mathbf{r}_i$:

- The midpoint method (Der-Kiureghian and Ke, 1987) divides the spatial domain into elements and approximates the random field in each element by the random variable $H(\mathbf{r}_i, \varpi)$, where $\mathbf{r}_i$ is the centroid of that particular element. Therefore, there are as many random variables used to approximate the random field as there are elements. This method over-represents the variability of the random field within each element.

- The integration point method (Matthies et al., 1997) is used when numerical in-

tegration is needed. Then, in the deterministic case, the integral is approximated by the integral of a Lagrange interpolating polynomial that matches the function to be integrated at some given coordinates, the Gauss points. The random variables used to approximate the random field are the random field evaluated at each Gauss point. In the context of the Finite Element method, this method can use directly the integration rules available for the construction of the element matrices. Results are accurate for short correlation lengths. However, the total number of random variables involved increases dramatically with the size of the problem.

- The shape function method (Liu et al., 1986c) divides the spatial domain $\mathcal{D}$ into elements and the nodes of these elements are the coordinates $\mathbf{r}_i$ used to approximate the random field. Polynomial shape functions N_i are associated with the element so that the random field approximation within each element is given by

$$\hat{H}(\mathbf{r}, \varpi) = \sum_{i=1}^{Q} N_i(\mathbf{r}) H(\mathbf{r}_i, \varpi) \tag{1.17}$$

with Q the number of nodes of the element.

- The optimal linear estimation method (OLE) or Kriging method, presented by Li and Der-Kiureghian (1993a), approximates the random field with random variables dependent on nodal values $\mathbf{X} = \{H(\mathbf{r}_1), \ldots, H(\mathbf{r}_Q)\}$. The dependence is linear

$$\hat{H}(\mathbf{r}) = a(\mathbf{r}) + \mathbf{b}^T(\mathbf{r})\mathbf{X} \tag{1.18}$$

and functions $a(\mathbf{r})$ and $b(r)$ are calculated minimizing the variance of the difference between the approximated and exact random field $\mathrm{Var}\left[H(\mathbf{r}) - \hat{H}(\mathbf{r})\right] = \mathrm{E}\left[(H(\mathbf{r}) - \hat{H}(\mathbf{r}))^2\right]$ while keeping the mean of that difference equal to zero $\mathrm{E}\left[H(\mathbf{r}) - \hat{H}(\mathbf{r})\right] = 0$.

1.4.2 Average discretization methods

This group of discretization methods uses random variables given by weighted integrals of the random field over a domain $\mathcal{D}_e$

$$X_i = \int_{\mathcal{D}_e} H(\mathbf{r}) w(\mathbf{r}) d\mathbf{r} \tag{1.19}$$

- Spatial average method (Vanmarcke and Grigoriu, 1983) uses one random variable per element to represent uncertainty. This random variable is the average of the original field over the element, i.e. $w(\mathbf{r}) = 1/|\mathcal{D}_e|$ in Equation (1.19). The variance of the spatial average over an element under-represents the local variance of the random field (Der-Kiureghian and Ke, 1987).

- The weighted integral method (Shinozuka and Deodatis, 1991, Deodatis, 1991, 1990) considers, for linear elasticity, the element stiffness matrices as random quantities: each random variable is the result of integrating the product of one of the monomials used in the FEM by the random field over each element.

1.4.3 Series expansion methods

The last group of discretization methods expands any realization of the original random field over a complete set of deterministic functions ϕ_i and truncates the series after a finite number of terms

$$\hat{H}(\mathbf{r}, \varpi) = \sum_{i=1}^{M} X_i(\varpi)\phi_i(\mathbf{r}) \tag{1.20}$$

- The most widely used of all series expansion method is the Karhunen-Loève expansion, which will be discussed in subsection 1.4.4.

- The Orthogonal Series Expansion method (OSE) (Zhang and Ellingwood, 1993) selects $\phi_i(\mathbf{r})$ as a set of Q deterministic orthogonal functions such that the random field is approximated by

$$\hat{H}(\mathbf{r}, \varpi) = \mathrm{E}\left[\hat{H}(\mathbf{r}, \varpi)\right] + \sum_{i=1}^{Q} X_i(\varpi)\phi_i(\mathbf{r}) \tag{1.21}$$

  The random variables X_j of the expansion are zero mean and correlated, such that the mean and variance of the approximation to the random field match the ones of the original random field.

- The Expansion Optimal Linear Estimation method (Li and Der-Kiureghian, 1993b) (EOLE) is an extension of OLE, where the number Q of random variables $\mathbf{X}$ from Equation (1.18) is reduced by using its spectral representation

$$\mathbf{X}(\varpi) = \mathrm{E}[\mathbf{X}(\varpi)] + \sum_{i=1}^{M} \sqrt{\lambda_i}\xi_i(\varpi)\boldsymbol{\phi}_i \tag{1.22}$$

with $\{\xi_1, \ldots, \xi_M\}$ a set of uncorrelated random variables, with $M < Q$ and where (λ_i, ϕ_i) are the eigenvalues and eigenvectors of the covariance matrix $\mathbf{\Sigma_{XX}} = \mathrm{E}\{\mathbf{X}^T\mathbf{X}\}$.

- The spectral representation (Vanmarcke, 1983, Stefanou, 2009) expands the stationary stochastic field as a sum of trigonometric functions with random phase angles $\hat{H}(\mathbf{r}, \varpi) = \mathrm{E}[H(\mathbf{r}, \varpi)] + \sum_{i=-K}^{K} Y_i(\mathbf{r}, \varphi)$, $Y_i(\mathbf{r}, \varphi) = A_i \cos(\eta_i \mathbf{r} + \phi_i)$, with A_i an amplitude verifying $\mathrm{E}[A_i]/2 = \mathrm{E}[Y_i^2(\mathbf{r}, \varphi)]$, ϕ_i a set of independent phase angles uniformly distributed in $[0, 2\pi]$ and frequencies $\eta_i = \pm[\Delta\eta(2i-1)/2]$. This expansion is asymptotically a Gaussian stochastic field, with mean and autocorrelation function identical to that of $H(\mathbf{r}, \varpi)$ as $N \to \infty$.

1.4.4 Karhunen-Loève expansion (KL expansion)

The Karhunen-Loève (KL) expansion was derived independently by two researchers (Karhunen, 1947, Loève, 1948)). It expands the random field with a Fourier-type series and is based on the spectral decomposition of the autocorrelation function, so that it minimizes the mean squared error. The basis functions obtained are the best possible basis for the random field expansion. The KL expansion of a random field $H(\mathbf{r}, \varpi)$ is given by

$$\hat{H}(\mathbf{r}, \varpi) = \mathrm{E}[H(\mathbf{r}, \varpi)] + \sum_{i=1}^{\infty} \sqrt{\nu_i}\xi_i\varphi_i(\mathbf{r}) \tag{1.23}$$

with $\mathrm{E}[H(\mathbf{r}, \varpi)]$ the mean of the random field, $\varphi_i(\mathbf{r})$ a set of orthonormal functions (i.e. $\int_{\mathcal{D}} \varphi_i(\mathbf{r})\varphi_j^*(\mathbf{r})d\mathbf{r} = \delta_{ij}$) and $(\xi_1, \ldots, \xi_n)$ a set of zero mean uncorrelated random variables. The constants ν_i and functions $\varphi_i(\mathbf{r})$ are the eigenvalues and eigenfunctions of the autocorrelation function $\mathrm{R}(\mathbf{r}_1, \mathbf{r}_2)$ of $H(\mathbf{r}, \varpi)$. That is, ν_i and $\varphi_i(\mathbf{r})$ are obtained from the equation

$$\int_{\mathcal{D}} \mathrm{R}(\mathbf{r}_1, \mathbf{r}_2)\varphi(\mathbf{r}_2)d\mathbf{r}_2 = \nu\varphi(\mathbf{r}_1) \tag{1.24}$$

Where $\mathcal{D}$ is the domain where the autocorrelation function is defined. The random variables are given by $\xi_i = \int_{\mathcal{D}} H(\mathbf{r}, \varpi)\varphi_i(\mathbf{r})d\mathbf{r}$. Then it can be shown that the approximation $\hat{H}$ converges to H in the mean squared sense $\mathrm{E}\left[|H(\mathbf{r}, \varpi) - \hat{H}(\mathbf{r}, \varpi)|^2\right] = 0$ $\mathbf{r} \in \mathcal{D}$. The KL expansion has some interesting properties (Sudret and Der-Kiureghian, 2000):

- The mean-square error, $\mathrm{E}\left[\left|H(\mathbf{r},\varpi) - \left(\mathrm{E}\left[H(\mathbf{r},\varpi)\right] + \sum_{i=1}^{M}\sqrt{\nu_i}\xi_i\varphi_i(\mathbf{r})\right)\right|^2\right]$, from a finite representation of the original process using the set of orthogonal functions $\varphi_i(\mathbf{r})$, is minimum.
- The KL expansion is unique.
- KL expansion is almost surely convergent for $H(\mathbf{r},\varpi)$ a Gaussian process, as the random variables appearing in the expansion are gaussian and uncorrelated.

We consider the KL expansion of a random field depending on the spatial variable x with exponential correlation function (Ghanem and Spanos, 1991)

$$\mathrm{R}(x_1,x_2) = e^{-|x_1-x_2|/b}, \qquad x \in [-a,a] \tag{1.25}$$

where b is the correlation length. The eigenfunctions φ and eigenvalues ν are the solution of the equation

$$\int_{-a}^{+a} e^{-|x_1-x_2|/b}\varphi(x_2)dx_2 = \nu\varphi(x_1) \tag{1.26}$$

The explicit expressions of the eigenfunctions and eigenvalues are given by:

$$\begin{cases} \varphi_i(x) = \dfrac{\cos(\omega_i x)}{\sqrt{a + \frac{\sin(2\omega_i a)}{2\omega_i}}} & \nu_i = \dfrac{2c}{\omega_i^2 + c^2} \quad \text{for } i \text{ odd} \\ \varphi_i^*(x) = \dfrac{\sin(\omega_i^* x)}{\sqrt{a - \frac{sin(2\omega_i^* a)}{2\omega_i^*}}} & \nu_i^* = \dfrac{2c}{\omega_i^{*2} + c^2} \quad \text{for } i \text{ even} \end{cases} \tag{1.27}$$

where $c = 1/b$ and ω_i being the solutions of the first equation and ω^* of the second:

$$\begin{cases} c - \omega\tan(\omega a) = 0 & \text{for } i \text{ odd} \\ \omega^* + c\tan(\omega^* a) = 0 & \text{for } i \text{ even} \end{cases} \tag{1.28}$$

The first step in the propagation of uncertainty is introducing the random field in the equation modelling the physical system. It is noted that, in the case of deterministic systems, the equations are generally solved using numerical methods such as the Finite Element method (Zienkiewicz and Taylor, 1991). The spatial discretization of an elliptic problem with random field discretized using the KL expansion is perused.

1.5 Stochastic Finite Element foundation

The KL expansion is nowadays the most widely used random field discretization method. Therefore, in this section, the propagation of the random field to system matrices is only described for this particular method. This section generalizes the equations from section 1.2 to the stochastic case.

Consider a bounded domain $\mathcal{D} \in \mathbb{R}^d$ with piecewise Lipschitz boundary $\partial\mathcal{D}$, where $d \leq 3$ is the spatial dimension. The stochastic elliptic partial differential equation (PDE) defined on a probability space $(\Omega, \mathcal{F}, P)$ is given by

$$-\nabla.\left[a(\mathbf{r},\varpi)\nabla u(\mathbf{r},\varpi)\right] = p(\mathbf{r}); \quad \mathbf{r} \text{ in } \mathcal{D} \quad \text{with} \quad u(\mathbf{r},\varpi) = 0; \quad \mathbf{r} \text{ on } \partial\mathcal{D} \tag{1.29}$$

Here $a : \mathbb{R}^d \times \Omega \rightarrow \mathbb{R}$ is assumed to be a stationary and square integrable random field representing the material constant and u and p are respectively the primary and source variables. Depending on the physical problem, the random field $a(\mathbf{r},\varpi)$ can be used to model different physical quantities. As an example, for a slow flow of an incompressible, viscous fluid through a porus media, $a(\mathbf{r},\varpi)$ would be the random field describing the permeability of the medium.

Truncating the series from Equation (1.23) after the M-th term, substituting $a(\mathbf{r},\varpi)$ in the governing PDE (1.29) and applying the boundary conditions, the discretized equation can be written as

$$\left[\mathbf{K}_0 + \sum_{i=1}^{M} \xi_i(\varpi)\mathbf{K}_i\right]\mathbf{u}(\varpi) = \mathbf{f} \tag{1.30}$$

The number of terms M in Equation (2.1) can be selected based on the 'amount of information' to be retained. This in turn is related to the number of eigenvalues retained, since the eigenvalues, ν_i, in Equation (1.23) are arranged in a decreasing order. For a 1-D problem, the element stiffness matrices are given by

$$\mathbf{K}_0^e = \int_{\mathcal{D}_e} \mathbf{B}^{(e)\,T}(x)\mathbf{D}\mathbf{B}^{(e)}(x)\,dx \tag{1.31}$$

$$\mathbf{K}_i^e = \sqrt{\nu_i}\int_{\mathcal{D}_e} \varphi_i(x)\mathbf{B}^{(e)\,T}(x)\mathbf{D}\mathbf{B}^{(e)}(x)\,dx \tag{1.32}$$

where $\mathbf{B}^{(e)} = d\mathbf{N}^{(e)}/dx$, $\mathbf{D}$, $\mathbf{u}$ and $\mathbf{f}$ have been defined in section 1.2, and matrices $\mathbf{K}_0$, $\mathbf{K}_i$ are deterministic. The necessary technical details to obtain the discrete stochas-

tic algebraic equations from the stochastic partial differential equation (1.29) has become standard in the literature. Excellent references, for example Ghanem and Spanos (1991), Matthies and Keese (2005), Babuska et al. (2005), are available on this topic. In Equation (1.30) $\mathbf{K}_0 \in \mathbb{R}^{n\times n}$ is a symmetric positive definite matrix, i.e. $\mathbf{x}^T\mathbf{K}_0\mathbf{x} > 0$ for all $\mathbf{x}$ and $\mathbf{K}_0^T = \mathbf{K}_0$, $\mathbf{K}_i \in \mathbb{R}^{n\times n}; i = 1, 2, \ldots, M$ are symmetric matrices, $\mathbf{u}(\varpi) \in \mathbb{R}^n$ is the solution vector and $\mathbf{f} \in \mathbb{R}^n$ is the force vector.

For the case of the random eigenvalue problem and of the dynamic problem, the mass matrix of the system is also needed, and if a parameter affecting this matrix, as, for example, the density (ρ), is expanded with a KL expansion, equations similar to Equations (1.31) and (1.32) can be obtained

$$\mathbf{M}_0^e = \int_{\mathcal{D}_e} \mathrm{E}\left[\rho\right] \mathbf{N}^{(e)\,T}(x)\mathbf{N}^{(e)}(x)\, dx \tag{1.33}$$

$$\mathbf{M}_i^e = \sqrt{\nu_i} \int_{\mathcal{D}_e} \varphi_i(x)\mathbf{N}^{(e)\,T}(x)\mathbf{N}^{(e)}(x)\, dx \tag{1.34}$$

It is noted that the system matrices are, in practical applications, positive definite. Modelling a system parameter with a Gaussian random field could lead to non-positive definite random matrices for some of the samples of the random field. To overcome this problem while using the KL discretization of a Gaussian random field, where the random variables appearing are independent and Gaussian, a transformation of the KL expansion can be used. This transformation has to ensure that the random field is positive and larger than zero for every point in the geometry. To this end, xi square or lognormal random fields can be used. In the first case, the squared value of the random part is used, i.e. $\hat{H}(\mathbf{r}, \varpi) = \mathrm{E}\left[H(\mathbf{r}, \varpi)\right] + \left(\sum_{i=1}^{M} \sqrt{\nu_i}\xi_i\varphi_i(\mathbf{r})\right)^2$. In the second case, the exponential function is used, i.e. $\hat{H}(\mathbf{r}, \varpi) = \mathrm{E}\left[H(\mathbf{r}, \varpi)\right] + \exp\left(\sum_{i=1}^{M} \sqrt{\nu_i}\xi_i\varphi_i(\mathbf{r})\right)$. This last representation has been used, for example, in fluids through porous media (Ghanem and Dham, 1998)

Characterizing parametric uncertainty follows several steps, namely, identification of the random parameters, probabilistic description of the parameters and mapping of the parameters into the system matrices. To quantify uncertainty in a system while avoiding these difficulties that are inherent to parametric uncertainty, Soize (2000) proposed a method that models each system matrix as a random matrix. This method is also applied to study non-parametric uncertainty.

1.6 Non-parametric uncertainty

Non-parametric uncertainties are generally related to uncertainties in the mathematical model. A model is a simplified representation of the phenomena under study, and a good one represents the system as simply as possible while providing a response with the required accuracy. Model uncertainties can arise by simplifications (e.g. approximating a nonlinear behavior by a linear one, nonproportional damping by proportional damping), model resolution arising in numerical models (e.g. size of the grid can introduce uncertainties), or by not including some phenomenon in the model. Quantification of non-parametric uncertainties, unlike parametric uncertainty, is not suited to the usual parameter estimation techniques. Methods to evaluate this type of uncertainties in the context of multiple-degrees-of-freedom systems can be based on random matrix theory (RMT) (Gupta and Nagar, 2000).

The matrix variate distributions used are obtained using the maximum entropy principle (Kapur, 1989, Gokhale, 1975, Soize, 2000). To this end, matrices and their inverses are assumed real, symmetric and positive definite. The mean of the matrices is also assumed to be known. The maximum entropy method allows to obtain a joint probability density function (pdf) of the elements of the random matrix. The obtained distribution has the pdf corresponding to the Wishart distribution or matrix variate gamma distribution, as these probability density functions (pdfs) coincide under some conditions (Gupta and Nagar, 2000, Muirhead, 1982). A different pdf was obtained by Mignolet and Soize (2008a) when the variance of some eigenvalues is also prescribed when applying the maximum entropy principle. A Wishart matrix distribution $W_n(p, \mathbf{\Sigma})$ is completely characterised by its parameters p and $\mathbf{\Sigma} \in \mathbb{R}^{n \times n}$. The parameters of the Wishart matrix variate distribution can be related to the mean of the distribution and to a measure of uncertainty, the dispersion parameter (Soize, 2000). Different criterion were proposed by Adhikari (2008) to fit the parameters arising in the Wishart distribution. Ghanem and Das (2009) have coupled frequency response function matrices with Wishart random matrices. Desceliers et al. (2004) proposed a hybrid method to model uncertainties, where nonlinear damping is modelled with parametric uncertainty and system matrices are modelled using the random matrix theory. In the case of elliptic partial differential equations, the maximum entropy principle has been used to model the real tensor of elastic coefficients (Soize, 2006, Guilleminot and

Soize, 2011) and reduced matrices (Soize, 2009). Positive definite matrices appearing in nonlinear problems have also been modelled with the proposed approach (Mignolet and Soize, 2008b). Both parametric and nonparametric uncertainties were considered bySoize (2010) for dynamic systems.

1.6.1 Maximum entropy

The concept of entropy (Shannon, 1948, Kapur, 1989) can be used to obtain the pdf of a random variable or random vector based on some knowledge (e.g. moments). The entropy of a random variable is a measure depending continuously on its pdf and equal to zero when there is no uncertainty. Furthermore, the entropy of the joint pdf of two independent random variables is the sum of the entropies of the pdfs of each random variable. Then, the entropy of a random variable X with pdf f_X defined on $[a, b]$ is given by $\mathcal{S}$

$$\mathcal{S}(f_X) = -\int_a^b f_X \ln f_X \, d\varpi \tag{1.35}$$

and is subjected to some given information, as, for example, $\int_a^b f_X \, d\varpi = 1$ and $\int_a^b f_X g(\varpi) \, d\varpi = \mathrm{E}[g]$. This information is introduced by using Lagrange multipliers γ_1, γ_2 and the entropy is maximised with respect to f_X

$$\frac{d}{f_X}\left(\mathcal{S}(f_X) - \gamma_1\left(\int_a^b f_X \, d\varpi - 1\right) - \gamma_2\left(\int_a^b f_X g(\varpi) \, d\varpi - \bar{g}\right)\right) = 0 \tag{1.36}$$

The functions g can be used to prescribe moments ($g = X^n$) or other types of functions such as $g = e^{-x}$, $g = \ln(1 + x)$ and other logarithms, and $\bar{g}$ is the prescribed value of $\int_a^b f_X g(\varpi) \, d\varpi$. The maximization of entropy implies the maximization of an integral function, and results from calculus of variations can be used (Dacorogna, 2004). For the multivariate case (i.e. vectors and matrices), considering the entries independent would lead to obtain their joint pdf as the product of their marginal pdfs. The introduction of statistical dependence between entries can be performed by introducing covariances between pairs of random variables, specifying a relationship among variables (e.g. the sum of some variables is a constant) or specifying moments for functions of all the variables.

As for the univariate case, a pdf can be obtained by maximizing the entropy $\mathcal{S}$ associated with the matrix variate probability density function $f_{\mathbf{G}}(\mathbf{G})$ (Gokhale, 1975,

Soize, 2001)

$$\mathcal{S}\left(f_{\mathbf{G}}\right) = -\int_{\mathbf{G}>0} f_{\mathbf{G}}\left(\mathbf{G}\right) \ln\left\{f_{\mathbf{G}}\left(\mathbf{G}\right)\right\} d\mathbf{G} \tag{1.37}$$

and the integrals are evaluated over the ensemble of symmetric positive definite matrices of size n, $\mathbb{M}_n^+$. The entropy equation is subjected to several constraints, that is, the matrix $\mathbf{G}$ is symmetric, positive definite and

$$\int_{\mathbf{G}>0} f_{\mathbf{G}}\left(\mathbf{G}\right) d\mathbf{G} = 1 \tag{1.38}$$

$$\mathrm{E}\left[\mathbf{G}\right] = \int_{\mathbf{G}>0} \mathbf{G}\, f_{\mathbf{G}}\left(\mathbf{G}\right) d\mathbf{G} = \overline{\mathbf{G}} \tag{1.39}$$

$$\mathrm{E}\left[\ln\left\{\det\left(\mathbf{G}\right)\right\}\right] = v \quad |v| < +\infty \tag{1.40}$$

where $\overline{\mathbf{G}}$ is the mean of matrix $\mathbf{G}$ and is prescribed. The last constraint allows to ensure the existence of moments of matrix $\mathbf{G}^{-1}$. In general, the probability density function resulting from this analysis is a matrix variate gamma distribution. The main difference between the matrix variate gamma distribution and the Wishart distribution is that historically only integer values were considered for the parameter p in the Wishart matrices. Then, the obtained pdf $f_{\mathbf{G}}$ of a Wishart distribution is given by (Muirhead, 1982)

$$f_{\mathbf{G}} = \{2^{\frac{1}{2}np}\Gamma_n(\frac{1}{2}p)\det(\mathbf{\Sigma})^{\frac{1}{2}p}\}^{-1}\det(\mathbf{G})^{\frac{1}{2}(p-n-1)}\mathrm{etr}(-\frac{1}{2}\mathbf{\Sigma}^{-1}\mathbf{G}), \mathbf{G} > 0, p \geq n \tag{1.41}$$

where $\Gamma_n(a)$ is the multivariate gamma function. This distribution will be referred as the Wishart distribution probability density function and the parameters of the distribution are p and $\mathbf{\Sigma} = \overline{\mathbf{G}}/p$, that is $\mathbf{G} \sim W_n\left(p, \overline{\mathbf{G}}/p\right)$.

The Wishart distribution is a symmetric positive definite matrix $\mathbf{G} \in \mathbb{R}^{n\times n}$. Any symmetric positive definite matrix can be given by $\mathbf{G} = \mathbf{Z}^T\mathbf{Z}$. The Wishart distribution is obtained when the $p \times n$ matrix $\mathbf{Z}$ is given by $N(\mathbf{0_{p\times n}}, \mathbf{I_p} \otimes \mathbf{\Sigma})$, that is, the p rows of $\mathbf{Z}$ are independent $N_n(\mathbf{0_{1\times n}}, \mathbf{\Sigma})$ random vectors, and $\mathbf{0_{n\times p}}$ is a matrix $\in \mathbb{R}^{n\times p}$ whose elements are all equal to zero. That is, a Wishart distribution is a n-variate generalization of χ^2 distribution denoted by $W_n(p, \mathbf{\Sigma})$ with parameters p, n and $\mathbf{\Sigma}(n \times n) > 0$, has dimension $n \times n$, is symmetric positive definite and its pdf is given by Equation (1.41). The distribution of the inverse Wishart matrix, that is, inverse of a Wishart matrix, has been derived analytically (see, e.g. Gupta and Nagar, 2000), and moments of this distribution are available (see, e.g. Letac and Massam, 2004).

The Wishart random matrix have been used to model system matrices **M**, **C** and **K** (Soize, 2000, 2005). In the next subsection, a method to identify parameters of a Wishart distribution from a system matrix **G** is described. Both the joint pdf of eigenvalues and eigenvectors of a Wishart matrix and the asymptotic marginal distribution of eigenvalues for a particular case of the Wishart matrix have been derived. These results can be useful for dynamic problems and are discussed in subsection 1.6.3.

1.6.2 Parameter selection of a Wishart random matrix

As already exposed, the mean of a matrix modelled with the random matrix approach coincides with the mean of the random matrix i.e. (Adhikari, 2008)

$$\mathrm{E}\left[\mathbf{G}\right] = \overline{\mathbf{G}} = p\boldsymbol{\Sigma} \tag{1.42}$$

This allows to determine matrix $\boldsymbol{\Sigma}$, but parameter p remains to be calculated. The dispersion parameter δ_G, a measure of the normalised standard deviation, was introduced by Soize (2000)

$$\delta_G^2 = \frac{\mathrm{E}\left[\|\mathbf{G} - \mathrm{E}\left[\mathbf{G}\right]\|_{\mathrm{F}}^2\right]}{\|\mathrm{E}\left[\mathbf{G}\right]\|_{\mathrm{F}}^2}. \tag{1.43}$$

where $\|\mathbf{A}\|_{\mathrm{F}}^2 = \mathrm{Trace}\left(\mathbf{A}^T\mathbf{A}\right)$ denotes the Frobenius norm of matrix **A**. For a Wishart distribution it has been shown that (Adhikari, 2008)

$$\delta_G^2 = \frac{1}{p}\left\{1 + \frac{\{\mathrm{Trace}\left(\overline{\mathbf{G}}\right)\}^2}{\mathrm{Trace}\left(\overline{\mathbf{G}}^2\right)}\right\} \tag{1.44}$$

When underlying parametric uncertainty is considered and no experimental data are available, the dispersion parameter can be considered as a parameter to perform a sensitivity analysis of the stochastic solution. If experimental data are available, the dispersion parameter can be estimated through an optimization process (Soize, 2010). The parameter p of Wishart distribution can be related to the dispersion parameter through Equation (1.44), leading to

$$p = \frac{1}{\delta_G^2}\left\{1 + \frac{\{\mathrm{Trace}\left(\overline{\mathbf{G}}\right)\}^2}{\mathrm{Trace}\left(\overline{\mathbf{G}}^2\right)}\right\}. \tag{1.45}$$

Therefore, the parameter p of the Wishart distribution can be calculated from the dispersion parameter and the mean of the matrix under consideration. It is noted here that other methods to fit the mean matrix have been proposed by Adhikari (2008), where several criteria were selected. Those criteria include the one adopted to derive Equation (1.45), where the mean of the stiffness matrix coincides with the mean of the random matrix. A second criterion stated that the mean of the inverse Wishart matrix coincides with the inverse of the mean stiffness matrix. The third criterion specified that the mean of the random matrix and the mean of the inverse of the random matrix are closest to the deterministic matrix and its inverse.

1.6.3 Eigenvalues and eigenvectors of a Wishart distribution

A well-known theorem of random matrix theory (Muirhead, 1982) states that the joint density function of the latent roots $l_1, \ldots, l_n$ of a $n \times n$ positive definite matrix $\mathbf{A}$ with density function $f(\mathbf{A})$ is given by

$$f(l_1, \ldots, l_n) = \frac{\pi^{n^2/2}}{\Gamma_n(n/2)} \prod_{i<j}^{n} (l_i - l_j) \int_{O(n)} f(\mathbf{\Psi L \Psi}^T)(d\mathbf{\Psi}) \tag{1.46}$$

where $\mathbf{\Psi}$ is an orthogonal matrix of the orthogonal group $O(n)$ such that $\mathbf{A} = \mathbf{\Psi L \Psi}^T$, with $\mathbf{L}$ a diagonal matrix with diagonal elements $(l_1, \ldots, l_n)$. The integral on the orthogonal group $O(n)$, $\int_{O(n)} f(\mathbf{\Psi L \Psi}^T)(d\mathbf{\Psi})$, is in general difficult to evaluate, but for some cases, eigenvalues and eigenvectors are independent, and the integral simplifies. One of the cases where the eigenvalues and eigenvectors of $\mathbf{A}$ are independent is when $f(\mathbf{A}) = f(\mathbf{\Theta A \Theta}^T)$, with $\mathbf{\Theta}$ any orthogonal matrix. For some distributions, including Wishart matrix distribution, eigenvalues and eigenvectors are asymptotically independent (Muirhead, 1982).

A Wishart matrix satisfying $f(\mathbf{A}) = f(\mathbf{\Theta A \Theta}^T)$ is known as the White Wishart matrix, where $\mathbf{\Sigma} = a^2/n\mathbf{I}$. The pdf of a White Wishart matrix is therefore orthogonal invariant. That is, if the orthogonal transformation $\mathbf{\Theta A \Theta}^T$ is performed on the White Wishart matrix $\mathbf{A}$ with $\mathbf{\Theta \Theta}^T = \mathbf{I}$, the resulting matrix is still a White Wishart matrix. Consider the eigensolution of a White Wishart matrix $\mathbf{A} = \mathbf{\Psi L \Psi}^T$ so that $\mathbf{\Theta A \Theta}^T = \mathbf{\Theta \Psi L \Psi}^T \mathbf{\Theta}^T$ is a White Wishart matrix. Its matrices of eigenvectors and eigenvalues are respectively $\mathbf{\Theta \Psi}$ and $\mathbf{L}$, and $\mathbf{\Theta A \Theta}^T$ has the same pdf as $\mathbf{A}$. Then, the eigenvectors

of a White Wishart are uniformly distributed over the $n-$ dimensional unit sphere, so that entries of the same eigenvector are independent and for each eigenvector $\psi^T\psi = \sum_{i=1}^{n}\psi_i^2 = 1$. Then, the mean of the product of two elements of the j-th eigenvector is given by Pastur and Shcherbina (2011)

$$\mathrm{E}[\psi_{kj}\psi_{lj}] = \delta_{jl}/n \tag{1.47}$$

and the mean of the product of four elements of the i-th and j-th eigenvector

$$\begin{aligned}\mathrm{E}[\psi_{ki}\psi_{li}\psi_{mj}\psi_{oj}] =& \frac{1}{n(n-1)(n+2)}((n+1)\delta_{kl}\delta_{mo} - (\delta_{km}\delta_{lo} + \delta_{ko}\delta_{lm}))+ \\ & \frac{1}{n(n-1)(n+2)}\delta_{ij}(-2\delta_{kl}\delta_{mo} + n(\delta_{km}\delta_{lo} + \delta_{ko}\delta_{ml}))\end{aligned} \tag{1.48}$$

The spectral analysis of large random matrices is an active field of research. Results on the limit distribution of eigenvalues of White Wishart matrices when the size of the matrix tends to infinity (i.e. asymptotic marginal distribution) have been obtained (Marčenko and Pastur, 1967, Bai and Silverstein, 2010, Pastur and Shcherbina, 2011). Here we briefly review the details. Define the normalised counting measure N_n

$$\mathrm{N}_n(\Delta) = \frac{1}{n}\sharp\{i \in \{1,\ldots,n\} : l_i^{(n)} \in \Delta\} \tag{1.49}$$

where Δ is an interval of $\mathbb{R}$ and $l_i^{(n)}$ are the eigenvalues of an $n \times n$ matrix. The Stieltjes transform (Marčenko and Pastur, 1967) of the normalised counting measure of matrix $\mathbf{H}$, defined for all nonreal z, is given by

$$\begin{aligned}s_n(z) &= \int \frac{\mathrm{N}_n(dl)}{l-z} = \frac{\mathrm{Trace}\left((\mathbf{H} - z\mathbf{I}_n)^{-1}\right)}{n} \\ &= \frac{1}{n}\sum_{k=1}^{n}\frac{1}{h_{kk} - z - \boldsymbol{\alpha}_k^*(\mathbf{H}_k - z\mathbf{I}_{n-1})^{-1}\boldsymbol{\alpha}_k}\end{aligned} \tag{1.50}$$

with $\mathbf{H}$ a symmetric matrix, $\mathbf{H}_k$ the $(n-1)\times(n-1)$ matrix obtained by removing the k-th row and column from matrix $\mathbf{H}$, $\boldsymbol{\alpha}_k$ is the k-th column of $\mathbf{H}$ with the k-th element removed and h_{kk} is the k-th diagonal element of $\mathbf{H}$. If the denominator $h_{kk} - z - \boldsymbol{\alpha}_k^*(\mathbf{H}_k - z\mathbf{I}_{n-1})^{-1}\boldsymbol{\alpha}_k$ is equal to $s(z, g_n(z)) + o(1)$ for some function g_n, the limiting spectral distribution N exists and its Stieltjes transform is the solution of $s = 1/g(z,s)$, with $o(1)$ the small O implying in this case that $|h_{kk} - z - \boldsymbol{\alpha}_k^*(\mathbf{H}_k - z\mathbf{I}_{n-1})^{-1}\boldsymbol{\alpha}_k - s(z, g_n(z))| << 1$.

Consider the matrix $\mathbf{H} = \mathbf{H}^{(0)} + n^{-1}\mathbf{Z}^T\mathbf{T}\mathbf{Z}$, where $\mathbf{H}^{(0)}$ and $\mathbf{T}$ are nonrandom symmetric matrices and the entries of $\mathbf{Z}$ are i.i.d. Gaussian random variables with $\mathrm{E}[Z_{ij}] = 0$, $\mathrm{E}[Z_{ij}Z_{kl}] = a^2\delta_{ik}\delta_{jl}$. The normalised counting measures of $\mathbf{H}^{(0)}$ and $\mathbf{T}$ converge respectively to $\mathrm{N}^{(0)}$ and t as $n \to \infty$, and the Stieltjes transform of $\mathrm{N}^{(0)}$ is $g^{(0)}$. The normalised counting measures of $\mathbf{H}$, N_n, converges asymptotically to N, and $p/n \to c \geq 1$ when $n \to \infty$. The Stieltjes transform g of N is uniquely determined by

$$g(z) = g^{(0)}\left(z - a^2 c \int \frac{\tau t(d\tau)}{1 + a^2\tau g(z)}\right) \tag{1.51}$$

When $\mathbf{H}^{(0)}$ is zero and $\mathbf{T} = \mathbf{I}$, its normalised counting measures are $N^{(0)} = \delta_0$ and $t = \delta_1$, i.e. all its eigenvalues are zero and one respectively. By introducing these results in Equation (1.51) and inverting the Stieltjes transform, the Marčenko-Pastur distribution can be obtained

$$N = \rho = \frac{\sqrt{a^+ - l}\sqrt{l - a^-}}{2\pi a^2 l} \quad \text{with} \quad a^- = a^2(1 - \sqrt{c})^2,\ a^+ = a^2(1 + \sqrt{c})^2 \tag{1.52}$$

The counting measure $\mathcal{N}_n(\Delta) = nN_n(\Delta)$ is a particular case of a linear statistic defined by a test function $\varphi : \mathbb{R} \to \mathbb{C}$

$$\mathcal{N}_n[\varphi] = \sum_{i=1}^{n} \varphi(l_i^{(n)}) = \int \varphi(l)\mathcal{N}_n(dl) = \mathrm{Trace}(\varphi(\mathbf{A})) \tag{1.53}$$

If $\mathcal{N}_n[\varphi]$ is a linear eigenvalue statistics of the White Wishart ensemble with φ a continuous bounded function with bounded derivative, the centralised linear statistic $n\mathrm{N}_n[\varphi] - \mathrm{E}[n\mathrm{N}_n[\varphi]]$ converges in distribution as $n \to \infty$ $p/n \to c \geq 1$ to the Gaussian random variable with zero mean and variance (Pastur and Shcherbina, 2011)

$$V_{Wish}[\varphi] = \frac{1}{2\pi^2}\int_{a^-}^{a^+}\int_{a^-}^{a^+}\left(\frac{\Delta\varphi}{\Delta l}\right)^2 \frac{4a^4c - (l_1/n - a_m)(l_2 - a_m)}{\sqrt{4a^4c - (l_1/n - a_m)^2}\sqrt{4a^4c - (l_2/n - a_m)^2}}(1/n^2)dl_1dl_2 \tag{1.54}$$

with $a_m = (a^+ + a^-)/2 = a^2(1 + c)$ and $\Delta\varphi = \varphi(l_2) - \varphi(l_1)$, $\Delta l = l_2 - l_1$. This integral can therefore be used to calculate the variance of a linear eigenvalue statistics.

1.7 Numerical methods for uncertainty propagation

A physical system can generally be modelled with a partial differential equation (e.g. elliptic PDE) and, in the deterministic case, the solution of this equation is approximated using a numerical method (e.g. the Finite Element method (FEM) (Zienkiewicz and Taylor, 1991)). When considering parametric uncertainty, the partial differential equation is affected by uncertainty through a source term or through the model of a geometric or material parameter such as Young's modulus and Poisson's ratio amongst others. Parametric uncertainty can be described using probability theory and modelled by a random field (Vanmarcke, 1983, Sudret and Der-Kiureghian, 2000, Stefanou, 2009), that is discretized with one of the methods formerly considered. It is assumed that the random field has finite variance, so that it can be discretized by projecting it on a basis of functions of the Hilbert space $\mathcal{L}^2(\Xi, dP_\Xi)$. Then, if n is the number of degrees of freedom of the system after discretization using the FEM, the vector of nodal response $\mathbf{u} \in \mathbb{R}^n$ results from a nonlinear transformation of the uncertainty affecting the system. Several methods aimed at obtaining the joint pdf of the elements of $\mathbf{u}$ have been developed. These methods can be divided into two groups, namely, sampling methods and non-sampling methods. Surrogate models interpolate or fit a curve using samples, so they may be considered as sampling methods, and are reviewed in subsection 1.7.2.

1.7.1 Sampling methods

The solution of a stochastic problem with a sampling method involves generating samples of the random field or multivariate parameter, solving the deterministic PDEs associated with these samples and finally analyzing the samples, i.e. obtaining the joint pdf or moments of the response vector $\mathbf{u}$. The samples can be generated through a random number generator, leading to procedures such a Monte Carlo Simulation, quasi-Monte Carlo and Latin Hypercube methods (Lemieux, 2009). Otherwise, the samples can be prescribed by the method, as in the case of surrogate models (Forrester et al., 2008).

Random number generators can be obtained from a physical system (e.g. the lottery, a substance undergoing atomic decay, thermal noise in a semiconductor) or through quasi-random number generators. Quasi-random number generators calculates a sequence of numbers that appear to be random $x_i = g(x_{i-1}, \ldots, x_{i-k})$, and the sequence is repeated after applying g a given number of times, called the period. These random

number generators are used to simulate uniformly distributed random variables. The uniform univariate distribution $U(0,1)$ has a probability density function given by

$$f(x) = \begin{cases} 1 & \text{if } 0 < x < 1 \\ 0 & \text{otherwise} \end{cases} \tag{1.55}$$

and its mean and variance are respectively $\mathrm{E}[X] = 1/2$, $\mathrm{Var}[X] = 1/12$. A random number generator for this pdf can be the linear congruential generator (Newman and Odell, 1971, Gentle, 2003), where parameters R_0, a, b, m are used to obtain the serie

$$R_{i+1} = (aR_i + b)(\mathrm{mod}\, m) \qquad a < m,\ b < m \tag{1.56}$$

where mod m indicates congruence modulo m, i.e. the difference $R_{i+1} - (aR_i + b)$ is divisible by m, so that R_{i+1} can be the residue of $(aR_i + b)/m$. Each term of the serie is then divided by m to scale it into the interval $(0,\ 1)$. The modulo m can be, for example, a Mersenne prime $m = 2^p - 1$ (with $p \leq 31$ a prime number), or, for a binary computer $m = 2^b$. The outcome of the congruential random number generator can be shuffled by using another generator to permute subsequences from the original generator. An extension of this method can be obtained by substituting a by a vector of k constants and R_i by a vector composed of the last k terms of the series. Also, the constant b can depend on the term of the series, as in the add-with-carry, subtract-with-borrow and multiply-with-carry generators. Nonlinear congruential generators have also been developed, such as inversive congruential generators or Blum, Blum and Shub. Methods based on combining different generators are also available. More details on random number generators can be found, for example, in the books by Newman and Odell (1971), Gentle (2003), Lemieux (2009).

Generally, samples of random variables with pdfs different from the uniform pdf are needed. A random variable X with continuous cumulative density function P_X can be related to a uniform random variable $U(0,1)$ through the inverse CDF method (Papoulis and Pillai, 2002, Gentle, 2003)

$$X = P_X^{-1}(U) \tag{1.57}$$

Although calculations of the inverse of the distribution P_X^{-1} can be difficult when available, and this inverse is many times not available. Alternative methods have been derived to circumvent this problem, such as acceptance/rejection methods, composi-

tion, convolution or methods based on the use of Markov chains (Markov Chain Monte Carlo) (Lemieux, 2009). For the case of a Gaussian random variable $N(0,1)$, samples can be obtained from samples of two independent uniform random variables U and V

$$X = (-2\ln U)^{1/2}\cos(2\pi V), \qquad Y = (-2\ln U)^{1/2}\sin(2\pi V) \tag{1.58}$$

so that X and Y are independent random variables with standard normal distribution.

Once the samples of the random variables are obtained, they are introduced in the PDE studied and the deterministic systems are solved. If MCS with N samples is used to obtain an estimation of the pdf of a random variable u (e.g. a term of the response vector $\mathbf{u}$), estimations of the mean and standard deviation are given by

$$\mathrm{E}[u] \approx \frac{1}{N}\sum_{i=1}^{N} u_i, \qquad \sigma \approx \sqrt{\frac{1}{N}\sum_{i=1}^{N}(u_i - \mathrm{E}[u])^2} \tag{1.59}$$

From the central limit theorem (Xiu, 2010), we can say that the error of the MCS approximation to an integral, using N samples, converges in distribution to a gaussian random variable with zero mean and stardard deviation $\sqrt{N}/\sigma$. The mean of a random variable given by Equation (1.12) is the result of evaluating a multivariate integral. The evaluation of moments using MCS given by Equation (1.59) is independent of the dimension of the integral evaluated, that is, an integral evaluated using MCS does not suffer from the curse of dimensionality. Furthermore, from the central limit theorem, it can be said that the probabilistic error of the Monte Carlo estimator is in $O(1/\sqrt{N})$, that is, for example, that to reduce the error by a factor of 10 the number of samples used should be increased by a factor of 100 (on average).

Some methods focus on reducing this error by finding a function whose integral leads to the same result as MCS but with a with smaller variance (Lemieux, 2009, Glasserman, 2004). This is obtained with variance reduction techniques such as antithetic variates, control variates, importance sampling, conditional Monte Carlo, stratification, common random numbers and Latin Hypercube Sampling (LHS).

Other methods, called quasi-Monte Carlo methods or low-discrepancy methods, focus on samplings techniques leading to a better convergence rate in error. These methods use a deterministic sequence of numbers such that the distance $D^*(P_n)$ between the empirical distribution and the uniform distribution is minimised, e.g. for a 1D problem

$D^*(P_n) = sup_{x\in[0,1)} |F(x) - \hat{F}_n(x)|$, where F is the CDF of the uniform distribution and $\hat{F}$ the one obtained from the samples. They are divided into two families, lattices and digital nets/sequences.

Nonlinear problems are often addressed with sampling methods (Bayer and Bucher, 1999, Matthies and Keese, 2005). The algebraic random eigenvalue problem where large amounts of uncertainty are considered has also been addressed with sampling methods. The strategies for the random eigenvalue problem are based on ordering the samples depending on the distance between them and on calculating the eigenvalues of a sample using the ones of a close sample. This ordering can be based on algorithms from the traveling salesman problem and space reduction (Szekely and Schuëller, 2001), component mode synthesis (Pradlwarter et al., 2002), or can be done in a tree-type data structure (Du et al., 2005). The relation between eigenvalues of close samples is obtained using different initialization strategies for the power method, so that the start-vector used in a sample is the result from the iteration process of the previous sample. The initialization strategies and size reduction methods reduce the computational time of MCS.

Random matrices can also be simulated with MCS. Consider the case of a Wishart distribution. The steps to perform the MCS simulation are (Adhikari, 2008):

1. Find the mean system matrix $\overline{\mathbf{G}}$, that is, the matrix obtained from the deterministic FEM and its dimension n. For complex engineering systems n can be in the order of several thousands or even millions.

2. Obtain the normalised standard deviations or the 'dispersion parameters' $\widetilde{\delta}_G$ corresponding to the system matrix, from experiment, experience or using the Stochastic FEM.

3. Calculate
$$p = \frac{1}{\delta_G^2}\left\{1 + \frac{\{\text{Trace}\,(\overline{\mathbf{G}})\}^2}{\text{Trace}\left(\overline{\mathbf{G}}^2\right)}\right\}. \tag{1.60}$$
and approximate it to its nearest integer. This approximation would introduce negligible error. Calculate $\boldsymbol{\Sigma} = \overline{\mathbf{G}}/p$.

4. Create a $p \times n$ matrix $\widetilde{\mathbf{X}}$ with Gaussian random numbers with zero mean and unit covariance i.e., $\widetilde{\mathbf{X}} \sim N_{p,n}\left(\mathbf{O}, \mathbf{I}_p \otimes \mathbf{I}_n\right)$. Obtain the Cholesky decomposition of the

positive definite matrix $\boldsymbol{\Sigma}$, $\boldsymbol{\Sigma} = \boldsymbol{\Gamma}\boldsymbol{\Gamma}^T$ and use it to calculate the matrix $\mathbf{Z}$ using the linear transformation

$$\mathbf{Z} = \widetilde{\mathbf{X}}\boldsymbol{\Gamma}^T \tag{1.61}$$

Following theorem 2.3.10 in Gupta and Nagar (2000) it can be shown that $\mathbf{X} \sim N_{n,p}(\mathbf{O}, \mathbf{I}_p \otimes \boldsymbol{\Sigma})$. Obtain the sample of the Wishart matrix $\mathbf{G} = \mathbf{Z}^T\mathbf{Z}$.

5. Perform steps 1 to 4 for all the system matrices modelled as Wishart matrices. In general, $\mathbf{G} = \{\mathbf{K}, \mathbf{M}, \mathbf{C}\}$ or system matrices reduced using a limited number of eigenvectors.

6. Solve the equation of motion for each sample to obtain the response statistics of interest. The equation to be solved can be, for example $\mathbf{Ku} = \mathbf{f}$, $\mathbf{Kv} = \lambda\mathbf{v}$ or $(s^2\mathbf{M} + s\mathbf{C} + \mathbf{K})\mathbf{u} = \mathbf{f}$ respectively for the linear problem, eigenvalue problem and dynamic problem in Laplace domain. Depending on the case, one or several of the matrices $\{\mathbf{K}, \mathbf{M}, \mathbf{C}\}$ might be modelled as Wishart matrices.

This procedure can be implemented easily. Alternatively, MATLAB® command `wishrnd` can be used to generate the samples of Wishart matrices modelling $\{\mathbf{K}, \mathbf{M}, \mathbf{C}\}$. MATLAB® can handle fractional values of p so that the approximation to its nearest integer in step 3 may be avoided.

1.7.2 Surrogate models

Surrogate models are used for cases where a quantity of interest of a system depends on some parameters through a function that is complicated or expensive to evaluate. Response surface methods, meta-modelling or surrogate models approximate the function by sampling the original function (Jones, 2001, Jin et al., 2000, Zhao and Xue, 2010), and the approximation can be smoothing (e.g. least squares method) or interpolating (e.g. collocation method using the Gauss points of a numerical integration procedure). The procedure is identical for all systems, that is, surrogate models can approximate equally the response from linear, non-linear, static and dynamic problems. Therefore, the difference between the procedure to obtain surrogate models of, for example, a linear system and of a non-linear system, is the deterministic systems corresponding to each sample. Surrogate models can then be specially suite for nonlinear systems, and some examples are given, for example, by Keese and Matthies (2003), Matthies and

Keese (2005), Deng et al. (2011). This subsection focuses in the interpolation procedure.

For non-interpolating or smoothing methods, a regression model, e.g. quadratic polynomial, is fitted to a set of points using the least squares method or maximum likelihood estimation (Jones, 2001, Forrester et al., 2008, Friswell and Mottershead, 1995). The least squares method minimises the sum of square residues $S = \sum_{i=1}^{N} r_i^2$. Each residue is a measure of distance between each sample y_i and the function $f(x, \boldsymbol{\beta})$, $r_i = y_i - f(x_i, \boldsymbol{\beta})$, where β is the set of parameters that have to be determined. If f is a polynomial $f = \sum_{j=0}^{k} \beta_j x_i^j$ the minimization of S with respect to β_l leads to $\sum_{i=1} x_i^l (\sum_{j=1}^{k} \beta_j x_i^j) = \sum_{i=1} x_i^l y_i$, from where a linear system of equations is obtained and the system matrix is the Vandermonde matrix. Simplifying the resulting system leads to a system $\mathbf{A}\boldsymbol{\beta} = \mathbf{f}$ where $\mathbf{A} \in \mathbb{R}^{N \times k}$ with elements $A_{ij} = x_i^j$ and vectors $\boldsymbol{\beta}$ and $\mathbf{f}$ are respectively the vector of coefficients β_j and response samples y_i. The coefficients $\boldsymbol{\beta}$ can be retrieved from $\boldsymbol{\beta} = (\mathbf{A}^T\mathbf{A})^{-1}\mathbf{A}^T\mathbf{f}$. The maximum likelihood method maximizes the probability of obtaining the data for a set of parameters β. Consider the data set $\{(x_1, y_1 \pm \epsilon_1), (x_2, y_2 \pm \epsilon_2), \ldots, (x_N, y_N \pm \epsilon_N)\}$ from $\hat{y}(x, \boldsymbol{\beta})$, the probability of its occurrence is

$$P = \prod_{i=1}^{N} \frac{1}{2\pi\sigma_i^2} e^{-(y_i - \hat{y}(x_i))^2 / 2\sigma_i^2} \epsilon_i \tag{1.62}$$

by assuming that the errors ϵ_i are independent and uniformly distributed and weighted by a normal distribution of y_i around $\hat{y}(x)$. This probability is maximized with respect to $\boldsymbol{\beta}$, or, equivalently, the negative of its natural logarithm is minimized. If all σ_i are the same and ϵ_i are constant, the least-square method is retrieved.

The surrogate model of a function y can be given by

$$\hat{y}(\mathbf{x}^*) = \sum_{k=1}^{m} a_k \pi_k(\mathbf{x}^*) + \sum_{j=1}^{n} b_j \phi(||\mathbf{x}^* - \mathbf{x}_j||) \tag{1.63}$$

where an initial set of points $\mathbf{x}_j$ has been used to fit polynomials π_k with the least squares method, that is, minimizing the squared errors between the function and the polynomial interpolation. A new set of points $\mathbf{x}^*$ is used to fit the remaining functions ϕ. These functions can be considered as radial basis functions as they depend on the distance between the original set of points and the new sampling points $r = ||\mathbf{x}^* - \mathbf{x}_j||$. The functions generally used can be polynomials, thin plate spline ($\phi = ||r||^2 \log(||r||)$),

multiquadric ($\phi = \sqrt{||r||^2 + \gamma^2}$), inverse multiquadric ($\phi = (||r||^2+\gamma^2)^{-1/2}$), Gaussian ($\phi = e^{-||r||^2/2\sigma^2}$) or Kriging ($\phi = \exp(-\sum_{l=1}^{d} \theta_l |x_l^* - x_{jl}|^{p_l})$) (Forrester et al., 2008). These methods are widely used in optimization problems. An example of application could be the use of Kriging method to calculate the instability in aeroelastic problems (Badcock et al., 2011).

The sampling techniques discussed in the previous section can be used to evaluate integrals appearing in the propagation of parametric uncertainty. But integrals can also be evaluated using numerical methods, such as quadrature methods (Xiu, 2007, 2009, Maître and Knio, 2010, Eldred and Burkardt, 2009, Bressolette et al., 2010). Consider a quantity of interest y of a system depending on a set of independent identically distributed random variables $\{\xi_1, \ldots, \xi_M\}$, where M is referred to as the dimension of the Polynomial Chaos, then, an approximation to y can be given by

$$\hat{y} = \sum_{i=1}^{P} y_i \Gamma_i, \quad y_i = \frac{\mathrm{E}[\Gamma_i y]}{\mathrm{E}[\Gamma_i^2]} \tag{1.64}$$

where Γ_i are a set of basis functions orthogonal with respect to the pdf of the random variables $\{\xi_1, \ldots, \xi_M\}$, i.e. $\int \Gamma_i \Gamma_j f_\xi d\xi = \delta_{ij} \int \Gamma_i^2 f_\xi d\xi$. The integral $\mathrm{E}[\Gamma_i^2]$ can be obtained analytically, and only $\mathrm{E}[\Gamma_i y]$ remains to be calculated. This mean can be evaluated through MCS, but numerical integration techniques are generally used. The set of functions Γ_i are generally orthogonal polynomials so that quadrature methods are used (Engels, 1980). The maximum order on the Hermite polynomials from which Γ_i is obtained is p, so that the maximum order of the polynomial in one variable to be integrated is $2p$. Quadrature methods integrate exactly polynomials of order $2p+1$ if the function is evaluated at the $p+1$ roots of the orthogonal polynomial of order $p+1$, and, if y depends only on one random variable, the resulting numerical integral is of the form

$$\mathrm{E}[\Gamma_i y] \approx \sum_{k=1}^{p+1} \Gamma_i(\xi_{j_k}) y(\xi_{j_k}) A_k \tag{1.65}$$

where ξ_{jk} are the roots of an orthogonal polynomial with respect to a weight function $W(\xi)$ and A_k are the corresponding weights. If Hermite polynomials are used, the weight function can be $W(\xi) = e^{-\xi^2/2}/2\pi$. If M random variables affect y, the integral from Equation (1.65) transforms into an M dimension integral. The most obvious way of numerically integrating a M-dimensional integral is to perform a tensor product of

M one dimensional integrals, so that y is evaluated at the tensor product of M sets of roots of the polynomial of order $p+1$, that is, y is evaluated at $(p+1)^M$ coordinates. A combination of values adopted by the random variables is denoted by $\xi_{1j_1}, \ldots, \xi_{Mj_M}$, so that ξ_{kj_k} is a zero of the Hermite polynomial. The tensor product approximation to the integral using quadrature formula is given by

$$\mathrm{E}\left[\Gamma_i \mathbf{u}\right] \approx \sum_{j=1}^{(p+1)^M} \left(\Gamma_i(\xi_{1j_1}, \ldots, \xi_{Mj_M}) \mathbf{u}(\xi_{1j_1}, \ldots, \xi_{Mj_M}) \prod_{k=1}^{M} A_{j_k} \right) \tag{1.66}$$

with each weight of the quadrature formula given by Engels (1980)

$$A_{j_k} = \int_{-\infty}^{+\infty} \frac{e^{-\xi_k^2/2}}{2\pi} \left(\prod_{l \neq k, l=1}^{p+1} \frac{\xi_k - \xi_{kj_l}}{\xi_{kj_k} - \xi_{kj_l}} \right)^2 d\xi_k \tag{1.67}$$

The weights can be calculated exactly, noting that the moments of a normal random variable are such that $\mathrm{E}\left[\xi^n\right] = \int_{-\infty}^{+\infty} \xi^n e^{-\xi^2/2}/2\pi d\xi = 1.3 \ldots (n-1)$ for n even and 0 for n odd.

As the number of random variables M becomes large, the method becomes computationally expensive, and sparse grid methods have been used to alleviate this burden, replacing the full tensor product approach (Xiu and Hesthaven, 2005). The sparse grid method or Smolyak algorithm allows to refine the multivariate approximation both by increasing the order of the polynomials and by dividing the random domain in different regions, allowing adaptivity (Bungartz and Dornseifer, 1997, Griebel, 1998, Gerstner and Griebel, 1998, Ma and Zabaras, 2009). Some adaptive variations of the method have been developed to deal with discontinuities in the function. An alternative to sparse grids can consist in iteratively identify which terms of the expansion are relevant to the response (Blatman and Sudret, 2010). Other efficient collocation methods have been proposed by Foo and Karniadakis (2010), Ma and Zabaras (2009). Padé-Legendre approximants have also been used (Chantrasmi et al., 2009). Coefficients of Polynomial Chaos expansion have also been calculated using mean-squared minimization (Berveiller et al., 2006).

When considering the random eigenvalue problem, the non-sampling methods used so far have been the dimensional decomposition method (Rahman, 2006, 2007, 2009), asymptotic integral method (Adhikari and Friswell, 2007, Adhikari, 2007), collocation methods (Bressolette et al., 2010), the use of interpolations, response surface methods

and meta-models (Pichler et al., 2009, Alibrandi et al., 2010, Goller et al., 2011).

1.7.3 Non-sampling methods

Non-sampling methods are similar to response surface methods in that they aim to obtain a simple approximation to a complicated function depending on a set of random variables. These methods can be divided into expansion-based methods (perturbation method (Kleiber and Hien, 1992), Neumann expansion method (Yamazaki et al., 1988)), spectral approach (Ghanem and Spanos, 1991, Nouy, 2009, Maître and Knio, 2010) and stochastic reduced basis method (SRBM) (Nair and Keane, 2002). These methods can be applied to different problems, but for each problem specific variations of the methods have been developed.

Elliptic problem

When considering the case of a linear partial differential equation (PDE) like Equation (1.29), the first step to solve it can consist in the propagation of the random field into the system matrix using the Finite Element method (Zienkiewicz and Taylor, 1991). If the KL expansion is used, the resulting equation can be given by Equation (1.30). The solution of this set of stochastic linear algebraic equations is a key step in the stochastic finite element analysis. As a result, several methods have been proposed.

One of the first methods used to study uncertainty propagation is the perturbation method (Kleiber and Hien, 1992, Liu et al., 1986), where terms are expanded with their Taylor series expansion around the mean value of the random parameters α_i, $i = 1, \ldots, M$, and these random parameters can be correlated. In Equation (1.30), these random parameters are denoted by ξ_i and are uncorrelated. For the elliptic problem, the Taylor series expansions of stiffness $\mathbf{K}$, response $\mathbf{u}$ and load vector $\mathbf{f}$ are truncated after the second order terms and introduced into $\mathbf{Ku} = \mathbf{f}$. Then, coefficients multiplying polynomials of the same order can be identified

$$\mathbf{u}_0 = \mathbf{K}_0^{-1}\mathbf{f}_0 \tag{1.68}$$

$$\mathbf{u}_i^I = \mathbf{K}_0^{-1}(\mathbf{f}_i^I - \mathbf{K}_i^I\mathbf{u}_0) \tag{1.69}$$

$$\mathbf{u}_{ij}^{II} = \mathbf{K}_0^{-1}(\mathbf{f}_{ij}^{II} - \mathbf{K}_i^I\mathbf{u}_j^I - \mathbf{K}_j^I\mathbf{u}_i^I - \mathbf{K}_{ij}^{II}\mathbf{u}_0) \tag{1.70}$$

where terms with subindexes 0, i and ij are respectively the matrix or vector evaluated

at $\boldsymbol{\alpha} = 0$, its first derivative (e.g. $\mathbf{K}_i^I = \left.\frac{\partial \mathbf{K}}{\partial \alpha_i}\right|_{\alpha=0}$) and its second derivative (e.g. $\mathbf{K}_{ij}^{II} = \left.\frac{\partial^2 \mathbf{K}}{\partial \alpha_i \partial \alpha_j}\right|_{\alpha=0}$) The statistics of $\mathbf{u}$ are derived from the second order Taylor expansion of $\mathbf{u}$ and the statistics of $\boldsymbol{\alpha}$

$$\mathrm{E}[\mathbf{u}] \approx \mathbf{u}_0 + \frac{1}{2}\sum_{i=1}^{M}\sum_{j=1}^{M}\mathbf{u}_{ij}^{II}\mathrm{Cov}[\alpha_i, \alpha_j] \tag{1.71}$$

$$\mathrm{Cov}[\mathbf{u}, \mathbf{u}] \approx \sum_{i=1}^{M}\sum_{j=1}^{M}\mathbf{u}_i^I.(\mathbf{u}_j^I)^T\mathrm{Cov}[\alpha_i, \alpha_j] \tag{1.72}$$

This method has been used following a discretization of the random field with the spatial average method (Baecher and Ingra, 1981, Vanmarcke and Grigoriu, 1983), the shape functions method (Liu et al., 1986a,b) and the weighted integral method (Deodatis, 1991, Deodatis and Shinozuka, 1991).

Another of the earlier approaches to uncertainty propagation is the Neumann expansion method, introduced into the field of structural mechanics by Shinozuka and Nomoto (1980). The theory states that if the inverse of an operator $[\mathbf{L} + \Pi]$ exists, it can be expanded in a convergent series in terms of the iterated kernels

$$\mathbf{u}(\alpha(\varpi), \mathbf{x}) = [\mathbf{L} + \Pi]^{-1}\mathbf{f} = \sum_{j=0}^{\infty}(-1)^j[\mathbf{L}^{-1}(\mathbf{x})\Pi(\alpha(\mathbf{x}, \varpi), \mathbf{x})]^j[\mathbf{L}^{-1}(\mathbf{x})\mathbf{f}(\mathbf{x}, \varpi)] \tag{1.73}$$

verifying that $\| \mathbf{L}^{-1}\Pi \| < 1$. When a random parameter $(\alpha(\mathbf{x}, \varpi))$ of the system is substituted by its KL expansion, Equation (1.30) is obtained and its solution is equivalent to the solution of the system

$$\left[\mathbf{I} + \sum_{i=1}^{M}\xi_n\mathbf{Q}^{(i)}\right]\mathbf{u} = \mathbf{g} \qquad \mathbf{Q}^{(n)} = \bar{\mathbf{K}}^{-1}\mathbf{K}^{(i)} \quad \mathbf{g} = \bar{\mathbf{K}}^{-1}\mathbf{f} \tag{1.74}$$

Where Neumann expansion is applied

$$\mathbf{u} = \sum_{j=0}^{\infty}(-1)^j\left[\sum_{i=1}^{M}\xi_i\mathbf{Q}^{(i)}\right]^j\mathbf{g} \tag{1.75}$$

This expression is computationally more tractable than the original Neumann expansion. The expansion is generally truncated after the second order terms.

Spectral stochastic finite element methods (SSFEM), another group of techniques to solve stochastic partial differential equations, have received significant attention (see

Nouy (2009), Xiu (2009), Panayirci and Schueller (2011) for reviews). These methods include the Wiener–Askey chaos expansions (Xiu and Karniadakis, 2002, Wan and Karniadakis, 2006), the most widely used one being polynomial chaos (PC) expansion (Ghanem and Spanos, 1991, Ghosh et al., 2005) and Galerkin methods (Babuska et al., 2004). According to the polynomial chaos expansion, a second-order random variable $u_j(\varpi)$ depending on the Gaussian random variable ξ can be represented by the mean-square convergent expansion

$$u_j(\varpi) = \sum_{i=1}^{\infty} u_i^{(j)} h_i \tag{1.76}$$

where u_i are deterministic constants, and h_i is the i^{th} order Hermite polynomial obtained from

$$h_i(\xi) = (-1)^i \exp(\xi^2/2) \frac{\partial^i \exp(-\xi^2/2)}{\partial^i \xi} \tag{1.77}$$

so that, for example (Ghanem and Spanos, 1991)

$$h_0(\xi) = 1 \tag{1.78}$$

$$h_1(\xi) = \xi \tag{1.79}$$

$$h_2(\xi) = \xi^2 - 1 \tag{1.80}$$

$$h_3(\xi) = \xi^3 - 3\xi \tag{1.81}$$

$$h_4(\xi) = \xi^4 - 6\xi^2 + 3 \tag{1.82}$$

The polynomials $h_i(\xi)$ are orthogonal with respect to the Gaussian probability density function, i.e.

$$\int_{-\infty}^{\infty} \frac{h_p(\xi) h_q(\xi) \exp(\xi^2/2)}{\sqrt{2\pi}} d\xi = p! \delta_{pq} \tag{1.83}$$

If $u_j(\varpi)$ depends on a set of i.i.d Gaussian random variables $\xi_1, \ldots, \xi_M$, a similar expansion can be obtained. If u_j is the j-th element of a vector $\mathbf{u} \in \mathbb{R}^n$, the expansion of $\mathbf{u}$ truncated after P terms is given by

$$\mathbf{u}(\varpi) = \sum_{i=1}^{P} \Gamma_i(\boldsymbol{\xi}_1(\varpi), \ldots, \boldsymbol{\xi}_M(\varpi)) \mathbf{u}_i \tag{1.84}$$

where $\mathbf{u}_i \in \mathbb{R}^n$ are vectors whose elements are constants and Γ_i is the i-th Polynomial Chaos. The Polynomial Chaoses are obtained as the product of several univariate Her-

mite polynomials, each of them depending on a random variable from $\{\xi_1, \ldots, \xi_M\}$. When these basis functions Γ_i are obtained from the terms of the tensor product of several univariate Hermite polynomials up to a fixed total-order specification r, this approach is referred to as "total-order expansion", and the number of polynomials obtained is

$$P = (M + r)!/M!r! \tag{1.85}$$

The same idea can be extended to non-Gaussian random variables, provided more generalised functional basis are used (Xiu and Karniadakis, 2002, Wan and Karniadakis, 2006). Consider that the response and forcing term are expanded with a PC expansion like the one in Equation (1.84), and the stiffness matrix is expanded with a KL expansion. Then, the vectors of coefficients $\mathbf{u}_i$ of the PC expansions can be retrieved by ensuring that the residual of $\mathbf{Ku} = \mathbf{f}$ is orthogonal to each basis Γ_i and this approach is sometimes referred as Galerkin method. Mathematically, this condition is achieved by multiplying this equation by each basis function Γ_p, $p = 1, \ldots, P$ and taking the mean of the resulting equation

$$\sum_{j=1}^{P} \left(\mathbf{K}_0 \mathrm{E}\left[\Gamma_j \Gamma_p\right] + \sum_{i=1}^{M} \mathbf{K}_i \mathrm{E}\left[\xi_i \Gamma_j \Gamma_p\right] \right) \mathbf{u}_j = \mathbf{f}_p \mathrm{E}\left[\Gamma_p^2\right] \qquad \mathbf{f}_p = \frac{\mathrm{E}\left[\mathbf{f}\Gamma_p\right]}{\mathrm{E}\left[\Gamma_p^2\right]} \tag{1.86}$$

A linear deterministic equation of size $n \times P$ is obtained

$$\begin{bmatrix} \mathbf{A}_{1,1} & \cdots & \mathbf{A}_{1,P} \\ \mathbf{A}_{2,1} & \cdots & \mathbf{A}_{2,P} \\ \vdots & \vdots & \vdots \\ \mathbf{A}_{P,1} & \cdots & \mathbf{A}_{P,P} \end{bmatrix} \begin{Bmatrix} \mathbf{u}_1 \\ \mathbf{u}_2 \\ \vdots \\ \mathbf{u}_P \end{Bmatrix} = \begin{Bmatrix} \mathbf{f}_1 \\ \mathbf{f}_2 \\ \vdots \\ \mathbf{f}_P \end{Bmatrix} \tag{1.87}$$

where matrix $\mathbf{A}_{j,k} = \mathbf{K}_0 \mathrm{E}\left[\Gamma_j \Gamma_k\right] + \sum_{i=1}^{M} \mathbf{K}_i \mathrm{E}\left[\xi_i \Gamma_i \Gamma_j\right]$. This system can be rewritten as

$$\mathbf{A}^{(\mathrm{PC})} \mathbf{u_c} = \mathbf{f_c} \qquad \mathbf{A}^{(\mathrm{PC})} = \left(\mathbf{c}_0 \otimes \mathbf{K}_0 + \sum_{i=1}^{M} \mathbf{c}_{1i} \otimes \mathbf{K}_i \right) \tag{1.88}$$

where $\otimes$ is the kronecker product and the vector of coefficients and the forcing vector are given respectively by $\mathbf{u_c} = \left[\mathbf{u}_1^T, \mathbf{u}_2^T, \ldots, \mathbf{u}_P^T\right]^T$ and $\mathbf{f_c} = \left[\mathrm{E}\left[\mathbf{f}\Gamma_1\right]^T, \ldots, \mathrm{E}\left[\mathbf{f}\Gamma_P\right]^T\right]^T$. The diagonal matrix $\mathbf{c}_0$ has diagonal entries $\mathbf{c}_{0_{ii}} = \mathrm{E}\left[\Gamma_i^2\right]$ and matrices $\mathbf{c}_{1i}$ have elements given by $\mathbf{c}_{1i_{jk}} = \mathrm{E}\left[\xi_i \Gamma_j \Gamma_k\right]$. These matrices depend on the polynomial chaoses used as basis functions, and are therefore problem-independent. It is noted that for a

deterministic forcing term, $\mathbf{f}_i = 0$ for $i > 1$ and $\mathbf{f}_1 = \mathbf{f}$, so that $\mathbf{f_c} = \left[\mathbf{f}^T, 0, \ldots, 0\right]^T$.

After obtaining the PC expansion of the response, the first and second moments of the response can be retrieved

$$\mathrm{E}\left[\mathbf{u}\right] = \sum_{i=1}^{P} \mathbf{u}_i \mathrm{E}\left[\Gamma_i\right] = \mathbf{u}_1 \quad \mathrm{E}\left[\mathbf{u}\mathbf{u}^T\right] = \sum_{i,j=1}^{P} \mathbf{u}_i \mathbf{u}_j^T \mathrm{E}\left[\Gamma_i \Gamma_j\right] = \sum_{i=1}^{P} \mathbf{u}_i \mathbf{u}_i^T \mathrm{E}\left[\Gamma_i^2\right] \quad (1.89)$$

and the standard deviation of the i-th element of vector $\mathbf{u}$, i.e. u_i, is given by

$$\sigma_{u_i}^2 = \sqrt{\mathrm{E}\left[u_i^2\right] - \mathrm{E}\left[u_i\right]^2} \quad (1.90)$$

where $\mathrm{E}\left[u_i^2\right]$ is the i-th diagonal element of the matrix $\mathrm{E}\left[\mathbf{u}\mathbf{u}^T\right]$.

The first applications of SFEM used Hermite polynomial chaos as basis functions Γ_i (Ghanem and Spanos, 1991), but other basis have been used, as the Wiener-Askey polynomial chaos (Xiu and Karniadakis, 2002), wavelets (Le Maître et al., 2004), multi-element method (Wan and Karniadakis, 2005, 2006, Mohan et al., 2008), finite elements (Babuska et al., 2004), optimal Galerkin approach (Grigoriu, 2006), or an orthogonal polynomial basis generated by a nonstandard pdf (Gautschi, 1982, Wan and Karniadakis, 2006).

Although SSFEM has been applied to various practical problems, one of the possible drawbacks is the high computational cost associated with large systems. Since P increases very rapidly with the order of the chaos r and the number of random variables M, the final number of unknown constants Pn becomes very large. As a results several methods have been developed (see for example Nair and Keane (2002), Sarkar et al. (2009), Blatman and Sudret (2010), Matthies and Keese (2005), Adhikari (2011), Doostan et al. (2007), Maute et al. (2009), Chentouf et al. (2011)) to reduce the computational cost and to reduce the size of the system. The reduction of the system can be done before or after applying the spectral decomposition such as the polynomial chaos (PC) expansion. For example, Sachdeva et al. (2006b) used the first basis vectors spanning the preconditioned stochastic Krylov subspace, and each vector was expressed as a linear combination of a deterministic vector and a PC. An orthogonalization of the deterministic response and its first-order derivative with respect to parameters and design parameters, calculated at calibration points was used by Maute et al. (2009). Recently Nouy (2007, 2008) discussed the possibility of an optimal spectral decomposition. A

different condensation method focused on dynamic systems was developed by Guedri et al. (2006), where the vectors used were a reduced basis, e.g. a Ritz basis of fixed or free normal modes, and a static displacement where the uncertainty in the dynamic stiffness matrix is taken into account. In Acharjee and Zabaras (2006) the generalised PC was applied to the diffusion equation, and the vectors used were the ones from the proper orthogonal decomposition obtained from the underlying deterministic diffusion problem.

Another method is the stochastic reduced basis method, introduced by Nair (2001), and further developed in Nair and Keane (2002), Bah et al. (2003), Sachdeva et al. (2006a,b) and Sachdeva (2006). This methods represents the response $\mathbf{u}(\varpi)$ as an element of the stochastic Krylov subspace $\mathcal{K}_m(\mathbf{K}(\varpi), \mathbf{f})$

$$\mathcal{K}_m(\mathbf{K}(\varpi), \mathbf{f}) = \text{span}\{\mathbf{f}, \mathbf{K}(\varpi)\mathbf{f}, \mathbf{K}(\varpi)^2\mathbf{f}, \ldots, \mathbf{K}(\varpi)^{m-1}\mathbf{f}\}. \tag{1.91}$$

Accuracy in the computation of the approximation needs a high degree of overlap of the PDFs of the eigenvalues of the matrix $\mathbf{K}(\varpi)$ if few basis vectors are going to be used. This is obtained with the use of a preconditioner, the matrix $\mathrm{E}\left[\mathbf{K}(\varpi)\right]^{-1} = \mathbf{K}_0^{-1}$. The response vector can then be expanded as

$$\mathbf{u}(\varpi) = \alpha_1\psi_1(\varpi) + \alpha_2\psi_2(\varpi) + \cdots + \xi_m\psi_m(\varpi) = \Psi(\varpi)\boldsymbol{\alpha} \tag{1.92}$$

with $\psi_1(\varpi) = \mathbf{K}_0^{-1}\mathbf{f}$, $\psi_2(\varpi) = \mathbf{K}_0^{-1}\mathbf{K}(\varpi)\psi_1(\varpi)$ and $\psi_3(\varpi) = \mathbf{K}_0^{-1}\mathbf{K}(\varpi)\psi_2(\varpi)$ the first three vectors of the Krylov subspace $\mathcal{K}_m(\mathbf{K}_0^{-1}\mathbf{K}(\varpi), \mathbf{f})$ and $\boldsymbol{\alpha}$ a vector of undetermined coefficients. When matrix $\mathbf{K}(\varpi)$ is expanded using a KL expansion $\mathbf{K}(\varpi) = \mathbf{K}_0 + \sum_{i=1}^{M}\xi_i\mathbf{K}_i$, these first three vectors are given by

$$\psi_1(\varpi) = \mathbf{u}_0, \qquad \psi_2(\varpi) = \sum_{i=1}^{M}\mathbf{d}_i\xi_i \quad \text{and} \quad \psi_3(\varpi) = \sum_{i=1}^{M}\sum_{j=1}^{M}\mathbf{e}_{ij}\xi_i\xi_j \tag{1.93}$$

With $\mathbf{u}_0 = \mathbf{K}_0^{-1}\mathbf{f}$, $\mathbf{d}_i = \mathbf{K}_0^{-1}\mathbf{K}_i\mathbf{u}_0$ and $\mathbf{e}_{ij} = \mathbf{K}_0^{-1}\mathbf{K}_i\mathbf{d}_j$. The residual error vector is

$$\epsilon(\varpi) = \left(\mathbf{K}_0 + \sum_{i=1}^{M}\mathbf{K}_i\xi_i\right)\Psi(\varpi)\boldsymbol{\alpha} - \mathbf{f} \tag{1.94}$$

where matrices $\mathbf{K}_i$ are symmetric. The coefficients $\boldsymbol{\alpha}$ can be calculated using Galerkin

condition

$$\left[\left(\mathbf{K}_0 + \sum_{i=1}^{M} \mathbf{K}_i \xi_i\right) \boldsymbol{\Psi}(\varpi)\boldsymbol{\alpha} - \mathbf{f}\right] \perp \boldsymbol{\Psi}(\varpi) \tag{1.95}$$

$$\mathrm{E}\left[\boldsymbol{\Psi}(\varpi)^T \mathbf{K}_0 \boldsymbol{\Psi}(\varpi) + \sum_{i=1}^{M} \xi_i \boldsymbol{\Psi}(\varpi)^T \mathbf{K}_i \boldsymbol{\Psi}(\varpi)\right] \boldsymbol{\alpha} = \mathrm{E}\left[\boldsymbol{\Psi}(\varpi)^T \mathbf{f}\right] \tag{1.96}$$

This last equation is a deterministic linear algebraic system of equations whose solution is $\boldsymbol{\alpha} \in \mathbb{R}^{3\times 1}$ if only three basis vectors are used in $\boldsymbol{\Psi}(\varpi)$. After solving this system, the response is retrieved from Equation (1.92), from where moments of the distribution can be calculated.

Other solution approaches are based on linear algebra results, and try to obtain a transformation that is close to diagonal to the system matrix $\mathbf{K}$ (Falsone and Impollonia, 2002, Li et al., 2006).

Dynamic and random eigenvalue problem

A structure is modelled as a dynamic system when vibrations are expected to occur during its lifespan. Examples of structures subjected to vibrations are mechanical equipments, vehicles or aircraft structures. Dynamic analysis of complex deterministic systems can be efficiently performed using the finite element method (FEM) (see, for example, Géradin and Rixen (1997)). The discretized equation of motion can be expressed by the system of n coupled second-order ordinary differential equations

$$\mathbf{M}\ddot{\mathbf{U}}(t) + \mathbf{C}\dot{\mathbf{U}}(t) + \mathbf{K}\mathbf{U}(t) = \mathbf{F}(t). \tag{1.97}$$

This matrix equation is characterised by the system mass, stiffness and damping matrices, the response vector and the forcing vector in time domain, denoted respectively by $\mathbf{M}$, $\mathbf{K}$, $\mathbf{C}$, $\mathbf{U}(t)$ and $\mathbf{F}(t)$. Taking the Laplace transform of Equation (1.97), and setting $s = \mathrm{i}\omega$ with $\mathrm{i} = \sqrt{-1}$, the equation of motion of a linear dynamical system in the frequency domain can be expressed as

$$\left(-\omega^2\mathbf{M} + \mathrm{i}\omega\mathbf{C} + \mathbf{K}\right)\mathbf{u} = \mathbf{f}. \tag{1.98}$$

Here ω is the frequency, $\mathbf{u}$ is the Laplace transform of $\mathbf{U}(t)$, and $\mathbf{f} = \int_{-\infty}^{\infty} \mathbf{F}(t)e^{-\mathrm{i}\omega t}dt + \mathrm{i}\omega\mathbf{M}\mathbf{U}_0 + \mathbf{M}\mathbf{U}_0' + \mathbf{C}\mathbf{U}_0$ is the forcing vector in the frequency domain. The initial con-

ditions are the displacement and velocity at time zero, given respectively by $\mathbf{U}_0$ and $\mathbf{U}'_0$.

The deterministic generalised eigenvalue problem is given by the equation

$$\mathbf{K}\boldsymbol{\phi}^{(j)} = \lambda^{(j)}\mathbf{M}\boldsymbol{\phi}^{(j)} \tag{1.99}$$

The eigenvalues $\lambda^{(j)}$ are the same as the ones from the eigenvalue problem

$$\mathbf{A}\mathbf{v}^{(j)} = \lambda^{(j)}\mathbf{v}^{(j)} \quad \text{with} \quad \mathbf{A} = \mathbf{M}^{-1/2}\mathbf{K}\mathbf{M}^{-1/2}, \quad \mathbf{v}^{(j)} = \mathbf{M}^{1/2}\boldsymbol{\phi}^{(j)} \tag{1.100}$$

where $\mathbf{A} \in \mathbb{R}^{n\times n}$ is the system matrix, $\mathbf{v}^{(j)}$ is its j-th eigenvector, $\lambda^{(j)}$ is the corresponding eigenvalue and n is the degrees of freedom of the system. The system matrix $\mathbf{A}$ is symmetric, as both $\mathbf{M}$ and $\mathbf{K}$ are symmetric. Proportional damping is assumed, that is, $\boldsymbol{\Phi}^T\mathbf{C}\boldsymbol{\Phi} = 2\boldsymbol{\zeta}\boldsymbol{\Omega}$ where $\boldsymbol{\zeta}$ and $\boldsymbol{\Omega}$ are diagonal matrices whose diagonal elements are respectively the damping ratios ζ_j and the square roots of the eigenvalues $\omega_j = \sqrt{\lambda^{(j)}}$. The response vector can be expressed in terms of the eigenvalues and eigenvectors of the generalised eigenvalue problem

$$\mathbf{u} = \left(-\omega^2\mathbf{M} + \mathrm{i}\omega\mathbf{C} + \mathbf{K}\right)^{-1}\mathbf{f} \tag{1.101}$$

$$= \sum_{j=1}^{N}\left[\frac{\boldsymbol{\phi}^{(j)}\left(\boldsymbol{\phi}^{(j)}\right)^T}{-\omega^2 + 2\mathrm{i}\omega\zeta_j\omega_j + \omega_j^2}\right]\mathbf{f} \tag{1.102}$$

where the term $\left(-\omega^2\mathbf{M} + \mathrm{i}\omega\mathbf{C} + \mathbf{K}\right)^{-1}$ is called the transfer function matrix. A necessary condition for the method to be accurate is that the dimension of each element is smaller than the wavelength (at most $1/7$-th of the wavelength). This condition is not a problem for low frequencies, but it can be at higher frequencies. As frequency increases, the number of elements needed to obtain an accurate approximation to the response grows too large, and the response sensitivity to small variations of the structure parameters rises. The consideration of uncertainty in the calculation of system response therefore becomes important for dynamic problems. There can be two broad routes to calculate the response statistics: through direct inversion of the dynamic stiffness matrix as in Equation (1.101), or via modal approach as in Equation (1.102). Here, only the modal approach is considered.

When uncertainties arise in the system parameters, boundary conditions and geome-

try, the system matrices can be considered as random matrices. Therefore, if the forcing term is considered deterministic, uncertainties in the system can be characterised by the joint probability density function (pdf) of the random matrices **M**, **C** and **K**, or, equivalently, by the joint pdf of their eigenvalues $\lambda^{(j)} = \omega_j^2$, eigenvectors $\phi^{(j)}$ and damping factors ζ_j. The system matrices remain symmetric and positive definite even if uncertainty is considered. It is generally considered that, at low frequencies, the study of propagation of uncertainty to the response **u** is best addressed by parametric approach. Then, stochastic finite element methods (SFEM) (Ghanem and Spanos, 1991) can be applied to obtain the statistics of the response or of the eigenvalues and eigenvectors.

Randomness in the matrix **A** from Equation (1.100) can be introduced by a random field (modelling, for example, Young's modulus) that can be discretized using the Karhunen-Loève (KL) expansion (Ghanem and Spanos, 1991) and truncated after M terms. Then, the system matrix **A** can be approximated by the following KL expansion

$$\mathbf{A} = \mathbf{A}_0 + \sum_{i=1}^{M} \xi_i \mathbf{A}_i \tag{1.103}$$

Here $\mathbf{A}_0$ is the mean of the system matrix and $\mathbf{A}_i$ are the matrices obtained from using the eigenfunctions of the KL expansion in the Finite Element formulation of **A**. It is observed that in a more general case than the KL expansion, the random system matrix **A** in Equation (1.103) can be approximated using a set of independent identically distributed random variables $\xi_1, \ldots, \xi_M$ such that

$$\mathbf{A} = \sum_{i=1}^{P} \Gamma_i \mathbf{A}_i \tag{1.104}$$

where Γ_q are a set of P polynomials of increasing order in $\xi_1, \ldots, \xi_M$ orthogonal with respect to the pdf of the random variables $\xi_1, \ldots, \xi_M$. Particular cases of these polynomials have already been discussed previously, such as the polynomials from the Wiener-Askey scheme (Xiu and Karniadakis, 2002), or more general ones (Wan and Karniadakis, 2006).

To solve the random eigenvalue problem, methods that can be applied to small uncertainties are based on the perturbation method (Kleiber and Hien, 1992). First applications date from the late sixties, and a series of modified methods have been developed (Boyce, 1968, Collins and Thomson, 1969, Fox and Kapoor, 1968, Hasselman

and Hart, 1972, Hart, 1973, Song et al., 1995, den Nieuwenhof and Coyette, 2003, Cha and Solberg, 2008). These methods work well when the uncertainties are small and the parameter distribution is Gaussian. A comparison of several of these methods is given by Chen et al. (2000). When considering the inverse problem, sensitivities of eigenvalues to control gains have been obtained using measured receptances (Mottershead et al., 2009). Other perturbation-based methods use Rayleigh quotient (Chen et al., 1994), iteration (Liu and Oliveira, 2003) or combination of deterministic and perturbed eigenvectors (Eldred, 1992, Nair and Keane, 2003) to deal with larger uncertainties or to allow reanalysis of structures. Other methods available are based on crossing theory (Grigoriu, 1992) and kronecker product (Lee and Singh, 1994). Williams (2010) used an auxiliary function where the derivative of the eigenvector equals the eigenvalue multiplied by the eigenvector. Asymptotic methods combined with the maximum entropy principle have been used to obtain estimated pdf of the eigenvalues (Adhikari and Friswell, 2007, Adhikari, 2006). The Ritz method (Hála, 1994, Mehlhose et al., 1999) has also been considered. The modal stability procedure has also been used (Arnoult et al., 2011).

Several authors have applied polynomial chaos (PC) (Ghanem and Spanos, 1991) based methods to the random algebraic eigenvalue problem. A PC expansion of eigenvalues and eigenvectors was obtained by Ghosh et al. (2005) using MCS for the calculation of the coefficients of the expansion. Verhoosel et al. (2006) developed an iterative procedure based on the inverse power method and Rayleigh quotient to obtain PC expansions of the eigensolutions. Ghanem and Ghosh (2007) substituted eigenvalues and eigenvectors by their PC expansion in the eigenvalue problem. Coefficients were obtained from the nonlinear problem with the help of a norm equation for the eigenvectors. A modification of the previous method using enrichment functions was derived by Ghosh and Ghanem (2008).

When considering the dynamic problem, results from the random eigenvalue problem can be used. Approaches obtaining response moments based on results from the random eigenvalue problem are mostly based on performing MCS on some approximation of $\phi^{(j)}$ and ω_j^2 and introducing it in Equation (1.102). A different approach followed by Udwadia (1987a,b) proposed exact analytical expressions of response statistics for a single-degree-of-freedom system. They were obtained from the pdf of eigenvalues, related to pdf of random parameters. Also, Laplace's integral has been used

to calculate moments and reliability of response, where the maximum and hessian of the logarithm of the integrated function are obtained through different numerical methods (Papadimitriou et al., 1997). Dynamic condensation methods have also been used (Guedri et al., 2006).

At high frequencies, several pdfs for eigenvalues are assumed (e.g. Poisson's distribution (Lyon and Dejong, 1995), gaussian orthogonal ensemble (Weaver, 1989)) to calculate space and frequency averaged energies in the context of statistical energy analysis (SEA). Non-parametric uncertainty can also be considered for high frequencies by modelling the system matrices as different types of random matrices, like gamma distribution matrices (Soize, 2000) or Wishart matrices (Adhikari, 2010). For medium-frequency vibration analysis in linear dynamical systems, both parametric and non-parametric uncertainties need to be considered, as in the papers by Mace and Shorter (2001), Sarkar and Ghanem (2002, 2003), Ghanem and Sarkar (2003), Cotoni et al. (2007).

1.8 Open problems

It has been observed that two kinds of uncertainty affect physical systems. When propagating these uncertainties, methods used to propagate parametric uncertainty can be computationally expensive while methods to propagate nonparametric uncertainty are based on MCS. Furthermore, both types of uncertainty are seldom considered in the same system. Therefore, the following open problems have been identified:

- The need of efficient parametric uncertainty propagation in the elliptic problem, using reduced methods based on the spectral decomposition of the system matrices.
- The need of reduction techniques for an efficient parametric uncertainty propagation in the random eigenvalue problem.
- The propagation of uncertainty from eigenvalues and eigenvectors to the dynamic response of the system.
- The propagation of both parametric and nonparametric uncertainties in a system, for the case where (a) both uncertainties affect different subdomains of the system, and (b) both uncertainties affect the whole domain of the physical system.

- The propagation of nonparametric uncertainty when considering a dynamic problem.

1.9 Layout of the dissertation

The dissertation is divided into 7 chapters, where the open problems identified in the previous section are investigated.

In Chapter 2 the stochastic finite element analysis of elliptic type partial differential equations is considered. A reduced method of the spectral stochastic finite element method using polynomial chaos is proposed. The method is based on the spectral decomposition of the deterministic system matrix. The reduction is achieved by retaining only the dominant eigenvalues and eigenvectors. The response of the reduced system is expanded as a series of Hermite polynomials, and a Galerkin error minimization approach is applied to obtain the deterministic coefficients of the expansion. The moments and probability density function of the solution are obtained by a process similar to the classical spectral stochastic finite element method. The method is illustrated using three numerical examples, namely, bending of a stochastic beam, flow through porous media with stochastic permeability and transverse bending of a plate with stochastic properties. The results obtained from the proposed method are compared with classical polynomial chaos and direct Monte Carlo simulation results.

Chapter 3 develops several methods to propagate parametric uncertainty into the random eigenvalue problem. The methods use polynomial chaos, system reduction and are based on available methods for the deterministic eigenvalue problem, namely, the power method, the inverse power method and the eigenvalue equation. The proposed methods are referred to as the reduced spectral power method (RSPM), the reduced spectral inverse power method (RSIPM), the reduced spectral constrained coefficients method (RSCCM) and the spectral constrained coefficients method (SCCM) and lead to a PC expansion of eigenvectors. A spectral representation of eigenvalues is obtained through a projection of the Rayleigh quotient on the polynomial chaos basis functions. The new methods are applied to the problem of an Euler Bernoulli beam and a thin plate with stochastic properties.

In Chapter 4 the moments of the response of a dynamic system are obtained, assuming the distribution of eigenvalues and moments of the eigenvectors are known.

Low frequency vibration of structural dynamic systems with uncertainty is considered. A method to calculate the statistics of transfer functions from the probability density functions of the eigenvalues is proposed. Firstly, single-degree-of-freedom-systems are considered and closed-form analytical expressions for the mean and variance is obtained using a hybrid Laplace's method. Several probability density functions, including gamma, normal and lognormal distributions are considered for the derivation of the analytical expressions. The method is extended to calculate the mean and variance of the frequency response function of multiple-degrees-of-freedom dynamic systems. Proportional damping is assumed and the eigenvalues are considered to be independent. Results are derived for several probability density functions and damping factors. The accuracy of the approach for both single and multiple-degrees-of-freedom systems is examined using the direct Monte Carlo simulation.

Chapter 5 focuses on the response of a dynamic system using non-parametric uncertainty to model system matrices. Firstly, the different models of nonparametric uncertainty affecting dynamic systems are reviewed. In the first model, both mass and stiffness matrices are Wishart matrices and in the second model, the eigenvalues matrix is modelled as a Wishart matrix. Methods to calculate the parameters of this Wishart distribution are discussed. A White Wishart matrix model is proposed to approximate the dynamic response. The first and second moments of the response for this system are approximated with a proposed numerical integration and compared to results from MCS.

Chapter 6 proposes two hybrid methods where both parametric and nonparametric uncertainties affect the elliptic problem. The first one deals with both uncertainties over the entire domain. Firstly, only parametric uncertainty is considered to obtain a Karhunen-Loève (KL) expansion of the system matrix. Then, this KL expansion is used as the mean matrix of the nonparametric model. The second hybrid method, considers different types of uncertainties over non-overlapping subdomains, where the matrix representing a subdomain is considered to be Wishart and the sub matrix considering the second subdomain is represented by a KL expansion. Both uncertainties are considered independent, and the two first moments of the response are calculated using Polynomial Chaos expansion and random matrix theory results.

Finally, Chapter 7 summarizes the work completed, outlines the contributions emerging from the studies carried out in the dissertation and suggests different research direc-

tions.

Chapter 2

A reduced polynomial chaos expansion method for linear problems

2.1 Introduction

It was noted in the previous Chapter that uncertainty needs to be quantified in physical problems to assess the degree of confidence of the prediction of a particular equation. Methods to solve the problem of parametric uncertainty propagation in the elliptic problem, given by Equation (1.30)

$$\left[\mathbf{K}_0 + \sum_{i=1}^{M} \xi_i(\varpi)\mathbf{K}_i\right]\mathbf{u}(\varpi) = \mathbf{f} \tag{2.1}$$

are an active field of research where solution procedures to obtain $\mathbf{u}(\varpi)$ for $\varpi \in \Omega$ are either only valid for small uncertainty or expensive. Consider the calculation of the solution of the full PC system from Equation (1.88)

$$\mathbf{A}^{(\mathrm{PC})}\mathbf{u_c} = \mathbf{f_c} \qquad \mathbf{A}^{(\mathrm{PC})} = \left(\mathbf{c}_0 \otimes \mathbf{K}_0 + \sum_{i=1}^{M} \mathbf{c}_{1i} \otimes \mathbf{K}_i\right) \tag{2.2}$$

We assume that the eigenvalues of $\mathbf{K}_0$ in Equation (2.1) are distinct. It is noted that the size of the system from Equation (2.2) is Pn, where P is the number of basis functions and n is the size of the deterministic system. The exponential growth of P with the maximum order of the polynomial expansion (r) and the number of random variables M was given in Equation (1.85), and can be observed in Table 2.1.

The solution of Equation (2.2) is computationally expensive, as the time required to solve the problem is proportional to $(Pn)^3$ (Golub and Loan, 2010). A reduction of

M	2	3	5	10	20	50	100
$r=2$	6	10	21	66	231	1326	5151
$r=3$	10	20	56	286	1771	23426	176851

Table 2.1: Number of basis functions P depending on the number of random variables M and the order of PC.

the size of the system to be solved is desirable to reduce the computation time. This reduction in the size cannot be accomplished by reducing the number of basis functions P used, as the accuracy in the uncertainty propagation assessment could be compromised. The proposed method aims at reducing the effective size (n) of the stochastic system. This is achieved through a space reduction of the original system, so as to relieve the computational burden of solving the full PC system from Equation (2.2). The reduction technique is developed in section 2.2. The post processing of the results to obtain the response moments, and an error estimation of the proposed method with respect to SSFEM are discussed in section 2.3. Based on the theoretical results, a simple computational approach is proposed in section 2.4. The new approach is applied to the stochastic mechanics of a beam in section 2.5, to a flow through a stochastic porus medium in section 2.6 and to the stochastic mechanics of a plate in section 2.7. From the theoretical developments and numerical results, some conclusions are drawn in section 2.8.

2.2 Development of the reduced polynomial chaos approach

Following the spectral stochastic finite element method, an approximation to the solution of Equation (2.1) can be expressed as a linear combination of functions of random variables and deterministic vectors. The aim is to use a small number of terms to reduce the computation time without loosing accuracy. Here a new approach is proposed to reduce the dimension of the Equation (2.2) arising in the PC method.

To illustrate the motivation behind the proposed reduced method, first consider the deterministic system

$$\mathbf{K}_0\mathbf{u}_0 = \mathbf{f} \tag{2.3}$$

Because $\mathbf{K}_0$ is a symmetric and positive definite matrix, its eigenvalues are positive and

its eigenvectors form a complete orthonormal basis. The eigenvalue problem can be expressed as

$$\mathbf{K}_0\boldsymbol{\phi}_j = \lambda_0^{(j)}\boldsymbol{\phi}_j; \quad j = 1, 2, \ldots n \tag{2.4}$$

For notational convenience, define the matrices of deterministic eigenvalues and eigenvectors

$$\boldsymbol{\Lambda}_0 = \text{diag}\left[\lambda_0^{(1)}, \lambda_0^{(2)}, \ldots, \lambda_0^{(n)}\right] \in \mathbb{R}^{n\times n} \quad \text{and} \quad \boldsymbol{\Phi}_0 = [\boldsymbol{\phi}_1, \boldsymbol{\phi}_2, \ldots, \boldsymbol{\phi}_n] \in \mathbb{R}^{n\times n} \tag{2.5}$$

Eigenvalues are ordered in the ascending order so that $\lambda_0^{(1)} < \lambda_0^{(2)} < \ldots < \lambda_0^{(n)}$. Since $\boldsymbol{\Phi}$ is an orthogonal matrix we have $\boldsymbol{\Phi}_0^{-1} = \boldsymbol{\Phi}_0^T$ so that the following identities can be easily established

$$\boldsymbol{\Phi}_0^T\mathbf{K}_0\boldsymbol{\Phi}_0 = \boldsymbol{\Lambda}_0; \quad \mathbf{K}_0 = \boldsymbol{\Phi}_0^{-T}\boldsymbol{\Lambda}_0\boldsymbol{\Phi}_0^{-1} \quad \text{and} \quad \mathbf{K}_0^{-1} = \boldsymbol{\Phi}_0\boldsymbol{\Lambda}_0^{-1}\boldsymbol{\Phi}_0^T \tag{2.6}$$

These equations are also valid for the case where multiplicities in eigenvalues arise. Using these, the solution of Equation (2.3) can be expressed as

$$\mathbf{u}_0 = \mathbf{K}_0^{-1}\mathbf{f} = \boldsymbol{\Phi}_0\boldsymbol{\Lambda}_0^{-1}(\boldsymbol{\Phi}_0^T\mathbf{f}) = \sum_{j=1}^{n}\frac{\boldsymbol{\phi}_j^T\mathbf{f}}{\lambda_0^{(j)}}\boldsymbol{\phi}_j \tag{2.7}$$

The series from Equation (2.7) can be truncated based on the magnitude of the eigenvalues as the higher terms becomes smaller. Therefore one could only retain the dominant terms in the series. If the system has an eigenvalue with multiplicities and small magnitude, all the series terms corresponding to this eigenvalue are retained in the truncated series. A similar model reduction technique has been widely used within the proper orthogonal decomposition method (Lenaerts et al., 2002) where the eigensolution of a symmetric positive definite matrix are used. One can select a small value ϵ such that $\lambda_0^{(1)}/\lambda_0^{(p)} < \epsilon$ for some value of p. Therefore, truncating the series in Equation (2.7) one can have

$$\mathbf{u}_0 \approx \sum_{j=1}^{p}\frac{\boldsymbol{\phi}_j^T\mathbf{f}}{\lambda_0^{(j)}}\boldsymbol{\phi}_j \tag{2.8}$$

We use this simple idea to develop the reduced PC (RPC) approach.

We form the reduced matrix of dominant eigenvalues and eigenvectors as

$$\mathbf{\Lambda}_{0_p} = \text{diag}\left[\lambda_0^{(1)}, \lambda_0^{(2)}, \ldots, \lambda_0^{(p)}\right] \in \mathbb{R}^{p\times p} \quad \text{and} \quad \mathbf{\Phi}_p = \left[\boldsymbol{\phi}_1, \boldsymbol{\phi}_2, \ldots, \boldsymbol{\phi}_p\right] \in \mathbb{R}^{n\times p} \tag{2.9}$$

Let us introduce the transformation

$$\mathbf{u}(\omega) = \mathbf{\Phi}_p \mathbf{y}(\omega) \tag{2.10}$$

where $\mathbf{y} \in \mathbb{R}^p$ is the new unknown random vector. Substituting in the original equation (2.1) and premultiplying by $\mathbf{\Phi}_p^T$ we have

$$\left[\mathbf{\Lambda}_{0_p} + \sum_{i=1}^{M} \xi_i(\varpi)\widetilde{\mathbf{K}}_i\right] \mathbf{y}(\varpi) = \widetilde{\mathbf{f}} \tag{2.11}$$

where the transformed reduced matrices and vector are given by

$$\widetilde{\mathbf{K}}_i = \mathbf{\Phi}_p^T \mathbf{K}_i \mathbf{\Phi}_p \in \mathbb{R}^{p\times p}; i = 1, 2, \ldots, M \quad \text{and} \quad \widetilde{\mathbf{f}} = \mathbf{\Phi}_p^T \mathbf{f} \tag{2.12}$$

The main idea is to expand the reduced random vector $\mathbf{y}(\varpi)$ with a polynomial chaos expansion. For a selected order of PC, the polynomial chaoses $\Gamma_i(\boldsymbol{\xi}(\varpi))$ will be identical to the ones used in the full system. Therefore, we have

$$\mathbf{y}(\varpi) = \sum_{k=1}^{P} \Gamma_k(\boldsymbol{\xi}(\varpi))\mathbf{y}_k \tag{2.13}$$

The unknown vectors $\mathbf{y}_i$ can be obtained by substituting $\mathbf{y}(\varpi)$ from the above expressions into the reduced Equation (2.11) and minimizing the error using the standard Galerkin approach (Ghanem and Spanos, 1991), as was done to derive Equation (2.2). It can be shown that we need to solve a $pP \times pP$ system of linear equation to obtain all $\mathbf{y}_i \in \mathbb{R}^p$:

$$\widetilde{\mathbf{A}}^{(\text{PC})}\mathbf{y_c} = \widetilde{\mathbf{f}}_\mathbf{c} \quad \text{where} \quad \widetilde{\mathbf{A}}^{(\text{PC})} = \left(\mathbf{c}_0 \otimes \mathbf{\Lambda}_{0_p} + \sum_{i=1}^{M} \mathbf{c}_{1i} \otimes \widetilde{\mathbf{K}}_i\right) \tag{2.14}$$

with $\mathbf{y_c} = \left[\mathbf{y}_1^T, \mathbf{y}_2^T, \ldots, \mathbf{y}_P^T\right]^T$ and $\widetilde{\mathbf{f}}_\mathbf{c} = \left[\text{E}\left[\widetilde{\mathbf{f}}\Gamma_1\right]^T, \ldots, \text{E}\left[\widetilde{\mathbf{f}}\Gamma_P\right]^T\right]^T$

The computational complexity of the matrix inversion problem scales in cubically with the dimension of the matrix in the worse case (Wilkinson, 1988). For many prac-

tical problems $p \ll n$, therefore $\mathcal{O}(P^3p^3) \ll \mathcal{O}(P^3n^3)$. As a result the RPC can offer significant computational reduction. This will be discussed further in the numerical examples later in the Chapter.

2.3 Moments of the response and error analysis

The mean and the covariance of the reduced system can be obtained using the standard PC approach. From properties of PC $\mathrm{E}[\mathbf{y}(\varpi)] = \mathbf{y}_1$. The covariance matrix of $\mathbf{y}(\varpi)$ can be obtained using the orthogonality property of the polynomial chaoses as

$$\boldsymbol{\Sigma}_y = \left(\sum_{k=1}^{P} \mathrm{E}\left[\Gamma_k^2(\boldsymbol{\xi}(\varpi))\right] \mathbf{y}_k \mathbf{y}_k^T \right) - \mathbf{y}_1 \mathbf{y}_1^T \tag{2.15}$$

The expressions of $\mathrm{E}[\Gamma_k^2(\boldsymbol{\xi}(\varpi))]$ can be obtained, for example, from Ghanem and Spanos (1991). Note that these calculations take less time than calculating the moments of the response using full PC, as the dimension of $\mathbf{y}_k$ is in general much smaller than the dimension of $\mathbf{u}_k$ from Equation (2.2). The mean and the covariance matrix of the response of the original system can be obtained as

$$\mathrm{E}[\mathbf{u}] = \boldsymbol{\Phi}_p \mathbf{y}_1 \quad \text{and} \quad \boldsymbol{\Sigma}_u = \boldsymbol{\Phi}_p \boldsymbol{\Sigma}_y \boldsymbol{\Phi}_p^T \tag{2.16}$$

The probability density function of $\mathbf{y}$ can be obtained by simulating Equation (2.13). The samples of $\mathbf{u}$ can be generated easily using the samples of $\mathbf{y}$. To estimate the error between full PC and the proposed RPC, two different error analysis are given to try to evaluate the effect of neglecting the projection of the response on the eigenvectors not included in the new basis, that is, the eigenvectors corresponding to the largest eigenvalues. The first error estimate is based on the Schur complement, and gives an exact relationship between the approximation method and the full PC response. The second one is an heuristic approximation of the error, to understand the physical meaning of the neglected terms. The error is expected to be small when the projection of the response in the sub-space spanned by the deterministic eigenvectors corresponding to the higher eigenvalues is relatively smaller.

2.3.1 Rigorous error analysis

If the PC method is applied to the original system where all the KL expansion matrices have been premultiplied by Φ_0^T, the change of variables $\mathbf{u} = \Phi_0 \mathbf{y}^*$ is introduced and $\mathbf{f}^* = \Phi_0^T \mathbf{f}$, the following system of equations is obtained

$$\left(\mathbf{c}_0 \otimes \Lambda_0 + \sum_{i=1}^{M} \mathbf{c}_{1i} \otimes \Phi_0^T \mathbf{K}_i \Phi_0 \right) \begin{Bmatrix} \mathbf{y}_1^* \\ \vdots \\ \mathbf{y}_P^* \end{Bmatrix} = \begin{Bmatrix} \mathbf{f}_1^* \\ \vdots \\ \mathbf{f}_P^* \end{Bmatrix} \tag{2.17}$$

The terms of the SSFEM deterministic matrix can be rearranged such that the matrix can be partitioned as follows

$$\begin{Bmatrix} \mathbf{B}_{11} & \mathbf{B}_{12} \\ \mathbf{B}_{21} & \mathbf{B}_{22} \end{Bmatrix} \begin{Bmatrix} \mathbf{y}^{p*} \\ \mathbf{y}^{2*} \end{Bmatrix} = \begin{Bmatrix} \mathbf{f}^{p*} \\ \mathbf{f}^{2*} \end{Bmatrix}, \text{ with } \begin{Bmatrix} \mathbf{y}^{p*} \\ \mathbf{y}^{2*} \end{Bmatrix} = \begin{Bmatrix} \mathbf{y}_{1_p}^* \\ \vdots \\ \mathbf{y}_{P_p}^* \\ \mathbf{y}_{1_2}^* \\ \vdots \\ \mathbf{y}_{P_2}^* \end{Bmatrix}, \begin{Bmatrix} \mathbf{f}^{p*} \\ \mathbf{f}^{2*} \end{Bmatrix} = \begin{Bmatrix} \widetilde{\mathbf{f}}_1 \\ \vdots \\ \widetilde{\mathbf{f}}_P \\ \mathbf{f}_{1_2}^* \\ \vdots \\ \mathbf{f}_{P_2}^* \end{Bmatrix} \tag{2.18}$$

The submatrices are given by

$$\mathbf{B}_{11} = \mathbf{c}_0 \otimes \Lambda_{0_p} + \sum_{1}^{M} \mathbf{c}_{1i} \otimes \widetilde{\mathbf{A}}_i, \qquad \mathbf{B}_{12} = \sum_{1}^{M} \mathbf{c}_{1i} \otimes \Phi_p^T \mathbf{A}_i \Phi_2 \tag{2.19}$$

$$\mathbf{B}_{21} = \sum_{1}^{M} \mathbf{c}_{1i} \otimes \Phi_2^T \mathbf{A}_i \Phi_p \quad \text{and} \qquad \mathbf{B}_{22} = \mathbf{c}_0 \otimes \Lambda_{0_2} + \sum_{1}^{M} \mathbf{c}_{1i} \otimes \Phi_2^T \mathbf{A}_i \Phi_2 \tag{2.20}$$

The vectors appearing in Equation (2.17) have been partitioned and rearranged in new vectors such that

$$\mathbf{y}_j^* = \begin{Bmatrix} \mathbf{y}_{j_p}^* \\ \mathbf{y}_{j_2}^* \end{Bmatrix}, \text{ with } \mathbf{y}^{p*} = \begin{Bmatrix} \mathbf{y}_{1_p}^* \\ \vdots \\ \mathbf{y}_{P_p}^* \end{Bmatrix} \quad \text{and} \quad \mathbf{y}^{2*} = \begin{Bmatrix} \mathbf{y}_{1_2}^* \\ \vdots \\ \mathbf{y}_{P_2}^* \end{Bmatrix} \tag{2.21}$$

The forcing term from Equation (2.17) is related to the one in Equation (2.18) through

$$\mathbf{f}_k^* = \begin{Bmatrix} \widetilde{\mathbf{f}}_k \\ \mathbf{f}_{k_2}^* \end{Bmatrix}, \text{ with } \mathbf{f}^{p*} = \begin{Bmatrix} \widetilde{\mathbf{f}}_1 \\ \vdots \\ \widetilde{\mathbf{f}}_P \end{Bmatrix} \quad \text{and} \quad \mathbf{f}^{2*} = \begin{Bmatrix} \mathbf{f}_{1_2}^* \\ \vdots \\ \mathbf{f}_{P_2}^* \end{Bmatrix} \tag{2.22}$$

Making use of the Schur complement (see, for example, Zhang (2005)), the partitioned solution can be written as

$$\begin{Bmatrix} \mathbf{y}^{p*} \\ \mathbf{y}^{2*} \end{Bmatrix} = \begin{Bmatrix} \left(\mathbf{B}_{11} - \mathbf{B}_{12}\mathbf{B}_{22}^{-1}\mathbf{B}_{21}\right)^{-1}\left(\mathbf{f}^{p*} - \mathbf{B}_{12}\mathbf{B}_{22}^{-1}\mathbf{f}^{2*}\right) \\ \left(\mathbf{B}_{22} - \mathbf{B}_{21}\mathbf{B}_{11}^{-1}\mathbf{B}_{12}\right)^{-1}\left(\mathbf{f}^{2*} - \mathbf{B}_{21}\mathbf{B}_{11}^{-1}\mathbf{f}^{p*}\right) \end{Bmatrix} \tag{2.23}$$

The response calculated by the proposed reduced method is given by $\mathbf{y}_p = \mathbf{B}_{11}^{-1}\mathbf{f}^{p*}$. As it can be observed, in the proposed method it is assumed that the non-diagonal block matrices are zero and that higher eigenvalues or the uncertainty linked to them have no effect on the response. The error associated to the proposed method with respect to the full system is given by

$$\varepsilon = (\mathbf{u}^* - \mathbf{u})^T(\mathbf{u}^* - \mathbf{u}),\ (\mathbf{u}^* - \mathbf{u}) = \left(\boldsymbol{\Phi}_0 \begin{bmatrix} \mathbf{y}_p^* \\ \mathbf{y}_2^* \end{bmatrix} - \boldsymbol{\Phi}_0 \begin{bmatrix} \mathbf{y}_p \\ 0 \end{bmatrix}\right) = \boldsymbol{\Phi}_0 \left(\begin{bmatrix} \mathbf{y}^{p*} - \mathbf{y}_p \\ \mathbf{y}^{2*} \end{bmatrix}\right) \tag{2.24}$$

An approximation can be introduced to the expression of $\mathbf{y}^{p*}$ using the Neumann expansion

$$\mathbf{y}^{p*} \approx \left(\sum_{s=0}^{\infty}(\mathbf{B}_{11}^{-1}\mathbf{B}_{12}\mathbf{B}_{22}^{-1}\mathbf{B}_{21})^s\right)\mathbf{B}_{11}^{-1}\left(\mathbf{f}^{p*} - \mathbf{B}_{12}\mathbf{B}_{22}^{-1}\mathbf{f}^{2*}\right) \tag{2.25}$$

and we obtain

$$\mathbf{y}^{p*} - \mathbf{y}^{p} \approx \left(\sum_{s=1}^{\infty}(\mathbf{B}_{11}^{-1}\mathbf{B}_{12}\mathbf{B}_{22}^{-1}\mathbf{B}_{21})^s\right)\mathbf{B}_{11}^{-1}\left(\mathbf{f}^{p*} - \mathbf{B}_{12}\mathbf{B}_{22}^{-1}\mathbf{f}^{2*}\right) + \mathbf{B}_{11}^{-1}\left(-\mathbf{B}_{12}\mathbf{B}_{22}^{-1}\mathbf{f}^{2*}\right) \tag{2.26}$$

These expressions, although correct, do not allow to grasp the physical meaning of neglecting the projection of the response on eigenvectors corresponding to the higher eigenvalues. The following approximate error analysis is given to fulfill this requirement.

2.3.2 Approximate error analysis

We consider an approximate error analysis to get an idea of the nature of the approximations involved in the proposed RPC. Let us partition the matrices of the eigenvalues and eigenvectors as

$$\boldsymbol{\Lambda}_0 = \left[\boldsymbol{\Lambda}_{0_p}|\boldsymbol{\Lambda}_{0_2}\right] \quad \text{and} \quad \boldsymbol{\Phi}_0 = \left[\boldsymbol{\Phi}_p|\boldsymbol{\Phi}_2\right] \tag{2.27}$$

Here the matrices $\Lambda_{0_2} \in \mathbb{R}^{(n-p)\times(n-p)}$ and $\Phi_2 \in \mathbb{R}^{n\times(n-p)}$ denote the blocks that have not been used in the reduced method. Following the analogy of Equation (2.7) and using the partitions in Equation (2.27), the response can be expressed as

$$\begin{aligned}\mathbf{u}_0 = \left[\Phi_0\Lambda_0^{-1}\Phi_0^T\right]\mathbf{f} &= \left(\left[\Phi_p|\Phi_2\right]\left[\Lambda_{0_p}|\Lambda_{0_2}\right]^{-1}\left[\Phi_p|\Phi_2\right]^T\right)\mathbf{f} \\ &= \left[\Phi_p\Lambda_{0_p}^{-1}\Phi_p^T\right]\mathbf{f} + \left[\Phi_2\Lambda_{0_2}^{-1}\Phi_2^T\right]\mathbf{f} = \Phi_p\mathbf{y}_0 + \left[\Phi_2\Lambda_{0_2}^{-1}\Phi_2^T\right]\mathbf{f} \quad (2.28)\end{aligned}$$

where $\mathbf{y}_0 = \Lambda_{0_p}^{-1}\Phi_p^T\mathbf{f}$. Clearly in the proposed reduced approach when only $\mathbf{y}_0$ is considered, the second term is neglected.

Suppose, the error associated with the PC expansion of $\mathbf{u}(\omega)$ and $\mathbf{y}(\omega)$ are respectively ε_u and ε_y. The *additional* error arising in the evaluation of $\mathbf{y}(\omega)$ comes from neglecting the term similar to the second term of Equation (2.28), given by

$$\varepsilon_2 = \left[\Phi_2\Lambda_{0_2}^{-1}\Phi_2^T\right]\mathbf{f} \quad (2.29)$$

Taking the l_2 norm we have

$$\|\varepsilon_2\| = \text{Trace}\left(\left(\left[\Phi_2\Lambda_{0_2}^{-1}\Phi_2^T\right]\mathbf{f}\right)\left(\left[\Phi_2\Lambda_{0_2}^{-1}\Phi_2^T\right]\mathbf{f}\right)^T\right) = \text{Trace}\left(\Phi_2^T\Phi_2\Lambda_{0_2}^{-1}\Phi_2^T\mathbf{f}\mathbf{f}^T\Phi_2\Lambda_{0_2}^{-1}\right) \quad (2.30)$$

Recalling that $\Phi_2^T\Phi_2$ is an identity matrix we have

$$\|\varepsilon_2\| = \text{Trace}\left(\Lambda_{0_2}^{-2}\Phi_2^T\mathbf{f}\mathbf{f}^T\Phi_2\right) \quad (2.31)$$

Since Φ_p is an orthonormal matrix, the error norm is invariant with respect to rotation in Φ_p. That is the error norm for $\mathbf{y}(\omega)$ and $\Phi_p\mathbf{y}(\omega)$ are identical. Therefore, from Equation (2.28) the error norm of $\mathbf{y}(\omega)$ and $\mathbf{u}(\omega)$ can be approximately related as

$$\|\varepsilon_u\| \gtrapprox \|\varepsilon_y\| + \text{Trace}\left(\Lambda_{0_2}^{-2}\Phi_2\mathbf{f}\mathbf{f}^T\Phi_2^T\right) \quad (2.32)$$

This expression shows that the difference between the error norm of $\mathbf{u}(\omega)$ and $\mathbf{y}(\omega)$ will be small when the eigenvalues in the diagonal matrix Λ_{0_2} are large.

2.4 Summary of the computational method

The reduced polynomial chaos (RPC) for the solution of the stochastic elliptic PDE (1.29) can be implemented as follows:

1. Obtain the system matrices $\mathbf{A}_i, i = 0, 1, 2, \ldots, M$ and the forcing vector $\mathbf{f}$ by discretizing the governing stochastic partial differential equation using the well established stochastic finite element methodologies.

2. Solve the eigenvalue problem associated with the mean matrix $\mathbf{A}_0$

$$\mathbf{A}_0 \mathbf{\Phi}_0 = \mathbf{\Lambda}_0 \mathbf{\Phi}_0 \tag{2.33}$$

3. Select a small value of ϵ, say $\epsilon = 10^{-3}$. Obtain the number of the reduced orthonormal basis p such that $\lambda_{0_1}/\lambda_{0_p} < \epsilon$.

4. Create the reduced matrix of eigenvalues and eigenvectors

$$\mathbf{\Lambda}_{0_p} = \text{diag}\left[\lambda_0^{(1)}, \lambda_0^{(2)}, \ldots, \lambda_0^{(p)}\right] \in \mathbb{R}^{p \times p} \quad \text{and} \quad \mathbf{\Phi}_p = \left[\boldsymbol{\phi}_1, \boldsymbol{\phi}_2, \ldots, \boldsymbol{\phi}_p\right] \in \mathbb{R}^{n \times p} \tag{2.34}$$

5. Calculate the transformed matrices and vector

$$\widetilde{\mathbf{A}}_i = \mathbf{\Phi}_p^T \mathbf{A}_i \mathbf{\Phi}_p \in \mathbb{R}^{p \times p}; i = 1, 2, \ldots, M \quad \text{and} \quad \widetilde{\mathbf{f}} = \mathbf{\Phi}_p^T \mathbf{f} \tag{2.35}$$

6. Obtain the reduced polynomial chaos expansion

$$\mathbf{y}(\omega) = \sum_{k=1}^{P} \Gamma_k(\boldsymbol{\xi}(\varpi)) \mathbf{y}_k \tag{2.36}$$

where the vectors $\mathbf{y}_k \in \mathbb{R}^p$ can be obtained by solving the $pP \times pP$ system from Equation (2.14)

$$\widetilde{\mathbf{A}}^{(\text{PC})} \mathbf{y_c} = \widetilde{\mathbf{f}}_\mathbf{c}, \qquad \widetilde{\mathbf{A}}^{(\text{PC})} = \left(\mathbf{c}_0 \otimes \mathbf{\Lambda}_{0_p} + \sum_{i=1}^{M} \mathbf{c}_{1i} \otimes \widetilde{\mathbf{K}}_i \right) \tag{2.37}$$

7. Calculate the mean and the covariance matrix of the response of the original system

$$\mathrm{E}\left[\mathbf{u}\right] = \mathbf{\Phi}_p \mathbf{y}_1 \quad \text{and} \quad \mathbf{\Sigma}_u = \mathbf{\Phi}_p \mathbf{\Sigma}_y \mathbf{\Phi}_p^T \tag{2.38}$$

where

$$\Sigma_y = \left(\sum_{k=1}^{P-1} \mathrm{E}\left[\Gamma_k^2(\boldsymbol{\xi}(\varpi))\right] \mathbf{y}_k \mathbf{y}_k^T \right) - \mathbf{y}_1 \mathbf{y}_1^T \tag{2.39}$$

The proposed RPC method is now applied to three numerical examples to verify the efficiency of the method.

2.5 Transversal deformation of a beam with stochastic properties

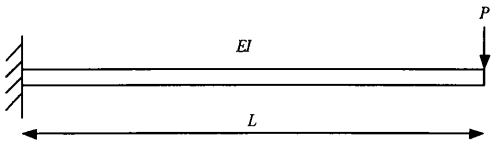

Figure 2.1: A clamped-free beam with random bending rigidity subjected to a point load at the end.

The method described is applied to the problem of a bending beam with stochastic flexural rigidity. We consider the numerical example of the clamped-free beam shown in Figure 2.1, subjected to a deterministic transversal load at its tip of $P = 0.4658$ N. The system is such that the finite element model of the beam has 50 elements and the associated deterministic matrix is of size $n = 100$. The length of the Euler Bernoulli beam is 1 m, and for the deterministic case, Young's modulus is E=69 GPa and the cross-section is a rectangle of length 40 mm and height 4 mm, its moment of inertia is I=9 10^{-11} m^4. The flexural rigidity of the beam, EI, is considered as a random field with mean $\mathrm{E}[EI] = 6.21$ Nm^2, standard deviation $0.2\mathrm{E}[EI]$ and exponential covariance function with correlation length the length of the beam. Two terms are kept in the KL expansion of the system stiffness matrix. The order of the polynomial chaos used is four, that is, from Equation (1.85) with $M = 2$ and $r = 4$, 15 polynomials are used in the expansion of the response.

The solution is obtained with different methods to compare their performance. MCS method is applied using 10000 samples. The PC method, called here full PC, is applied, and the linear system to be solved is of size 1500. Two reduced systems are considered, using the first 3 and 6 eigenvectors. The ratio between the first and the $n - th$ eigenvalue is shown in Figure 2.2, together with the first four eigenvectors for the transverse

displacement. The red circles show the ratio of eigenvalues for the two reduced systems used in the numerical examples, i.e. for the number of eigenvalues 3 and 6. The two

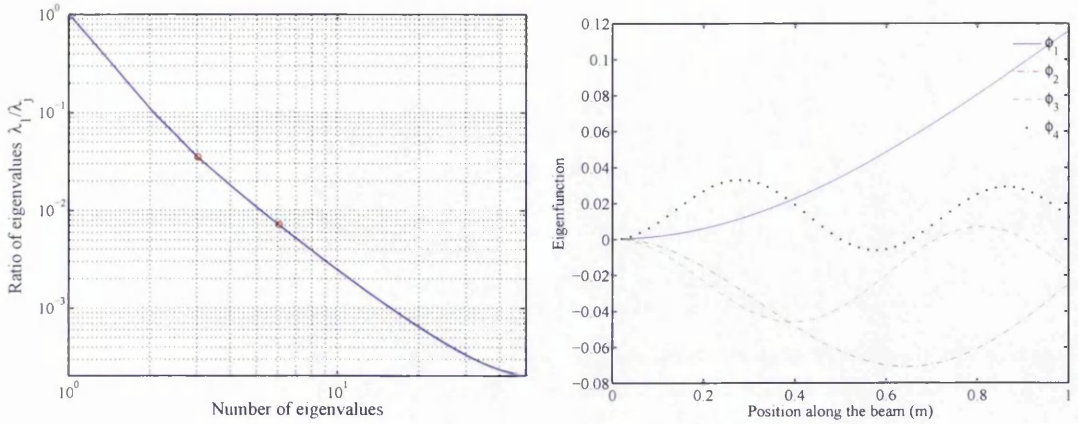

(a) Ratio of eigenvalues (b) Eigenvectors

Figure 2.2: Ratio of eigenvalues and eigenvectors for the beam problem.

reduced PC system matrices are of sizes 45 and 90 for transformed stiffness matrices of sizes 3 and 6 respectively. Values of the mean and standard deviation of the vertical displacement for all the nodes are shown in Figure 2.3. The displacement is normalised by $PL^3/3EI$ such that the deterministic vertical displacement at the tip is unity. The

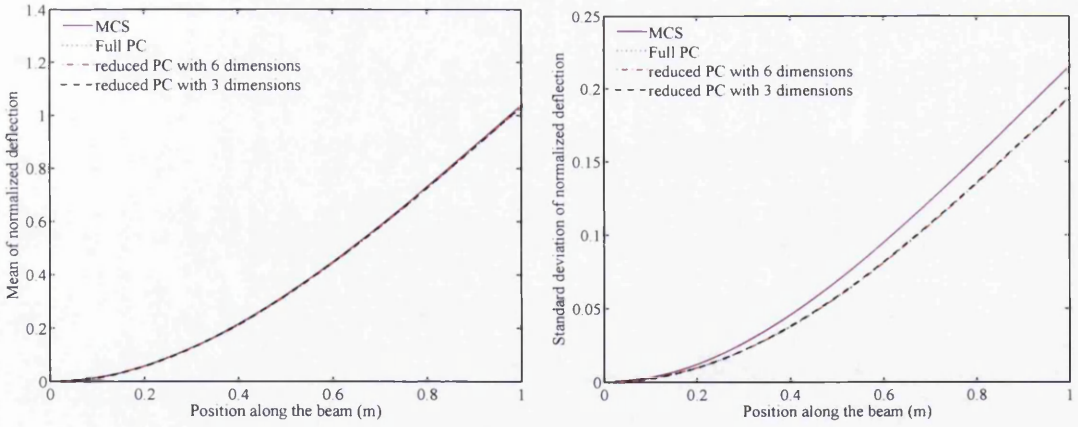

(a) Mean (b) Standard deviation

Figure 2.3: Mean and standard deviation of the normalised vertical displacement for the beam problem.

error associated with using RPC instead of the full PC is shown in Figure 2.4 for all the nodes of the beam. The percentage error is represented as

$$\varepsilon_{\%} = 100 \times \frac{|\text{fPC} - \text{RPC}|}{\text{fPC}} \tag{2.40}$$

	MCS	Full PC ($n = 100$)	RPC ($n = 3$)	RPC ($n = 6$)
CPU time (s)	1.1508	0.0238	0.0063	0.0071

Table 2.2: CPU times (sec) of calculations for the full PC and in the proposed reduced method. The cost of calculating complete eigensolutions is 0.0073s.

where fPC are the results from full PC and RPC are the ones from the reduced PC. It is

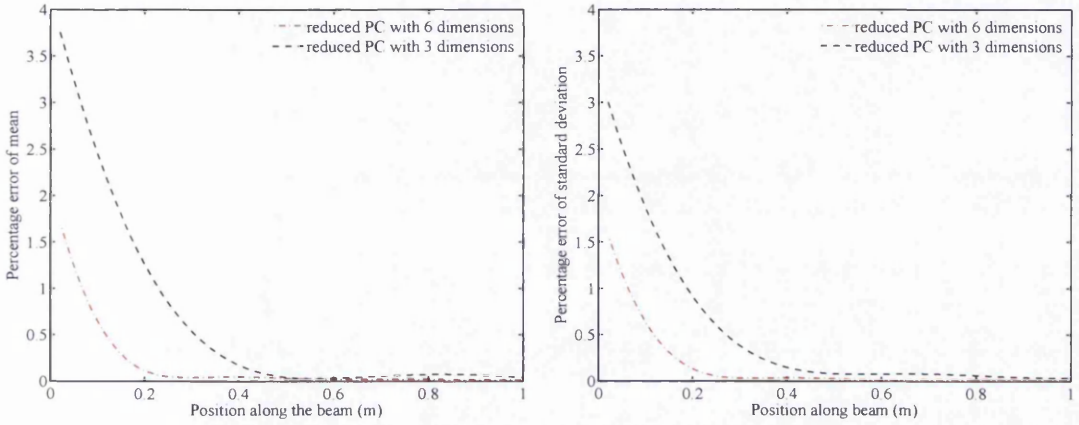

(a) Percentage error of mean (b) Percentage error of standard deviation

Figure 2.4: Percentage error of mean and standard deviation of the normalised vertical displacement, between full PC and reduced PC.

observed that the error is higher at position $x = 0$ m, as values near the origin are close to zero. It is also observed that errors at the tip of the beam are negligible. We can also observe that there is a significant different between the results obtained from PC (both full and reduced) and MCS. The accuracy of the methods can be improved by using polynomials of higher order, that is, using more basis functions Γ_i in the PC expansio of the response. As expected, the proposed method generates a response with an accuracy similar to the one of full PC, but at lower cost. This cost is described in Table 2.2, where the CPU time of calculations for the four methods is given. Figure 2.5(a) shows the pdf of the tip vertical displacement for MCS, full PC and the two reduced systems. The error of the vertical displacement associated with using a reduced system instead of the full PC for the tip node is shown in Figure 2.5(b), for different orders of the reduced system. One can observe that with 6 dimensions, the proposed RPC produce results comparable with the full PC with dimension 100. Figure 2.5(b) shows that the error compared to the full PC reduces significantly when the size of the reduced system is beyond 10.

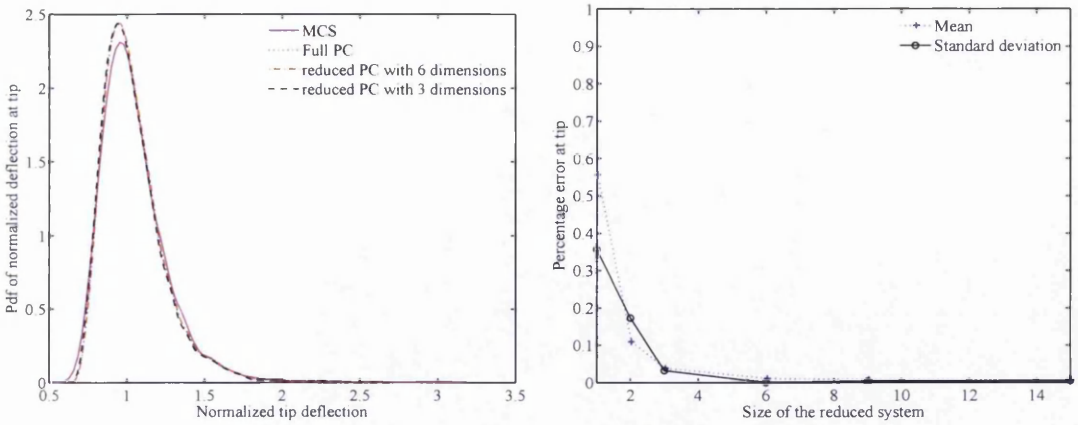

(a) Pdf of the normalised tip displacement.

(b) Percentage errors of mean and standard deviation.

Figure 2.5: The pdf of the normalised vertical displacement at tip of the beam obtained with MCS, full PC and reduced PC with $n = 3$ and n =6. Percentage errors of mean and standard deviation of the normalised tip displacement using different reduced systems.

2.6 Flow through a stochastic medium

A numerical example of a steady flow through a porous media is now considered to investigate the efficiency of the proposed method for a problem of higher spatial dimension than the previous example. The equation of motion is the Poissons equation, i.e. $-\nabla.(k\nabla h) = q$, where k is the hydraulic conductivity, h is the head and q is the specific flux or sources. The two-dimensional domain is a rectangle of length L=1 m and width W=0.6 m, as shown in Figure 2.6. The domain is divided with a uniform mesh of 70 by 42 square elements. The domain is subjected to a constant flux $q_b = 1$ cm/s along the portion of its boundary verifying $y = -0.3$ m and $x \in [0.3\,,\,0.5]$ m (last 14 elements on x direction), in coordinates of the KL expansion. The head is fixed at value $h_b = 0$ cm along the portion of the boundary such that $x = -0.5$ m, $y \in [0.1714\,,\,0.3]$ m (last 9 elements in y direction). The deterministic system has $n = 584$ degrees of freedom. A Gaussian hydraulic conductivity (k) with 2D exponential covariance function is considered. The 2D covariance function is obtained by multiplying a 1D exponential covariance function depending on x, with correlation length $b_x = L/5$; and a 1D exponential covariance function depending on y, with correlation length $b_y = W/5$. Two terms of the KL expansion in each direction are kept, that is, the KL expansion has four matrices for the whole system. The mean value of the hydraulic conductivity is given by $\mathrm{E}[k] = 1$ cm/s, and its standard deviation is $\sigma = 0.2\mathrm{E}[k]$. The stiffness element

matrices are given by

$$\mathbf{K}_{I_{ij}} = \int_0^a \int_0^b \sqrt{\nu} \frac{dN_i}{dx} \frac{dN_j}{dx} \varphi(x,y)\, dxdy \tag{2.41}$$

$$\mathbf{K}_{II_{ij}} = \int_0^a \int_0^b \sqrt{\nu} \frac{dN_i}{dy} \frac{dN_j}{dy} \varphi(x,y)\, dxdy \tag{2.42}$$

The stiffness matrix of the system is given by $\mathbf{K} = \mathbf{K}_I + \mathbf{K}_{II}$, where $\mathbf{K}_I$ and $\mathbf{K}_{II}$

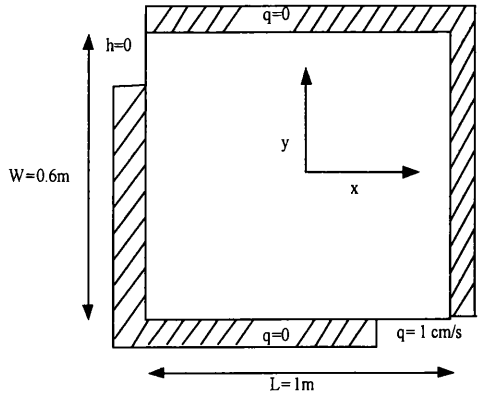

Figure 2.6: Flow through a rectangular porous media. The porous media is assumed to have stochastically inhomogeneous hydraulic conductivity.

are obtained by assembling the respective matrices given above. The details of the finite element model can be found, for example, in Reddy (1984). The random variable appearing in the stiffness matrix is k. The eigenfunction and eigenvectors equal $\varphi(x,y) = 1$, $\nu = \mathrm{E}[k]$ for the deterministic stiffness matrix, and it depends on the covariance function when considering a KL expansion matrix. The polynomial chaos used is of fourth order, so that the total number of polynomials is 70.

As formerly, the response is obtained using different methods to compare their performance. MCS is applied using 10000 samples. The size of the linear system to be solved when applying full PC is 40880. The two reduced systems considered use the first 5 and 20 eigenvectors respectively. The ratio between the first and the $n-th$ eigenvalue is shown in Figure 2.7, where the two red circles show this ratio for the two examples considered, and the contours of the first four eigenvectors are shown in Figure 2.8.

The two reduced PC system matrices are of sizes 350 and 1400 for the transformed stiffness matrices of sizes 5 and 20 respectively. Contour plots of the mean and standard deviation obtained with the different methods are shown respectively in Figure 2.9 and Figure 2.10. The contours of the percentage errors in mean and standard deviation

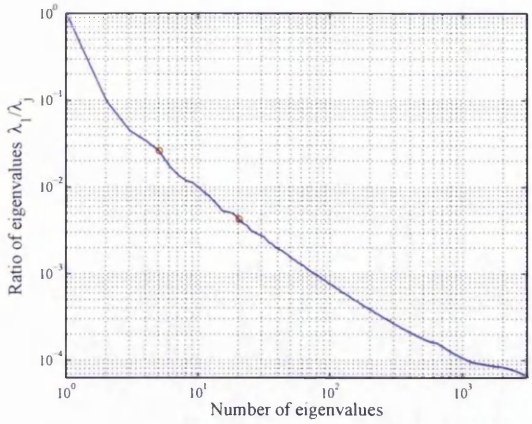

Figure 2.7: Ratio of eigenvalues for the flow through porous media problem.

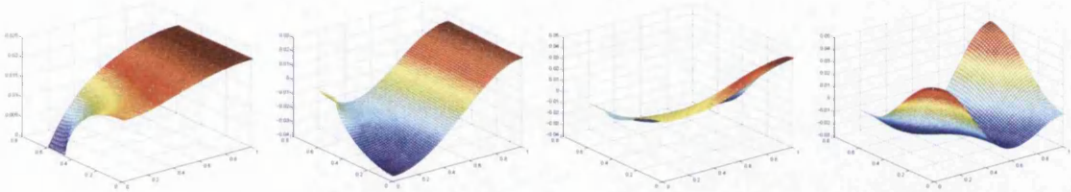

(a) First eigenvector. (b) Second eigenvector. (c) Third eigenvector. (d) Fourth eigenvector.

Figure 2.8: First four eigenvectors of the stiffness matrix for the flow through porous media problem.

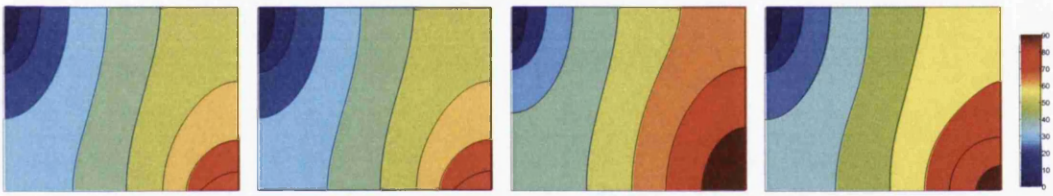

(a) MCS, 10k samples. (b) Full PC ($n = 584$). (c) RPC ($n = 5$). (d) RPC ($n = 20$).

Figure 2.9: Contour of the mean of head (cm) obtained with MCS, full PC and reduced systems using the first five and twenty eigenvectors respectively. x and y axis are respectively the positions in x direction with $x \in [-0.5, 0.5]$ and y direction with $y \in [-0.3, 0.3]$.

between the reduced systems and the full PC are shown in Figure 2.11. The percentage error is calculated with Equation (2.40). As formerly, the accuracy of the response with the proposed method is similar to the one of full PC, but is obtained at a lower cost. This cost is described in Table 2.3, where the CPU time of calculations for the four methods is given. The pdf of the response at coordinate $(x, y) = (0.1714, -0.2857)$ is shown in Figure 2.12 for MCS, full PC and the two reduced order models. This coordinate is close to the boundary in which the specific flux is prescribed, and far from the boundary

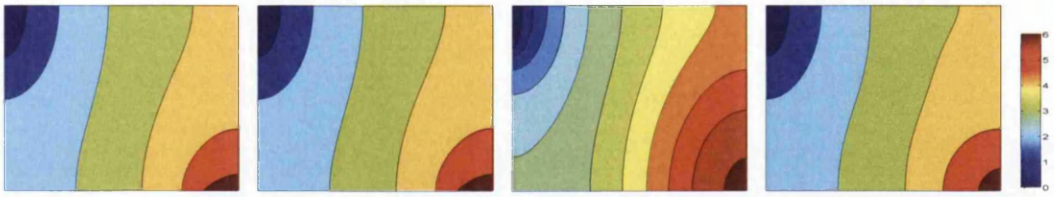

(a) MCS, 10k samples. (b) Full PC ($n = 584$). (c) RPC ($n = 5$). (d) RPC ($n = 20$).

Figure 2.10: Contour of the standard deviation of head (cm) obtained with MCS, full PC and reduced systems using the first five and twenty eigenvectors respectively. x and y axis are respectively the positions in x direction with $x \in [-0.5, 0.5]$ and y direction with $y \in [-0.3, 0.3]$.

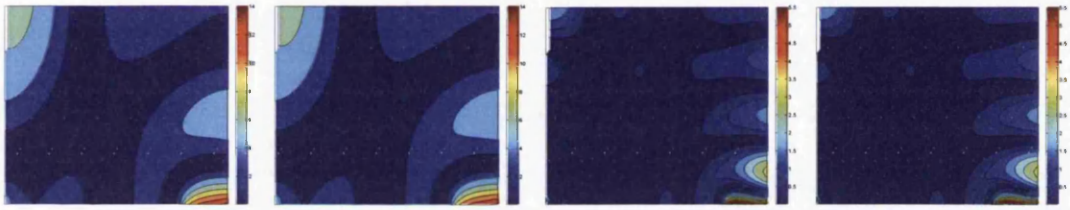

(a) $\varepsilon_{\%}$ of mean ($n = 5$). (b) $\varepsilon_{\%}$ of σ ($n = 5$). (c) $\varepsilon_{\%}$ of mean ($n = 20$). (d) $\varepsilon_{\%}$ of σ ($n = 20$).

Figure 2.11: Contour of percentage error ($\varepsilon_{\%}$) of mean and standard deviation (σ) of RPC (with $n = 5$ and $n = 20$) compared to full PC. x and y axis are respectively the positions in x direction with $x \in [-0.5, 0.5]$ and y direction with $y \in [-0.3, 0.3]$.

for which the head is fixed, so that the effect of uncertainty on the head should be larger than at other coordinates in the geometry. One can observe that with 20 dimensions, the proposed RPC produce results comparable with the full PC with dimension 584. Figure 2.12(b) shows that the error compared to the full PC reduces significantly when the size of the reduced system is beyond 50.

2.7 Bending of an elastic plate with stochastic properties

Numerical example of a plate bending problem is given to investigate the efficiency of the proposed method. The domain is a rectangular plate of length $L = 1$ m and width

	MCS	full PC ($n = 584$)	RPC ($n = 5$)	RPC ($n = 20$)
CPU time (s)	8.3371×10^3	192.1206	0.8293	0.9569

Table 2.3: CPU times (sec) of calculations for the full PC and in the proposed reduced method. The cost of calculating complete eigensolutions is 119.7236s.

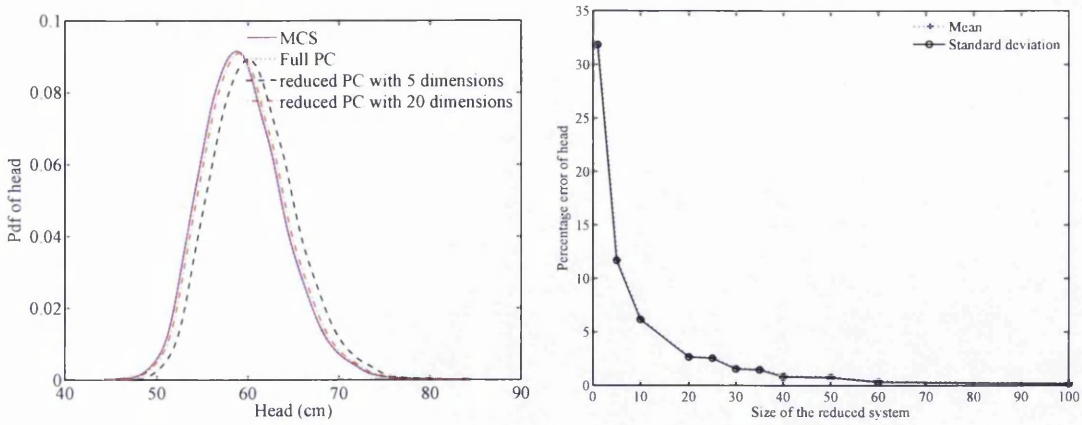

(a) Pdf. (b) Error of mean and standard deviation.

Figure 2.12: Pdf of head and percentage errors of mean and standard deviation of head at $(x, y) = (0.1714, -0.2857)$.

$W = 0.6$ m, as shown in Figure 2.13. The plate is clamped along its width (coordinate

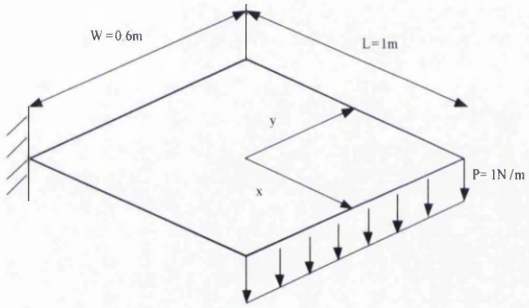

Figure 2.13: A rectangular elastic plate with stochastic bending rigidity subjected to a line load along one edge.

$x = -0.5$ m) and a uniform distributed load of value $P = 1$ N/m is applied at $x = 0.5$ m. The plate has 30 elements in x direction and 18 elements in y direction. The deterministic system stiffness matrix is of dimension $n = 1710$. The variable $D = \frac{Et^3}{12(1-\nu^2)}$ is modelled as a Gaussian random field, where its 2D covariance function is obtained by multiplying an 1D exponential covariance function depending on x, with correlation length $b_x = 0.2$ m; and another 1D exponential covariance function depending on y, with correlation length $b_y = 0.12$ m. The mean $\mathrm{E}[D]$ of D is calculated with $E = 200$ GPa, $t = 3$ mm and $\nu = 0.3$, and its standard deviation is $\sigma = 0.2\mathrm{E}[D]$. Two terms are kept in each 1D KL expansion, therefore, the KL expansion is the sum of a deterministic matrix and four matrices multiplied by independent random variables. Details on the FE method can be found, for example, in Dawe (1984).

The vertical displacement of the system is calculated with four methods: a MCS

using 10000 samples, full PC and two reduced systems, where the system is reduced using the two and five first eigenvectors respectively. The ratio between the first and the $n-th$ eigenvalue is shown in Figure 2.14. First four eigenvectors for the vertical displacement are shown in Figure 2.15. The two reduced PC system matrices are of

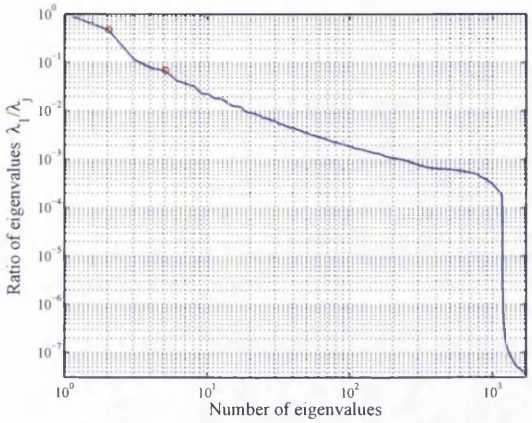

Figure 2.14: Ratio of eigenvalues for the plate bending problem.

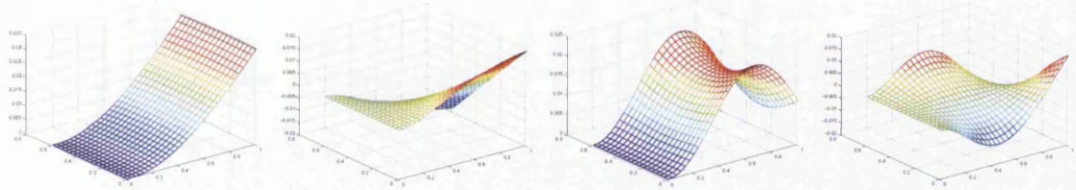

(a) First eigenvector. (b) Second eigenvector. (c) Third eigenvector. (d) Fourth eigenvector.

Figure 2.15: First four eigenvectors of the stiffness matrix for the plate bending problem. Only the degrees of freedom corresponding to vertical displacement are represented.

sizes $n = 140$ and $n = 350$ for transformed stiffness matrices of sizes two and five respectively. Contours of the mean and standard deviation for the four methods are shown respectively in Figure 2.16 and Figure 2.17. The percentage error associated with using RPC instead of full PC is shown in Figure 2.18. The percentage error is given by Equation (2.40). As formerly, it is observed that the percentage error between both methods is small, while the computation time is very different, as shown in Table 2.4. Coordinate $(x, y) = (0.1667, 0)$ is chosen to show some features of the method, as the pdf of the vertical displacement at Subfigure 2.19(a). At this position, the percentage errors of mean and standard deviation of the vertical displacement for different reduced systems compared to full PC are shown in Subfigure 2.19(b). One can observe that with 5 dimensions, the proposed RPC produce results comparable with the full PC with

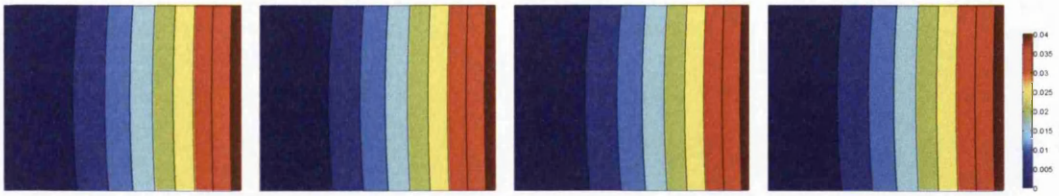

(a) MCS, 10k samples. (b) Full PC (n = 1710). (c) RPC ($n = 2$). (d) RPC ($n = 5$).

Figure 2.16: Contours of the mean of vertical displacement (m) obtained with MCS, full PC and reduced systems using the first two and five eigenvectors respectively. x and y axis are the positions in x direction with $x \in [-0.5, 0.5]$ and y direction with $y \in [-0.3, 0.3]$.

(a) MCS, 10k samples. (b) Full PC (n = 1710). (c) RPC ($n = 2$). (d) RPC ($n = 5$).

Figure 2.17: Contours of the standard deviation of vertical displacement (m) obtained with MCS, full PC and reduced PC using the first two and five eigenvectors respectively. x and y axis are respectively the positions in x direction with $x \in [-0.5, 0.5]$ and y direction with $y \in [-0.3, 0.3]$.

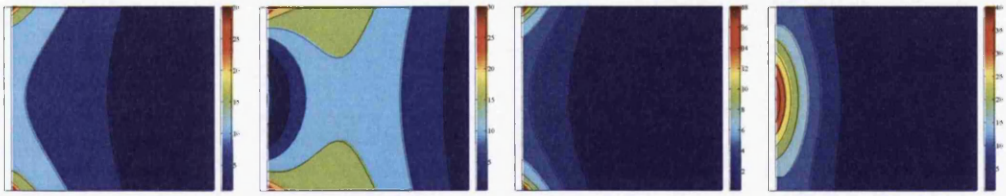

(a) $\varepsilon_{\%}$ of mean (n = 2). (b) $\varepsilon_{\%}$ of σ ($n = 2$). (c) $\varepsilon_{\%}$ of mean (n = 5). (d) $\varepsilon_{\%}$ of σ ($n = 5$).

Figure 2.18: Contour of percentage error ($\varepsilon_{\%}$) of mean and standard deviation (σ) of vertical displacement. x and y axis are respectively the positions in x direction with $x \in [-0.5, 0.5]$ and y direction with $y \in [-0.3, 0.3]$.

dimension 1710. Figure 2.19(b) shows that the error compared to the full PC reduces significantly when the size of the reduced system is beyond 20.

	MCS	full PC ($n = 1710$)	RPC ($n = 2$)	RPC ($n = 5$)
CPU time	1.6054×10^4	389.2569	0.3751	0.5074

Table 2.4: CPU times (sec) of calculations for the full PC and in the proposed reduced method. The cost of calculating complete eigensolutions is 38.0243s.

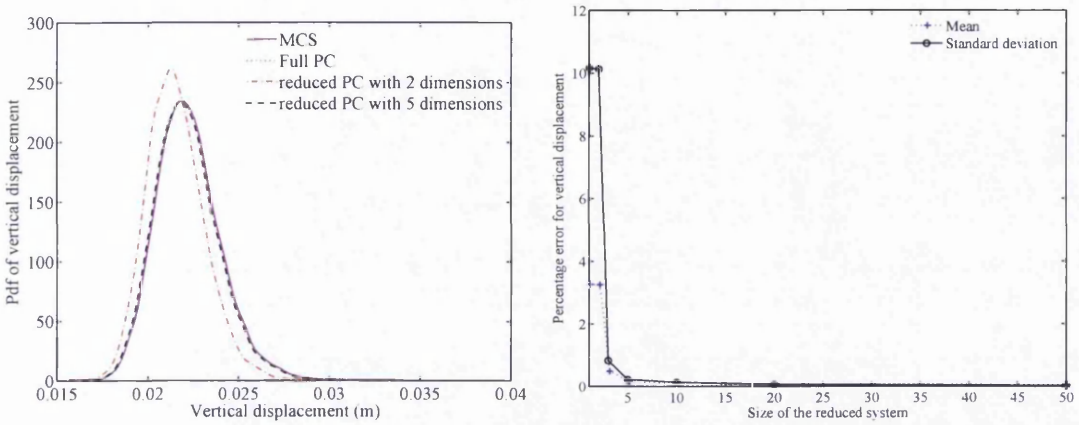

(a) Pdf.

(b) Error of mean and standard deviation.

Figure 2.19: Pdf and percentage error of mean and standard deviation of vertical displacement, at position $(x, y) = (0.1667, 0)$.

2.8 Conclusions

In this Chapter discretized stochastic elliptic partial differential equations have been considered. In the classical spectral stochastic finite element approach, each element of the response vector is projected into a basis of polynomials orthogonal with respect to a given pdf, and the associated vectors of coefficients multiplying each polynomial are obtained using a Galerkin type of error minimization approach. Here an alternative approach is investigated. The solution is firstly projected into a finite dimensional orthonormal vector basis, and each element of the associated reduced response vector is then projected into the basis of orthogonal polynomials. As formerly, the constants arising from the projections are obtained using a Galerkin type of error minimization approach. This error minimization approach is twofold as both projections, in the vector space and in the functions space, need to be taken into account. The dimension of the linear system to be solved with the classical spectral stochastic finite element approach is obtained by multiplying the number of polynomials used in the projection by the dimension of the system stiffness matrix. In the proposed approach, the dimension of the linear system to be solved is obtained by multiplying the number of polynomials by the number of vectors in the projection basis used. The vectors used in the projection

basis are chosen amongst the eigenvectors of the deterministic stiffness matrix, and are the ones corresponding to the p smaller eigenvalues, so that p is the size of the reduced system.

The reduced system can be considered as a preconditioned submatrix of the original system, so that an approximate relation between the errors of the two methods can be derived. The method has been applied to three different systems with random parameters, a bending beam, a flow through porous media with random permeability and a bending plate. For the three systems, a reduction of the system with the method leads to a reduction in computation time with respect to the classical spectral stochastic finite element approach. The accuracy remained similar to that of the original method, in spite of the reduction in the spatial dimension. Keeping the computational cost fixed, the proposed reduced polynomial chaos (RPC) approach allows one to solve a system of larger dimension, or to consider higher order polynomial chaos expansion.

A related approach will be investigated for the random eigenvalue problem in Chapter 3, where new methods based on polynomial chaos and size reduction are proposed.

Chapter 3

Hybrid perturbation-polynomial chaos approaches to the random algebraic eigenvalue problem

3.1 Introduction

In Chapter 1 the random eigenvalue problem was discussed, and its importance in dynamic problems was commented. It was observed that even if research has been carried out both on the perturbation and PC methods for the random eigenvalue problem, no method hybridizing both approaches is yet available. Efficient methods hybridizing PC and other methods have been proposed for the elliptic problem (Sachdeva et al., 2006b, Maute et al., 2009), where a reduction of the size of the linear system to be solved, different from the one exposed in Chapter 2, was achieved. The aim of the present Chapter is to gain efficiency on the PC algorithms for random eigenvalue problems through the use of results from the perturbation method. The outline of the Chapter is as follows. The basic theories of the perturbation method and PC are discussed respectively in subsections 3.2.1 and 3.2.2. PC expansion of eigenvalues is obtained in section 3.3 using the Rayleigh quotient where eigenvectors are obtained from the perturbation method or from one of the methods developed to update eigenvectors. Four new methods, namely reduced spectral power method (RSPM), reduced spectral inverse power method (RSIPM), reduced spectral constrained coefficients method (RSCCM) and spectral constrained coefficients method (SCCM) are proposed to update the eigenvectors in section 3.4. The four methods allow us to obtain an updated PC expansion

of the eigenvectors and eigenvalues using Rayleigh quotient. A summary of the proposed methods is given in section 3.5. A comparison of the methods is performed for the problem of a beam with stochastic properties in section 3.6 and for a thin plate with stochastic properties in section 3.7.

3.2 A brief overview of available techniques tackling the random eigenvalue problem

The generalised eigenvalue problem was given in Equation (1.99)

$$\mathbf{K}\boldsymbol{\phi}^{(j)} = \lambda^{(j)}\mathbf{M}\boldsymbol{\phi}^{(j)} \tag{3.1}$$

The eigenvalues $\lambda^{(j)}$ are the same as the ones from the eigenvalue problem

$$\mathbf{A}\mathbf{v}^{(j)} = \lambda^{(j)}\mathbf{v}^{(j)} \qquad \mathbf{A} = \sum_{i=1}^{P} \Gamma_i \mathbf{A}_i \tag{3.2}$$

where $\mathbf{A} = \mathbf{M}^{-1/2}\mathbf{K}\mathbf{M}^{-1/2}$ is the system matrix and $\mathbf{v}^{(j)} = \mathbf{M}^{1/2}\boldsymbol{\phi}^{(j)}$ is the j-th eigenvector. It is noted that, when $\mathbf{M}$ is a deterministic matrix and $\mathbf{K} = \sum_{i=1}^{P} \Gamma_i \hat{\mathbf{K}}_i$, the system matrix is given by $\mathbf{A}_i = \mathbf{M}^{-1/2}\hat{\mathbf{K}}_i\mathbf{M}^{-1/2}$. For the case of the system matrix in Equation (1.30), $\hat{\mathbf{K}}_1 = \mathbf{K}_0$ and $\hat{\mathbf{K}}_{i+1} = \mathbf{K}_i$ for $i = 1, \ldots, M$ in the case of Γ_i the basis functions of PC. When uncertainty affects both mass and stiffness matrices, the system matrix $\mathbf{A}$ can still be represented with a PC expansion, but the obtention of matrices $\mathbf{A}_i$ is not straightforward. Identifying these matrices would imply projecting the product of the three matrices $\mathbf{M}^{-1/2}\mathbf{K}\mathbf{M}^{-1/2}$ into the basis functions Γ_i as, in general, $\mathbf{A}_i = \mathrm{E}\left[\mathbf{A}\Gamma_i\right]/\mathrm{E}\left[\Gamma_i^2\right]$.

The propagation of uncertainty from $\mathbf{A}$ to eigenvectors $\mathbf{v}^{(j)}$ and eigenvalues $\lambda^{(j)}$ has been studied with several methods, amongst them, the perturbation method and PC expansion.

3.2.1 Perturbation method for the random eigenvalue problem

The perturbation method is widely used due to its simplicity and computational efficiency. The different perturbation methods available to analyze the random eigenvalue problem are based on keeping different number of terms in the Taylor series expansions.

The first order perturbation of the j-th eigenvalue is given by

$$\lambda^{(j)} = \lambda_0^{(j)} + \sum_{i=1}^{M} \xi_i \frac{\partial \lambda^{(j)}}{\partial \xi_i} \quad \text{where} \quad \frac{\partial \lambda^{(j)}}{\partial \xi_i} = \mathbf{v}_{j0}^T \frac{\partial \mathbf{A}}{\partial \xi_i} \mathbf{v}_{j0} \tag{3.3}$$

For the case where $\mathbf{A}$ is given by a KL expansion as in Equation (1.103), $\partial \mathbf{A}/\partial \xi_i = \mathbf{A}_i$. Perturbation methods can also be applied to eigenvectors, and the eigenvalues can then be obtained using the Rayleigh quotient. This approximation of eigenvalues is more accurate than the one obtained by directly applying the perturbation method via the Taylor series expansions (Chen et al., 2000). If $\lambda_0^{(j)}$ and $\mathbf{v}_{j0}$ are the j-th deterministic eigenvalue and the corresponding eigenvector, an expression for the first-order perturbation of the eigenvector can be given by (Hasselman and Hart, 1972)

$$\mathbf{v}^{(j)} = \mathbf{v}_{j0} + \sum_{i=1}^{M} \xi_i \frac{\partial \mathbf{v}^{(j)}}{\partial \xi_i} \tag{3.4}$$

The deterministic eigenvectors satisfy the following properties

$$\mathbf{v}_{j0}^T \mathbf{v}_{j0} = 1 \qquad \text{and} \qquad \mathbf{v}_{j0}^T \frac{\partial \mathbf{v}^{(j)}}{\partial \xi_i} = 0 \tag{3.5}$$

Different methods have been developed to calculate the derivatives of the eigenvectors. One of these methods expands the derivative of eigenvectors as a linear combination of deterministic eigenvectors (Bellman, 1960, Fox and Kapoor, 1968), so that

$$\mathbf{v}_{ji} = \frac{\partial \mathbf{v}^{(j)}}{\partial \xi_i} = \sum_{m=1, m \neq j}^{N} \alpha_{jim} \mathbf{v}_{m0} \qquad \text{where} \qquad \alpha_{jim} = \frac{1}{\lambda_0^{(j)} - \lambda_0^{(m)}} \mathbf{v}_{m0}^T \frac{\partial \mathbf{A}}{\partial \xi_i} \mathbf{v}_{j0} \tag{3.6}$$

This equation is used when all deterministic eigenvectors are calculated. If only a limited number of eigenvectors were calculated, other methods described by Nelson (1976) could be applied. The case of complex or repeated eigenvalues is not dealt with here. The perturbation method for such cases is derived, for example in Ojalvo (1987), Mills-Curran (1988), Friswell (1996), Adhikari (2000). For the case of repeated eigenvalues, the space corresponding to a given eigenvalue is the space spanned by its two eigenvectors, so that the proposed methods would be valid for the eigenvalues that are not repeated but not for the repeated one. The case of veering of modes is dealt with, for example in du Bois et al. (2011), Gallina et al. (2011), and the proposed method does not allow to deal with this problem.

3.2.2 Polynomial chaos approach for the random eigenvalue problem

The eigensolutions are assumed to have finite second-order moments, and can be represented as an expansion using a basis of functions in the space of square integrable functions. The representations of $\lambda^{(j)}$ and $\mathbf{v}^{(j)}$ on the basis functions Γ_k truncated after P terms can be given by

$$\lambda^{(j)}(\xi_1, \ldots \xi_M) = \sum_{k=1}^{P} \lambda_{jk} \Gamma_k(\xi_1, \ldots \xi_M) \tag{3.7}$$

$$\mathbf{v}^{(j)}(\xi_1, \ldots \xi_M) = \sum_{k=1}^{P} \mathbf{v}_k^{(j)} \Gamma_k(\xi_1, \ldots \xi_M) \tag{3.8}$$

where λ_{jk} and $\mathbf{v}_k^{(j)}$ are unknowns and the basis functions considered here are PC (Ghanem and Spanos, 1991). Details on the PC expansion have already been given in Chapter 1.

PC has already been used in the context of the algebraic random eigenvalue problem by Ghanem and Ghosh (2007). Ghanem and Ghosh (2007) substituted eigenvalues and eigenvectors by their expansions, i.e., $\lambda^{(j)}$ and $\mathbf{v}^{(j)}$ are replaced in Equation (3.2) by their expansions from Equations (3.7) and (3.8). The resulting equation is projected on the basis functions Γ_i through the Galerkin method, that is, the equation is multiplied by each basis function Γ_p and subsequently the mean of the equation is taken. The resulting system of equations of size $P \times n$ relating the unknowns λ_{jl} and $\mathbf{v}_l^{(j)}$ can be given by

$$\left(\sum_{r=1}^{P} \mathbf{e}_{0r} \otimes \mathbf{A}_r \right) \begin{bmatrix} \mathbf{v}_1^{(j)} \\ \vdots \\ \mathbf{v}_P^{(j)} \end{bmatrix} = \sum_{l=1}^{P} \lambda_{jl} \mathbf{e}_{0l} \otimes \mathbf{I}_n \begin{bmatrix} \mathbf{v}_1^{(j)} \\ \vdots \\ \mathbf{v}_P^{(j)} \end{bmatrix} \tag{3.9}$$

For the case of a KL expansion of the random field such as in Equation (1.103), the matrix on the left hand side reduces to $\left(\mathbf{c}_0 \otimes \mathbf{A}_0 + \sum_{i=1}^{M} \mathbf{c}_{1i} \otimes \mathbf{A}_i \right)$. Here the elements in the k-th row and p-th column of the $P \times P$ matrices $\mathbf{c}_0$, $\mathbf{c}_{1i}$ and $\mathbf{e}_{0l}$ are respectively $c_{0kp} = \mathrm{E}\left[\Gamma_k \Gamma_p\right]$, $c_{1ikp} = \mathrm{E}\left[\xi_i \Gamma_k \Gamma_p\right]$, with $i = 1, \ldots M$ and $e_{0lkp} = \mathrm{E}\left[\Gamma_k \Gamma_p \Gamma_l\right]$ with $l = 1, \ldots P$, and $\otimes$ denotes the kronecker product. If the norm of the eigenvectors is also prescribed, the nonlinear system of equations can be solved with iterative techniques. A good initial approximation is often needed to obtain a fast convergence.

An iterative procedure to obtain PC expansions of eigenvalues and eigenvectors has

been proposed by Verhoosel et al. (2006) based on the inverse power method. The algorithm of the iteration can be concisely described by the following steps:

1. $\lambda^{(j)}_{(q+1)} = \left(\mathbf{v}^{(j)}_{(q)}\right)^T (\mathbf{A}_0 + \sum_{i=1}^{M} \xi_i \mathbf{A}_i)\mathbf{v}^{(j)}_{(q)}$.
2. $\mathbf{v}^{(j)}_{(q+1)} = \left(\lambda^{(j)}_{(q+1)} - \lambda^{(j)}_0\right) \left[\mathbf{A}_0 + \sum_{i=1}^{M} \xi_i \mathbf{A}_i - \lambda^{(j)}_0 \mathbf{I}\right]^{-1} \mathbf{v}^{(j)}_{(q)}$.
3. $\mathbf{v}^{(j)}_{(q+1)} \rightarrow \frac{\mathbf{v}^{(j)}_{(q+1)}}{||\mathbf{v}^{(j)}_{(q+1)}||_{L^2_S}}$ where $||\mathbf{v}^{(j)}_{(q+1)}||_{L^2_S} = \sqrt{\sum_{k=1}^{P} \mathrm{E}\left[\Gamma^2_k\right] \left(\mathbf{v}^{(j)}_{k(q+1)}\right)^T \mathbf{v}^{(j)}_{k(q+1)}}$.
4. Define errors $\epsilon_{1_{q+1}} = ||[\mathbf{A}_0 + \sum_{i=1}^{M} \xi_i \mathbf{A}_i - \lambda^{(j)}_{(q+1)} \mathbf{I}_n]||_{L^2_S}$ and $\epsilon_{2_{(q+1)}} = \frac{|V_{\lambda^{(j)}_{(q+1)}} - V_{\lambda^{(j)}_{(q)}}|}{|V_{\lambda^{(j)}_{(q)}}|}$ with $V_{\lambda^{(j)}_{(q)}} = \frac{\sqrt{\sum_{k=1}^{P} \lambda^2_{jk(q)} \mathrm{E}\left[\Gamma^2_k\right]}}{\lambda_{j1(q)}}$, the coefficient of variation of the eigenvalue.

For all the steps of the iterative procedure where it is needed, the coefficients of the PC expansions are obtained using the Galerkin method. The subscripts (q) and $(q+1)$ denote the number of the iteration. That is, $\lambda^{(j)}_{(q)}$ is the PC expansion of the j-th eigenvalue at iteration q, while $\lambda_{jk(q)}$ denotes the k-th coefficient of the expansion, so that $\lambda^{(j)}_{(q)} = \sum_{k=1}^{P} \lambda_{jk(q)} \Gamma_k$. Similarly, $\mathbf{v}^{(j)}_{(q)}$ is the PC expansion of the j-th eigenvector at iteration q, so that $\mathbf{v}^{(j)}_{(q)} = \sum_{k=1}^{P} \mathbf{v}^{(j)}_{k(q)} \Gamma_k$.

The two methods discussed here can be used to obtain the eigenvalue and eigenvector coefficients λ_{jk} and $\mathbf{v}^{(j)}_k$ of the PC expansions given by Equations (3.7) and (3.8). From these PC expansions, the pdf of eigenvalues and eigenvectors can be obtained by a Monte Carlo simulation. This is done by sampling the set of independent Gaussian random variables $\xi_1, \ldots, \xi_M$. The corresponding values of the basis functions Γ_k are calculated and subsequently introduced in the PC expansions of eigenvalues and eigenvectors given by Equations (3.7) and (3.8). A numerical approximation to the pdf of eigenvalues from the samples of eigenvalues can then be obtained. Moments of eigenvalues and eigenvectors can also be derived from Equations (3.7) and (3.8). The first and second moments of eigenvalues are given by

$$\mathrm{E}\left[\lambda^{(j)}\right] = \sum_{k=1}^{P} \lambda_{jk} \mathrm{E}\left[\Gamma_k\right] = \lambda_{j1} \tag{3.10}$$

$$\mathrm{E}\left[\left(\lambda^{(j)}\right)^2\right] = \sum_{k,l=1}^{P} \lambda_{jk}\lambda_{jl} \mathrm{E}\left[\Gamma_k \Gamma_l\right] = \sum_{k=1}^{P} \lambda^2_{jk} \mathrm{E}\left[\Gamma^2_k\right] \tag{3.11}$$

Similarly, the first and second moments of the eigenvectors can be calculated

$$\mathrm{E}\left[\mathbf{v}^{(j)}\right] = \sum_{k=1}^{P} \mathbf{v}_k^{(j)} \mathrm{E}\left[\Gamma_k\right] = \mathbf{v}_1^{(j)} \tag{3.12}$$

$$\mathrm{E}\left[\mathbf{v}^{(j)}\left(\mathbf{v}^{(j)}\right)^T\right] = \sum_{k,l=1}^{P} \mathbf{v}_k^{(j)}\left(\mathbf{v}_l^{(j)}\right)^T \mathrm{E}\left[\Gamma_k\Gamma_l\right] = \sum_{k=1}^{P} \mathbf{v}_k^{(j)}\left(\mathbf{v}_k^{(j)}\right)^T \mathrm{E}\left[\Gamma_k^2\right] \tag{3.13}$$

3.3 Rayleigh quotient method for the polynomial chaos expansion of eigenvalues

The Rayleigh quotient can be used to obtain an approximation to the eigenvalue $\lambda^{(j)}$ if an approximation to eigenvector $\mathbf{v}^{(j)}$ is available

$$\lambda^{(j)} = \frac{\left(\mathbf{v}^{(j)}\right)^T \mathbf{A}\mathbf{v}^{(j)}}{\left(\mathbf{v}^{(j)}\right)^T \mathbf{v}^{(j)}} \tag{3.14}$$

This method to obtain eigenvalues is similar to step 1 of the algorithm by Verhoosel et al. (2006), but here, the eigenvectors do not need to be normalised as the Rayleigh quotient already removes the effect of the norm of eigenvectors on eigenvalues through the denominator. The eigenvalues of the random algebraic eigenvalue problem can be expanded with a PC expansion such that the j-th eigenvalue is given by Equation (3.7). Substituting this expansion in the expression of the Rayleigh quotient in Equation (3.14) leads to

$$\left(\sum_{k=1}^{P} \lambda_{jk}\Gamma_k\right)\left(\mathbf{v}^{(j)}\right)^T \mathbf{v}^{(j)} = \left(\mathbf{v}^{(j)}\right)^T \left(\sum_{r=1}^{P} \Gamma_r \mathbf{A}_r\right) \mathbf{v}^{(j)} \tag{3.15}$$

In the following subsections, the eigenvectors $\mathbf{v}^{(j)}$ will be substituted by different approximations, allowing to obtain the coefficients λ_{jk} from a linear system of equations. It is noted that, once a description of eigenvectors is available, two approaches to calculate the PC expansion of eigenvalues are available. Here, the expansion is obtained using Galerkin method, but nonintrusive methods could also be applied (Maître and Knio, 2010).

3.3.1 Perturbation of the eigenvectors

Using the first-order perturbation of the j-th eigenvector, the corresponding eigenvalue can be approximated using the Rayleigh quotient by substituting $\mathbf{v}^{(j)}$ from Equations

(3.4) and (3.6) into Equation (3.15)

$$\left(\sum_{k=0}^{P}\lambda_{jk}\Gamma_k\right)\left(\mathbf{v}_{j0}^T\mathbf{v}_{j0}+2\sum_{i=1}^{M}\xi_i\mathbf{v}_{j0}^T\mathbf{v}_{ji}+\sum_{i,g=1}^{M}\xi_i\xi_g\mathbf{v}_{ji}^T\mathbf{v}_{gi}\right)=\sum_{r=1}^{P}\mathbf{v}_{j0}^T\mathbf{A}_r\mathbf{v}_{j0}\Gamma_r+$$
$$2\sum_{r=1}^{P}\sum_{g=1}^{M}\mathbf{v}_{j0}^T\mathbf{A}_r\mathbf{v}_{jg}\xi_g\Gamma_r+\sum_{r=1}^{P}\sum_{g,h=1}^{M}\mathbf{v}_{jg}^T\mathbf{A}_r\mathbf{v}_{jh}\xi_g\xi_h\Gamma_r \quad (3.16)$$

The Galerkin method is applied to Equation (3.16) (i.e. the equation is multiplied by the p-th PC basis function Γ_p and mean of the equation is taken) and the resulting equation is simplified using properties given by Equation (3.5). Then, coefficients λ_{jk} of the PC expansion of $\lambda^{(j)}$ can be obtained from the equations

$$\sum_{k=1}^{P}\lambda_{jk}\left(c_{0kp}+\sum_{i,g=1}^{M}\mathbf{v}_{ji}^T\mathbf{v}_{jg}c_{2igkp}\right)=\sum_{r=1}^{P}\mathbf{v}_{j0}^T\mathbf{A}_r\mathbf{v}_{j0}c_{0rp}+2\sum_{r=1}^{P}\sum_{g=1}^{M}\mathbf{v}_{j0}^T\mathbf{A}_r\mathbf{v}_{jg}c_{1grp}+$$
$$\sum_{r=1}^{P}\sum_{g,h=1}^{M}\mathbf{v}_{jg}^T\mathbf{A}_r\mathbf{v}_{jh}c_{2ghrp} \quad (3.17)$$

This equation reduces, for the case of $\mathbf{A}$ given by equation (1.103), to

$$\sum_{k=1}^{P}\lambda_{jk}\left(c_{0kp}+\sum_{i,g=1}^{M}\mathbf{v}_{ji}^T\mathbf{v}_{jg}c_{2igkp}\right)=\lambda_0^{(j)}d_{0p}+\sum_{i=1}^{M}\mathbf{v}_{j0}^T\mathbf{A}_i\mathbf{v}_{j0}d_{1ip}+\sum_{i,g=1}^{M}\left(2\mathbf{v}_{j0}^T\mathbf{A}_i\mathbf{v}_{jg}+\right.$$
$$\left.\mathbf{v}_{jg}^T\mathbf{A}_0\mathbf{v}_{ji}\right)d_{2igp}+\sum_{i,g,h=1}^{M}\mathbf{v}_{jg}^T\mathbf{A}_i\mathbf{v}_{jh}d_{3ighp} \quad (3.18)$$

where $p=1,\ldots,P$. Matrix $\mathbf{c}_0$ has already been defined as a diagonal matrix with element in the k-th row and p-th column given by $c_{0kp}=\mathrm{E}[\Gamma_k\Gamma_p]$. Similarly, the $P\times P$ matrix $\mathbf{c}_{2ig}$ has elements $c_{2igkp}=\mathrm{E}[\Gamma_k\Gamma_p\xi_i\xi_g]$ and column vectors of length P $\mathbf{d}_0$, $\mathbf{d}_{1i}$, $\mathbf{d}_{2ig}$ and $\mathbf{d}_{3igh}$ have their p-th term given by $d_{0p}=\mathrm{E}[\Gamma_p]$, $d_{1ip}=\mathrm{E}[\Gamma_p\xi_i]$, $d_{2igp}=\mathrm{E}[\Gamma_p\xi_i\xi_g]$ and $d_{3ighp}=\mathrm{E}[\Gamma_p\xi_i\xi_g\xi_h]$ respectively. This notation for matrices $\mathbf{c}$ and $\mathbf{d}$ is such that for each matrix the mean of the product of, respectively, one and two polynomials Γ_k is calculated. The numerical subindex (e.g. 1, 2) indicate the number of random variables multiplying those polynomials inside the mean operator. Equation

(3.18) can be represented by the linear system of equations

$$\left(\mathbf{c}_0 + \sum_{i,g=1}^{M} \mathbf{v}_{ji}^T \mathbf{v}_{jg} \mathbf{c}_{2ig}\right) \begin{bmatrix} \lambda_{j1} \\ \vdots \\ \lambda_{jP} \end{bmatrix} = \lambda_0^{(j)} \mathbf{d}_0 + \sum_{i=1}^{M} \mathbf{v}_{j0}^T \mathbf{A}_i \mathbf{v}_{j0} \mathbf{d}_{1i} + \sum_{i,g=1}^{M} \left(2\mathbf{v}_{j0}^T \mathbf{A}_i \mathbf{v}_{jg} + \mathbf{v}_{jg}^T \mathbf{A}_0 \mathbf{v}_{ji}\right) \mathbf{d}_{2ig} + \sum_{i,g,h=1}^{M} \mathbf{v}_{jg}^T \mathbf{A}_i \mathbf{v}_{jh} \mathbf{d}_{3igh} \tag{3.19}$$

and the coefficients λ_{jk} of the eigenvalue expansion can be obtained by solving the $P \times P$ linear system given by Equation (3.19).

3.3.2 Reduced polynomial chaos eigenvectors

The PC expansion of an eigenvector is given by Equation (3.8). A possible approach to reduce the size of the system is to assume the vectors $\mathbf{v}_k^{(j)}$ can be expressed as a linear combination of the vectors $\mathbf{v}_{j0}$ and $\mathbf{v}_{ji}$, such that

$$\mathbf{v}_k^{(j)} = a_{0k}^{(j)} \mathbf{v}_{j0} + \sum_{i=1}^{M} a_{ik}^{(j)} \mathbf{v}_{ji} \tag{3.20}$$

The reduction is performed when $M+1 < n$, otherwise, the system obtained is equivalent to the full system where the eigenvector is given in Equation (3.8), for $M+1 = n$, or the vectors $\mathbf{v}_{j0}$, $\mathbf{v}_{ji}$ are linearly dependent, for $M+1 > n$. In the cases where $M+1 \geq n$, the system is not reduced, but a projection of the eigenvectors on the deterministic eigenvectors can be performed. This procedure will be developed in subsection 3.3.3. The idea of expanding the random eigenvectors into a basis formed by the deterministic eigenvector and its first derivative has already been used by Nair and Keane (2003), and an accurate approximation to eigenvectors was obtained. Substituting Equation (3.20) in Equation (3.8), the eigenvector can be expanded as

$$\mathbf{v}^{(j)} = \left(\sum_{k=1}^{P} a_{0k}^{(j)} \Gamma_k\right) \mathbf{v}_{j0} + \sum_{i=1}^{M} \left(\sum_{k=1}^{P} a_{ik}^{(j)} \Gamma_k\right) \mathbf{v}_{ji} = \mathbf{V}_j \begin{bmatrix} \sum_{k=1}^{P} a_{0k}^{(j)} \Gamma_k \\ \vdots \\ \sum_{k=1}^{P} a_{Mk}^{(j)} \Gamma_k \end{bmatrix} \tag{3.21}$$

where the rectangular matrix $\mathbf{V}_j$ is formed with the columns of the deterministic eigenvector and its derivatives with respect to each random variable

$$\mathbf{V}_j = \begin{bmatrix} \mathbf{v}_{j0} & \mathbf{v}_{j1} & \dots & \mathbf{v}_{jM} \end{bmatrix} \in \mathbb{R}^{n\times(M+1)} \tag{3.22}$$

This expansion will be used in the next section, where coefficients $a_{0k}^{(j)}$, $a_{ik}^{(j)}$ will be obtained. After obtaining the set of coefficients $a_{0k}^{(j)}$, $a_{ik}^{(j)}$, the PC expansion of the j-th eigenvalue is obtained using the Rayleigh quotient. That is, the new eigenvectors from Equation (3.21) are substituted in Equation (3.15)

$$\begin{aligned}\left(\sum_{k=0}^{P}\lambda_{jk}\Gamma_k\right)\left(\sum_{l,m=1}^{P}a_{0m}^{(j)}a_{0l}^{(j)}\Gamma_l\Gamma_m\mathbf{v}_{j0}^T\mathbf{v}_{j0}+2\sum_{i=1}^{M}\sum_{l,m=1}^{P}a_{0m}^{(j)}a_{gl}^{(j)}\Gamma_l\Gamma_m\mathbf{v}_{j0}^T\mathbf{v}_{ji}+\right.\\ \left.\sum_{i,g=1}^{M}\sum_{l,m=1}^{P}a_{im}^{(j)}a_{gl}^{(j)}\Gamma_l\Gamma_m\mathbf{v}_{ji}^T\mathbf{v}_{gi}\right)=\sum_{r,l,m=1}^{P}a_{0m}^{(j)}a_{0l}^{(j)}\Gamma_r\Gamma_l\Gamma_m\mathbf{v}_{j0}^T\mathbf{A}_r\mathbf{v}_{j0}+\\ 2\sum_{i=1}^{M}\sum_{r,l,m=1}^{P}a_{0m}^{(j)}a_{il}^{(j)}\Gamma_r\Gamma_l\Gamma_m\mathbf{v}_{j0}^T\mathbf{A}_r\mathbf{v}_{ji}+\sum_{i,g=1}^{M}\sum_{r,l,m=1}^{P}a_{im}^{(j)}a_{gl}^{(j)}\Gamma_r\Gamma_l\Gamma_m\mathbf{v}_{jg}^T\mathbf{A}_r\mathbf{v}_{ji}\end{aligned} \tag{3.23}$$

As in the previous subsection, the equation is simplified using properties given by Equation (3.5). Then, the equation is multiplied by Γ_p and mean is taken. The coefficients of the eigenvalue expansion can be retrieved from the set of equations

$$\begin{aligned}\sum_{k=1}^{P}\lambda_{jk}\sum_{l,m=1}^{P}g_{lmpk}\left(a_{0l}^{(j)}a_{0m}^{(j)}+\sum_{i,g=1}^{M}a_{im}^{(j)}a_{gl}^{(j)}\mathbf{v}_{ji}^T\mathbf{v}_{jg}\right)=\\ \sum_{r,l,m=1}^{P}g_{rlmp}\left(a_{0l}^{(j)}a_{0m}^{(j)}\mathbf{v}_{j0}^T\mathbf{A}_r\mathbf{v}_{j0}+2\sum_{i=1}^{M}a_{0m}^{(j)}a_{il}^{(j)}\mathbf{v}_{j0}^T\mathbf{A}_r\mathbf{v}_{ji}+\sum_{g,i=1}^{M}a_{gm}^{(j)}a_{il}^{(j)}\mathbf{v}_{jg}^T\mathbf{A}_r\mathbf{v}_{ji}\right)\end{aligned} \tag{3.24}$$

If the system matrix is given by Equation (1.103), the previous equation reduces to

$$\begin{aligned}\sum_{k=1}^{P}\lambda_{jk}\sum_{l,m=1}^{P}g_{lmpk}\left(a_{0l}^{(j)}a_{0m}^{(j)}+\sum_{i,g=1}^{M}a_{im}^{(j)}a_{gl}^{(j)}\mathbf{v}_{ji}^T\mathbf{v}_{jg}\right)=\\ \sum_{l,m=1}^{P}a_{0l}^{(j)}a_{0m}^{(j)}\left(\lambda_{0j}e_{0lmp}+\sum_{i=1}^{M}\mathbf{v}_{j0}^T\mathbf{A}_i\mathbf{v}_{j0}e_{1ilmp}\right)+\sum_{l,m=1}^{P}a_{0l}^{(j)}\sum_{i,g=1}^{M}a_{im}^{(j)}2\mathbf{v}_{j0}^T\mathbf{A}_g\mathbf{v}_{ji}e_{1glmp}+\\ \sum_{l,m=1}^{P}\sum_{i,g}^{M}a_{im}^{(j)}a_{gl}^{(j)}\left(\mathbf{v}_{ji}^T\mathbf{A}_0\mathbf{v}_{jg}e_{0lmp}+\sum_{h=1}^{M}\mathbf{v}_{ji}^T\mathbf{A}_h\mathbf{v}_{jg}e_{1hlmp}\right)\end{aligned} \tag{3.25}$$

Here $p = 1, \ldots, P$, $e_{0lmp} = \mathrm{E}\left[\Gamma_l \Gamma_m \Gamma_p\right]$, $e_{1glmp} = \mathrm{E}\left[\Gamma_m \Gamma_l \Gamma_p \xi_g\right]$, $g_{klmp} = \mathrm{E}\left[\Gamma_k \Gamma_l \Gamma_m \Gamma_p\right]$. As formerly, the set of coefficients λ_{jk} can be found solving a linear equation similar to the one obtained in Equation (3.19). The set of coefficients $a_{0k}^{(j)}$, $a_{ik}^{(j)}$ have yet not been defined. They are calculated in the next section, following three approaches, namely, the reduced spectral power method, the reduced spectral inverse method and the reduced spectral constrained coefficients method.

3.3.3 Polynomial chaos eigenvectors projected on deterministic eigenvectors

The PC expansion of an eigenvector is given by Equation (3.8). The vectors $\mathbf{v}_k^{(j)}$ can be expressed as a linear combination of the deterministic eigenvectors $\mathbf{v}_{j0}$, such that

$$\mathbf{v}_k^{(j)} = \sum_{i=1}^{n} \left(\sum_{k=1}^{P} a_k^{(ji)} \Gamma_k \right) \mathbf{v}_{i0} = \mathbf{V}_0 \begin{bmatrix} \sum_{k=1}^{P} a_k^{(j1)} \Gamma_k \\ \vdots \\ \sum_{k=1}^{P} a_k^{(jn)} \Gamma_k \end{bmatrix} = \mathbf{V}_0 \left(\mathbf{I}_n \otimes \left[\Gamma_1 \ \ldots \ \Gamma_P \right] \right) \begin{bmatrix} a_1^{(j1)} \\ \vdots \\ a_P^{(j1)} \\ \vdots \\ a_P^{(jn)} \end{bmatrix} \tag{3.26}$$

where $\mathbf{V}_0$ is the matrix of deterministic eigenvectors. This calculation of the Rayleigh quotient uses the coefficients $a_{0k}^{(j)}$, $a_{ik}^{(j)}$ obtained from the spectral constrained coefficients method obtained in subsection 3.4.4. After obtaining the set of coefficients $a_{0k}^{(j)}$, $a_{ik}^{(j)}$, the PC expansion of the j-th eigenvalue is obtained using the Rayleigh quotient. That is, the new eigenvectors from Equation (3.26) are substituted in Equation (3.15)

$$\left(\sum_{k=1}^{P} \lambda_{jk} \Gamma_k \right) \left(\sum_{k=1}^{n} \sum_{l,m=1}^{P} a_m^{(jk)} a_l^{(jk)} \Gamma_l \Gamma_m \right) = \sum_{r,l,m=1}^{P} \sum_{g,k=1}^{n} \mathbf{v}_{g0}^T \mathbf{A}_r \mathbf{v}_{k0} a_m^{(jk)} a_l^{(jg)} \Gamma_l \Gamma_m \Gamma_r \tag{3.27}$$

Equation (3.27) is multiplied by Γ_p and mean is taken, leading to

$$\left(\sum_{k=1}^{n} \sum_{l,m=1}^{P} a_m^{(jk)} a_l^{(jk)} \mathbf{g}_{lm} \right) \begin{bmatrix} \lambda_{j1} \\ \vdots \\ \lambda_{jP} \end{bmatrix} = \sum_{r,l,m=1}^{P} \sum_{g,k=1}^{n} \mathbf{v}_{g0}^T \mathbf{A}_r \mathbf{v}_{k0} a_m^{(jk)} a_l^{(jg)} \mathbf{g}_{lmr} \tag{3.28}$$

which, if the system matrix is given by a KL expansion, reduces to

$$\left(\sum_{k=1}^{n}\sum_{l,m=1}^{P} a_m^{(jk)} a_l^{(jk)} \mathbf{g}_{lm}\right)\begin{bmatrix}\lambda_{j1}\\ \vdots \\ \lambda_{jP}\end{bmatrix} = \sum_{k=1}^{n}\lambda_0^{(k)}\sum_{l,m=1}^{P} a_m^{(jk)} a_l^{(jk)}\mathbf{e}_{0lm} + \sum_{g,k=1}^{n}\sum_{i}^{M}\mathbf{v}_{g0}^T\mathbf{A}_i\mathbf{v}_{k0}^T\sum_{l,m=1}^{P} a_m^{(jk)} a_l^{(jg)}\mathbf{e}_{1ilm} \quad (3.29)$$

where $\mathbf{g}_{lm}$ is a matrix indexed by (k,p) and $\mathbf{e}_{0lm}$, $\mathbf{e}_{1ilm}$ and $\mathbf{g}_{lmr}$ are vectors indexed by p. The set of coefficients $a_k^{(ji)}$ have yet not been defined. They are calculated in the next section, following the spectral constrained coefficient method.

3.4 Updating of the eigenvectors

When considering a deterministic eigenvalue problem, several iterative methods are available to approximate each eigenvector with a desired accuracy (Wilkinson, 1965). The power method is based on the fact that a symmetric matrix $\mathbf{B}$ with eigenvalues χ_i and eigenvectors $\mathbf{x}_i$ multiplied s times by itself can be expressed in terms of the s-th power of its eigenvalues through $\mathbf{B}^s = \sum_{i=1}^{n}\chi_i^s\mathbf{x}_i\mathbf{x}_i^T$. If the eigenvalues have distinct values, the expression is dominated by $\sum_{i=1}^{r}\chi_i^s\mathbf{x}_i\mathbf{x}_i^T$ where χ_i are the r larger or dominant eigenvalues. Therefore, the power method is an iterative method that allows the eigenvector corresponding to the largest eigenvalue to be obtentained through $\mathbf{B}^s\mathbf{w}$, where $\mathbf{w}$ is the start-vector of the iteration algorithm, and s is the step of the iteration. A shift of origin (i.e. $(\mathbf{B}-p\mathbf{I}_n)$, where $p\in\mathbb{R}$) allow convergence of $(\mathbf{B}-p\mathbf{I}_n)^s\mathbf{w}$ to different eigenvectors. When the inverse of $\mathbf{B}$ is considered, it is observed that $\mathbf{B}^{-s}$ is dominated by $\sum_{i=1}^{r}(1/\chi_i^s)\,\mathbf{x}_i\mathbf{x}_i^T$ where χ_i are the r smallest eigenvalues. If the power method is applied to the matrix $(\mathbf{B}-p\mathbf{I}_n)^{-1}$, the inverse power method is obtained, and the product $(\mathbf{B}-p\mathbf{I}_n)^{-s}\mathbf{w}$ converges to the eigenvector corresponding to the eigenvalue closest to p (Wilkinson, 1965). In a deterministic system, these two methods allow to update a given approximation to an eigenvector. In the following subsections, the power and inverse power methods are extended to the stochastic case for updating the PC expansions of the eigenvectors. Two other methods are also developed to update eigenvectors, based on the eigenvalue equation $(\mathbf{A}-\lambda^{(j)}\mathbf{I})\mathbf{v}^{(j)}=0$. It is noted that if the eigenvalue is assumed to be the first order perturbation from Equation (3.3) and the

eigevector $\mathbf{v}^{(i)}$ is assumed to be the deterministic eigenvalue plus a summation of coefficients α_{ji} multiplying the other deterministic eigenvectors, the coefficients α_{ji} obtained are the ones from the first order perturbation method. The RSCCM and SCCM are expected to improve the first order perturbation method for two reasons. Firstly, the approximation to λ^j used is more accurate that the one used for the first order perturbation. Secondly, the eigenvector is given by the deterministic eigenvalue plus a summation of coefficients multiplying a set of vectors spanning a subspace orthogonal to the deterministic eigenvector, and these coefficients are given by PC expansions instead of the scalars used in the first order perturbation method.

It is noted that the methods applied do not enforce the orthogonality of eigenvectors, and neither is it enforced in the perturbation method. The eigenvectors will be orthogonal if the PC expansion obtained is an accurate representation of the eigenvectors.

3.4.1 Reduced spectral power method

The power method has been used in the context of spectral stochastic finite element method (SSFEM) by Lee and Singh (1994) to obtain the mean and covariance of the eigenvectors. Only one iteration was performed, so that the random eigenvectors were obtained by multiplying the deterministic eigenvectors by the system stochastic matrix from Equation (1.103). Here, the equation used to derive the reduced spectral power method (RSPM) is based on the deterministic power method equation

$$\lambda^{(j)}_{(q)}\mathbf{v}^{(j)}_{(q+1)} = \mathbf{A}\mathbf{v}^{(j)}_{(q)} \tag{3.30}$$

where the subscripts (q) and $(q+1)$ indicate the number of the iteration. Substituting the PC expansion of eigenvalues from Equation (3.7) into Equation (3.30) leads to

$$\left(\sum_{k=1}^{P}\lambda_{jk(q)}\Gamma_k\right)\mathbf{v}^{(j)}_{(q+1)} = \mathbf{A}\mathbf{v}^{(j)}_{(q)} \tag{3.31}$$

where the initial approximation to the eigenvector is given by

$$\mathbf{v}^{(j)}_{(0)} = \mathbf{v}_{j0} + \sum_{i=1}^{M}\xi_i\mathbf{v}_{ji} \tag{3.32}$$

Substituting Equation (3.8) into Equation (3.31) and applying the Galerkin method to the resulting equation would lead to a $P \times n$ linear system from where the unknown vectors $\mathbf{v}_k^{(j)}$ could be retrieved. A reduction in the system is performed by projecting the q-th iteration of the j-th eigenvector $\mathbf{v}_{(q)}^{(j)}$ into the subspace defined by the deterministic eigenvector and its derivatives, as in Equation (3.20). In the iterative case, eigenvector and constants $\mathbf{v}^{(j)}$, $a_{0k}^{(j)}$ and $a_{ik}^{(j)}$ are obtained from an iteration and, therefore, are expressed respectively as $\mathbf{v}_{(q)}^{(j)}$, $a_{0k,(q)}^{(j)}$ and $a_{ik,(q)}^{(j)}$. The system is reduced from a $P \times n$ system to a $(M+1) \times P$ system, and the unknowns of the reduced system are the set of coefficients $a_{0k}^{(j)}$, $a_{ik}^{(j)}$ for $k = 1, \ldots, P$ and $i = 1, \ldots M$. Equation (3.31) projected in the subspace span$\{\mathbf{v}_{j0}, \ldots, \mathbf{v}_{ji}\}$ can be rewritten as

$$\left(\sum_{l=1}^{P} \lambda_{jl(q)} \Gamma_l\right) \mathbf{V}_j^T \mathbf{V}_j \begin{bmatrix} \sum_{k=1}^{P} a_{0k,(q+1)}^{(j)} \Gamma_k \\ \vdots \\ \sum_{k=1}^{P} a_{Mk,(q+1)}^{(j)} \Gamma_k \end{bmatrix} = \mathbf{V}_j^T \mathbf{A} \mathbf{V}_j \begin{bmatrix} \sum_{k=1}^{P} a_{0k,(q)}^{(j)} \Gamma_k \\ \vdots \\ \sum_{k=1}^{P} a_{Mk,(q)}^{(j)} \Gamma_k \end{bmatrix} \tag{3.33}$$

The iterative algorithm can be derived easily by multiplying Equation (3.33) by Γ_p and taking the mean

$$\sum_{l=1}^{P} \lambda_{jl(q)} \mathbf{V}_j^T \mathbf{V}_j \begin{bmatrix} \sum_{k=1}^{P} a_{0k,(q+1)}^{(j)} \mathrm{E}\left[\Gamma_k \Gamma_l \Gamma_p\right] \\ \vdots \\ \sum_{k=1}^{P} a_{Mk,(q+1)}^{(j)} \mathrm{E}\left[\Gamma_k \Gamma_l \Gamma_p\right] \end{bmatrix} = \mathrm{E}\left[\Gamma_p \mathbf{V}_j^T \mathbf{A} \mathbf{V}_j \begin{bmatrix} \sum_{k=1}^{P} a_{0k,(q)}^{(j)} \Gamma_k \\ \vdots \\ \sum_{k=1}^{P} a_{Mk,(q)}^{(j)} \Gamma_k \end{bmatrix} \right] \tag{3.34}$$

An expression for $\mathbf{v}_{(1)}^{(j)}$ is calculated, which corresponds to one iteration. An accurate solution is expected from one iteration as the first-order perturbation of eigenvectors are close to the exact solution. Furthermore, accuracy might be compromised if a large number of iterations are performed. This is so because the deterministic power method converges to the eigenvector corresponding to the largest eigenvalue when a considerable number of iterations are performed. The first iteration is obtained from Equation (3.34) where $a_{01,(0)} = a_{i2,(0)} = 1$ and all the other coefficients are 0 and $\lambda_{jl(0)}$ are obtained from Equation (3.19). The vector of unknown coefficients $\mathbf{a} = [a_{01(1)}^{(j)} \cdots a_{0M(1)}^{(j)} a_{11(1)}^{(j)} \cdots a_{ip(1)}^{(j)} \cdots a_{MP(1)}^{(j)}]^T$ is the solution to the the linear system

$$\left(\sum_{l=1}^{P} (\lambda_{jl(0)} \mathbf{V}_j^T \mathbf{V}_j \otimes \mathbf{e}_{0l})\right) \mathbf{a} = \mathbf{f} \tag{3.35}$$

The $P \times P$ matrices $\mathbf{e}_{0l}$ are such that their k-th row and p-th element is e_{0lkp} and

$$\mathbf{f} = \begin{bmatrix} \sum_{r=1}^{P} \mathbf{v}_{j0}^T \mathbf{A}_r \mathbf{v}_{j0} \mathbf{c}_{0r} + \sum_{i=1}^{M} \sum_{r=1}^{P} \mathbf{v}_{j0}^T \mathbf{A}_r \mathbf{v}_{jk} \mathbf{c}_{1ir} \\ \sum_{r=1}^{P} \mathbf{v}_{j1}^T \mathbf{A}_r \mathbf{v}_{j0} \mathbf{c}_{0r} + \sum_{i=1}^{M} \sum_{r=1}^{P} \mathbf{v}_{j1}^T \mathbf{A}_r \mathbf{v}_{jk} \mathbf{c}_{1ir} \\ \vdots \\ \sum_{r=1}^{P} \mathbf{v}_{jM}^T \mathbf{A}_r \mathbf{v}_{j0} \mathbf{c}_{0r} + \sum_{i=1}^{M} \sum_{r=1}^{P} \mathbf{v}_{jM}^T \mathbf{A}_r \mathbf{v}_{jk} \mathbf{c}_{1ir} \end{bmatrix} \tag{3.36}$$

can be rewritten, for the case of a system matrix given by a KL expansion, as

$$\mathbf{f} = \begin{bmatrix} \lambda_0^{(j)} \mathbf{d}_0 + \sum_{i=1}^{M} \mathbf{v}_{j0}^T \mathbf{A}_i \mathbf{v}_{j0} \mathbf{d}_{1i} + \sum_{i,k=1}^{M} \mathbf{v}_{j0}^T \mathbf{A}_i \mathbf{v}_{jk} \mathbf{d}_{2ik} \\ \sum_{i=1}^{M} \left(\mathbf{v}_{j1}^T \mathbf{A}_0 \mathbf{v}_{ji} + \mathbf{v}_{j1}^T \mathbf{A}_i \mathbf{v}_{0j} \right) \mathbf{d}_{1i} + \sum_{i,k=1}^{M} \mathbf{v}_{j1}^T \mathbf{A}_i \mathbf{v}_{jk} \mathbf{d}_{2ik} \\ \vdots \\ \sum_{i=1}^{M} \left(\mathbf{v}_{jM}^T \mathbf{A}_0 \mathbf{v}_{ji} + \mathbf{v}_{jM}^T \mathbf{A}_i \mathbf{v}_{0j} \right) \mathbf{d}_{1i} + \sum_{i,k=1}^{M} \mathbf{v}_{jM}^T \mathbf{A}_i \mathbf{v}_{jk} \mathbf{d}_{2ik} \end{bmatrix} \tag{3.37}$$

The deterministic power method can update the eigenvectors if the initial approximation is close to the solution, but as the number of iterations increases, the method converges to the eigenvector corresponding to the largest eigenvalue. The reduced spectral power method is likely to suffer from the same drawback. The reduced spectral inverse power method is derived in the next subsection to try to overcome this difficulty.

3.4.2 Reduced spectral inverse power method

The reduced spectral inverse power method (RSIPM) developed here is based on the deterministic inverse power method equation

$$\left(\mathbf{A} - \lambda_0^{(j)} \mathbf{I}_n \right) \mathbf{v}_{(q+1)}^{(j)} = \left(\lambda_{(q)}^{(j)} - \lambda_0^{(j)} \right) \mathbf{v}_{(q)}^{(j)} \tag{3.38}$$

where the subscripts (q) and $(q+1)$ indicate the number of the iteration. Substitution of the PC expansion of eigenvalues from Equation (3.7) into Equation (3.38) leads to

$$\left(\mathbf{A} - \lambda_0^{(j)} \mathbf{I}_n \right) \mathbf{v}_{(q+1)}^{(j)} = \left(\sum_{k=1}^{P} \lambda_{jk(q)} \Gamma_k - \lambda_0^{(j)} \right) \mathbf{v}_{(q)}^{(j)} \tag{3.39}$$

where the initial approximation to the eigenvector is given by Equation (3.32). As in the previous subsection, an approximation to $\mathbf{v}_{(q+1)}^{(j)}$ could be obtained by applying the Galerkin method to Equation (3.39). This approximation requires the solution of a $P \times n$ linear system. A reduction of the size of the system is achieved by projecting the equation in the subspace span$\{\mathbf{v}_{j0}, \ldots, \mathbf{v}_{ji}\}$ where the size of the new system is

$(M+1) \times P$. The approximation to the j-th eigenvector $\mathbf{v}_{(q+1)}^{(j)}$ can be expressed as the eigenvector from Equation (3.21) where subscripts $(q+1)$ are added to $\mathbf{v}^{(j)}$, $a_{0k}^{(j)}$ and $a_{ik}^{(j)}$. The projection of Equation (3.39) leads to

$$\left(\mathbf{V}_j^T \mathbf{A} \mathbf{V}_j - \lambda_0^{(j)} \mathbf{V}_j^T \mathbf{V}_j\right) \begin{bmatrix} \sum_{k=1}^{P} a_{0k,(q+1)}^{(j)} \Gamma_k \\ \vdots \\ \sum_{k=1}^{P} a_{Mk,(q+1)}^{(j)} \Gamma_k \end{bmatrix} = \left(\sum_{k=1}^{P} \lambda_{jk(q)} \Gamma_k - \lambda_0^{(j)}\right) \mathbf{V}_j^T \mathbf{V}_j \begin{bmatrix} \sum_{k=1}^{P} a_{0k,(q)}^{(j)} \Gamma_k \\ \vdots \\ \sum_{k=1}^{P} a_{Mk,(q)}^{(j)} \Gamma_k \end{bmatrix} \tag{3.40}$$

The unknowns of the iteration can be obtained by multiplying Equation (3.40) by Γ_p and taking the mean

$$\sum_{r=1}^{P} \mathbf{V}_j^T \mathbf{A}_r \mathbf{V}_j \begin{bmatrix} \sum_{k=1}^{P} a_{0k,(q+1)}^{(j)} \mathrm{E}\left[\Gamma_r \Gamma_k \Gamma_p\right] \\ \vdots \\ \sum_{k=1}^{P} a_{Mk,(q+1)}^{(j)} \mathrm{E}\left[\xi_i \Gamma_k \Gamma_p\right] \end{bmatrix} - \lambda_0^{(j)} \mathbf{V}_j^T \mathbf{V}_j \begin{bmatrix} \sum_{k=1}^{P} a_{0k,(q+1)}^{(j)} \mathrm{E}\left[\Gamma_k \Gamma_p\right] \\ \vdots \\ \sum_{k=1}^{P} a_{Mk,(q+1)}^{(j)} \mathrm{E}\left[\Gamma_k \Gamma_p\right] \end{bmatrix} =$$
$$\sum_{l=1}^{P} \lambda_{jk(q)} \mathbf{V}_j^T \mathbf{V}_j \begin{bmatrix} \sum_{k=1}^{P} a_{0k,(q)}^{(j)} \mathrm{E}\left[\Gamma_k \Gamma_l \Gamma_p\right] \\ \vdots \\ \sum_{k=1}^{P} a_{Mk,(q)}^{(j)} \mathrm{E}\left[\Gamma_k \Gamma_l \Gamma_p\right] \end{bmatrix} - \lambda_0^{(j)} \mathbf{V}_j^T \mathbf{V}_j \begin{bmatrix} \sum_{k=1}^{P} a_{0k,(q)}^{(j)} \mathrm{E}\left[\Gamma_k \Gamma_p\right] \\ \vdots \\ \sum_{k=1}^{P} a_{Mk,(q)}^{(j)} \mathrm{E}\left[\Gamma_k \Gamma_p\right] \end{bmatrix} \tag{3.41}$$

For the first iteration, the approximation to the j-th eigenvalue $\sum_{k=1}^{P} \lambda_{jk(q)} \Gamma_k$ can be obtained from Equation (3.19), that is, after applying the Rayleigh quotient using the first-order perturbation of eigenvectors. The coefficients used for the first iteration are $a_{01,(0)} = a_{i2,(0)} = 1$ and all the other coefficients of vector $\mathbf{a}$ are 0. The unknown coefficients $a_{0k,(1)}$ and $a_{ik,(1)}$ can be found by solving a linear system of equations where

$$\mathbf{S} = \left(\sum_{r=1}^{P} (\mathbf{V}_j^T \mathbf{A}_r \mathbf{V}_j) \otimes \mathbf{e}_{0q} - \lambda_0^{(j)} (\mathbf{V}_j^T \mathbf{V}_j) \otimes \mathbf{c}_0\right) \tag{3.42}$$

reduces, if the system matrix is given by a KL expansion, to

$$\mathbf{S} = \left(\sum_{i=1}^{M} (\mathbf{V}_j^T \mathbf{A}_i \mathbf{V}_j) \otimes \mathbf{c}_{1i} + (\mathbf{V}_j^T (\mathbf{A}_0 - \lambda_0^{(j)} \mathbf{I}) \mathbf{V}_j) \otimes \mathbf{c}_0\right) \tag{3.43}$$

such that

$$\mathbf{S}\begin{bmatrix} a_{01(1)} \\ \vdots \\ a_{0M(1)} \\ a_{11(1)} \\ \vdots \\ a_{ip(1)} \\ \vdots \\ a_{MP(1)} \end{bmatrix} = \begin{bmatrix} \lambda_{j1(0)}\mathrm{E}\left[\Gamma_1^2\right] - \lambda_0^{(j)}\mathrm{E}\left[\Gamma_1\right] \\ \vdots \\ \lambda_{jP(0)}\mathrm{E}\left[\Gamma_P^2\right] - \lambda_0^{(j)}\mathrm{E}\left[\Gamma_P\right] \\ \sum_{g=1}^{M}(\mathbf{v}_{j1})^T\mathbf{v}_{jg}(\sum_{k=1}^{P}\lambda_{jk(0)}\mathbf{c}_{1gk1} - \lambda_0^{(j)}\mathbf{d}_{1g1}) \\ \vdots \\ \sum_{g=1}^{M}(\mathbf{v}_{ji})^T\mathbf{v}_{jg}(\sum_{k=1}^{P}\lambda_{jk(0)}\mathbf{c}_{1gkp} - \lambda_0^{(j)}\mathbf{d}_{1gp}) \\ \vdots \\ \sum_{g=1}^{M}(\mathbf{v}_{jM})^T\mathbf{v}_{jg}(\sum_{k=1}^{P}\lambda_{jk(0)}\mathbf{c}_{1gkP} - \lambda_0^{(j)}\mathbf{d}_{1gP}) \end{bmatrix} \tag{3.44}$$

In the next section, a third method to update the eigenvectors is proposed.

3.4.3 Reduced spectral constrained coefficients method

The reduced spectral constrained coefficients method (RSCCM) developed here is based on the eigenvalue equation

$$\left(\mathbf{A} - \lambda_{(q)}^{(j)}\mathbf{I}_n\right)\mathbf{v}_{(q+1)}^{(j)} = \mathbf{0}_n \tag{3.45}$$

where the subscripts (q) and $(q+1)$ indicate the number of the iteration and $\mathbf{0}_n = [0\ldots0]^T \in \mathbb{N}^n$. The quantity $\lambda_{(q)}^{(j)}$ is the PC expansion of the jth eigenvalue from the q-th iteration. Substitution of the PC expansion of eigenvalues from Equation (3.7) into Equation (3.45) leads to

$$\left(\mathbf{A} - \sum_{k=1}^{P}\lambda_{jk(q)}\Gamma_k\mathbf{I}_n\right)\mathbf{v}_{(q+1)}^{(j)} = \mathbf{0}_n \tag{3.46}$$

where the initial approximation to the eigenvalues is given by Equation (3.19). As in the previous subsections, an approximation to $\mathbf{v}_{(q+1)}^{(j)}$ could be obtained by applying the Galerkin method to Equation (3.46) and assuming a term of $\mathbf{v}_{(q+1)}^{(j)} = [v_{1(q+1)}^{(j)}\ldots v_{n(q+1)}^{(j)}]^T$ is known and equal to one. This assumption allows the removal of the singularity of the linear matrix. The 'constrained' term, that is the term set to one, is the element whose value is expected to be the largest. Heuristically, it is assumed that this term is the term of $\mathbf{v}_{(q+1)}^{(j)}$ in the position of the largest term of the deterministic eigenvector. If another term of the PC expansion of the eigenvector were to be larger, our assumption of the position of the largest term of the vector would not be correct. Therefor, the method

would be repeated by constraining this term, that is, the term in the position of the obtained largest term, to one. This approximation requires the solution of a $P \times (n-1)$ linear system.

A reduction to the size of the system is achieved by projecting the equation in the subspace span$\{\mathbf{v}_{j0}, \ldots, \mathbf{v}_{ji}\}$ where the size of the new system matrix is $n \times (M+1)$. This projection is equivalent to express the j-th eigenvector $\mathbf{v}^{(j)}_{(q+1)}$ as the eigenvector from Equation (3.21) where subscripts $(q+1)$ are added to $\mathbf{v}^{(j)}$, $a^{(j)}_{0k}$ and $a^{(j)}_{ik}$. The projection of Equation (3.46) leads to

$$\left(\mathbf{V}_j^T\mathbf{A}\mathbf{V}_j - \sum_{k=1}^{P}\lambda_{jk(q)}\Gamma_k\mathbf{V}_j^T\mathbf{V}_j\right)\begin{bmatrix}\sum_{k=1}^{P} a^{(j)}_{0k,(q+1)}\Gamma_k \\ \vdots \\ \sum_{k=1}^{P} a^{(j)}_{Mk,(q+1)}\Gamma_k\end{bmatrix} = \mathbf{0}_{M+1} \tag{3.47}$$

The unknowns of the iteration can be obtained by multiplying Equation (3.47) by Γ_p and taking the mean

$$\left(\sum_{i=1}^{P}\left(\mathbf{V}_j^T\mathbf{A}_i\mathbf{V}_j - \lambda_{ji(q)}\mathbf{V}_j^T\mathbf{V}_j\right)\right)\begin{bmatrix}\sum_{k=1}^{P} a^{(j)}_{0k,(q+1)}\mathrm{E}\left[\Gamma_i\Gamma_k\Gamma_p\right] \\ \vdots \\ \sum_{k=1}^{P} a^{(j)}_{Mk,(q+1)}\mathrm{E}\left[\Gamma_i\Gamma_k\Gamma_p\right]\end{bmatrix} = \mathbf{0}_{M+1} \tag{3.48}$$

Reordering the rows and columns obtained from the previous system considering $k = 1, \ldots, P$, the coefficients $[a_{01}, \ldots, a_{0M}, a_{11}, \ldots, a_{ip}, \ldots, a_{MP}]$ are the solution of the system

$$\left(\sum_{i=1}^{P}(\mathbf{V}_j^T\mathbf{A}_i\mathbf{V}_j - \lambda_{ji(q)}(\mathbf{V}_j^T\mathbf{V}_j)) \otimes \mathbf{e}_{0i}\right)\mathbf{a} = \mathbf{0}_{P(M+1)} \tag{3.49}$$

If the system matrix is given by a KL expansion,this system of equations reduces to

$$\left((\mathbf{V}_j^T\mathbf{A}_0\mathbf{V}_j) \otimes \mathbf{c}_0 + \sum_{i=1}^{M}(\mathbf{V}_j^T\mathbf{A}_i\mathbf{V}_j) \otimes \mathbf{c}_{1i} - \sum_{i=1}^{P}\lambda_{ji(q)}(\mathbf{V}_j^T\mathbf{V}_j) \otimes \mathbf{e}_{0i}\right)\mathbf{a} = \mathbf{0}_{P(M+1)} \tag{3.50}$$

As in the case of the full system, it is assumed that vector $[a^{(j)}_{01(q+1)} \ldots a^{(j)}_{0P(q+1)}] = [1\,0\,\ldots\,0]$, and a squared system matrix of dimension $P \times M$ is obtained. For the first iteration, the approximation to the j-th eigenvalue $\sum_{k=1}^{P}\lambda_{jk}\Gamma_k$ can be obtained from Equation (3.19), that is, after applying the Rayleigh quotient using the first-order perturbation of eigenvectors.

3.4.4 Spectral constrained coefficients method

The spectral constrained coefficients method (SCCM) developed here is based on the eigenvalue equation given by Equation (3.45), where the eigenvector $\mathbf{v}_{(q+1)}^{(j)}$ is projected in the set of deterministic eigenvectors $\mathbf{V}_0$, as in Equation (3.26), such that

$$\mathbf{V}_0^T \left(\mathbf{A} - \lambda_{(q)}^{(j)} \mathbf{I}_n \right) \mathbf{V}_0 \begin{bmatrix} \sum_{k=1}^{P} a_{k(q+1)}^{(j1)} \Gamma_k \\ \vdots \\ \sum_{k=1}^{P} a_{k(q+1)}^{(jn)} \Gamma_k \end{bmatrix} = \mathbf{0}_n \tag{3.51}$$

It is assumed that the vector of coefficient multiplying the j-th eigenvector is $[a_{1(q+1)}^{(jj)} \dots a_{P(q+1)}^{(jj)}] = [1\, 0 \dots 0]$. The rectangular matrix of eigenvectors where the j-th eigenvector is not included is denoted by $\mathbf{V}_{0j}$ and the resulting system is given by

$$\left(\sum_{k=1}^{P} \left(\mathbf{V}_{0j}^T \mathbf{A}_k \mathbf{V}_{0j} - \lambda_{jk} \mathbf{I}_{n-1} \right) \Gamma_k \right) \begin{bmatrix} \sum_{k=1}^{P} a_{k(q+1)}^{(j1)} \Gamma_k \\ \vdots \\ \sum_{k=1}^{P} a_{k(q+1)}^{(j(j-1))} \Gamma_k \\ \sum_{k=1}^{P} a_{k(q+1)}^{(j(j+1))} \Gamma_k \\ \vdots \\ \sum_{k=1}^{P} a_{k(q+1)}^{(jn)} \Gamma_k \end{bmatrix} = - \begin{bmatrix} \sum_{i=1}^{P} \mathbf{v}_{10}^T \mathbf{A}_i \mathbf{v}_{j0} \Gamma_i \\ \vdots \\ \sum_{i=1}^{P} \mathbf{v}_{(j-1)0}^T \mathbf{A}_i \mathbf{v}_{j0} \Gamma_i \\ \sum_{i=1}^{P} \mathbf{v}_{(j+1)0}^T \mathbf{A}_i \mathbf{v}_{j0} \Gamma_i \\ \vdots \\ \sum_{i=1}^{P} \mathbf{v}_{N0}^T \mathbf{A}_i \mathbf{v}_{j0} \Gamma_i \end{bmatrix} \tag{3.52}$$

As formerly, the system of equations is multiplied by Γ_p and mean is taken

$$\left(\sum_{k=1}^{P} (\mathbf{V}_{0j}^T \mathbf{A}_k \mathbf{V}_{0j} - \lambda_{jk(q)} \mathbf{I}_{n-1}) \otimes \mathbf{e}_{0k} \right) \begin{bmatrix} a_{1(q+1)}^{(j(1))} \\ \vdots \\ a_{P(q+1)}^{(j(j-1))} \\ a_{1(q+1)}^{(j(j+1))} \\ \vdots \\ a_{P(q+1)}^{(jn)} \end{bmatrix} = - \sum_{i=1}^{P} \left(\mathbf{V}_0^T \mathbf{A}_i \mathbf{v}_{j0} \right) \otimes \mathbf{c}_{0i} \tag{3.53}$$

where -th column of matrix $\mathbf{c}_0$. $\mathbf{c}_{0i}$ is the iIf the system matrix can be expressed through a KL expansion, the previous equation reduces to

$$\left(\mathbf{\Lambda}_{0j}\otimes\mathbf{c}_0+\sum_{i=1}^{M}\mathbf{V}_{0j}^T\mathbf{A}_i\mathbf{V}_{0j}\otimes\mathbf{c}_{1i}-\sum_{k=1}^{P}\lambda_{jk(q)}\mathbf{I}_{n-1}\otimes\mathbf{e}_{0k}\right)\begin{bmatrix}a_{1(q+1)}^{(j(1))}\\ \vdots\\ a_{P(q+1)}^{(j(j-1))}\\ a_{1(q+1)}^{(j(j+1))}\\ \vdots\\ a_{P(q+1)}^{(jn)}\end{bmatrix}=-\sum_{i=1}^{M}\left(\mathbf{V}_0^T\mathbf{A}_i\mathbf{v}_{j0}\right)\otimes\mathbf{d}_{1i} \tag{3.54}$$

where $\mathbf{\Lambda}_{0j}$ is a diagonal matrix whose diagonal elements are the set of deterministic eigenvalues $\lambda_0^{(j)}$. The initial approximation $\lambda_{(0)}^{(j)}$ is j-th diagonal term from $\mathbf{V}_0^T\mathbf{A}\mathbf{V}_0$. In the next section, the proposed methods are summarized.

3.5 Summary of the proposed methods

Three hybrid perturbation-PC approximations and an approximation based on a projection on the deterministic eigenvectors basis are proposed for the solution of the algebraic random eigenvalue problem arising in structural dynamics. The random eigenvalues are firstly approximated with a PC expansion using the first-order perturbation of eigenvectors in the Rayleigh quotient. These results can be further improved if the eigenvectors are updated using the reduced spectral power method, the reduced spectral inverse power method, the reduced spectral constrained coefficients method or the spectral constrained coefficients method (RSPM, RSIPM, RSCCM and SCCM) respectively. These methods allow us to obtain PC expansions of the eigenvectors. These expansions are then used in the Rayleigh quotient to obtain an improved PC expansion of each eigenvalue. Alternatively, direct MCS can be performed on the Rayleigh quotient to obtain the moments of the eigenvalues. The proposed methods can be implemented by the following steps:

1. Calculate $\mathbf{A}_0$ and the system KL expansion matrices $\mathbf{A}_i\ \forall i=1,\ldots,M$.
2. Obtain the deterministic eigenvalues and eigenvectors $\lambda_0^{(j)}$, $\mathbf{v}_{0j}$.
3. Use Equation (3.6) to obtain the first-order perturbation of eigenvectors $\mathbf{v}^{(j)}=\mathbf{v}_{0j}+\sum_{i=1}^{M}\xi_i\partial\mathbf{v}^{(j)}/\partial\xi_i$.

4. Calculate the PC expansion of eigenvalues using the Rayleigh quotient from Equation (3.19), obtained using the first-order perturbation of eigenvectors and the truncated Karhunen-Loève expansion of the stiffness matrix.

5. Calculate a new approximation to eigenvectors using one of the four proposed methods:

   - The coefficients of the PC expansions involved in each eigenvector approximation are obtained with the reduced spectral power method (RSPM) from Equation (3.35).
   - The coefficients of the PC expansions involved in each eigenvector approximation are obtained with the reduced spectral inverse power method (RSIPM) from Equation (3.44).
   - The coefficients of the PC expansions involved in each eigenvector approximation are obtained with the reduced spectral constrained coefficients method (RSCCM) from Equation (3.49) or Equation (3.50) if the system matrix is given by a KL expansion.
   - The coefficients of the PC expansions involved in each eigenvector approximation are obtained with the spectral constrained coefficients method (SCCM) from Equation (3.53) or Equation (3.54) if the system matrix is given by a KL expansion.

6. Calculate the PC expansion of eigenvalues using Rayleigh quotient as in step 4 if another step of the iteration is going to be performed.

7. Calculate the first and second moments of the eigenvalues using Equation (3.10) and (3.11) or through direct MCS of the Rayleigh quotient using the PC expansion of the eigenvectors.

3.6 Numerical example: Euler-Bernoulli beam with stochastic properties

A clamped-free beam with equation of motion

$$-\frac{\partial^2}{\partial x^2}\left(EI(x,\varpi)\frac{\partial^2 v}{\partial x^2}\right)-\rho A\frac{\partial^2 v}{\partial t^2}+p_y=0 \quad \text{Throughout} \quad -L/2\leq x\leq L/2 \tag{3.55}$$

with v the vertical displacement of the centroidal axis, p_y the vertical load applied to the beam and $EI(x,\theta)$ is represented by a random field. The system is shown in Figure 3.1, where the values of the parameters appearing in the equation are given. The

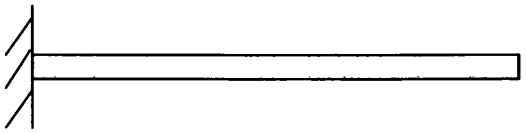

Figure 3.1: Euler-Bernoulli beam with spatially varying random bending rigidity $w(x,\varpi)$. The length of the beam is $L = 1.65$ m, the section area is $A = 8.2123e-5$ m^2, the density is $\rho = 7800$ kg/m^3 and the mean of the bending rigidity random field is $\mathrm{E}\left[w(x,\varpi)\right] = 5.7520$ kg.m^2.

system is discretized with the finite element method, using $n = 100$ elements. Details of the method can be found, for example, in the book by Dawe (1984). Uncertainty is introduced in the system by a Gaussian random field representing the bending rigidity, that is, $w(x,\varpi) = EI$ with mean $\mathrm{E}\left[w(x,\varpi)\right] = 5.7520$ kg.m^2. The discretization of $w(x,\varpi)$ is done by the KL decomposition of the exponential autocorrelation function $C(x_1,x_2) = e^{-|x_1-x_2|/L}$ as explained in subsection 1.4.4. The KL expansion is truncated after $M = 5$ terms, so that the corresponding KL expansion of the stiffness matrix is $\mathbf{A} = \mathbf{A}_0 + \sum_{i=1}^{5} \xi_i \mathbf{A}_i$. The effect of two different standard deviations of the random field is studied. These standard deviations are respectively 7% and 15% of the mean of the random field. These standard deviations are considered with the view that they represent the cases of low and high randomness without producing a swapping of the modes. The maximum order of the Hermite polynomial used is 4, so that $P = 126$ polynomials are used as basis functions. Only the results corresponding to the first 10 eigenvalues are considered as the chances of modal overlap increases for higher modes.

Results obtained with the proposed methods are compared against the results from first-order perturbation method from Equation (3.3) and MCS with 5000 samples. Convergence of the MCS results is ensured by choosing this number of samples. The moments are obtained by performing MCS on the Rayleigh quotients using PC expansion of eigenvectors and 5000 samples. Figures 3.2 and 3.3 show the mean and standard deviation of the eigenvalues obtained with the first order perturbation and proposed methods for a standard deviation of 7% of the mean of the random field. In these figures the variation of percentage error of the corresponding quantities with respect to MCS results are also shown. The percentage errors are explicitly reported in Tables 3.1

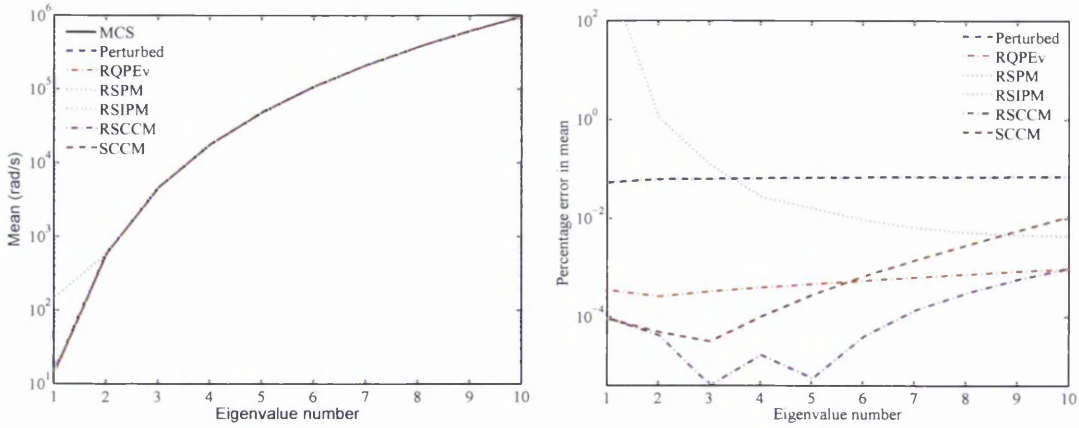

(a) Mean of the eigenvalues.

(b) Percentage error in the mean.

Figure 3.2: Mean and corresponding percentage error of the first ten eigenvalues of the beam obtained with Monte Carlo Simulation (MCS) using 5000 samples, first-order perturbation method (Perturbed), Rayleigh quotient using first-order perturbation of eigenvectors (RQPEv) the proposed reduced spectral power method (RSPM), reduced spectral inverse power method (RSIPM), reduced spectral constrained coefficient method (RSCCM) and spectral constrained coefficient method (SCCM). The standard deviation of the discretized random field is 7% of the mean value.

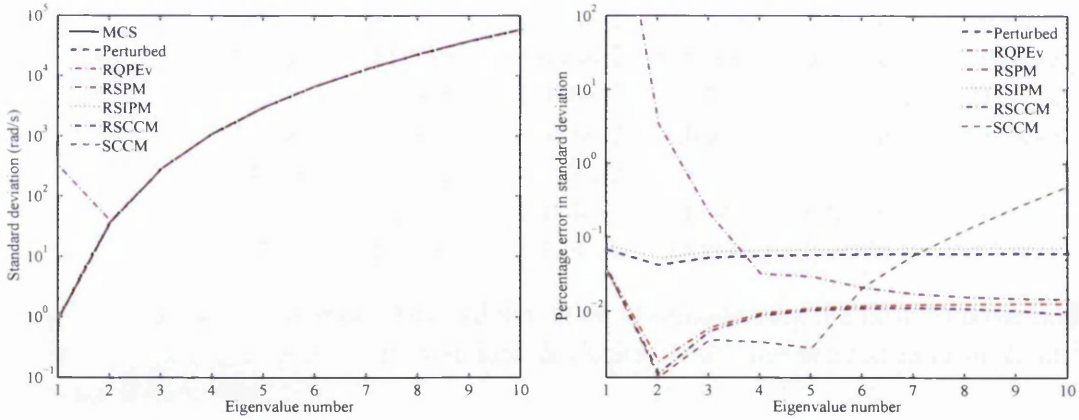

(a) Standard deviation of the eigenvalues.

(b) Percentage error in the standard deviation.

Figure 3.3: Standard deviation and corresponding percentage error of the first ten eigenvalues of the beam obtained with Monte Carlo Simulation (MCS) using 5000 samples, Perturbed, RQPEv, RSPM, RSIPM, RSCCM and SCCM. The standard deviation of the random field is 7% of the mean value.

and 3.2 to show the relative accuracies of the different methods.

Now we consider the case of higher uncertainty. Figures 3.4 and 3.5 show the mean and standard deviation of the eigenvalues obtained with the first order perturbation and the proposed methods for a standard deviation of 15% of the mean of the random field.

The variation of percentage error with different modes with respect to MCS results

Eigenvalue Number	Perturbed	RQPEv	RSPM	RSIPM	SRCCM	SCCM
$\lambda^{(1)}$	5.191e-2	3.441e-4	8.992e+2	5.190e-2	9.358e-5	9.012e-5
$\lambda^{(2)}$	6.079e-2	2.562e-4	1.077e+0	6.079e-2	4.161e-5	4.877e-5
$\lambda^{(3)}$	6.158e-2	3.244e-4	1.206e-1	6.158e-2	4.050e-6	3.156e-5
$\lambda^{(4)}$	6.372e-2	3.872e-4	2.686e-2	6.372e-2	1.660e-5	9.959e-5
$\lambda^{(5)}$	6.504e-2	4.519e-4	1.553e-2	6.504e-2	5.550e-6	2.764e-4
$\lambda^{(6)}$	6.584e-2	5.236e-4	9.030e-3	6.584e-2	3.941e-5	6.475e-4
$\lambda^{(7)}$	6.633e-2	6.053e-4	6.235e-3	6.633e-2	1.333e-4	1.373e-3
$\lambda^{(8)}$	6.665e-2	6.982e-4	4.975e-3	6.665e-2	2.969e-4	2.762e-3
$\lambda^{(9)}$	6.687e-2	8.026e-4	4.436e-3	6.687e-2	5.569e-4	5.427e-3
$\lambda^{(10)}$	6.702e-2	9.188e-4	4.274e-3	6.702e-2	9.474e-4	1.067e-2

Table 3.1: Percentage errors in mean obtained using the proposed methods for the first ten eigenvalues. The standard deviation of the discretized random field is 7% of the mean value.

Eigenvalue Number	Perturbed	RQPEv	RSPM	RSIPM	SRCCM	SCCM
$\lambda^{(1)}$	6.637e-2	3.550e-2	3.101e+4	7.637e-2	3.492e-2	3.491e-2
$\lambda^{(2)}$	4.129e-2	2.095e-3	3.372e+0	5.128e-2	1.442e-3	1.285e-3
$\lambda^{(3)}$	5.174e-2	5.921e-3	2.050e-1	6.174e-2	5.311e-3	4.053e-3
$\lambda^{(4)}$	5.472e-2	9.169e-3	3.143e-2	6.471e-2	8.549e-3	3.806e-3
$\lambda^{(5)}$	5.650e-2	1.083e-2	2.884e-2	6.650e-2	1.015e-2	3.165e-3
$\lambda^{(6)}$	5.747e-2	1.154e-2	2.026e-2	6.747e-2	1.072e-2	2.074e-2
$\lambda^{(7)}$	5.804e-2	1.190e-2	1.674e-2	6.804e-2	1.081e-2	5.613e-2
$\lambda^{(8)}$	5.840e-2	1.211e-2	1.523e-2	6.840e-2	1.057e-2	1.230e-1
$\lambda^{(9)}$	5.864e-2	1.225e-2	1.454e-2	6.864e-2	9.965e-3	2.472e-1
$\lambda^{(10)}$	5.881e-2	1.236e-2	1.423e-2	6.880e-2	8.899e-3	4.813e-1

Table 3.2: Percentage errors in standard deviation obtained using the proposed methods for the first ten eigenvalues. The standard deviation of the discretized random field is 7% of the mean value.

are also shown. The percentage errors are again explicitly given in Tables 3.3 and 3.4 to show the relative accuracies of the different methods. As expected, in general the errors are larger than the ones from the previous case where the amount of randomness in the system was comparatively lower.

It can be observed that the error of the RSIPM and the first-order perturbation method are very close. This is due to the fact that, if the random variables are set to zero, the matrix of the RSIPM becomes singular. For small standard deviation, it is heuristically expected that the projection of the updated eigenvector on the deterministic eigenvector is much larger than the projection on the other vectors. An eigenvector updated with RSIPM is consequently likely to be close to the related deterministic

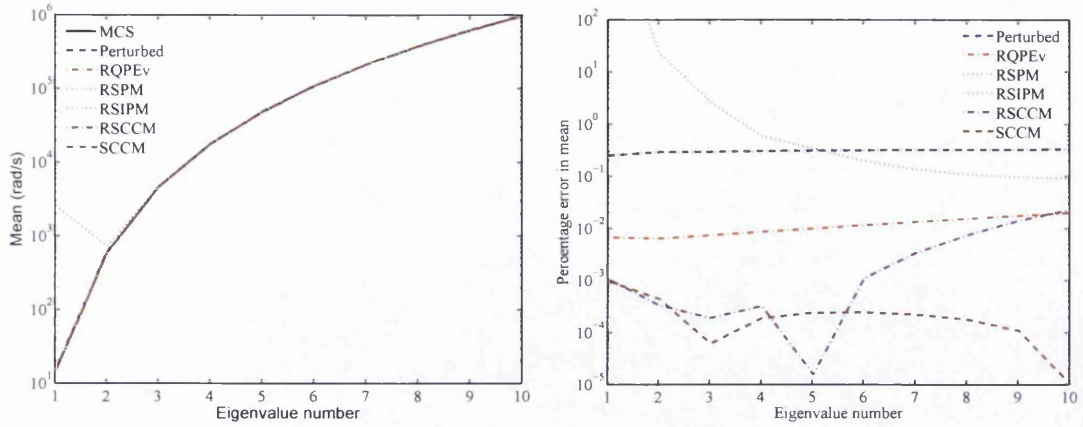

(a) Mean of the eigenvalues.

(b) Percentage error in the mean.

Figure 3.4: Mean and corresponding percentage error of the first ten eigenvalues of the beam obtained with Monte Carlo Simulation (MCS) using 5000 samples, Perturbed, RQPEv, RSPM, RSIPM, RSCCM and SCCM. The standard deviation of the random field is 15% of the mean value.

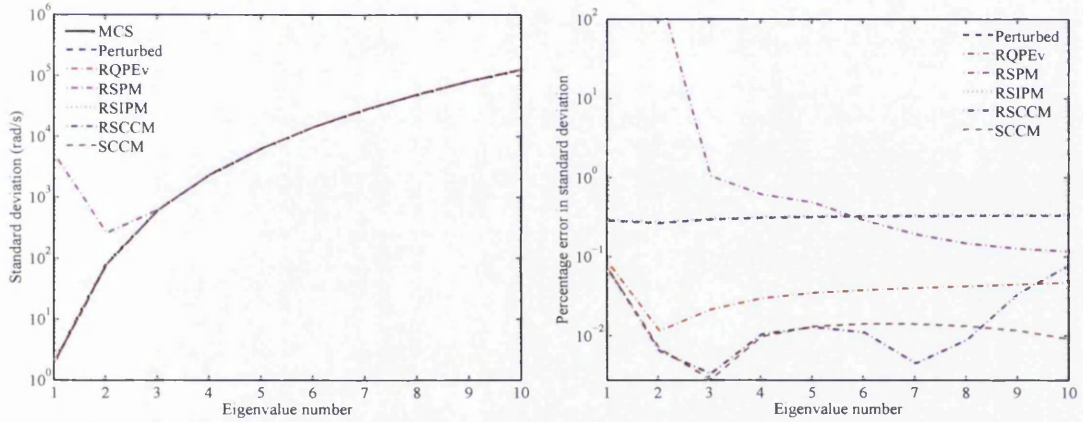

(a) Standard deviation of the eigenvalues.

(b) Percentage error in the standard deviation.

Figure 3.5: Standard deviation and corresponding percentage error of the first ten eigenvalues of the beam obtained with Monte Carlo Simulation (MCS) using 5000 samples, Perturbed, RQPEv, RSPM, RSIPM, RSCCM and SCCM. All the standard deviations of Rayleigh quotients have been obtained with MCS using 5000 samples. The standard deviation of the discretized random field is 15% of the mean value.

eigenvector. The first-order perturbation method can be considered as the result of applying the Rayleigh quotient using the deterministic eigenvectors. Consequently, it is expected that both methods lead to similar results.

For the RSPM it can be observed that the error of the first eigenvalue is the highest of all. It has already been commented that the power method converges to the largest eigenvalues, and this fact is likely to be the reason behind the error in the approximation to the first eigenvalues. Consequently, the RSPM is expected to lead to good results for

Eigenvalue Number	Perturbed	RQPEv	RSPM	RSIPM	SRCCM	SCCM
$\lambda^{(1)}$	2.436e-1	6.603e-3	1.694e+4	2.436e-1	1.037e-3	9.479e-4
$\lambda^{(2)}$	2.846e-1	6.281e-3	2.324e+1	2.846e-1	3.263e-4	4.351e-4
$\lambda^{(3)}$	2.884e-1	7.245e-3	2.638e+0	2.884e-1	1.856e-4	5.955e-5
$\lambda^{(4)}$	2.986e-1	8.433e-3	5.809e-1	2.986e-1	3.142e-4	1.837e-4
$\lambda^{(5)}$	3.048e-1	9.715e-3	3.356e-1	3.048e-1	1.530e-5	2.338e-4
$\lambda^{(6)}$	3.086e-1	1.116e-2	1.940e-1	3.086e-1	1.080e-3	2.371e-4
$\lambda^{(7)}$	3.109e-1	1.280e-2	1.330e-1	3.109e-1	3.284e-3	2.144e-4
$\lambda^{(8)}$	3.124e-1	1.465e-2	1.053e-1	3.124e-1	7.208e-3	1.705e-4
$\lambda^{(9)}$	3.134e-1	1.669e-2	9.297e-2	3.134e-1	1.360e-2	1.039e-4
$\lambda^{(10)}$	3.141e-1	1.891e-2	8.865e-2	3.141e-1	2.189e-2	9.950e-6

Table 3.3: Percentage errors in mean obtained using the proposed methods for the first ten eigenvalues. The standard deviation of the discretized random field is 15% of the mean value.

Eigenvalue Number	Perturbed	RQPEv	RSPM	RSIPM	SRCCM	SCCM
$\lambda^{(1)}$	2.782e-1	8.210e-2	2.258e+5	2.882e-1	6.755e-2	6.727e-2
$\lambda^{(2)}$	2.591e-1	1.134e-2	2.222e+2	2.690e-1	6.361e-3	6.800e-3
$\lambda^{(3)}$	2.875e-1	2.097e-2	1.026e+0	2.975e-1	3.262e-3	2.751e-3
$\lambda^{(4)}$	3.012e-1	2.915e-2	5.953e-1	3.112e-1	1.024e-2	9.579e-3
$\lambda^{(5)}$	3.090e-1	3.392e-2	4.719e-1	3.190e-1	1.262e-2	1.285e-2
$\lambda^{(6)}$	3.134e-1	3.676e-2	2.779e-1	3.234e-1	1.077e-2	1.385e-2
$\lambda^{(7)}$	3.161e-1	3.898e-2	1.862e-1	3.261e-1	4.393e-3	1.377e-2
$\lambda^{(8)}$	3.178e-1	4.105e-2	1.428e-1	3.278e-1	8.731e-3	1.292e-2
$\lambda^{(9)}$	3.190e-1	4.312e-2	1.222e-1	3.290e-1	3.322e-2	1.131e-2
$\lambda^{(10)}$	3.198e-1	4.527e-2	1.130e-1	3.298e-1	7.636e-2	8.809e-3

Table 3.4: Percentage errors in standard deviation obtained using the proposed methods for the first ten eigenvalues. The standard deviation of the discretized random field is 15% of the mean value.

the larger eigenvalues, which are not studied here.

We note that the SRCCM and the SCCM results are more accurate than the ones obtained with the Rayleigh quotient using first-order perturbation eigenvectors. This observation is particularly true for the mean results. For standard deviation, the results for the three methods are very similar for the case of lower standard deviation of $w(x, \varpi)$, although SCCM performs better for few eigenvalues. For the case of higher standard deviation of $w(x, \varpi)$, SCCM performs better than the other two methods. Based on relative accuracy of the different methods, it is finally observed that the most promising method aimed at updating eigenvectors from first-order perturbation method is SCCM.

3.7 Numerical example: Thin plate with stochastic properties

A clamped-free plate is considered, where its equation of motion is given by

$$\frac{\partial Q_x}{\partial x} + \frac{\partial Q_y}{\partial y} - 2\rho h\ddot{w} + p = 0 \quad \text{where} \quad \begin{cases} Q_x = \frac{\partial M_x}{\partial x} + \frac{\partial M_{xy}}{\partial y} \\ Q_y = \frac{\partial M_y}{\partial y} + \frac{\partial M_{xy}}{\partial y} \end{cases} \tag{3.56}$$

In the above equation M_x, M_y, M_{xy} are the bending moments per unit length given by

$$\boldsymbol{\mathcal{M}} = \begin{bmatrix} M_x \\ M_y \\ M_{xy} \end{bmatrix} = -D(x,y,\varpi) \begin{bmatrix} \begin{bmatrix} \frac{\partial^2 w}{\partial x^2} + \nu \frac{\partial^2 w}{\partial y^2} \\ \frac{\partial^2 w}{\partial y^2} + \nu \frac{\partial^2 w}{\partial x^2} \end{bmatrix} \\ (1-\nu)\frac{\partial^2 w}{\partial x \partial y} \end{bmatrix} \tag{3.57}$$

where $D(x,y,\varpi)$ is the random bending rigidity, ν is Poisson's ratio, p is the force applied to the plate and w is the vertical displacement. The system is shown in Figure 3.6, where values of the parameters appearing in the equation are provided. The system is

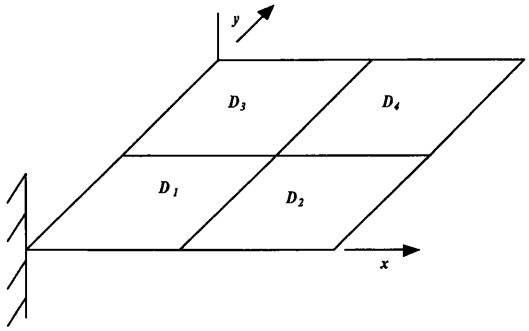

Figure 3.6: Kirchhoff-Love plate with $D(x,y,\varpi)$ given by $D_i = D_0(1+\epsilon\xi_i)$ for each subsystem. The length $L_x = 1.0$ m, width $L_y = 0.6$ m, Poisson's ratio $\nu = 0.3$, modulus of elasticity $E = 200$ GPa, thickness $h = 3$ mm and density $\rho = 7860$ kg/m^3 when the mean system is considered.

discretized with the finite element method, using a rectangular mesh with $n_x = 10$ elements on the length of the plate and $n_y = 6$ elements on its width. Details of the method can be found, for example, in the book by Dawe (1984). Uncertainty is introduced in the system by a set of independent normal Gaussian random variables ξ_i, each one affecting a different substructure of the plate. The plate is divided into 4 substructures and each of them is affected by uncertainty through the effect of $D_i = D_0(1+\epsilon\xi_i)$,

with $D_0 = Eh^3/12(1-\nu^2)$. The plate is divided into 4 rectangular plates as can be seen in Figure 3.6, so that the first substructure is composed by the first five elements in x direction and first three in y direction. The global stiffness matrix of the system can then be represented by $\mathbf{A} = \mathbf{A}_0 + \sum_{i=1}^{4} \xi_i \mathbf{A}_i$, where $\mathbf{A}_0$ is the deterministic system matrix and $\mathbf{A}_i$ are obtained by considering only the elements of a given subsystem, it is noted that ϵ is included in $\mathbf{A}_i$. The effect of two different standard deviations of the random variables is studied. These standard deviations are respectively $\epsilon = 0.07$ and $\epsilon = 0.15$. As formerly, standard deviations of 7% and 15% are considered with the view that they represent the cases of low and high randomness without producing a swapping of the modes. The maximum order of the Hermite polynomial used is 4, so that $P = 70$ polynomials are used as basis functions. Only the results corresponding to the first 10 eigenvalues are considered as the chances of modal overlap increases for higher modes.

Results obtained with the proposed methods are compared against the results from first-order perturbation method from Equation (3.3) and MCS with 5000 samples. Convergence of the MCS results is ensured by choosing this number of samples. The moments are obtained by performing MCS on the Rayleigh quotients using PC expansion of eigenvectors and 5000 samples. Figures 3.7 and 3.8 show the mean and standard deviation of the eigenvalues obtained with the first order perturbation and proposed methods for a standard deviation of 7% of the mean of the random field. In these figures the variation of percentage error of the corresponding quantities with respect to MCS results are also shown. The percentage errors are explicitly reported in Tables 3.5 and 3.6 to show the relative accuracies of the different methods.

For the case of a standard deviation of 15% of the mean of the random variables D_i, Figures 3.9 and 3.10 show the mean and standard deviation of the eigenvalues obtained with the first order perturbation and the proposed methods

The variation of percentage error with different modes with respect to MCS results are also shown. The percentage errors are again explicitly given in Tables 3.7 and 3.8 to show the relative accuracies of the different methods. As formerly, in general the errors are larger than the ones from the previous case where the amount of randomness in the system was comparatively lower.

The results observed for the plate problem are quantitatively similar to the ones of the beam problem. That is, results from the RSIPM and the first-order perturbation method are very close, the RSPM leads to the highest error for the smallest eigenvalues,

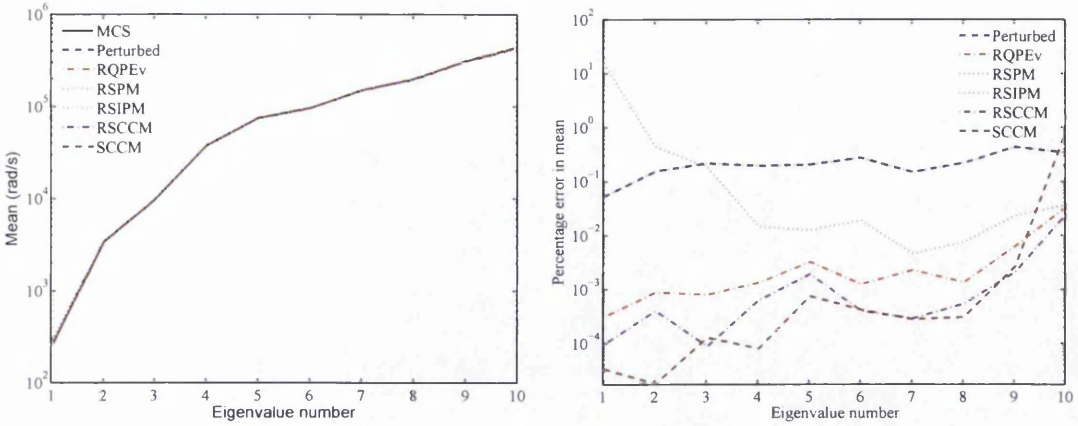

(a) Mean of the eigenvalues.

(b) Percentage error in the mean.

Figure 3.7: Mean and corresponding percentage error of the first ten eigenvalues of the plate obtained with Monte Carlo Simulation (MCS) using 5000 samples, first-order perturbation method (Perturbed), Rayleigh quotient using first-order perturbation of eigenvectors (RQPEv) the proposed reduced spectral power method (RSPM), reduced spectral inverse power method (RSIPM), reduced spectral constrained coefficient method (RSCCM) and spectral constrained coefficient method (SCCM). The standard deviation of the discretized random variables is 7% of the mean value.

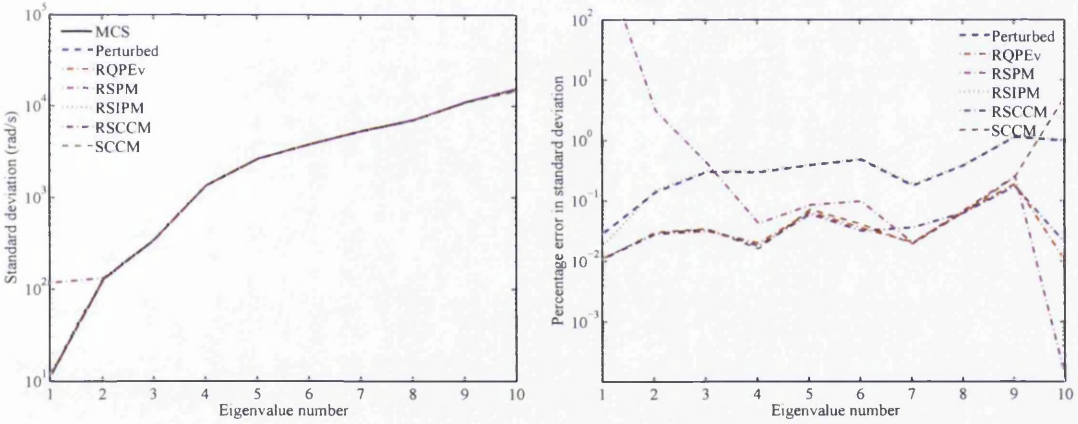

(a) Standard deviation of the eigenvalues.

(b) Percentage error in the standard deviation.

Figure 3.8: Standard deviation and corresponding percentage error of the first ten eigenvalues of the plate obtained with Monte Carlo Simulation (MCS) using 5000 samples, Perturbed, RQPEv, RSPM, RSIPM, RSCCM and SCCM. The standard deviation of the random variables is 7% of the mean value.

and the SRCCM and the SCCM results are more accurate than the ones obtained with the Rayleigh quotient using first-order perturbation eigenvectors for the mean results and very similar for standard deviation.

Eigenvalue Number	Perturbed	RQPEv	RSPM	RSIPM	SRCCM	SCCM
$\lambda^{(1)}$	5.107e-2	3.001e-4	1.509e+1	5.107e-2	9.311e-5	3.232e-5
$\lambda^{(2)}$	1.506e-1	8.505e-4	4.325e-1	1.506e-1	3.916e-4	1.737e-5
$\lambda^{(3)}$	2.120e-1	7.736e-4	1.807e-1	2.120e-1	8.601e-5	1.248e-4
$\lambda^{(4)}$	1.917e-1	1.298e-3	1.449e-2	1.917e-1	6.129e-4	7.883e-5
$\lambda^{(5)}$	2.025e-1	3.185e-3	1.238e-2	2.025e-1	1.888e-3	7.403e-4
$\lambda^{(6)}$	2.704e-1	1.223e-3	1.885e-2	2.704e-1	3.949e-4	4.149e-4
$\lambda^{(7)}$	1.467e-1	2.251e-3	4.536e-3	1.467e-1	2.854e-4	2.762e-4
$\lambda^{(8)}$	2.185e-1	1.333e-3	7.507e-3	2.185e-1	5.322e-4	3.022e-4
$\lambda^{(9)}$	4.268e-1	6.113e-3	2.266e-2	4.268e-1	2.037e-3	2.555e-3
$\lambda^{(10)}$	3.368e-1	3.303e-2	3.620e-2	3.368e-1	2.412e-2	8.304e-1

Table 3.5: Percentage errors in mean obtained using the proposed methods for the first ten eigenvalues. The standard deviation of the random variables is 7% of the mean value.

Eigenvalue Number	Perturbed	RQPEv	RSPM	RSIPM	SRCCM	SCCM
$\lambda^{(1)}$	2.812e-2	1.082e-2	8.969e+2	1.811e-2	1.071e-2	1.077e-2
$\lambda^{(2)}$	1.326e-1	2.689e-2	3.017e+0	1.426e-1	2.762e-2	2.892e-2
$\lambda^{(3)}$	2.908e-1	3.028e-2	4.031e-1	3.007e-1	3.221e-2	3.302e-2
$\lambda^{(4)}$	2.843e-1	1.918e-2	4.057e-2	2.943e-1	1.723e-2	1.553e-2
$\lambda^{(5)}$	3.745e-1	6.247e-2	8.215e-2	3.844e-1	5.818e-2	6.927e-2
$\lambda^{(6)}$	4.636e-1	3.406e-2	9.456e-2	4.735e-1	3.059e-2	3.949e-2
$\lambda^{(7)}$	1.707e-1	1.984e-2	1.925e-2	1.807e-1	3.490e-2	1.870e-2
$\lambda^{(8)}$	3.748e-1	6.264e-2	6.717e-2	3.848e-1	6.113e-2	6.195e-2
$\lambda^{(9)}$	1.101e+0	1.829e-1	2.444e-1	1.111e+0	1.667e-1	2.387e-1
$\lambda^{(10)}$	9.523e-1	9.147e-3	1.032e-4	9.622e-1	1.849e-2	5.505e+0

Table 3.6: Percentage errors in standard deviation obtained using the proposed methods for the first ten eigenvalues. The standard deviation of the random variables is 7% of the mean value.

3.8 Conclusions

In this Chapter, four new methods have been proposed and compared to improve the accuracy of the approximate solution of the random eigenvalue problem for symmetric matrices. The first two methods, namely the reduced spectral power method (RSPM) and the reduced spectral inverse power method (RSIPM), are based on approaches used in the context of the deterministic eigenvalue problem to obtain eigenvectors, respectively, the power method and the inverse power method. The next two methods, namely, the reduced spectral constrained coefficients method (RSCCM) and the spectral constrained coefficients method (SCCM), are based on the equation of the eigenvalue prob-

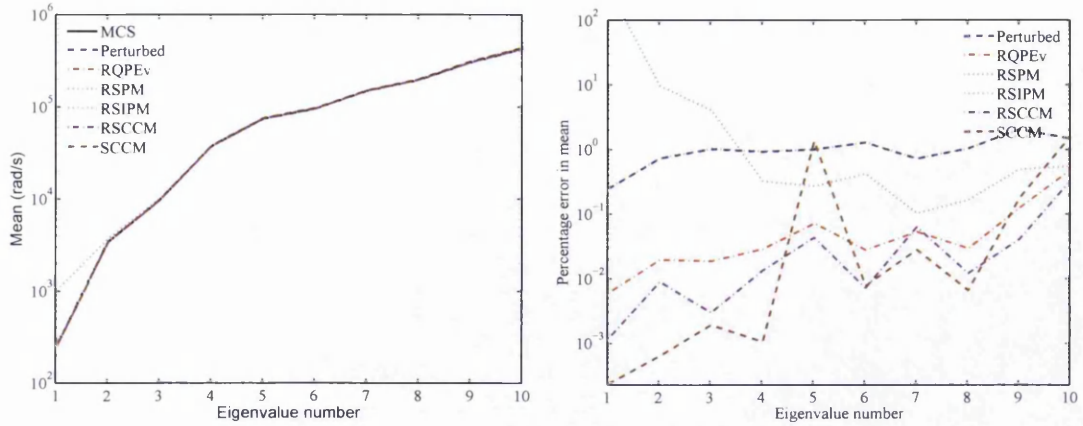

(a) Mean of the eigenvalues. (b) Percentage error in the mean.

Figure 3.9: Mean and corresponding percentage error of the first ten eigenvalues of the plate obtained with Monte Carlo Simulation (MCS) using 5000 samples, Perturbed, RQPEv, RSPM, RSIPM, RSCCM and SCCM. The standard deviation of the random variables is 15% of the mean value.

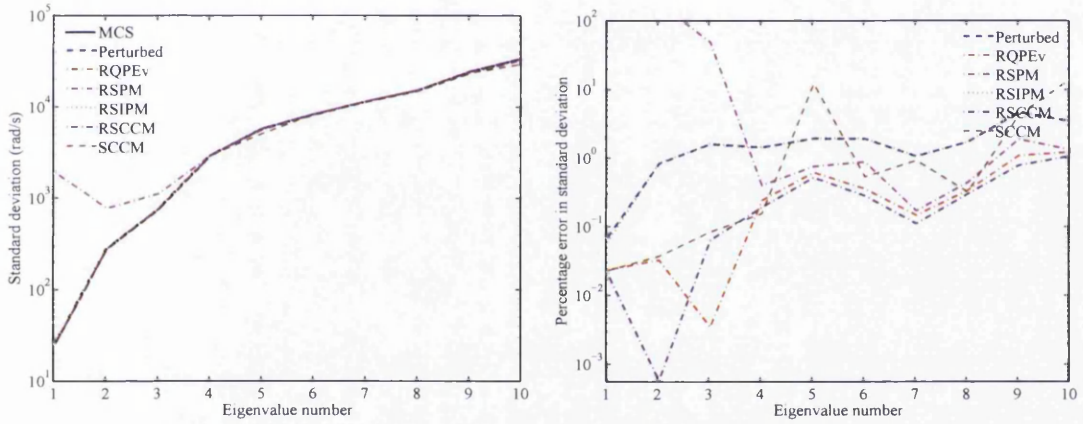

(a) Standard deviation of the eigenvalues. (b) Percentage error in the standard deviation.

Figure 3.10: Standard deviation and corresponding percentage error of the first ten eigenvalues of the plate obtained with Monte Carlo Simulation (MCS) using 5000 samples, Perturbed, RQPEv, RSPM, RSIPM, RSCCM and SCCM. All the standard deviations of Rayleigh quotients have been obtained with MCS using 5000 samples. The standard deviation of the random variables is 15% of the mean value.

lem. The deterministic methods to update the eigenvectors are adapted to the stochastic case through a projection in a truncated set of basis functions of a Hilbert space. These basis functions are the multivariate Hermite polynomials used in the PC method. The four proposed methods lead to a polynomial chaos (PC) expansion of eigenvectors. Furthermore, a size reduction of the equations is achieved by assuming that, in the PC expansion of eigenvectors, the coefficient vectors belong to the subspace spanned by the deterministic vector and its derivatives with respect to the random variables. Eigen-

Eigenvalue Number	Perturbed	RQPEv	RSPM	RSIPM	SRCCM	SCCM
$\lambda^{(1)}$	2.397e-1	5.774e-3	3.052e+2	2.397e-1	1.143e-3	2.260e-4
$\lambda^{(2)}$	7.094e-1	1.887e-2	9.392e+0	7.094e-1	8.680e-3	6.156e-4
$\lambda^{(3)}$	9.930e-1	1.808e-2	3.961e+0	9.930e-1	2.910e-3	1.862e-3
$\lambda^{(4)}$	9.039e-1	2.799e-2	3.142e-1	9.039e-1	1.306e-2	1.026e-3
$\lambda^{(5)}$	9.804e-1	7.018e-2	2.652e-1	9.804e-1	4.247e-2	1.332e+0
$\lambda^{(6)}$	1.259e+0	2.718e-2	4.131e-1	1.259e+0	7.032e-3	7.573e-3
$\lambda^{(7)}$	7.082e-1	5.194e-2	1.008e-1	7.082e-1	6.192e-2	2.750e-2
$\lambda^{(8)}$	1.021e+0	2.886e-2	1.624e-1	1.021e+0	1.194e-2	6.461e-3
$\lambda^{(9)}$	1.993e+0	1.229e-1	4.831e-1	1.993e+0	3.995e-2	1.732e-1
$\lambda^{(10)}$	1.445e+0	4.774e-1	5.438e-1	1.445e+0	3.263e-1	1.592e+0

Table 3.7: Percentage errors in mean obtained using the proposed methods for the first ten eigenvalues. The standard deviation of the random variables is 15% of the mean value.

Eigenvalue Number	Perturbed	RQPEv	RSPM	RSIPM	SRCCM	SCCM
$\lambda^{(1)}$	6.671e-2	2.246e-2	7.305e+3	5.671e-2	2.012e-2	2.201e-2
$\lambda^{(2)}$	8.021e-1	3.122e-2	1.753e+2	8.120e-1	5.569e-4	3.573e-2
$\lambda^{(3)}$	1.544e+0	3.329e-3	4.659e+1	1.554e+0	6.104e-2	8.079e-2
$\lambda^{(4)}$	1.384e+0	2.318e-1	3.848e-1	1.394e+0	1.841e-1	1.491e-1
$\lambda^{(5)}$	1.869e+0	5.965e-1	7.282e-1	1.879e+0	5.037e-1	1.182e+1
$\lambda^{(6)}$	1.858e+0	3.449e-1	8.519e-1	1.868e+0	2.738e-1	5.179e-1
$\lambda^{(7)}$	1.037e+0	1.423e-1	1.655e-1	1.047e+0	1.079e-1	8.992e-1
$\lambda^{(8)}$	1.677e+0	3.303e-1	4.297e-1	1.687e+0	2.914e-1	3.134e-1
$\lambda^{(9)}$	4.542e+0	1.061e+0	1.833e+0	4.551e+0	7.637e-1	4.138e+0
$\lambda^{(10)}$	3.358e+0	1.189e+0	1.288e+0	3.368e+0	1.042e+0	1.382e+1

Table 3.8: Percentage errors in standard deviation obtained using the proposed methods for the first ten eigenvalues. The standard deviation of the discretized random field is 15% of the mean value.

values are obtained from the updated eigenvectors using the Rayleligh quotient, where the eigenvectors are given by the PC expansion obtained from one of the four proposed methods. A PC expansion of each eigenvalue is proposed by projecting the Rayleigh quotient into the PC basis functions. Numerical results suggest that the Rayleigh quotient using first-order perturbed eigenvectors outperforms RSPM and RSIPM when considering the smallest eigenvectors. The only methods leading to an improvement of the results would then be SCCM and RSCCM. This can be due to several facts. Firstly, the RSPM is expected to converge to the highest eigenvector, while the other methods should converge to all of them. Secondly, the RSIPM equation becomes singular for the case where the random variables are equal to zero, and as it has been observed,

the eigenvectors converge to the deterministic eigenvectors and the eigenvalues to the first order perturbation eigenvalues. Finally, the two other methods are based on the eigenvalue equation in the same way as the first order perturbation method for eigenvectors, but two improvements are introduced. The first one is that the approximation to the eigenvalue used in the equation is more accurate, and the second one is that the coefficients multiplying the vectors spanning a subspace orthogonal to the deterministic eigenvector are polynomials (i.e. given by PC expansions) instead of being scalars.

It was noted in Chapter 1 that the random eigenvalue problem is important in the context of structural dynamics. In this Chapter, the first two moments of eigenvalues and eigenvectors have been derived. Based on these moments, pdfs for the eigenvalues could be obtained using the maximum entropy principle (Kapur, 1989). In the next Chapter, the first two moments of the response of a dynamic system are calculated using moments of eigenvalues and eigenvectors.

Chapter 4

Low-Frequency response of stochastic dynamic systems

4.1 Introduction

In this Chapter the dynamic problem is considered, when the response is obtained through the modal decomposition of the operator. The work carried out considers vibrations in the low frequency domain, such as, for example, the ones originated during earthquakes, affecting civil structures like buildings, in the region of 0 to 125 rad/s (Filiatrault, 2002). Other vibrations affecting these structures can be caused by machinery and are in the region of 370 to 1200 rad/s. In the previous Chapter, methods to obtain a spectral representation for the eigensolution of a dynamic system were derived and, based on these, the moments of eigenvalues and eigenvectors could be obtained. We recall that the frequency response function (FRF) of a dynamic system as a function of the eigenvalues and eigenvectors $\lambda^{(j)} = \omega_j^2$, $\boldsymbol{\phi}^{(j)}$ is given by (Meirovitch, 1967)

$$\mathbf{u} = \sum_{j=1}^{N} \left[\frac{\boldsymbol{\phi}^{(j)} \left(\boldsymbol{\phi}^{(j)} \right)^T}{-\omega^2 + 2\mathrm{i}\omega\zeta_j\omega_j + \omega_j^2} \right] \mathbf{f} \tag{4.1}$$

It was observed in Chapter 1 that, on the one hand, efforts have been made to obtain results on systems eigenvalues and eigenvectors statistics. On the other hand, few works investigate about response statistics of dynamic problems based on those results. In this Chapter, a pdf is assumed for each random eigenvalue, and eigenvalues are assumed independent. This assumption may not be valid for high frequencies, where overlap between eigenvalues appears. Therefore, the proposed method is expected to work well

at low frequencies.

This Chapter focuses on obtaining the mean and variance of the response from the pdf of the eigenvalues. The outline of the Chapter is as follows. In section 4.2, single-degree-of-freedom (SDOF) systems are investigated. The calculation of the response pdf is outlined in subsection 4.2.1 and the expressions for the mean and standard deviation are derived in subsection 4.2.2. These expressions depend on the calculation of three integrals, which are evaluated through Laplace's method and through a proposed modified Laplace's method in Subsections 4.2.2 and 4.2.2. Exact expressions of the mean and standard deviation are obtained for the uniform distribution of eigenvalues in subsection 4.3.1. Laplace's method and modified Laplace's method are used for normal, gamma and lognormal distributions respectively in Subsections 4.3.2, 4.3.3 and 4.3.4. The method is extended to obtain mean and standard deviation of the response for a multiple-degrees-of-freedom (MDOF) system in section 4.4. A numerical example for a MDOF system is shown in subsection 4.4.4, where the proposed methods are compared to MCS. The main results and the key conclusions of the Chapter are discussed in sections 4.5 and 4.6.

4.2 Single-degree-of-freedom (SDOF) systems

A single-degree-of-freedom system is the simplest way to model a structural dynamic system. The study of SDOF systems is often undertaken prior to the study of multiple-degrees-of-freedom systems due to physical insights and analytical conveniences. Solutions of an SDOF problem are easily obtained in comparison to MDOF problems. They are also useful when investigating the response of general MDOF problems, as MDOF problems with proportional damping reduce to a linear combination of SDOF problems. For an SDOF, the transfer function normalised with the mass is given by (Meirovitch, 1967)

$$h(\mathrm{i}\omega) = \frac{1}{(-\omega^2 + \mathrm{i}2\omega_n\zeta_n\omega + \omega_n^2)} \tag{4.2}$$

where ω_n and ζ_n are respectively the natural frequency and the damping factor, and ω is the frequency. The transfer function is a complex number for every nonzero ω, therefore, its moments can be related to the moments of its real and imaginary parts and its absolute value. The real and imaginary parts of the transfer function and its absolute

value are respectively given by

$$\Re\left(h(\omega,\omega_n)\right) = \frac{\omega_n^2 - \omega^2}{(\omega_n^2-\omega^2)^2 + 4\zeta_n^2\omega_n^2\omega^2} \tag{4.3}$$

$$\Im\left(h(\omega,\omega_n)\right) = \frac{-2\zeta_n\omega_n\omega}{(\omega_n^2-\omega^2)^2 + 4\zeta_n^2\omega_n^2\omega^2} \tag{4.4}$$

$$|h(\omega,\omega_n)| = \frac{1}{\sqrt{(\omega_n^2-\omega^2)^2 + 4\zeta_n^2\omega_n^2\omega^2}}. \tag{4.5}$$

In this set of equations, the squared natural frequency of the system ω_n^2 is assumed to be a random variable.

4.2.1 The probability density function of the response

Probability density functions of the real part, the imaginary part and the absolute value of the response can be found analytically if these quantities are considered as functions of one random variable, i.e. $x = \omega_n^2$. These functions (denoted by z) have to satisfy that their domain include the range of ω_n^2, z are Borel functions and $z(x,\omega) = \pm\infty$ has zero probability. All these conditions are ratified if $\zeta_n \neq 0$ and $\omega_n^2 = 0$ has zero probability. This is a physically realistic situation as it points to a damped system with positive natural frequency. If the new random variables $\Re\left(h(x,\omega)\right)$, $\Im\left(h(x,\omega)\right)$ and $|h(x,\omega)|$ are denoted by z, their pdf (denoted by f_z) can be derived using the transformation of random variables (see for example Papoulis and Pillai (2002))

$$z = z(x_1) = \cdots = z(x_n) = \ldots \tag{4.6}$$

$$f_z(z) = \frac{f_x(x_1)}{|z'(x_1)|} + \cdots + \frac{f_x(x_n)}{|z'(x_n)|} + \ldots \tag{4.7}$$

Here x_n are the real roots of $z = z(x)$, and $z'(x_n)$ is the derivative of $z(x)$ evaluated at x_n. The pdf of the real and imaginary parts of the transfer function and its absolute value are derived below.

- To obtain the pdf or the real part of the transfer function from Equation (4.7), the roots of Equation (4.6) with $z = \Re\left(h(x,\omega)\right)$ have to be obtained. The real part of the transfer function and its derivative with respect to x are given by

$$z = \frac{x-\omega^2}{(x-\omega^2)^2 + 4\zeta_n^2 x\omega^2}, \qquad z'(x) = \frac{-(x-\omega^2)^2 + 4\zeta_n^2 x\omega^2}{((x-\omega^2)^2 + 4\zeta_n^2 x\omega^2)^2}. \tag{4.8}$$

  The roots of $z = \Re\left(h(x,\omega)\right)$ are the roots of a second order polynomial, and are

given by

$$x_1 = \frac{-B - \sqrt{B^2 - 4AC}}{2A}, \quad x_2 = \frac{-B + \sqrt{B^2 - 4AC}}{2A} \tag{4.9}$$

with

$$A = z \tag{4.10}$$

$$B = z2\omega^2(2\zeta_n^2 - 1) - 1 \tag{4.11}$$

$$C = z\omega^4 + \omega^2. \tag{4.12}$$

The pdf of the real part of the transfer function is obtained by introducing $z'(x_i)$ and $f(x_i)$ in Equation (4.7), that is $f_{\Re}(z) = (f_x(x_1))/|z'(x_1)| + (f_x(x_2))/|z'(x_2)|$.

- For the imaginary part of response ($z = \Im(h(x,\omega))$), Equation (4.6) reduces to

$$z = \frac{-2\zeta_n\sqrt{x}\omega}{(x-\omega^2)^2 + 4\zeta_n^2 x\omega^2}. \tag{4.13}$$

From this equation, it can be derived that x_n are the roots of a third order polynomial

$$x_n^3 z^2 + x_n^2 4z^2\omega^2(2\zeta_n^2 - 1) + x_n 6\omega^4 z^2 + (4z^2\omega^6(2\zeta_n^2 - 1) + 4\zeta_n^2\omega^2) = 0. \tag{4.14}$$

The first derivative of z with respect to x is given by

$$z'(x) = -2\zeta_n\omega \frac{\frac{1}{2}x^{-1/2}((x-\omega^2)^2 + 4\zeta_n^2 x\omega^2) - (2(x-\omega^2) + 4\zeta_n^2\omega^2)x^{1/2}}{((x-\omega^2)^2 + 4\zeta_n^2 x\omega^2)^2}. \tag{4.15}$$

The pdf of the imaginary part of the transfer function is obtained by introducing $z'(x_n)$ and $f(x_n)$ into Equation (4.7).

- And finally, the absolute value of response and its derivative with respect to x are given by

$$z = \frac{1}{\sqrt{(x-\omega^2)^2 + 4\zeta_n^2 x\omega^2}} \tag{4.16}$$

$$z'(x) = -\frac{(2(x-\omega^2) + 4\zeta_n^2\omega^2)((x-\omega^2)^2 + 4\zeta_n^2 x\omega^2)^{-1/2}}{(x-\omega^2)^2 + 4\zeta_n^2 x\omega^2} \tag{4.17}$$

and the roots of $z = |h(x,\omega)|$ are the roots of a second order polynomial, and are

given by

$$x = \frac{-B \pm \sqrt{B^2 - 4AC}}{2A} \tag{4.18}$$

with

$$A = z \tag{4.19}$$

$$B = z^2 2\omega^2 (2\zeta_n^2 - 1) \tag{4.20}$$

$$C = -z^2\omega^4 - 1\,. \tag{4.21}$$

The pdf of the absolute value of the transfer function is obtained by introducing $z'(x)$ and $f(x_n)$ into Equation (4.7).

The derivation of the pdf of the response is not straightforward even for single-degree-of-freedom system. For multiple-degrees-of-freedom systems, the problem becomes even more difficult, and, generally, not analytically solvable.

4.2.2 Response statistics

It has been seen that the calculation of the pdf of the quantities of interest (i.e. real and imaginary parts of the FRF and its absolute value) is not straightforward. Therefore, we focus on the calculation of their moments. A method to calculate the moments could be MCS. Unfortunately, if few random variables are considered in the problem, the rate of convergence of MCS is slow (Babuska et al., 2005), so a different method is investigated. As formerly, a probability density function $f_x(x)$ is assumed for the random variable $x = \omega_n^2$, where $f_x(x \leq 0) = 0$. The first moment (mean) of the real part, imaginary part and the absolute value of the transfer function, derived from Equations (4.3), (4.4) and (4.5), are given by

$$\mathrm{E}\left[\Re(h)\right] = \int_{\mathcal{D}} \frac{x f_x(x)}{(x-\omega^2)^2 + 4\zeta_n^2\omega^2 x}\, dx - \omega^2 \int_{\mathcal{D}} \frac{f_x(x)}{(x-\omega^2)^2 + 4\zeta_n^2\omega^2 x}\, dx \tag{4.22}$$

$$\mathrm{E}\left[\Im(h)\right] = -2\zeta_n\omega \int_{\mathcal{D}} \frac{\sqrt{x} f_x(x)}{(x-\omega^2)^2 + 4\zeta_n^2\omega^2 x}\, dx \tag{4.23}$$

$$\mathrm{E}\left[|h|\right] = \sigma_h^2 + |\mathrm{E}\left[h\right]|^2 = \int_{\mathcal{D}} \frac{f_x(x)}{(x-\omega^2)^2 + 4\zeta_n^2\omega^2 x}\, dx \tag{4.24}$$

here $\mathcal{D}$ is the domain of x, $\mathrm{E}\left[h\right] = \mathrm{E}\left[\Re(h)\right] + \mathrm{i}\mathrm{E}\left[\Im(h)\right]$ is the mean of the transfer function and σ_h is its standard deviation. The square of the absolute value of the mean

is obtained by multiplying the mean by its complex conjugate, so that

$$|\mathrm{E}[h]|^2 = \mathrm{E}[\Re(h)]^2 + \mathrm{E}[\Im(h)]^2. \tag{4.25}$$

In the next section, integrals appearing in Equations (4.22), (4.23) and (4.24) are approximated with Laplace's method.

Laplace's method

Integrals appearing in Equations (4.22), (4.23) and (4.24) can be related to the Laplace's integral (see, for example, Erdèlyi (1956))

$$I(w) = \int_{x_1}^{x_2} g(x) e^{wy(x)}\, dx. \tag{4.26}$$

It is known that if w is a large positive number, the major contribution to the integral comes from the vicinity of points at which $y(x)$ assumes its largest value. If g is continuous, y is twice continuously differentiable and $y'(\theta) = 0$, $y''(\theta) < 0$, this integral can be approximated with Laplace's method as

$$I(w) \backsim g(\theta) e^{wy(\theta)} \left[\frac{-2\pi}{wy''(\theta)}\right]^{\frac{1}{2}}. \tag{4.27}$$

We will assume $g(x) = 1$ and $w = 1$. Then

$$I(w) \backsim \sqrt{2\pi} e^{y(\theta)} \left[-y''(\theta)\right]^{-\frac{1}{2}}. \tag{4.28}$$

A general function $y(x, a)$, obtained from integrals appearing in Equations (4.22), (4.23) and (4.24), can be given by

$$y(x, a) = \ln(f_x(x)) + a \ln(x) - \ln(|h(\omega, x)|^2) \tag{4.29}$$

where

$$a = 0 \quad \text{for} \quad \int_{\mathcal{D}} \frac{f_x(x)}{(x-\omega^2)^2 + 4\zeta_n^2\omega^2 x}\, dx \tag{4.30}$$

$$a = \frac{1}{2} \quad \text{for} \quad \int_{\mathcal{D}} \frac{\sqrt{x} f_x(x)}{(x-\omega^2)^2 + 4\zeta_n^2\omega^2 x}\, dx \tag{4.31}$$

$$a = 1 \quad \text{for} \quad \int_{\mathcal{D}} \frac{x f_x(x)}{(x-\omega^2)^2 + 4\zeta_n^2\omega^2 x}\, dx. \tag{4.32}$$

Function $y(x,a)$ is maximum at $x=\theta_a$. Therefore, θ_a is the solution of

$$\frac{f'_x(\theta_a)}{f_x(\theta_a)}+\frac{a}{\theta_a}-\frac{2(\theta_a-\omega^2)+4\omega^2\zeta_n^2}{(\theta_a-\omega^2)^2+4\zeta_n^2\omega^2\theta_a}=0 \tag{4.33}$$

for which $y(\theta_a,a)$ is the absolute maximum. The second derivative of $y(x,a)$ is

$$y''(x,a)=\bar{f}(x)-\frac{a}{x^2}-\bar{h}(x) \tag{4.34}$$

where

$$\bar{h}(x,\omega) = \frac{2}{(-\omega^2+x)^2+4\zeta_n^2\omega^2x}-\left(\frac{2(-\omega^2+x)+4\zeta_n^2\omega^2}{(-\omega^2+x)^2+4\zeta_n^2\omega^2x}\right)^2 \tag{4.35}$$

and $\bar{f}(x)$ depends on the pdf of the random variable x. The Laplace's method will be applied for different pdfs in the remaining of the Chapter.

Hybrid Laplace-numerical integration and modified Laplace

Laplace's method approximates Equation (4.29) with a second-degree polynomial given by the first two terms of Taylor expansion of $y(x)$ around its maximum θ_a. The method works well if the behavior of $y(x)$ in the vicinity of its absolute maximum point θ_a is well represented by the approximation used. From Equation (4.29) it may be observed that $y(x)$ is obtained through the addition of three functions. The first one, $\ln(f_x(x))$ is related to the pdf of the distribution of the random variable x. This pdf is chosen such that it has only one maximum, situated at $x=\mu$, with μ the mean of the distribution. It is expected that $\ln(f_x(x))$ will have its maximum at μ. The second function added to obtain $y(x)$ is $a\ln(x)$, an increasing function. The last function, $-\ln(|h(\omega,x)|^2)$, is related to the transfer function and therefore has its maximum at $\omega^2(1-2\zeta_n^2)$. The function $-\ln(|h(\omega,x)|^2)$ has three points (x_{h1}, x_{h2} and x_{h3}) where its third derivative is zero. These three points are

$$x_{h1} = \omega^2(1-2\zeta_n^2)-2\sqrt{3}\omega^2\zeta_n\sqrt{1-\zeta_n^2} \tag{4.36}$$

$$x_{h2} = \omega^2(1-2\zeta_n^2) \tag{4.37}$$

$$x_{h3} = \omega^2(1-2\zeta_n^2)+2\sqrt{3}\omega^2\zeta_n\sqrt{1-\zeta_n^2}\,. \tag{4.38}$$

Therefore, $y(x)$ can have up to two local maximums, the first one, $\theta_{a\,\mu}$, is close to μ and the second one ($\theta_{a\,\omega^2}$) is close to $\omega^2(1-2\zeta_n^2)$. That is, a Newton iteration (Press

et al., 2007) with these starting points should converge to the solution in few steps if the two maximums exist. Three roots of $y'''(x) = 0$ can appear close to x_{h1}, x_{h2} and x_{h3}, respectively, $x_1 \approx x_{h1}$, $x_2 \approx x_{h2}$ and $x_3 \approx x_{h3}$. As formerly, Newton iteration is a procedure leading to the solution in few steps if the three points, x_{h1}, x_{h2} and x_{h3}, exist. Function $y(x)$ can have different shapes, and depending on it, a different method to calculate the integral is applied:

- The function has two maximums and $y(\theta_{a\omega^2}) < y(\theta_{a\mu})$, then, Laplace's method is used.

- The function has two maximums and $y(\theta_{a\mu}) \leq y(\theta_{a\omega^2})$. Laplace's approximation does not work well, in this case, a numerical integration (i.e. Gaussian quadrature, trapezoidal method) is a good alternative to approximate the integral.

- The function has only one maximum, $\theta_{a\mu}$, and x_1, x_2 and x_3 do not exist or are situated at the same side of $\theta_{a\mu}$, that is, $x_3 < \theta_{a\mu}$ or $\theta_{a\mu} < x_1$. Then, Laplace's method is used.

- The function has only one maximum, $\theta_{a\omega^2}$, and x_1, x_2 and x_3 exist and are such that $x_1 < \theta_{a\omega^2} < x_3$. In those situations, Laplace's approximation can work well if no discontinuity has appeared both in $\theta(a\,\omega)$ and $y''(\theta(a\,\omega))$. Generally, Laplace's approximation will provide a value smaller than the exact one. A different second order polynomial, having its maximum at θ_a and going through x_1 if $\theta_a > \mu$ and through θ_3 if $\theta_a \leq \mu$ can be used instead of the Taylor expansion used in Laplace's method. Then

$$I(\omega) = e^{y(\theta_a)}\sqrt{\frac{-\pi(\theta_a - x_1)^2}{y(x_1) - y(\theta_a)}} \quad \text{if} \quad \theta_a > \mu \tag{4.39}$$

$$I(\omega) = e^{y(\theta_a)}\sqrt{\frac{-\pi(\theta_a - x_3)^2}{y(x_3) - y(\theta_a)}} \quad \text{if} \quad \theta_a \leq \mu\,. \tag{4.40}$$

  This second approximation to the integral provides, mostly, a larger value than the exact result. This approximation will be referred as modified Laplace's method.

If Laplace's method is applied when leading to a good approximation and numerical integration is applied in the remaining frequencies, the resulting method is called Hybrid Laplace-numerical integration. If Laplace's method or modified Laplace's method are

applied when leading to a good approximation and numerical integration is performed for the remaining frequencies, the resulting method is referred to as modified Laplace.

4.3 FRF statistics for different probability density functions of the natural frequency

The pdfs of $x = \omega_n^2$ have to satisfy that $f_x(x \leq 0) = 0$, as it is not physically possible to have a negative or zero squared natural frequency. It is observed that $x = \omega_n^2$ is the solution to the random eigenvalue problem $\det(\mathbf{K} - \omega_n^2\mathbf{M}) = 0$, such that its pdf would be directly obtained when solving the random eigenvalue problem. The purpose of this section is to understand how different possible pdfs of ω_n^2 influence the dynamic response. The pdfs studied can be obtained with the maximum entropy principle, if some information on the eigenvalues is available (Kapur, 1989). That is, the pdfs are the functions maximizing the following entropy equation

$$S(f_x) = -\int f_x(x)\ln(f_x(x))dx - \gamma_0\left(\int f_x(x)dx - 1\right) - \sum_{i=1}^{M}\gamma_i g_i(x) \qquad (4.41)$$

where γ_0, γ_i for $i = 1, \ldots, M$ are Lagrange multipliers and g_i are functions related to the constraints imposed on the pdf f_x. Numerical examples are provided, where $\mathrm{E}[x] = 9$, $\sigma_x = 1$ and the damping factor has values $\zeta_n = 0.1$ or $\zeta_n = 0.01$. The chosen pdfs, other than the uniform distribution, are assumed to be unimodal with maximum at $x = \mu$. The number of samples in MCS is 10,000. A summary of results based on SDOF and MDOF systems is given later in the Chapter.

4.3.1 Uniform distribution

The pdf of an uniform distribution $U(u_1, u_2)$ is defined by a constant α_u over the interval $x \in [u_1, u_2]$. Parameters α_u, u_1 and u_2 of the distribution can be expressed through its mean (μ_x) and variance (σ_x)

$$u_1 = \mathrm{E}[x] - \sqrt{3\sigma_x} \qquad (4.42)$$

$$u_2 = \mathrm{E}[x] + \sqrt{3\sigma_x} \qquad (4.43)$$

$$\alpha_u = \frac{1}{2\sqrt{3\sigma_x}}. \qquad (4.44)$$

This pdf can be obtained with the maximum entropy principle, where the boundaries of integration are u_1 and u_2 and there are no constraints g_i imposed on the entropy equation. Eigenvalues for which first and second moments are known have been modelled with uniform distributions, for example, by den Nieuwenhof and Coyette (2003). For this pdf, all integrals appearing in Equations (4.30), (4.31) and (4.32) can be calculated exactly. For example if $a = 0$

$$I(\omega) = \hat{I}_0(u_2, \omega) - \hat{I}_0(u_1, \omega) \tag{4.45}$$

$$\text{where } \hat{I}_0(x, \omega) = \frac{\alpha_u}{2\omega^2\zeta_n\sqrt{1-\zeta_n^2}} \arctan \frac{x - \omega^2(1-2\zeta_n^2)}{2\omega^2\zeta_n\sqrt{1-\zeta_n^2}} \tag{4.46}$$

For $a = 1$ we have

$$I(\omega) = \hat{I}_1(u_2, \omega) - \hat{I}_1(u_1, \omega) \tag{4.47}$$

$$\text{where } \hat{I}_1(x, \omega) = \alpha_u \frac{\log(\omega^2(\omega^2 - 2x(1-2\zeta_n^2)) + x^2)}{2} - \alpha_u \frac{\sqrt{1-4\zeta_n^2(1-\zeta_n^2)}}{2\zeta_n\sqrt{1-\zeta_n^2}} \arctan \frac{(\omega^2(2\zeta_n^2-1)+2x)\sqrt{1-4\zeta_n^2(1-\zeta_n^2)}}{\omega^2(2\zeta_n^2-1)2\zeta_n\sqrt{1-\zeta_n^2}} \tag{4.48}$$

An expression for $a = 0.5$ can also be calculated analytically. In Figs. 4.1 and 4.2 we compared the results of the analytical expressions and MCS for different ζ_n and same uniform distribution $U(9-\sqrt{3}, 9+\sqrt{3})$ for x. Note the significant difference between

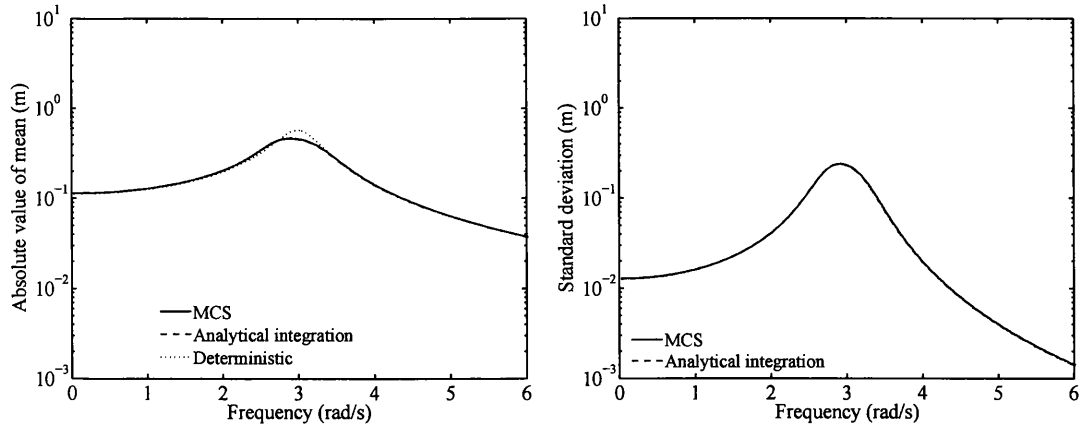

(a) Absolute value of mean.

(b) Standard deviation.

Figure 4.1: Mean and standard deviation of the absolute value of the transfer function for uniform distribution with $\zeta_n = 0.1$.

the mean and the deterministic results for the smaller value of the damping factor in Figure 4.2 compared to that for a higher value of the damping factor in Figure 4.1.

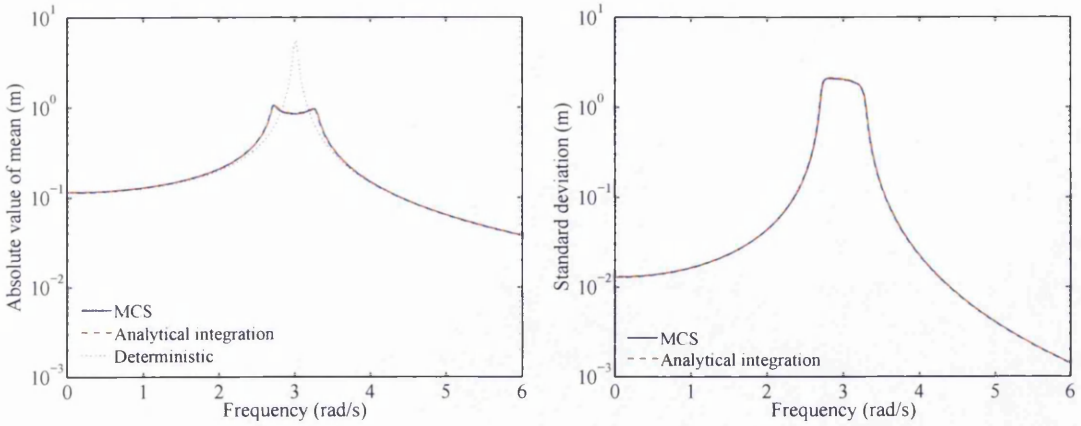

(a) Absolute value of mean.

(b) Standard deviation.

Figure 4.2: Mean and standard deviation of the absolute value of the transfer function for uniform distribution with $\zeta_n = 0.01$.

4.3.2 Normal distribution

The pdf $f_x(x)$ and $f'_x(x)/f_x(x)$ of the normal distribution conditional to $x > 0$ are given by

$$f_x(x) = \frac{e^{-(x-\mathrm{E}[x])^2/2\sigma_x^2}}{\sqrt{2\pi\sigma_x^2 P(0)}} \quad x \in (0,\, +\infty)\,, \qquad \frac{f'_x(x)}{f_x(x)} = -\frac{x - \mathrm{E}\,[x]}{\sigma_x^2} \tag{4.49}$$

where $\mathrm{E}\,[x]$ and σ_x^2 are respectively the mean and the variance of the distribution and $P(0)$ is the probability of $x \leq 0$ for a normal distribution $N(\mathrm{E}\,[x]\,,\, \sigma_x)$. This pdf can be obtained with the maximum entropy principle, where the constraints g_i imposed on the entropy equation are that the mean and variance of the random variable x are known. From experiments on alloy weels, the marginal distribution obtained for the eigenvalues are close to normal (Hinke et al., 2009).

From Equation (4.33), the parameter θ_a can be identified as the solution of a fourth order polynomial

$$b_{1_a} x^4 + b_{2_a} x^3 + b_{3_a} x^2 + b_{4_a} x + b_{5_a} = 0 \tag{4.50}$$

with coefficients

$$\begin{aligned} b_{1_b} &= -1 & b_{3_b} &= -\omega^4 + (a-2)\sigma_x^2 + \mathrm{E}\,[x]\,\bar{\zeta}_\omega \\ b_{2_b} &= -\bar{\zeta}_\omega + \mu_x & b_{4_b} &= (1+a)\sigma_x^2\bar{\zeta}_\omega + \mathrm{E}\,[x]\,\omega^4 \\ & & b_{5_b} &= a\sigma_x^2\omega^4 \end{aligned} \tag{4.51}$$

and $\bar{\zeta}_\omega = 2\omega^2(2\zeta_n^2 - 1)$. Up to four solutions can be expected, and we assume the existence of a first real solution close to the mean of the distribution, $\theta_{a\,\mu}$. If a second real solution $\theta_{a\,\omega^2}$ exists and is not a saddle point, a relative minimum between the two relative maximums exists. The remaining real solution is a spurious value, and likely to be negative or close to zero. Depending on the shape of $y(x)$, and as indicated in section 4.2.2, Laplace's method may be applied to approximate the integrals appearing in expressions of $\mathrm{E}[h]$ and $\mathrm{E}[|h|^2]$, given by Equations (4.22), (4.23) and (4.24). The second derivative of $y(x)$ is given by Equation (4.34) where $\bar{h}(x,\omega)$ is given by Equation (4.35) and

$$\bar{f}(x) = -\frac{1}{\sigma_x^2}. \tag{4.52}$$

The Laplace's approximation assuming normal distribution is therefore given by

$$I(\omega, a) \backsim \frac{\theta_a^a \sqrt{2\pi} e^{-(\theta_a - \mathrm{E}[x])^2/2\sigma_x^2}}{P(0)\sqrt{2\pi\sigma_x^2}\left((\theta_a - \omega^2)^2 + 4\zeta_n^2\omega^2\theta_a\right)^{a/2}} \left[\frac{1}{\sigma_x^2} - \frac{a}{\theta_a^2} + \bar{h}(\theta_a)\right]^{-\frac{1}{2}} \tag{4.53}$$

where a is given in Equations (4.30), (4.31) and (4.32). Parameters $\mathrm{E}[x]$ and σ_x are the mean and standard deviation of $x = \omega_n^2$. Another approximation of the integral can be obtained from Equations (4.39) and (4.40). Plots of approximations for an SDOF with $\mathrm{E}[x] = 9$ and $\sigma_x = 1$ are displayed, in Figure 4.3 for $\zeta_n = 0.1$ and in Figure 4.4 for $\zeta_n = 0.01$. For the small damping case one can again observe the significant

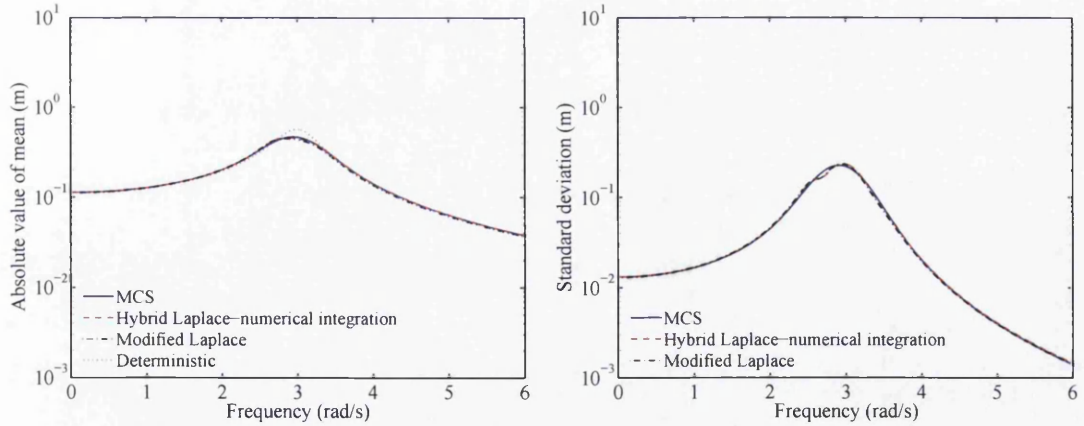

(a) Absolute value of mean.

(b) Standard deviation.

Figure 4.3: Mean and standard deviation of the absolute value of the transfer function for normal distribution with $\zeta_n = 0.1$.

difference between the deterministic response and the mean response. Additionally, it can be noted that hybrid modified Laplace method also produced some discrepancies

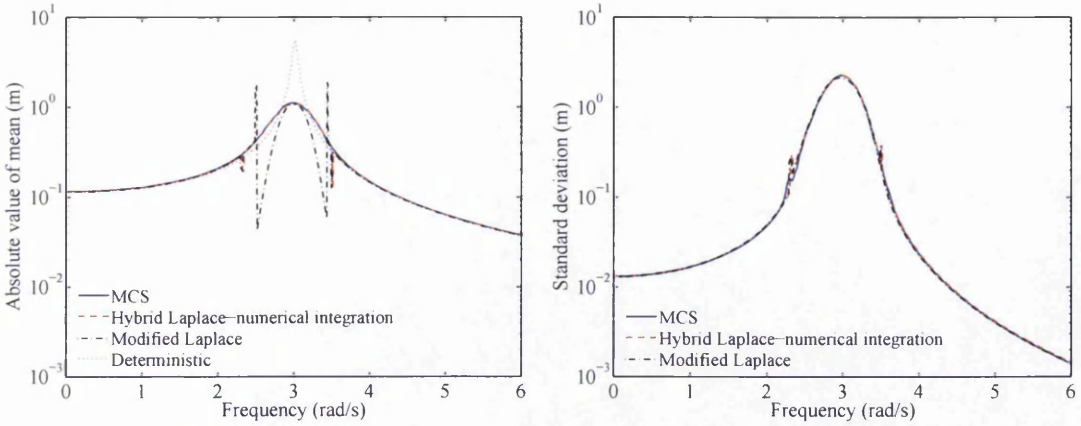

(a) Absolute value of mean.

(b) Standard deviation.

Figure 4.4: Mean and standard deviation of the absolute value of the transfer function for normal distribution with $\zeta_n = 0.01$.

for the low damping case.

4.3.3 Gamma distribution

The probability density function $f_x(x)$ and $f'_x(x)/f_x(x)$ of the gamma distribution, defined in the interval $[0, \infty)$, are given by

$$f_x(x) = \frac{x^{\alpha_g - 1}}{\Gamma(\alpha_g)\beta_g^{\alpha_g}} e^{-x/\beta_g}, \qquad \frac{f'_x(x)}{f_x(x)} = \frac{\alpha_g - 1}{x} - \frac{1}{\beta_g}. \tag{4.54}$$

Relationships between mean μ_x, variance σ_x^2 and parameters α_g and β_g are given by

$$\mu_x = \alpha_g \beta_g \,, \qquad \sigma_x^2 = \alpha_g \beta_g^2 \tag{4.55}$$

$$\alpha_g = \frac{\mu_x^2}{\sigma_x^2} \,, \qquad \beta_g = \frac{\sigma_x^2}{\mu_x}. \tag{4.56}$$

This pdf can be obtained with the maximum entropy principle, where the constraints g_i imposed on the entropy equation are that the random variable belongs to the interval $[0, \infty)$ and the means of the random variable x and of $\ln x$ are known. That is, a gamma random variable is positive, its mean is known and the first moment of its inverse is finite. This distribution has been used in reliability (Rausand and Hoyland, 2004). As formerly, θ_a is the real solution of the third order polynomial

$$b_{1_a} x^3 + b_{2_a} x^2 + b_{3_a} x + b_{4_a} = 0 \tag{4.57}$$

with coefficients

$$\begin{aligned} b_{1_a} &= -\frac{1}{\beta_g}, & b_{2_a} &= -\frac{\bar{\zeta}_\omega}{\beta_g} + \alpha_g + a - 3 \\ b_{4_a} &= \omega^4(\alpha_g + a - 1), & b_{3_a} &= \bar{\zeta}_\omega\,(\alpha_g + a - 2) - \frac{\omega^4}{\beta_g} \end{aligned} \tag{4.58}$$

and $\bar{\zeta}_\omega = 2\omega^2\,(2\zeta_n^2 - 1)$, at which $y(x)$ is maximum. A third-order polynomial has three solutions. Amongst these solutions, the ones that can be considered as plausible solutions to our problem are real and satisfy $x > 0$, $y'(x,a) = 0$ and $y"(x,a) < 0$. As we have already stated, one of the solutions is close to μ, and a second plausible solution is close to $x_{h2} = \omega^2(1 - 2\zeta_n^2)$. The third real solution of the polynomial would then be the relative minimum point situated between the two relative maximums, and verifies $y"(x,a) > 0$. Otherwise, two of the solutions are complex and there is only one real solution. We can then find an approximation to the solutions using Newton iteration method to Equation (4.57). As indicated in section 4.2.2, Laplace's method will be a good option to approximate the integrals depending on the shape of $y(x)$. The second derivative of $y(x,a)$ is given at Equation (4.34) where $\bar{h}(x,\omega)$ is given by Equation (4.35) and

$$\bar{f}(x) = \frac{1 - \alpha_g}{x^2}. \tag{4.59}$$

From Equation (4.28), an analytical approximation to the integrals appearing in the expressions of the two first moments of the absolute value of the FRF is given by

$$I(\omega,a) \backsim \frac{\sqrt{2\pi}\theta_a^{\alpha_g - 1 + a} e^{-\theta_a/\beta_g}}{\Gamma(\alpha_g)\beta_g^{\alpha_g}((\theta_a - \omega^2)^2 + 4\zeta_n^2\omega^2\theta_a)} \left[\frac{\alpha_g - 1 - a}{\theta_a^2} + \bar{h}(\theta_a)\right]^{-\frac{1}{2}} \tag{4.60}$$

where a is given in Equations (4.30), (4.31) and (4.32). Parameters α_g and β_g can be derived from Equation (4.56) if the mean μ_x and the standard deviation σ_x of ω_n^2 are known. Plots of approximations for an SDOF with $\mu_x = 9$ and $\sigma_x = 1$ are displayed, in Figure 4.5 for $\zeta_n = 0.1$ and in Figure 4.6 for $\zeta_n = 0.01$. Again note the difference between the results for small and high damping.

4.3.4 Lognormal distribution

A lognormal distribution is a probability distribution obtained by taking the exponential of a normal distribution of mean μ and standard deviation σ, $N(\mu,\sigma)$. A lognormal

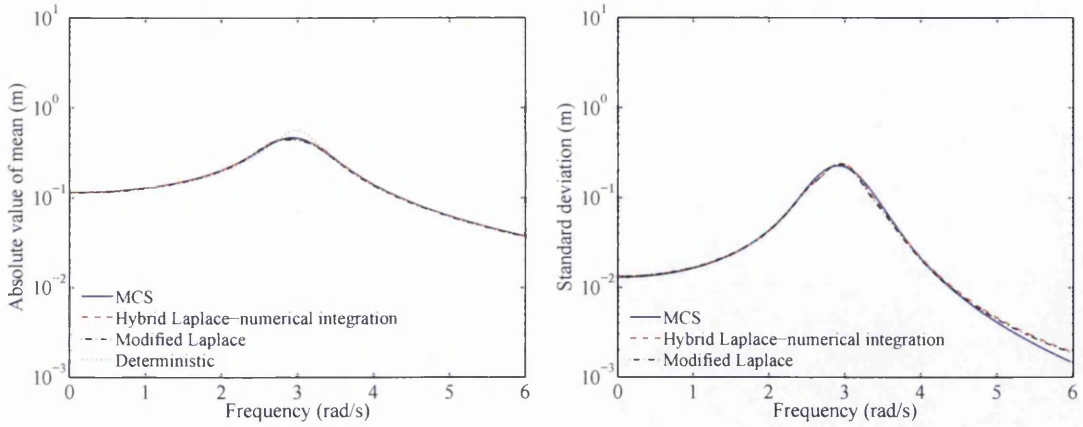

(a) Absolute value of mean. (b) Standard deviation.

Figure 4.5: Mean and standard deviation of the absolute value of the transfer function for gamma distribution with $\zeta_n = 0.1$.

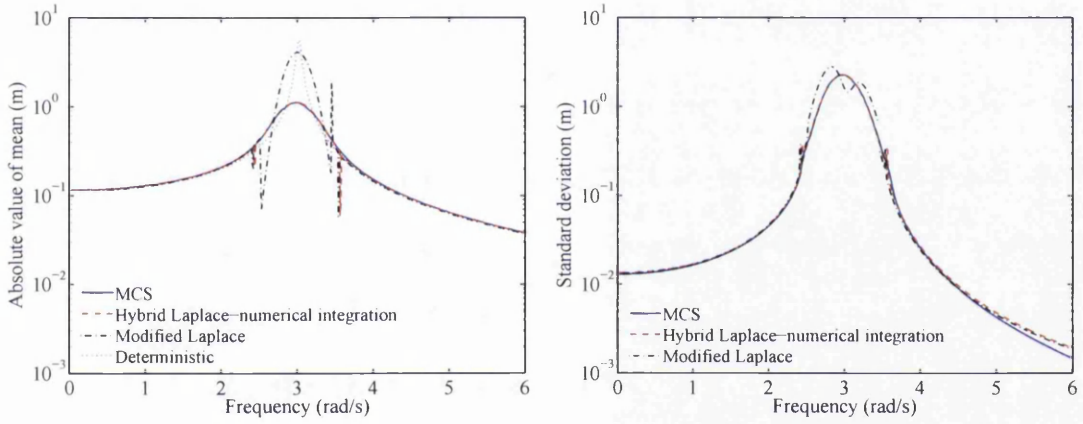

(a) Absolute value of mean. (b) Standard deviation.

Figure 4.6: Mean and standard deviation of the absolute value of the transfer function for gamma distribution with $\zeta_n = 0.01$.

random variable is always positive, so that it has been used to model random variables in reliability (Papadimitriou et al., 1997) and random fields in SFEM (Ghanem and Dham, 1998). The probability density function $f_x(x)$, and $f'_x(x)/f_x(x)$ of lognormal distribution, defined in the interval $(0, \infty)$, is given by

$$f_x(x) = \frac{e^{-(\ln x - \mu)^2/2\sigma^2}}{x\sqrt{2\pi\sigma^2}}, \qquad \frac{f'_x(x)}{f_x(x)} = -\frac{\sigma^2 \ln x - \mu}{x\sigma^2} \tag{4.61}$$

with mean μ_x and variance σ_x of lognormal distribution related to μ and σ by

$$\mu_x = e^{\mu+\sigma^2/2}, \qquad \sigma_x^2 = (e^{\sigma^2} - 1)e^{2\mu+\sigma^2} \tag{4.62}$$

$$\mu = \ln \mu_x - \frac{1}{2} \ln \left(1 + \frac{\sigma_x}{\mu_x^2} \right), \qquad \sigma = \ln \left(\frac{\sigma_x}{\mu_x^2} + 1 \right). \tag{4.63}$$

This pdf can be obtained with the maximum entropy principle, where the constraint g_i imposed on the entropy equation is that the mean of $\ln x$ and of $(\ln x)^2$ are known and the limits of integration are $x \in [0, \infty)$. From Equation (4.33) can be identified parameter θ_a as the solution to the equation

$$y'(\theta_a, a) = -\frac{\sigma^2 + \ln \theta_a - \mu}{\theta_a \sigma^2} + \frac{a}{\theta_a} - \frac{(2(\theta_a - \omega^2) + 4\zeta_n^2)}{(\theta_a - \omega^2)^2 + 4\zeta_n^2 \theta_a} = 0. \tag{4.64}$$

As indicated in section 4.2.2, we will assume here that one solution, $\theta_{a\,\mu}$, is close to the mean of the distribution and that another relative maximum of $y(x)$, $\theta_{a\,\omega^2}$, can arise together with a relative minimum situated between those two maximums. We can then find an approximation to these solutions using Newton method. From Equation (4.28) and depending on the shape of $y(x)$, an analytical approximation to the integrals appearing in the expressions of $\mathrm{E}[h]$ and of $\mathrm{E}[|h|^2]$ allows to find an approximation to those moments. This analytical approximation to integrals is given by

$$I(\omega, a) \backsim \frac{\theta_a^{a-1} e^{-(\ln \theta_a - \mu)^2 / 2\sigma^2}}{\sqrt{\sigma^2((\theta_a - \omega^2)^2 + 4\zeta_n^2 \omega^2 \theta_a)}} \left[\frac{\sigma^2(a-1) - \ln \theta_a + \mu}{\sigma^2 \theta_a^2} + \bar{h}(\theta_a) \right]^{-\frac{1}{2}} \tag{4.65}$$

with a given in Equations (4.30), (4.31) and (4.32). Parameters μ and σ can be found if μ_x and σ_x are known. Plots of the approximations for an SDOF with $\mu_x = 9$ and $\sigma_x = 1$ are displayed, in Figure 4.7 for $\zeta_n = 0.1$ and in Figure 4.8 for $\zeta_n = 0.01$. Like

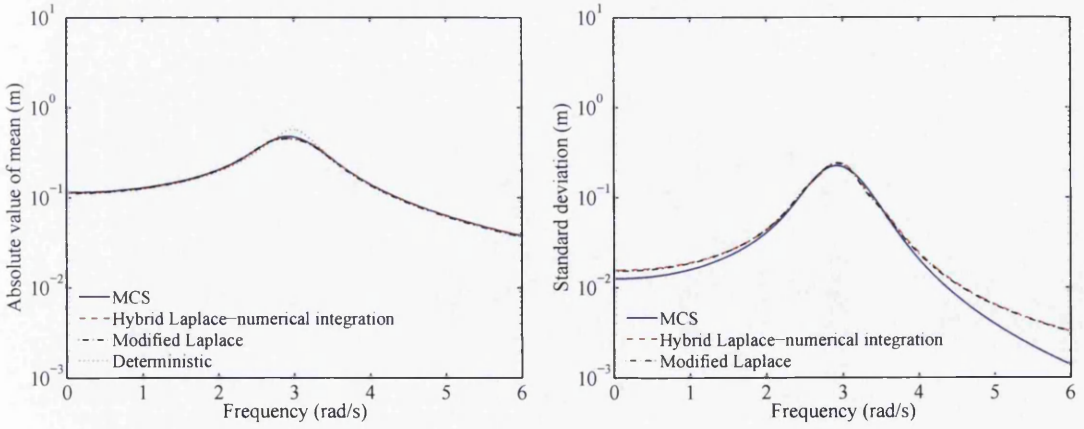

(a) Absolute value of mean.

(b) Standard deviation.

Figure 4.7: Mean and standard deviation of the absolute value of the transfer function for lognormal distribution with $\zeta_n = 0.1$.

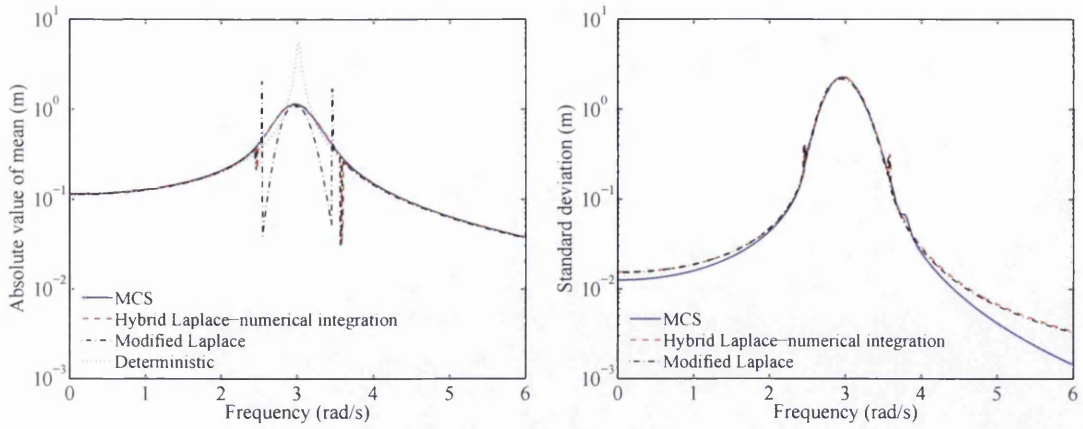

(a) Absolute value of mean.

(b) Standard deviation.

Figure 4.8: Mean and standard deviation of the absolute value of the transfer function for lognormal distribution with $\zeta_n = 0.01$.

the previous pdfs, the difference in results between the low and high damping can also be seen here.

4.4 Multiple-degrees-of-freedom (MDOF) systems

4.4.1 Response calculation

Applying finite element method to structural dynamic systems leads, generally, to an MDOF problem where a displacement vector $\mathbf{u}$ is the unknown. The frequency response vector of the MDOF system can be given by (see, for example, Géradin and Rixen (1997))

$$\mathbf{u} = \mathbf{\Phi}[-\omega^2\mathbf{I} + \mathrm{i}\omega 2\boldsymbol{\zeta}\mathbf{\Omega} + \mathbf{\Omega}^2]^{-1}\mathbf{\Phi}^T\mathbf{f} = \mathbf{\Phi}\mathbf{H}'\mathbf{\Phi}^T\mathbf{f} \tag{4.66}$$

where $\mathbf{\Phi}$ is the matrix of eigenvectors (modal matrix) and $\mathbf{\Omega}$ is a diagonal matrix of natural frequencies of the system. The frequency response can be expressed as

$$\begin{aligned}\mathbf{u} &= \mathbf{\Phi}\left[\sum_{j=1}^{N}\frac{e_j e_j^T}{-\omega^2 + 2\mathrm{i}\omega\zeta_j\omega_j + \omega_j^2}\right]\mathbf{\Phi}^T\mathbf{f} \\ &= \mathbf{\Phi}\left[\sum_{j=1}^{N}\frac{e_j e_j^T}{-\omega^2 + 2\mathrm{i}\omega\zeta_j\omega_j + \omega_j^2}\right]\mathbf{F}\end{aligned} \tag{4.67}$$

where e_j is the j-th unit vector, or j-th column of an identity matrix, and matrix $\mathbf{H}'$ is therefore diagonal. We denote by $\mathbf{x}^*$ and $\mathbf{H}'^*$ the complex conjugate of $\mathbf{u}$ and $\mathbf{H}'$

respectively. The j-th diagonal element of matrix $\mathbf{H}'$ is denoted by h'_j, and h'^*_j is its complex conjugate. Vector $\mathbf{\Phi}_i$ is the i-th row of matrix $\mathbf{\Phi}$, and $\mathbf{\Phi}_{i_j}$ is its j-th element. The j-th element of vector $\mathbf{F} = \mathbf{\Phi}^T\mathbf{f}$ is denoted by F_j. Uncertainty is introduced by the diagonal terms of $\mathbf{H}'$, and therefore, all other vectors and matrices are deterministic. From Equation (4.67), an expression of u_i, the i-th term of vector $\mathbf{u}$, and of $|u_i|^2$ can be derived

$$u_i = \sum_{j=1}^{N} \mathbf{\Phi}_{i_j} h'_j F_j \tag{4.68}$$

$$|u_i|^2 = u_i^T u_i^* = \sum_{j=1}^{N}\sum_{k=1}^{N} F_j h'_j \mathbf{\Phi}_{i_j}\mathbf{\Phi}_{i_k} h'^*_k F_k. \tag{4.69}$$

Denoting $C_j = F_j\mathbf{\Phi}_{i_j}$, the expression of $|u_i|^2$ can be simplified

$$|u_i|^2 = \sum_{j=1}^{N} C_j^2 h'_j h'^*_j + \sum_{k=1}^{N-1}\sum_{j=k+1}^{N} C_j C_k \left(h'_j h'^*_k + h'^*_j h'_k\right) \tag{4.70}$$

$$= \sum_{j=1}^{N} C_j^2 |h'_j|^2 + \sum_{k=1}^{N-1}\sum_{j=k+1}^{N} C_j C_k 2\Re(h'_j h'^*_k). \tag{4.71}$$

Mean of $|u_i|^2$ is equal to the second moments of $|u_i|$ and u_i.

4.4.2 Mean of real and imaginary parts of the response

Expressions of real and imaginary parts of u_i can be derived from Equation (4.68)

$$\Re(\mathrm{x}_i) = \sum_{j=1}^{N} C_j \Re\left(h'_j\right) \quad \text{with} \quad \Re\left(h'_j\right) = \frac{\omega_j^2 - \omega^2}{(\omega_j^2 - \omega^2)^2 + 4\zeta_j^2\omega^2\omega_j^2} \tag{4.72}$$

$$\Im(\mathrm{x}_i) = \sum_{j=1}^{N} C_j \Im\left(h'_j\right) \quad \text{with} \quad \Im\left(h'_j\right) = \frac{-2\zeta_j\omega\omega_j}{(\omega_j^2 - \omega^2)^2 + 4\zeta_j^2\omega^2\omega_j^2}. \tag{4.73}$$

Mean is a linear operator, therefore, the mean of each product $C_j\Re\left(h'_j\right)$, $C_j\Im\left(h'_j\right)$, $C_j^2|h'_j|^2$ and $C_jC_k2\Re(h'_jh'^*_k)$ is needed.

In Chapter 1 the joint pdf of eigenvalues and eigenvectors of a symmetric matrix was given, and it was noted that for some distributions, they are independent or asymptotically independent. Furthermore, applying the maximum entropy principle to obtain joint distribution of eigenvalues and eigenvectors where no data is available on the joint pdf leads to independent eigenvalues and eigenvectors. In the previous chapter, eigen-

values and eigenvectors were expanded with a PC expansion in Equations (3.7) and (3.8), so that the covariance between two different eigenvalues and an eigenvalue and its correspondent eigenvector is given by

$$\mathrm{E}\left[\lambda^{(i)}\lambda^{(j)}\right] - \mathrm{E}\left[\lambda^{(i)}\right]\mathrm{E}\left[\lambda^{(j)}\right] = \sum_{k=1}^{P} \lambda_{ik}\lambda_{jk}\mathrm{E}\left[\Gamma_k^2\right] - \lambda_{i1}\lambda_{j1} \tag{4.74}$$

$$\mathrm{E}\left[\lambda^{(j)}\mathbf{v}^{(j)}\right] - \mathrm{E}\left[\lambda^{(j)}\right]\mathrm{E}\left[\mathbf{v}^{(j)}\right] = \sum_{k=1}^{P} \lambda_{jk}\mathbf{v}_k^{(j)}\mathrm{E}\left[\Gamma_k^2\right] - \lambda_{j1}\mathbf{v}_1^{(j)} \tag{4.75}$$

The covariance between an eigenvalue and its eigenvector, using the first order perturbation of the system matrix $\mathbf{A}$ from Equation (3.2) and the first order perturbation of its eigenvector from Equation (3.6), can be approximated by

$$\mathrm{E}\left[\lambda^{(j)}\mathbf{v}^{(j)}\right] - \mathrm{E}\left[\lambda^{(j)}\right]\mathrm{E}\left[\mathbf{v}^{(j)}\right] \approx \mathrm{E}\left[\mathbf{A}\mathbf{v}^{(j)}\right] - \lambda_0^{(j)}\mathbf{v}_{j0} \approx \sum_{i=1}^{M}\sum_{m=1,m\neq j}^{n} \alpha_{jim}\mathbf{A}_i\mathbf{v}_{m0} \tag{4.76}$$

where coefficients α_{jim} are small compared to one and the order of magnitude of the random part of the system matrix $\mathbf{A}$, i.e. $\sum_{i=1}^{M}\mathbf{A}_i$, is smaller than that of $\mathbf{A}$. We can then assume that the correlation between an eigenvalue and its eigenvector is small when the first order approximation is accurate, that is, at low frequencies. When considering two eigenvalues, the marginal pdf and correlation coefficients of eigenvalues of alloy wheels for low frequencies have been obtained from experimental measurements, where the marginal pdfs were close to normal distributions, and correlation coefficients between eigenvalues was small (Hinke et al., 2009). We assume that eigenvalues and eigenvectors can be modelled as independent if they are uncorrelated, or if this correlation is small. Therefore, it is assumed that, for low frequencies, eigenvectors and eigenvalues are independent.

The independence of eigenvalues and eigenvectors of a positive definite matrix implies that

$$\mathrm{E}\left[C_j\Re\left(h_j'\right)\right] = \mathrm{E}\left[C_j\right]\mathrm{E}\left[\Re\left(h_j'\right)\right] \quad \mathrm{E}\left[C_j\Im\left(h_j'\right)\right] = \mathrm{E}\left[C_j\right]\mathrm{E}\left[\Im\left(h_j'\right)\right] \tag{4.77}$$

where $\mathrm{E}\left[C_j\right] = \sum_{k=1}^{n}\mathrm{E}\left[\Phi_{i_j}\Phi_{k_j}\right]\mathbf{f}_k$ can be obtained from the second moment of the j-th eigenvalue, with $\mathbf{f}_k$ the k-th element of the forcing term. Only means $\mathrm{E}\left[\Re\left(h_j'\right)\right]$ and $\mathrm{E}\left[\Im\left(h_j'\right)\right]$ remain to be calculated to obtain $\mathrm{E}\left[\Re\left(u_i\right)\right]$ and $\mathrm{E}\left[\Im\left(u_i\right)\right]$. These means

are given by

$$\mathrm{E}\left[\Re\left(h'_j\right)\right] = I_{2_j} - \omega^2 I_{1_j} \tag{4.78}$$

$$\mathrm{E}\left[\Im\left(h'_j\right)\right] = -2\zeta_j \omega I_{3_j}. \tag{4.79}$$

If uncorrelated random variables are assumed, integrals I_{1_j}, I_{2_j} and I_{3_j} are given by

$$I_{1_j} = \int_{\mathcal{D}} \frac{f_x}{(x_j - \omega^2)^2 + 4\zeta_j^2 \omega^2 x_j}\, dx_j \tag{4.80}$$

$$I_{2_j} = \int_{\mathcal{D}} \frac{x_j f_x}{(x_j - \omega^2)^2 + 4\zeta_j^2 \omega^2 \omega_j^2}\, dx_j \tag{4.81}$$

$$I_{3_j} = \int_{\mathcal{D}} \frac{\sqrt{x_j} f_x}{(x_j - \omega^2)^2 + 4\zeta_j^2 \omega^2 x_j}\, dx_j. \tag{4.82}$$

An analytical approximation to these integrals could be given, depending on the shape of the integrand, by Equations (4.53), (4.60) and (4.65) for normal, gamma and lognormal distributions respectively. Parameter $a = 0$ for I_{1_j}, $a = 1$ for I_{2_j} and $a = 1/2$ for I_{3_j}.

4.4.3 Variance of response

Expressions of the second moment of response can be derived from Equation (4.71), remembering that mean is a linear operator and that eigenvalues and eigenvectors are assumed independent

$$\mathrm{E}\left[|u_i|^2\right] = \sum_{j=1}^{N} \mathrm{E}\left[C_j^2\right] \mathrm{E}\left[|h'_j|^2\right] + \sum_{k=1}^{N-1} \sum_{j=k+1}^{N} \mathrm{E}\left[C_j C_k\right] 2\mathrm{E}\left[\Re(h'_j h'^{*}_k)\right] \tag{4.83}$$

$$\mathrm{E}\left[|u_i|^2\right] = \sum_{j=1}^{N} \mathrm{E}\left[C_j^2\right] I_{1_j} + \sum_{k=1}^{N-1} \sum_{j=k+1}^{N} \mathrm{E}\left[C_j C_k\right] 2\mathrm{E}\left[\Re(h'_j h'^{*}_k)\right] \tag{4.84}$$

$$\mathrm{E}\left[\Re(h'_j h'^{*}_k)\right] = \left(I_{2_j} - \omega^2 I_{1_j}\right)\left(I_{2_k} - \omega^2 I_{1_k}\right) + 4\zeta_j \zeta_k \omega^2 I_{3_j} I_{3_k}. \tag{4.85}$$

Means $\mathrm{E}\left[C_j^2\right]$ can be obtained from the fourth moment of the j-th eigenvector and $\mathrm{E}\left[C_j C_k\right]$ from the fourth moment of the eigenvector matrix Φ. The second moment is given by

$$\mathrm{E}\left[|u_i|^2\right] = \mu_{u_i}^2 + \sigma_{u_i}^2 \tag{4.86}$$

where mean of response and squared value of mean are given by

$$\mu_{u_i} = \mathrm{E}\left[\Re\left(u_i\right)\right] + \mathrm{iE}\left[\Im\left(u_i\right)\right] \tag{4.87}$$

$$\mu_{u_i}^2 = \mathrm{E}\left[\Re\left(u_i\right)\right]^2 + \mathrm{E}\left[\Im\left(u_i\right)\right]^2. \tag{4.88}$$

And finally the variance can be obtained as

$$\sigma_{u_i}^2 = \mathrm{E}\left[|u_i|^2\right] - \mu_{u_i}^2. \tag{4.89}$$

In the next section, numerical results are shown for an MDOF system with random eigenvalues with the different distributions already discussed.

4.4.4 Numerical example

A proportionally damped system consisting of a linear array of spring-mass oscillators is considered to illustrate the proposed approach. Figure 4.9 shows the model system. N masses, each of nominal mass m; are connected by springs of nominal stiffness k. The system considered uses the mean of eigenvalues and eigenvectors obtained from

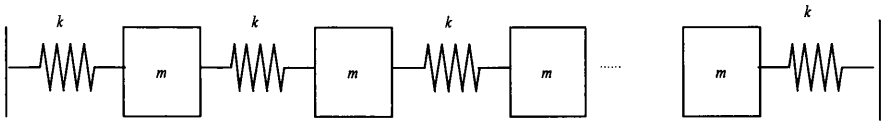

Figure 4.9: Linear array of N spring-mass oscillators, $N = 20$, $m = 1$ Kg and $k = 350$ N/m. A proportional damping model with damping factor 0.1 and 0.01 is assumed.

the deterministic mass and stiffness matrices $\mathbf{M}$ and $\mathbf{K}$, and forcing vector $\mathbf{f}$ as

$$\mathbf{M} = m\mathbf{I}_N\,, \qquad \mathbf{K} = k\begin{bmatrix} 2 & -1 & 0 & \dots & 0 \\ -1 & 2 & \ddots & & \vdots \\ 0 & \ddots & \ddots & \ddots & 0 \\ \vdots & \ddots & \ddots & 2 & -1 \\ 0 & \dots & 0 & -1 & 2 \end{bmatrix}, \qquad \mathbf{f} = \begin{Bmatrix} 1 \\ 0 \\ \vdots \\ 0 \end{Bmatrix} \tag{4.90}$$

with $\mathbf{I}_N$ the identity matrix. The number of degrees of freedom of the system is 20, therefore, matrices $\mathbf{M}$ and $\mathbf{K}$ become 20×20 matrices. Mass and stiffness constants are given by $m = 1$ kg and $k = 350$ N/m. The eigenvectors used are the ones obtained from the deterministic matrices $\mathbf{M}$ and $\mathbf{K}$ matrices, that is, they are considered deterministic,

or with central moments equal to zero. It is observed that the eigenvalue problem $k\mathbf{K} = \lambda m\mathbf{I}_N$ here reduces to $\mathbf{K} = (\lambda m/k)\mathbf{I}$, such that the eigenvectors are deterministic and the pdf of the eigenvalues depends on that of m/k. Mean eigenvalues are obtained from the deterministic matrices $\mathbf{M}$ and $\mathbf{K}$, and the standard deviation σ of each eigenvalue is given by a percentage of the mean of the considered eigenvalue. Each percentage is obtained through a sample of the uniform distribution $U(10, 15)$. Damping factors are assumed to be all equal to $\zeta_j = 0.1$ or to $\zeta_j = 0.01$. The number of samples for MCS is 10,000. Results are obtained for normal distribution with damping factors $\zeta_j = 0.1$ in Figure 4.10 and $\zeta_j = 0.01$ in Figure 4.11. Figures 4.12 and 4.13 show Gamma distribution results for $\zeta_j = 0.1$ and $\zeta_j = 0.01$ respectively. Lognormal distribution results for $\zeta_j = 0.1$ and $\zeta_j = 0.01$ are respectively displayed in Figs. 4.14 and 4.15. In all the figures, a comparison between mean and standard deviation obtained through approximations and MCS is facilitated. Uniform distribution results are not shown as an analytical expression to integrals is available and results match exactly MCS results.

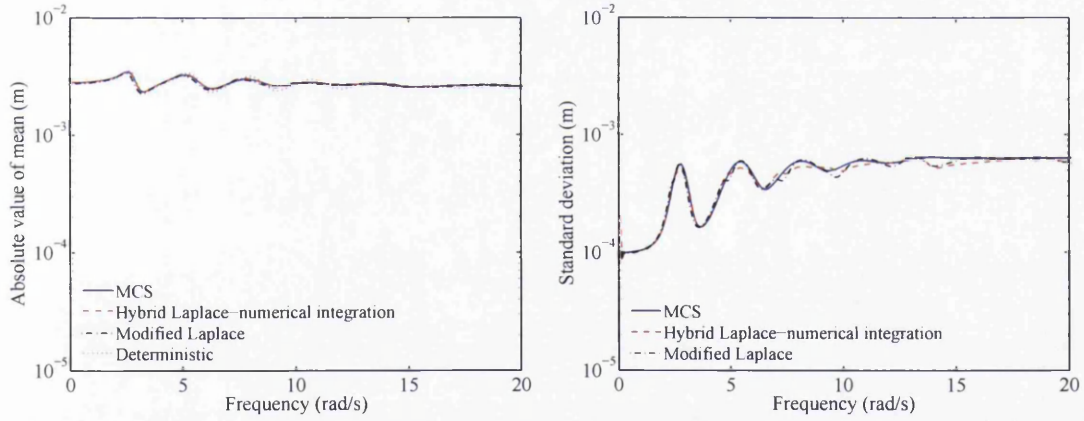

(a) Absolute value of mean.

(b) Standard deviation.

Figure 4.10: Mean and standard deviation of the absolute value of the transfer function for normal distribution with $\zeta_n = 0.1$.

4.5 Results and discussion

4.5.1 Discussion of the proposed methods

In this Chapter, the mean and variance of frequency response function of single and multiple-degrees-of-freedom systems are calculated from the pdf of independent eigen-

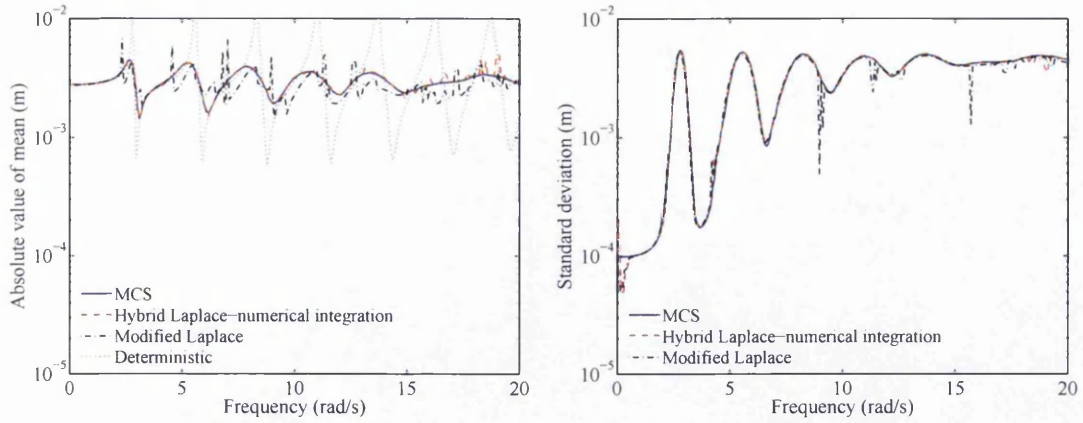

(a) Absolute value of mean. (b) Standard deviation.

Figure 4.11: Mean and standard deviation of the absolute value of the transfer function for normal distribution with $\zeta_n = 0.01$.

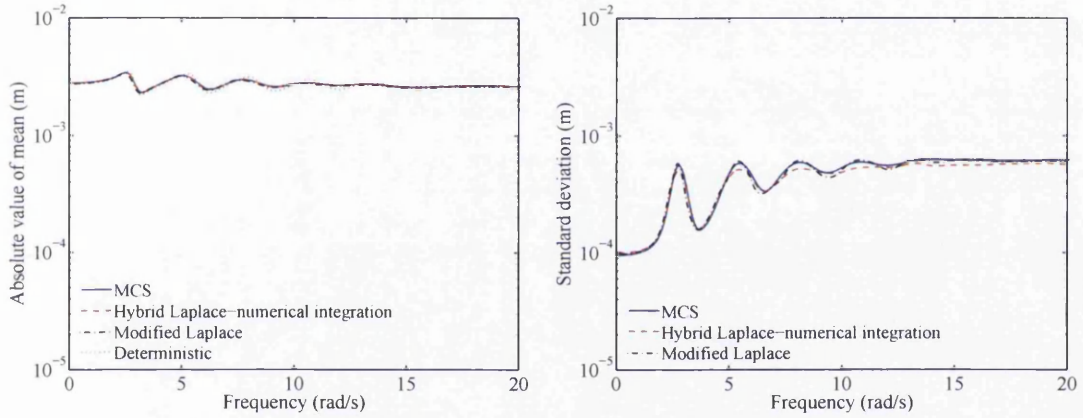

(a) Absolute value of mean. (b) Standard deviation.

Figure 4.12: Mean and standard deviation of the absolute value of the transfer function for gamma distribution with $\zeta_n = 0.1$.

values. This method needs the calculation of three integrals per frequency and degree of freedom, namely the ones appearing in Equations (4.30) to (4.32). Unfortunately, exact analytical integration is only available when the random variable, i.e. the squared natural frequency, has uniform distribution. Therefore, the main problem of the method is the calculation of the integrals. Numerical calculation of the integrals or evaluation through MCS can become computationally expensive for systems with large degrees of freedom. This problem can be overcome if integrals can be approximated using one of the two methods proposed in this Chapter.

The first method, referred as hybrid Laplace-numerical integration, is a hybrid method between Laplace's method and numerical integration. Laplace's method is used to ap-

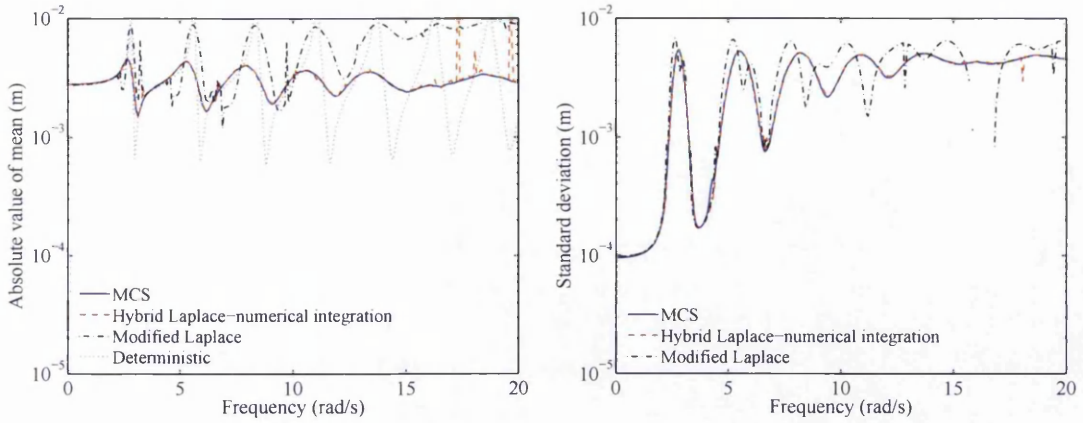

(a) Absolute value of mean. (b) Standard deviation.

Figure 4.13: Mean and standard deviation of the absolute value of the transfer function for gamma distribution with $\zeta_n = 0.01$.

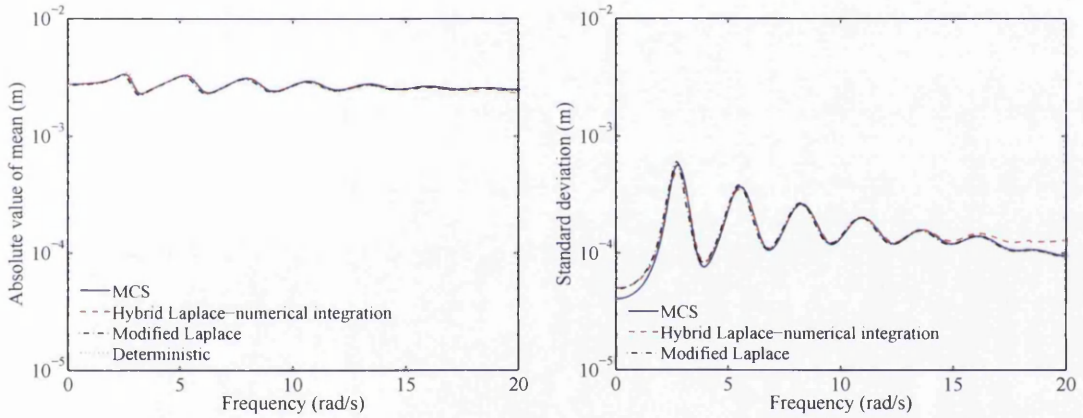

(a) Absolute value of mean. (b) Standard deviation.

Figure 4.14: Mean and standard deviation of the absolute value of the transfer function for lognormal distribution with $\zeta_n = 0.1$.

proximate the integrals at those frequencies where the method is expected to give a good approximation, and numerical integration is used for the remaining frequencies. The second method, i.e. hybrid modified Laplace, also approximates the integrals with Laplace's method when it is supposed to give a good approximation. The remaining integrals are approximated, when possible, with a modified Laplace's method and with numerical integration otherwise. For the frequencies where the modified Laplace's method can be applied, it is observed that Laplace's method provides an approximation smaller than the exact value, while the modified Laplace's method provides mostly a larger approximation. The modified Laplace's approximation gives good approximation at resonance points both for lognormal and normal distribution, but results are too

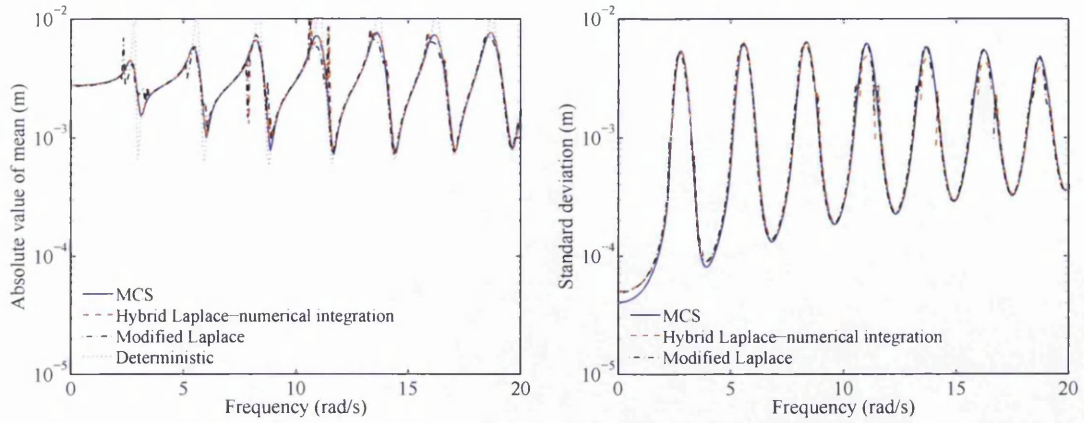

(a) Absolute value of mean.

(b) Standard deviation.

Figure 4.15: Mean and standard deviation of the absolute value of the transfer function for lognormal distribution with $\zeta_n = 0.01$.

large when dealing with the gamma distribution.

It is observed, in all figures where the mean of the system is calculated, that the difference between mean and deterministic system is larger at frequencies in the neighborhood of resonance frequencies than at other frequencies. This is due to the fact that each deterministic FRF corresponding to a sample of the natural frequency ω_n has a sharp peak at frequency $\omega_n\sqrt{1-2\zeta_n^2}$. The effect of taking the mean is equivalent to add up those FRFs with peaks at different frequencies and dividing the result by the number of samples. As a result, the mean appears more damped than the deterministic system in the neighborhood of the mean natural frequency and is closer to the deterministic system at other frequencies. It is also observed that for gamma distribution, the modified Laplace's method leads to results significatively larger than the ones from MCS. This is due to the fact that, while for other distributions the methods provides a good approximation for the resonance frequency, for gamma distribution the method leads to a result close to the deterministic response. The accuracy of the modified Laplace's method is therefore dependent on the pdf of the random variable.

Overall, the level of damping has significant impact on the Laplace's method for both SDOF and MDOF systems. When the systems are reasonably damped (about 10% damping), all the proposed methods work well and the results agree with each other. But the situation changes dramatically when damping becomes small (about 1% or smaller). In this case only numerical integration is able to produced results which agree with the direct Monte Carlo simulation results, at frequencies in the vicinity of

resonance. Therefore, one of the key conclusion from this work is that care should be taken for dynamic analysis of stochastic systems with very light damping.

4.5.2 Summary of results

It can be observed that damping has an important effect on the standard deviation of the response. The higher is the damping, the smaller is the standard deviation compared to the mean. This is observed for both SDOF and MDOF systems, but is more evident for MDOF systems. This effect is independent of the distribution of the random variable. Comparing results of mean and standard deviation for SDOF systems, it is observed that mean and standard deviation of all the pdfs give similar results. On the other side, this is only observed for frequencies near the first natural frequency for MDOF systems. For higher frequencies, mean of the FRF for normal distribution appears more damped than the ones obtained with other distributions, and standard deviation is generally larger than the one for other distributions. Values of mean and standard deviation of FRF for MDOF for lognormal, gamma and uniform distribution are almost coincident for every frequency.

4.6 Conclusions

This Chapter considers the calculation of response statistics of stochastic linear dynamical systems in the low-frequency region. Considering the distribution of the system eigenvalues, two novel semi-analytical methods, namely hybrid Laplace-numerical integration and hybrid modified Laplace methods have been proposed. The proposed methods have been extended to general multiple degree of freedom systems assuming uncorrelated eigensolutions. Due to the semi-analytical nature of the results, the proposed methods can offer computational advantages over direct Monte Carlo simulations for structures with very large number of degrees of freedom.

Mean of the real and imaginary parts of the response vector and second moment of its absolute value are calculated making use of the proposed methods. Four probability density functions, namely uniform, normal, log-normal and gamma, are considered for the natural frequencies. Exact closed-form expressions for the response moments have been obtained for the uniform distribution. It is observed that the accuracy of the proposed method depends on the pdf of the random variable, on the damping factor and

on the frequency at which the integral is evaluated. In general lightly damped systems show less accuracy compared to systems with more damping.

The assumption of uncorrelated eigenvalues is valid for low frequencies, where less overlap between the eigenvalues is expected. In the next Chapter, the dynamic response for a system modelled with non-parametric uncertainty is considered.

Chapter 5

Non-parametric uncertainty in dynamic systems

5.1 Introduction

In the previous Chapter, a method to calculate the first two moments of the frequency response function (FRF) of a dynamic system for low frequencies was proposed. Low frequencies affect civil structures such as buildings, but many aerospace structures are affected by high frequencies, as Keane and Price (1997) mentioned "it is estimated that the Saturn launch vehicle possessed approximately 500000 natural frequencies in the range 0 to 2000 Hz". A method developed to deal with high frequencies is statistical energy analysis (Lyon and Dejong, 1995), and it's original purpose was to model the exchange of energy between different parts of space rockets. When considering high frequencies, the effect of uncertainties in system matrices becomes less straightforward and a nonparametric modelling of the matrices is often preferred (Adhikari, 2010). In this Chapter, the moments of the FRF of a system with nonparametric uncertainty are calculated. All previous works calculating the response of a dynamic system with nonparametric uncertainty used MCS to simulate the system matrices so as to calculate the statistics of their eigenvalues, eigenvectors and the FRF. In section 5.2, a system whose system matrices are modelled with Wishart matrices is described and the nonparametric uncertainty introduced by both system matrices is approximated by a nonparametric uncertainty modelled using a single Wishart matrix. This matrix is approximated with a further simplified Wishart matrix known as White Wishart matrix in section 5.3. Based on the White Wishart approximation, analytical expressions are investigated in

section 5.4. The efficiency of the approximations and of the analytical expressions is illustrated with the numerical example of a thin plate in section 5.5. Conclusions of the Chapter are derived in section 5.6.

5.2 Wishart matrices for linear dynamic systems

5.2.1 Mass and stiffness matrices modelled as independent Wishart matrices

The Wishart random matrix was described in section 1.6 as a model for nonparametric uncertainty. Consider a dynamical system, discretized with the Finite Element method. The response of the system in the frequency domain is given by the solution of Equation (1.98), that is,

$$(-\omega^2\mathbf{M} + \mathrm{i}\omega\mathbf{C} + \mathbf{K})\mathbf{u} = \mathbf{f}, \tag{5.1}$$

where $\mathbf{M}$, $\mathbf{C}$, and $\mathbf{K}$ are respectively the generalised mass, damping, and stiffness matrices, all of them $n \times n$ real symmetric and positive definite. Vector $\mathbf{u}$ is the n-dimensional vector of complex generalised coordinates and $\mathbf{f}$ is the n-dimensional force vector.

The response of the system from Equation (5.1) can be obtained by applying modal analysis, for which the eigenvalues and eigenvectors of the system are calculated. The undamped eigenvalues and eigenvectors of the system, respectively $\lambda^{(j)}$ and $\boldsymbol{\phi}_j$, are obtained from

$$\mathbf{K}\boldsymbol{\phi}_j = \lambda^{(j)}\mathbf{M}\boldsymbol{\phi}_j, \ j = 1, \ldots, n \text{ with } \quad \boldsymbol{\Phi}^T\mathbf{M}\boldsymbol{\Phi} = \mathbf{I}_n, \quad \boldsymbol{\Phi}^T\mathbf{K}\boldsymbol{\Phi} = \boldsymbol{\Lambda} \tag{5.2}$$

or, equivalently,

$$\mathbf{M}^{-1/2}\mathbf{K}\mathbf{M}^{-1/2}\mathbf{v}_j = \lambda^{(j)}\mathbf{v}_j, \ j = 1, \ldots, n \text{ with } \quad \boldsymbol{\phi}_j = \mathbf{M}^{-1/2}\mathbf{v}_j, \quad \mathbf{V}^T\mathbf{V} = \mathbf{I}_n. \tag{5.3}$$

In the previous identities, $\mathbf{V} = [\mathbf{v}_1 \ldots \mathbf{v}_n]$ is the matrix of eigenvectors of $\mathbf{M}^{-1/2}\mathbf{K}\mathbf{M}^{-1/2}$. The matrices of eigenvectors and eigenvalues of the system are given respectively by $\boldsymbol{\Phi} = [\boldsymbol{\phi}_1 \ldots \boldsymbol{\phi}_n]$ and a diagonal matrix $\boldsymbol{\Lambda}$ whose diagonal elements are the eigenvalues $\lambda^{(j)}$. Proportional damping is assumed, so that

$$\boldsymbol{\Phi}^T\mathbf{C}\boldsymbol{\Phi} = 2\boldsymbol{\zeta}^*\boldsymbol{\Lambda}^{1/2}, \tag{5.4}$$

where $\boldsymbol{\zeta}^*$ is a diagonal matrix whose diagonal elements are the damping ratios ζ_j^*. Introducing the change of variables $\mathbf{u} = \boldsymbol{\Phi}\mathbf{q}$ into Equation (5.1), and premultiplying by $\boldsymbol{\Phi}^T$, the equation of motion of the system becomes

$$(-\omega^2\mathbf{I}_n + \mathrm{i}\omega 2\boldsymbol{\zeta}^*\boldsymbol{\Lambda}^{1/2} + \boldsymbol{\Lambda})\mathbf{q} = \boldsymbol{\Phi}^T\mathbf{f}, \tag{5.5}$$

and this equation is equivalent to

$$(-\omega^2\mathbf{I}_n + \mathrm{i}\omega\mathbf{V}^T\mathbf{M}^{-1/2}\mathbf{C}\mathbf{M}^{-1/2}\mathbf{V} + \mathbf{V}^T\mathbf{M}^{-1/2}\mathbf{K}\mathbf{M}^{-1/2}\mathbf{V})\mathbf{V}^T\mathbf{M}^{1/2}\mathbf{u} = \mathbf{V}^T\mathbf{M}^{-1/2}\mathbf{f} \tag{5.6}$$

The response vector is obtained

$$\mathbf{u} = \sum_{j=1}^{n} \frac{\boldsymbol{\phi}_j\boldsymbol{\phi}_j^T\mathbf{f}}{-\omega^2 + \mathrm{i}\omega 2\zeta_j^*\lambda_j^{1/2} + \lambda_j} \tag{5.7}$$

It is observed that, by applying the maximum principle of entropy to both mass and stiffness matrices in Equation (5.1), both matrices can be modelled using independent Wishart matrices. In that case, the mean and second moment of the response are approximated using MCS, as analytical expressions for the eigenvalues and eigenvectors of two independent Wishart matrices are not available. The response moments approximated using N_{MCS} number of samples of the independent Wishart matrices modelling $\mathbf{M}$ and $\mathbf{K}$ are given by

$$\mathrm{E}[\mathbf{u}] = \frac{1}{N_{MCS}} \sum_{i_S=1}^{N_{MCS}} \left(\sum_{j=1}^{n} \frac{\boldsymbol{\phi}_{jS}\boldsymbol{\phi}_{jS}^T\mathbf{f}}{-\omega^2 + \mathrm{i}\omega 2\zeta\lambda_{jS}^{1/2} + \lambda_{jS}} \right) \tag{5.8}$$

$$\mathrm{E}[\mathbf{u}\mathbf{u}^T] = \frac{1}{N_{MCS}} \sum_{i_S=1}^{N_{MCS}} \sum_{j,k=1}^{n} \frac{\boldsymbol{\phi}_{jS}\boldsymbol{\phi}_{jS}^T\mathbf{f}\mathbf{f}^T\boldsymbol{\phi}_{kS}\boldsymbol{\phi}_{kS}^T}{(-\omega^2 + \mathrm{i}\omega 2\zeta_{jS}^*\lambda_{jS}^{1/2} + \lambda_{jS})(-\omega^2 + \mathrm{i}\omega 2\zeta_{kS}^*\lambda_{kS}^{1/2} + \lambda_{kS})} \tag{5.9}$$

where λ_{jS}, $\boldsymbol{\phi}_{jS}$ are the j-th eigenvalue and eigenvector obtained from the i_S-th sample of $\mathbf{M}$ and $\mathbf{K}$, and ζ_{jS}^* is the j-th damping ratio of the system sample.

5.2.2 Eigenvalues matrix modelled with a Wishart matrix

In this subsection, the nonparametric uncertainty in both matrices is approximated using a single Wishart matrix. To this end, the matrix $\boldsymbol{\Lambda} = \mathbf{V}^T\mathbf{M}^{-1/2}\mathbf{K}\mathbf{M}^{-1/2}\mathbf{V}$ from Equation

(5.5) is modelled by a Wishart matrix. Then, a new eigenvalue problem arises

$$\mathbf{\Lambda}\boldsymbol{\psi}_j = l_j\boldsymbol{\psi}_j, \qquad j = 1,\ldots,n \qquad \mathbf{L} = \mathbf{\Psi}^T\mathbf{\Lambda}\mathbf{\Psi} \tag{5.10}$$

from where the matrices of eigenvalues $\mathbf{L}$ and of eigenvectors $\mathbf{\Psi} = [\boldsymbol{\psi}_1,\ldots,\boldsymbol{\psi}_n]$ of matrix $\mathbf{\Lambda}$ are obtained. Consider also that $\boldsymbol{\zeta} = \mathbf{\Psi}^T\boldsymbol{\zeta}^*\mathbf{\Psi}$ is a diagonal matrix. Then, the equation of motion of the system (5.1) where the eigenvalues matrix is modelled with a Wishart matrix is given by

$$(-\omega^2\mathbf{I}_n + \mathrm{i}\omega 2\boldsymbol{\zeta}\mathbf{L}^{1/2} + \mathbf{L})\mathbf{w} = \mathbf{\Psi}^T\mathbf{\Phi}^T\mathbf{f} \tag{5.11}$$

where $\mathbf{q} = \mathbf{\Psi}\mathbf{w}$. Then the response of Equation (5.1) is given by

$$\mathbf{u} = \mathbf{\Phi}\mathbf{\Psi}(-\omega^2\mathbf{I}_n + \mathrm{i}\omega 2\boldsymbol{\zeta}\mathbf{L}^{1/2} + \mathbf{L})^{-1}\mathbf{\Psi}^T\mathbf{\Phi}^T\mathbf{f} \tag{5.12}$$

and its first and second moments are given by

$$\mathrm{E}[\mathbf{u}] = \mathbf{\Phi}\left(\sum_{j=1}^{n}\mathrm{E}\left[\frac{\boldsymbol{\psi}_j\boldsymbol{\psi}_j^T}{-\omega^2 + \mathrm{i}\omega 2\zeta l_j^{1/2} + l_j}\right]\right)\mathbf{\Phi}^T\mathbf{f} \tag{5.13}$$

$$\mathrm{E}[\mathbf{u}\bar{\mathbf{u}}^T] = \sum_{i,j=1}^{n}\mathrm{E}\left[\frac{\mathbf{\Phi}\boldsymbol{\psi}_i\boldsymbol{\psi}_i^T\mathbf{\Phi}^T\mathbf{f}\mathbf{f}^T\mathbf{\Phi}\boldsymbol{\psi}_j\boldsymbol{\psi}_j^T\mathbf{\Phi}^T}{(-\omega^2 + i\omega 2\zeta l_i^{1/2} + l_i)(-\omega^2 + \mathrm{i}\omega 2\zeta l_j^{1/2} + l_j)}\right] \tag{5.14}$$

wtih $\bar{\mathbf{u}}$ the complex conjugate of $\mathbf{u}$. The joint distribution of eigenvalues and eigenvectors of a Wishart matrix was given in Equation (1.46). It was also pointed out that, for a White Wishart matrix, i.e. $W_n(cn, a^2/n\mathbf{I}_n)$, the eigenvalues and eigenvectors are independent. In the next section, methods to calculate the parameters of the White Wishart matrix from the system mass and stiffness matrices are exposed.

5.3 Selection of parameters

Based on the available information on eigenvalues of the system, the dispersion parameter δ_Λ of the Wishart matrix $\mathbf{\Lambda}$ from Equation (5.5) can be derived. Three methods are proposed in this section.

5.3.1 Maximum uncertainty modelling

A White Wishart matrix $\mathbf{G} \sim W_n(p, a^2/n\mathbf{I}_n)$, with $p = cn$ is here used to approximate the Wishart matrix $\mathbf{\Lambda}$. In the model used for the White Wishart matrix, parameters a and c have to be obtained from the original system. It is observed that, in the Marčenko-Pastur distribution from Equation (1.52) (Pastur and Shcherbina, 2011), the minimum and maximum of the eigenvalues of a White Wishart matrix are given by

$$a^+ = a^2(1+\sqrt{c})^2, \quad a^- = a^2(1-\sqrt{c})^2 \tag{5.15}$$

That is, the interval for which the marginal pdf of an eigenvalue is defined is $[a^-, a^+]$ When approximating matrix $\mathbf{\Lambda}$ with a White Wishart model, it is expected that the range of eigenvalues of both matrices will be the same. Assume that the minimum and maximum eigenvalues of the mean of $\mathbf{\Lambda}$ are the minimum and maximum eigenvalues of the system, then

$$\lambda^{(1)} = a^-, \qquad \lambda^{(n)} = a^+. \tag{5.16}$$

Parameters c and a can be retrieved from Equation (5.15), i.e.

$$c = \left(\frac{\sqrt{\lambda^{(n)}} + \sqrt{\lambda^{(1)}}}{\sqrt{\lambda^{(n)}} - \sqrt{\lambda^{(1)}}}\right)^2, \quad a = \frac{\sqrt{\lambda^{(n)}} + \sqrt{\lambda^{(1)}}}{2} \tag{5.17}$$

The dispersion parameter of the White Wishart matrix are produced from Equation (1.44)

$$\delta_G^2 = \frac{1}{p}\left\{1 + \frac{\{\text{Trace}\,(\overline{\mathbf{G}})\}^2}{\text{Trace}\left(\overline{\mathbf{G}}^2\right)}\right\} = \frac{1}{cn}\left\{1 + \frac{(ncna^2/n)^2}{n(cna^2/n)^2}\right\} = \frac{1+n}{cn} \tag{5.18}$$

by noting that $p = cn$ and $\overline{\mathbf{G}} = p\mathbf{\Sigma}_G = cna^2/n\mathbf{I}_n$.

5.3.2 Uncertainty information available for system matrices

In nonparametric uncertainty, the dispersion parameter of a Wishart matrix is given by Equation (1.43), and when considering the case of Equation (5.5), the matrix from which the dispersion parameter is derived can be $\mathbf{G} = \mathbf{V\Lambda V}^T = \mathbf{M}^{-1/2}\mathbf{K}\mathbf{M}^{-1/2}$. The matrix considered previously as Wishart was $\mathbf{\Lambda}$, but $\mathbf{G}$ is also a Wishart matrix of size $n \times n$, with $p_G = p_\Lambda$, $\mathbf{\Sigma}_G = \mathbf{V\Sigma}_\Lambda\mathbf{V}^T$, with the same eigenvalues as $\mathbf{\Lambda}$ and its eigenvec-

tors equal to the eigenvectors of $\mathbf{\Lambda}$ premultiplied by $\mathbf{V}$. The dispersion parameter of $\mathbf{G}$ is given by

$$\delta_G^2 = \frac{\mathrm{E}\left[\left\|\mathbf{M}^{-1/2}\mathbf{K}\mathbf{M}^{-1/2} - \mathrm{E}\left[\mathbf{M}^{-1/2}\mathbf{K}\mathbf{M}^{-1/2}\right]\right\|_{\mathrm{F}}^2\right]}{\left\|\mathrm{E}\left[\mathbf{M}^{-1/2}\mathbf{K}\mathbf{M}^{-1/2}\right]\right\|_{\mathrm{F}}^2} \tag{5.19}$$

$$= \frac{\mathrm{E}\left[\mathrm{Tr}(\mathbf{M}^{-1}\mathbf{K}\mathbf{M}^{-1}\mathbf{K})\right]}{\mathrm{Tr}(\mathrm{E}\left[(\mathbf{M}^{-1/2}\mathbf{K}\mathbf{M}^{-1/2})\right]^T \mathrm{E}\left[(\mathbf{M}^{-1/2}\mathbf{K}\mathbf{M}^{-1/2})\right])} - 1 \tag{5.20}$$

the second equation is obtained by noting that matrices $\mathbf{M}$, $\mathbf{M}^{-1/2}$ and $\mathbf{K}$ are symmetric, so that $\mathrm{Tr}((\mathbf{M}^{-1/2}\mathbf{K}\mathbf{M}^{-1/2})^T(\mathbf{M}^{-1/2}\mathbf{K}\mathbf{M}^{-1/2})) = \mathrm{Tr}(\mathbf{M}^{-1}\mathbf{K}\mathbf{M}^{-1}\mathbf{K})$. Consider that mass and stiffness matrices are modelled by the independent Wishart matrices $\mathbf{K} \sim W_n(p_K, \mathbf{\Sigma}_K)$ and $\mathbf{M} \sim W_n(p_M, \mathbf{\Sigma}_M)$, with known dispersion parameters δ_K^2, δ_M^2 and matrices means $\overline{\mathbf{K}} = \mathrm{E}[\mathbf{K}]$, $\overline{\mathbf{M}} = \mathrm{E}[\mathbf{M}]$. Parameters p_K, p_M, $\mathbf{\Sigma}_K$ and $\mathbf{\Sigma}_M$ in the distributions can be derived from Equations (1.42) and (1.45). Given a Wishart random matrix $\mathbf{W} \sim W_n(p, \mathbf{\Sigma})$, the following moments can be obtained (Gupta and Nagar, 2000)

$$\mathrm{E}[\mathbf{WBW}] = p\mathbf{\Sigma}\mathbf{B}^T\mathbf{\Sigma} + p\mathrm{Trace}(\mathbf{\Sigma}\mathbf{B})\mathbf{\Sigma} + p^2\mathbf{\Sigma}\mathbf{B}\mathbf{\Sigma} \tag{5.21}$$

$$\mathrm{E}\left[\mathbf{W}^{-1}\mathbf{A}\mathbf{W}^{-1}\right] = c_1\mathbf{\Sigma}^{-1}\mathbf{A}\mathbf{\Sigma}^{-1} + c_2\left[\mathbf{\Sigma}^{-1}\mathbf{A}^T\mathbf{\Sigma}^{-1} + \mathrm{Trace}\left(\mathbf{A}\mathbf{\Sigma}^{-1}\right)\mathbf{\Sigma}^{-1}\right] \tag{5.22}$$

$$\mathrm{E}\left[\mathrm{Trace}\left(\mathbf{A}\mathbf{W}^{-1}\right)\mathbf{W}^{-1}\right] = c_1\mathrm{Trace}\left(\mathbf{A}\mathbf{\Sigma}^{-1}\right) + c_2(\mathbf{\Sigma}^{-1}\mathbf{A}^T\mathbf{\Sigma}^{-1} + \mathbf{\Sigma}^{-1}\mathbf{A}\mathbf{\Sigma}^{-1}) \tag{5.23}$$

with $c_1 = (p-n-2)c_2$ and $c_2 = 1/\left((p-n)(p-n-1)(p-n-3)\right)$. Then

$$\mathrm{E}\left[(\mathbf{M}^{-1}\mathbf{K})^2\right] = \mathrm{E}\left[p_K\mathbf{M}^{-1}\mathbf{\Sigma}_K\mathbf{M}^{-1}\mathbf{\Sigma}_K + p_K\mathrm{Trace}\left(\mathbf{\Sigma}_K\mathbf{M}^{-1}\right)\mathbf{M}^{-1}\mathbf{\Sigma}_K\right] + \mathrm{E}\left[p_K^2\mathbf{M}^{-1}\mathbf{\Sigma}_K\mathbf{M}^{-1}\mathbf{\Sigma}_K\right] \tag{5.24}$$

$$= \frac{(1+p_K+p_M-n-2)\mathrm{Trace}\left(\mathbf{\Sigma}_M^{-1}\overline{\mathbf{K}}\right)\mathbf{\Sigma}_M^{-1}\overline{\mathbf{K}}}{p_K(p_M-n)(p_M-n-1)(p_M-n-3)} + \frac{((1+p_K)(p_M-n-1)+2)\mathbf{\Sigma}_M^{-1}\overline{\mathbf{K}}\mathbf{\Sigma}_M^{-1}\overline{\mathbf{K}}}{p_K(p_M-n)(p_M-n-1)(p_M-n-3)} \tag{5.25}$$

$$= \frac{p_M^2\left((p_K+p_M-n-1)\mathrm{Trace}\left((\overline{\mathbf{M}})^{-1}\overline{\mathbf{K}}\right)(\overline{\mathbf{M}})^{-1}\overline{\mathbf{K}}\right)}{p_K(p_M-n)(p_M-n-1)(p_M-n-3)} + \frac{p_M^2\left(((1+p_K)(p_M-n-1)+2)(\overline{\mathbf{M}})^{-1}\overline{\mathbf{K}}(\overline{\mathbf{M}})^{-1}\overline{\mathbf{K}}\right)}{p_K(p_M-n)(p_M-n-1)(p_M-n-3)} \tag{5.26}$$

can be derived using Equation (5.21), $\overline{\mathbf{K}} = \mathrm{E}[\mathbf{K}] = p_K \boldsymbol{\Sigma}_K$, Equations (5.22), (5.23) and $\boldsymbol{\Sigma}_M^{-1} = (\overline{\mathbf{M}})^{-1} p_M$.

To calculate $\mathrm{E}\left[\mathbf{M}^{-1/2}\mathbf{K}\mathbf{M}^{-1/2}\right]$ we firstly recall that any Wishart matrix $\mathbf{A}$ can be obtained from $\mathbf{A} = \mathrm{E}[\mathbf{A}]^{1/2}\, \mathbf{W}^{(A)} \mathrm{E}[\mathbf{A}]^{1/2}$, where $\mathbf{W}^{(A)}$ is a White Wishart matrix of size n with parameters p_A and $\boldsymbol{\Sigma}_{WA} = \mathbf{I}_n / p_A$. This matrix can be decomposed using its eigenvalues and eigenvectors $\mathbf{W}^{(A)} = \sum_{i=1}^{n} \boldsymbol{\psi}_i \boldsymbol{\psi}_i^T l_i$, so that

$$\mathbf{A}^{-1} = \mathbf{A}^{-1/2}\mathbf{A}^{-1/2} \tag{5.27}$$

$$\mathbf{A}^{-1} = (\mathrm{E}[\mathbf{A}])^{-1/4} \left(\sum_{i,j=1}^{n} \frac{\boldsymbol{\psi}_i \boldsymbol{\psi}_i^T (\mathrm{E}[\mathbf{A}])^{-1/2} \boldsymbol{\psi}_j \boldsymbol{\psi}_j^T}{\sqrt{l_i l_j}} \right) (\mathrm{E}[\mathbf{A}])^{-1/4} \tag{5.28}$$

$$\mathrm{E}\left[\mathbf{A}^{-1}\right] = (\mathrm{E}[\mathbf{A}])^{-1/4} \mathrm{E}\left[\left(\sum_{i,j=1}^{n} \frac{\boldsymbol{\psi}_i \boldsymbol{\psi}_i^T (\mathrm{E}[\mathbf{A}])^{-1/2} \boldsymbol{\psi}_j \boldsymbol{\psi}_j^T}{\sqrt{l_i l_j}} \right) \right] (\mathrm{E}[\mathbf{A}])^{-1/4} \tag{5.29}$$

the mean of the inverted Wishart matrix is given, for example, in Gupta and Nagar (2000)

$$\mathrm{E}\left[\mathbf{A}^{-1}\right] = \frac{\boldsymbol{\Sigma}_A^{-1}}{p_A - n - 1} = \frac{\mathrm{E}[\mathbf{A}]^{-1/4}\, \mathrm{E}[\mathbf{A}]^{-1/2}\, \mathrm{E}[\mathbf{A}]^{-1/4}}{p_A (p_A - n - 1)} \tag{5.30}$$

So that

$$\mathrm{E}\left[\left(\sum_{i,j=1}^{n} \frac{\boldsymbol{\psi}_i \boldsymbol{\psi}_i^T (\mathrm{E}[\mathbf{A}])^{-1/2} \boldsymbol{\psi}_j \boldsymbol{\psi}_j^T}{\sqrt{l_i l_j}} \right) \right] = \frac{p_A \mathrm{E}[\mathbf{A}]^{-1/2}}{(p_A - n - 1)} \tag{5.31}$$

It is noted that

$$\mathbf{M}^{-1/2}\overline{\mathbf{K}}\mathbf{M}^{-1/2} = (\overline{\mathbf{M}})^{-1/4} \left(\sum_{i,j=1}^{n} \frac{\boldsymbol{\psi}_i \boldsymbol{\psi}_i^T ((\overline{\mathbf{M}})^{-1/4} \overline{\mathbf{K}} (\overline{\mathbf{M}})^{-1/4}) \boldsymbol{\psi}_j \boldsymbol{\psi}_j^T}{\sqrt{l_i l_j}} \right) (\overline{\mathbf{M}})^{-1/4} \tag{5.32}$$

substituting $\mathrm{E}[\mathbf{A}]^{-1/2}$ by $(\overline{\mathbf{M}})^{-1/4}\overline{\mathbf{K}}(\overline{\mathbf{M}})^{-1/4}$ in Equation (5.31), we obtain

$$\mathrm{E}\left[\mathbf{M}^{-1/2}\overline{\mathbf{K}}\mathbf{M}^{-1/2}\right] = \frac{p_M (\overline{\mathbf{M}})^{-1/2} \overline{\mathbf{K}} (\overline{\mathbf{M}})^{-1/2}}{(p_M - n - 1)} \tag{5.33}$$

From Equations (5.20), (5.33) and (5.26), the dispersion parameter of $\mathbf{G} = \mathbf{M}^{-1/2}\mathbf{K}\mathbf{M}^{-1/2}$ can be obtained

$$\delta_G^2 = \frac{(p_M - n - 1)^2 (p_K + p_M - n - 1) T_1^2 + ((1 + p_K)(p_M - n + 1) + 2) T_2}{p_K (p_M - n)(p_M - n - 1)(p_M - n - 3) T_2} - 1 \tag{5.34}$$

with

$$T_1 = \mathrm{Trace}\left((\overline{\mathbf{M}})^{-1}\overline{\mathbf{K}}\right) \quad \text{and} \quad T_2 = \mathrm{Trace}\left(((\overline{\mathbf{M}})^{-1}\overline{\mathbf{K}})^2\right). \tag{5.35}$$

Equation (5.34) allows to obtain the dispersion parameter of a Wishart matrix whose mean is the eigenvalues matrix. This matrix is approximated with a White Wishart matrix. Parameters c and a of this White Wishart matrix have to be identified. To this end, it is assumed, firstly, that both matrices have the same dispersion parameter

$$\frac{1+n}{cn} = \frac{(p_M-n-1)^2(p_K+p_M-n-1)T_1^2+((1+p_K)(p_M-n+1)+2)T_2}{p_K(p_M-n)(p_M-n-1)(p_M-n-3)T_2} - 1 \tag{5.36}$$

and secondly, that the traces of the means of both matrices are equal

$$\text{Trace}\left(\frac{cna^2}{n}\mathbf{I}\right) = \text{Trace}\left(\text{E}\left[\mathbf{M}^{-1/2}\overline{\mathbf{K}}\mathbf{M}^{-1/2}\right]\right). \tag{5.37}$$

Finally, parameters a^2 and c for a White Wishart matrix approximating the matrix of eigenvalues of two independent Wishart matrices can be given by

$$c = \frac{(1+n)}{n\left(\frac{(p_M-n-1)^2(p_K+p_M-n-1)T_1^2+((1+p_K)(p_M-n+1)+2)T_2}{p_K(p_M-n)(p_M-n-1)(p_M-n-3)T_2} - 1\right)} \tag{5.38}$$

$$a^2 = \frac{p_M \text{Trace}\left((\overline{\mathbf{M}})^{-1/2}\overline{\mathbf{K}}(\overline{\mathbf{M}})^{-1/2}\right)}{cn(p_M-n-1)} \tag{5.39}$$

5.3.3 Uncertainty information available for the eigenvalues

It is observed that for any symmetric matrices **M** and **K**

$$\text{E}\left[\text{Trace}(\mathbf{M}^{-1}\mathbf{K}\mathbf{M}^{-1}\mathbf{K})\right] = \sum_{j=1}^{n}\text{E}\left[\lambda_j^2\right] \tag{5.40}$$

$$\text{Trace}(\text{E}\left[(\mathbf{M}^{-1/2}\mathbf{K}\mathbf{M}^{-1/2})\right]^T \text{E}\left[(\mathbf{M}^{-1/2}\mathbf{K}\mathbf{M}^{-1/2})\right]) = \sum_{j=1}^{n}\text{E}\left[\lambda_j\right]^2 \tag{5.41}$$

from Equation (5.20) the dispersion parameter is related to the first and second moments of eigenvalues

$$\delta_G^2 = \frac{\sum_{j=1}^{n}\text{E}\left[\lambda_j^2\right]}{\sum_{j=1}^{n}\text{E}\left[\lambda_j\right]^2} - 1 \tag{5.42}$$

so that, if information on the eigenvalues of the system is available, the dispersion parameter can be retrieved.

The parameters of the system matrices can be obtained from the first two moments

of the eigenvalues. Parameter p_M can be derived from Equation (5.33)

$$\sum_{j=1}^{n} \mathrm{E}\left[\lambda_j\right] = \frac{p_M \mathrm{Trace}\left((\overline{\mathbf{M}})^{-1/2}\overline{\mathbf{K}}(\overline{\mathbf{M}})^{-1/2}\right)}{p_M - n - 1} \tag{5.43}$$

$$p_M = \frac{(n+1)\sum_{j=1}^{n} \mathrm{E}\left[\lambda_j\right]}{\sum_{j=1}^{n} \mathrm{E}\left[\lambda_j\right] - \mathrm{Trace}\left((\overline{\mathbf{M}})^{-1/2}\overline{\mathbf{K}}(\overline{\mathbf{M}})^{-1/2}\right)} \tag{5.44}$$

and p_k can be obtained from Equations (5.34) using p_M from Equation (5.44) and the dispersion parameter from Equation (5.42), so that

$$p_K = \frac{(p_M - n - 1)^3 T_1^2 + (p_M - n + 3)(T_2)}{(n_1 - p_M)T_1^2 + (p_M - n)T_2((p_M - n)(p_M - n - 3)(\delta_G^2 - 1) - 1)} \tag{5.45}$$

with T_1 and T_2 given at Equation (5.35). It is observed that a mean matrix for both stiffness and mass matrices are needed in the calculation of p_M and p_K, and these matrices can be the ones obtained from a FE analysis.

In the next section, analytical expression for the mean and variance of the response are obtained for the case of the eigenvalues and eigenvectors of a White Wishart. These expressions are valid for all the methods to calculate White Wishart matrix parameters exposed in this section.

5.4 Analytical expressions for the response statistics

Based on Equations (5.13) and (5.14), the first two moments of the response of a dynamic system where the matrix $\mathbf{\Lambda}$ is modelled as a White Wishart matrix are derived.

5.4.1 Mean of the response

For the case of a White Wishart, eigenvalues and eigenvectors are independent (Muirhead, 1982), so that

$$\mathrm{E}[\mathbf{u}] = \mathbf{\Phi}\left(\sum_{j=1}^{n} \mathrm{E}\left[\boldsymbol{\psi}_j \boldsymbol{\psi}_j^T\right] \mathrm{E}\left[\frac{1}{-\omega^2 + \mathrm{i}\omega 2\zeta l_j^{1/2} + l_j}\right]\right) \mathbf{\Phi}^T \mathbf{f} \tag{5.46}$$

From Equation (1.47), it is noticed that $\mathrm{E}\left[\boldsymbol{\psi}_j \boldsymbol{\psi}_j^T\right] = 1/n\mathbf{I}_n$ is the same for all eigenvectors. It is also noticed that the marginal distributions of all eigenvalues are identical,

so that

$$\mathrm{E}[\mathbf{u}] = \mathbf{\Phi}\left(\sum_{j=1}^{n}\frac{1}{n}\mathbf{I}_n\mathrm{E}\left[\frac{1}{-\omega^2+\mathrm{i}\omega 2\zeta l_j^{1/2}+l_j}\right]\right)\mathbf{\Phi}^T\mathbf{f} \tag{5.47}$$

$$= \mathbf{\Phi}\left(\mathbf{I}_n\mathrm{E}\left[\frac{1}{-\omega^2+\mathrm{i}\omega 2\zeta l_j^{1/2}+l_j}\right]\right)\mathbf{\Phi}^T\mathbf{f} \tag{5.48}$$

Separating the real and imaginary parts, we have

$$\mathrm{E}\left[\frac{1}{-\omega^2+\mathrm{i}\omega 2\zeta l_j^{1/2}+l_j}\right] = \mathrm{E}\left[\frac{-\omega^2+l_j}{(-\omega^2+l_j)^2+4\omega^2\zeta^2 l_j}\right] - \mathrm{iE}\left[\frac{\omega 2\zeta l_j^{1/2}}{(-\omega^2+l_j)^2+4\omega^2\zeta^2 l_j}\right] \tag{5.49}$$

The marginal distributions of the eigenvalues are now approximated by the Marčenko-Pastur distribution, given by Equation (1.52). Then, each of the means appearing in Equation (5.49) can be approximated by

$$\mathrm{E}[g(l)] = \int_{a^-}^{a^+} g(l)\frac{\sqrt{a^+-l}\sqrt{l-a^-}}{2\pi a^2 l}dl \tag{5.50}$$

where $a^- = a^2(1-\sqrt{c})^2$, $a^+ = a^2(1+\sqrt{c})^2$ and $g(l)$ can be, for instance, the real and imaginary parts of which mean is taken in Equation (5.49). Introducing the change of variables $l = a^+\cos^2\theta$, the previous equation reduces to

$$\mathrm{E}[g(l)] = \int_{\theta^-}^{0} -g(a^+\cos^2\theta)\frac{\sqrt{a^+}\sin^2\theta\sqrt{a^+\cos^2\theta-a^-}}{\pi a^2\cos\theta}d\theta \tag{5.51}$$

with $\theta^- = \cos^{-1}(-\sqrt{a^-/a^+})$, and, when $c=1$, this integral can be rewritten as

$$\mathrm{E}[g(l)] = \int_{-\pi/2}^{0} -g(4a^2\cos^2\theta)\frac{\sin^2\theta}{\pi}d\theta \tag{5.52}$$

It is noted that this change of variables is introduced to avoid the singularity arising when $c=1$. Then, Equation (5.47) can be written as

$$\mathrm{E}[\mathbf{u}] = \left[\int_{\theta^-}^{0}\frac{-\frac{\omega^2}{a^+}+\cos^2\theta}{(-\frac{\omega^2}{a^+}+\cos^2\theta)^2+4\frac{\omega^2}{a^+}\zeta^2\cos^2\theta}\frac{\sin^2\theta\sqrt{a^+cos^2\theta-a^-}}{\sqrt{a^+}\pi a^2\cos\theta}d\theta - \right.$$
$$\left.\mathrm{i}\int_{\theta^-}^{0}\frac{\frac{\omega}{\sqrt{a^+}}2\zeta\cos\theta}{(-\frac{\omega^2}{a^+}+a^+\cos^2\theta)^2+4\frac{\omega^2}{a^+}\zeta^2\cos^2\theta}\frac{\sin^2\theta\sqrt{a^+\cos^2\theta-a^-}}{\sqrt{a^+}\pi a^2\cos\theta}d\theta\right]\mathbf{\Psi}\mathbf{\Psi}^T\mathbf{f} \tag{5.53}$$

The two integrals can be calculated using numerical methods. Another change of variables that can be performed, but would not be valid for the case $c = 1$, would be $l = a^+ \exp(x)$. With this change of variables Equation (5.50) transforms to

$$\mathrm{E}[g(l)] = \int_{\log(a^-/a^+)}^{0} g(a^+ \exp(x)) \frac{\sqrt{a^+}}{2\pi a^2} \sqrt{1 - \exp(x)} \sqrt{a^+ \exp(x) - a^-} dx \tag{5.54}$$

This change of variables is useful when c is close to one, but still larger than one, say $1 < c < 1.2$.

5.4.2 Variance of the response

Noting that eigenvalues and eigenvectors of a White Wishart matrix are independent, Equation (5.14) leads to

$$\begin{aligned} \mathrm{E}[\mathbf{u}\bar{\mathbf{u}}^T] =& \boldsymbol{\Phi} \left(\sum_{i,j=1}^{n} \mathrm{E}[\boldsymbol{\psi}_i \boldsymbol{\psi}_i^T \boldsymbol{\Phi}^T \mathbf{f}\mathbf{f}^T \boldsymbol{\Phi} \boldsymbol{\psi}_j \boldsymbol{\psi}_j^T] \right. \\ & \left. \mathrm{E}\left[\frac{1}{(-\omega^2 + i\omega 2\zeta l_i^{1/2} + l_i)(-\omega^2 - \mathrm{i}\omega 2\zeta l_j^{1/2} + l_j)} \right] \right) \boldsymbol{\Phi}^T \end{aligned} \tag{5.55}$$

The term $\mathrm{E}[\boldsymbol{\psi}_i \boldsymbol{\psi}_i^T \boldsymbol{\Phi}^T \mathbf{f}\mathbf{f}^T \boldsymbol{\Phi} \boldsymbol{\psi}_j \boldsymbol{\psi}_j^T]$ can be obtained using Equation (1.48)

$$\begin{aligned} \mathrm{E}[\boldsymbol{\psi}_i \boldsymbol{\psi}_i^T \boldsymbol{\Phi}^T \mathbf{f}\mathbf{f}^T \boldsymbol{\Phi} \boldsymbol{\psi}_j \boldsymbol{\psi}_j^T] = & \frac{\left((n+1)\boldsymbol{\Phi}^T \mathbf{f}\mathbf{f}^T \boldsymbol{\Phi} - (\boldsymbol{\Phi}^T \mathbf{f}\mathbf{f}^T \boldsymbol{\Phi} + \mathbf{f}^T \boldsymbol{\Phi}\boldsymbol{\Phi}^T \mathbf{f}\mathbf{I}_n)\right)}{n(n-1)(n+2)} + \\ & \frac{\delta_{ij}(-2\boldsymbol{\Phi}^T \mathbf{f}\mathbf{f}^T \boldsymbol{\Phi} + n(\boldsymbol{\Phi}^T \mathbf{f}\mathbf{f}^T \boldsymbol{\Phi} + \mathbf{f}^T \boldsymbol{\Phi}\boldsymbol{\Phi}^T \mathbf{f}\mathbf{I}_n))}{n(n-1)(n+2)} \end{aligned} \tag{5.56}$$

The variance of $\mathbf{u}$ is given by

$$\mathrm{Var}[\mathbf{u}] = \mathrm{E}[\mathbf{u}\bar{\mathbf{u}}^T] - \mathrm{E}[\mathbf{u}]\mathrm{E}[\bar{\mathbf{u}}]^T = \mathrm{Var}[\Re[\mathbf{u}]] + \mathrm{Var}[\Im[\mathbf{u}]] \tag{5.57}$$

with $\bar{\mathbf{u}}$ the complex conjugate of $\mathbf{u}$. Consider $h_i = \frac{1}{-\omega^2 + i\omega 2\zeta l_i^{1/2} + l_i} = \Re(h_i) + \mathrm{i}\Im(h_i)$, then, the variance of $\mathbf{u}$ is given by

$$\begin{aligned} \mathrm{Var}[\mathbf{u}] \quad = & \boldsymbol{\Phi} \left(\frac{(n+1)\boldsymbol{\Phi}^T \mathbf{f}\mathbf{f}^T \boldsymbol{\Phi} - (\boldsymbol{\Phi}^T \mathbf{f}\mathbf{f}^T \boldsymbol{\Phi} + \mathbf{f}^T \boldsymbol{\Phi}\boldsymbol{\Phi}^T \mathbf{f}\mathbf{I}_n)}{n(n-1)(n+2)} \sum_{i,j=1}^{n} \mathrm{E}\left[h_i \bar{h_j}\right] + \right. \\ & \left. \frac{(-2\boldsymbol{\Phi}^T \mathbf{f}\mathbf{f}^T \boldsymbol{\Phi} + n(\boldsymbol{\Phi}^T \mathbf{f}\mathbf{f}^T \boldsymbol{\Phi} + \mathbf{f}^T \boldsymbol{\Phi}\boldsymbol{\Phi}^T \mathbf{f}\mathbf{I}_n))}{n(n-1)(n+2)} \sum_{i=1}^{n} \mathrm{E}\left[(\Re^2(h_i) + \Im^2(h_i))\right] \right) \boldsymbol{\Phi}^T - \\ & \left(\left(\mathrm{E}\left[\Re(h_i)\right]\right)^2 + \left(\mathrm{E}\left[\Im(h_i)\right]\right)^2 \right) \boldsymbol{\Phi}\boldsymbol{\Phi}^T \mathbf{f}\mathbf{f}^T \boldsymbol{\Phi}\boldsymbol{\Phi}^T \end{aligned} \tag{5.58}$$

Consider a diagonal tensor whose i-th diagonal element is the function g_i, denote its trace by $\text{Trace}\,(\mathbf{G}(\omega)) = \sum_{i=1}^{n} g_i(\omega)$, so that

$$\text{Var}[\text{Trace}\,(\mathbf{G}(\omega))] = \sum_{i,j=1}^{n} (\text{E}[g_i(\omega)g_j(\omega)] - \text{E}[g_i(\omega)]\text{E}[g_j(\omega)]) \tag{5.59}$$

Adding and subtracting to Equation (5.58) the term

$$\mathbf{\Psi}\left(\frac{(n+1)\mathbf{\Psi}^T\mathbf{f}\mathbf{f}^T\mathbf{\Psi} - (\mathbf{\Psi}^T\mathbf{f}\mathbf{f}^T\mathbf{\Psi} + \mathbf{f}^T\mathbf{\Psi}\mathbf{\Psi}^T\mathbf{f}\mathbf{I}_n)}{n(n-1)(n+2)}\left(\sum_{i,j=1}^{n}\left(\text{E}\left[h_i\right]\text{E}\left[\bar{h}_j\right]\right)\right)\right)\mathbf{\Psi}^T$$

leads to

$$\begin{aligned}\text{Var}[\mathbf{u}] = \mathbf{\Phi}\Bigg(&\frac{(n+1)\mathbf{\Phi}^T\mathbf{f}\mathbf{f}^T\mathbf{\Phi} - (\mathbf{\Phi}^T\mathbf{f}\mathbf{f}^T\mathbf{\Phi} + \mathbf{f}^T\mathbf{\Phi}\mathbf{\Phi}^T\mathbf{f}\mathbf{I}_n)}{n(n-1)(n+2)}\text{Var}\left[\text{Tr}(\mathbf{H})\right] + \\ &\left(\frac{(n-2)\mathbf{\Phi}^T\mathbf{f}\mathbf{f}^T\mathbf{\Phi} + n\mathbf{f}^T\mathbf{\Phi}\mathbf{\Phi}^T\mathbf{f}\mathbf{I}_n}{(n-1)(n+2)}\right)\left(\text{Var}\left[\Re(h_i)\right] + \text{Var}\left[\Im(h_i)\right]\right)\Bigg)\mathbf{\Phi}^T\end{aligned} \tag{5.60}$$

with $\mathbf{H}$ the diagonal matrix whose diagonal entries are h_i. We now calculate $\text{Var}\left[h_i\right] = \text{Var}\left[\Re(h_i)\right] + \text{Var}\left[\Im(h_i)\right]$ and $\text{Var}\left[\text{Trace}(\mathbf{H})\right]$. For the first of these variances, only the marginal distribution of the eigenvalues are needed. When $n \to \infty$, this distribution tends to the Marčenko-Pastur distribution, so that the variance is approximated by

$$\begin{aligned}\text{Var}\left[h_i\right] = &\int_{a^-}^{a^+}\left(\frac{1}{(-\omega^2+l_i)^2 + 4\omega^2\zeta^2 l_i}\right)\frac{\sqrt{a^+ - l_i}\sqrt{l - a^-}}{2\pi a^2 l_i}dl_i \\ &- \left(\int_{a^-}^{a^+}\left(\frac{-\omega^2+l_i}{(-\omega^2+l_i)^2 + 4\omega^2\zeta^2 l_i}\right)\frac{\sqrt{a^+ - l_i}\sqrt{l_i - a^-}}{2\pi a^2 l_i}dl\right)^2 \\ &- \left(\int_{a^-}^{a^+}\left(\frac{2\omega\zeta\sqrt{l_i}}{(-\omega^2+l_i)^2 + 4\omega^2\zeta^2 l_i}\right)\frac{\sqrt{a^+ - l_i}\sqrt{l_i - a^-}}{2\pi a^2 l}dl_i\right)^2\end{aligned} \tag{5.61}$$

where the same change of variables as in Equation (5.51) can be performed.

The term $\text{Var}\left[\text{Trace}(\mathbf{H})\right] = \text{Var}\left[\text{Trace}(\Re(\mathbf{H}))\right] + \text{Var}\left[\text{Trace}(\Im(\mathbf{H}))\right]$ is obtained from Equation (1.54). In this equation, we perform change of variables $l - a_m = 2a^2\sqrt{c}\cos\theta$, for both $l = l_1$ and $l = l_2$, so that the jacobian of the transformation is $dl_1 dl_2 = 4a^4 c \sin\theta_1 \sin\theta_2 d\theta_1 d\theta_2$. The integral reduces to

$$V_{Wish}[\varphi] = \frac{1}{2\pi^2}\int_{-\pi}^{0}\int_{-\pi}^{0}\left(\frac{\Delta\varphi}{\Delta l}\right)^2 4a^4 c(1 - cos\theta_1\cos\theta_2)d\theta_1 d\theta_2 \tag{5.62}$$

For the calculation of the two variances $\text{Var}\left[\text{Trace}\left(\Re(\mathbf{H})\right)\right]$ and $\text{Var}\left[\text{Trace}\left(\Im(\mathbf{H})\right)\right]$, the

term $(\Delta\varphi/\Delta l)^2$ has to be calculated to implement numerical integration. Firstly, the calculation of Var [Trace $(\Re(\mathbf{H}))$] is performed. Here, $\varphi(l) = (-\omega^2+l)/((-\omega^2+l)^2 + 4\zeta^2\omega^2 l)$, so that

$$\frac{\Delta\varphi}{\Delta l} = \frac{(-\omega^2+l_2)(-\omega^2+l_1) - 4\zeta^2\omega^4}{((-\omega^2+l_2)^2+4\zeta^2\omega^2 l_1)((-\omega^2+l_1)^2+4\zeta^2\omega^2 l_2)} \tag{5.63}$$

We focus now on the calculation of Var [Trace $(\Im(\mathbf{H}))$]. We notice that $l_2 - l_1 = (\sqrt{l_2}-\sqrt{l_1})(\sqrt{l_2}+\sqrt{l_1})$, so that now

$$\frac{\Delta\varphi}{\Delta l} = \frac{1}{\sqrt{l_2}+\sqrt{l_1}} \frac{2\zeta\omega(-\omega^4+2\omega^2\sqrt{l_1 l_2}+\sqrt{l_1 l_2}(l_1+l_2+\sqrt{l_1 l_2})+4\zeta^2\omega^2)}{((-\omega^2+l_2)^2+4\zeta^2\omega^2 l_1)((-\omega^2+l_1)^2+4\zeta^2\omega^2 l_2)} \tag{5.64}$$

The two terms contributing to the covariance are of different order. Consider that the forcing vector applied to the structure is such that, for all the possible Finite Element discretizations possible, $\mathbf{f}^T\mathbf{u} \approx C$, that is, the work of the force is the same. It is noted that when the size n of the vectors increases, the elements of $\mathbf{u}$ remain of the same order for all discretizations. Then, if the force applied is distributed, the order of the elements of $\mathbf{f}$ is $O(1/n)$. Then, it is noted that the term multiplying Var [Trace $(\mathbf{H})$] is of order $O(1/n^4)$ while the one multiplying (Var $[\Re(h_i)]$ + Var $[\Im(h_i)]$) is of order $O(1/n^2)$. Then, to simplify calculations, only this last term is considered when calculating the variance.

Then, for the numerical examples, the variance of the response is calculated with

$$\text{Var}[\mathbf{u}] \approx \mathbf{\Phi}\left(\left(\frac{(n-2)\mathbf{\Phi}^T\mathbf{f}\mathbf{f}^T\mathbf{\Phi} + n\mathbf{f}^T\mathbf{\Phi}\mathbf{\Phi}^T\mathbf{f}\mathbf{I}_n}{(n-1)(n+2)}\right)\text{Var}\left[h_i\right]\right)\mathbf{\Phi}^T \tag{5.65}$$

where Var $[h_i]$ is given by Equation (5.61) and each of the integrals is calculated using the changes of variables introduced at Equation (5.51) or at Equation (5.54).

5.5 Numerical example

The numerical example of a plate bending problem is given to investigate the efficiency of the proposed method. The domain of the plate is a rectangle of length $L = 1$ m and width $W = 0.6$ m, as shown in Figure 5.1. The plate is clamped along its width (coordinate $x = -0.5$ m) and an impulse load of value $P = 1$ N is applied at $(x, y) = (0.5, 0)$ m in time domain, that is, a constant force in frequency domain. The system is modelled

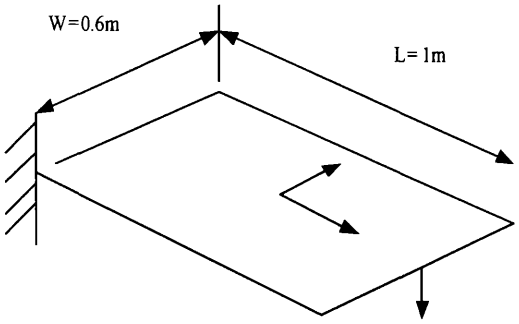

Figure 5.1: A rectangular elastic plate subjected to an impulse load.

applying the Finite Element method with rectangular elements, where 10 elements in x direction and 6 elements in y direction are used. The deterministic system matrices are of dimension $n = 210$. Details on the FE method can be found, for example, in Dawe (1984).

Firstly, the case where both system matrices are modelled with independent Wishart matrices is perused in subsection 5.5.1, and the effect of different combinations of dispersion parameters for both matrices is compared. Then, The matrix $\mathbf{\Lambda}$ is modelled as a White Wishart matrix in subsection 5.5.2, where two methods to obtain the dispersion parameter are applied, namely, the methods proposed in subsection 5.3.1 and subsection 5.3.2 respectively. Finally, the analytical expressions from section 5.4 are compared with MCS in subsection 5.5.3.

5.5.1 System matrices modelled with independent Wishart matrices

The vertical displacement of the system where **M** and **K** are modelled with Wishart matrices is calculated with MCS using 2000 samples. The Wishart distributions are obtained using different values of δ_M^2= [0.003, 0.093, 0.181, 0.271] and δ_K^2= [δ_{K1}^2, δ_{K2}^2, δ_{K3}^2, δ_{K4}^2] with $\delta_{K1}^2 = 0.003$, $\delta_{K2}^2 = 0.088$, $\delta_{K3}^2 = 0.173$, $\delta_{K4}^2 = 0.258$]. The absolute value of the mean and the standard deviation of the response at the right corner of the plate are shown for each δ_M in increasing order in Figure 5.2, Figure 5.3, Figure 5.4 and Figure 5.5. It is observed that, when comparing the mean of the absolute value of the response for the two smallest uncertainties in the mass matrix (i.e. Subfigure 5.2(a) and Subfigure 5.3(a)) the smaller the uncertainty in the stiffness matrix leads to higher values of the absolute value of the mean higher. It is also observed that, as the parameter

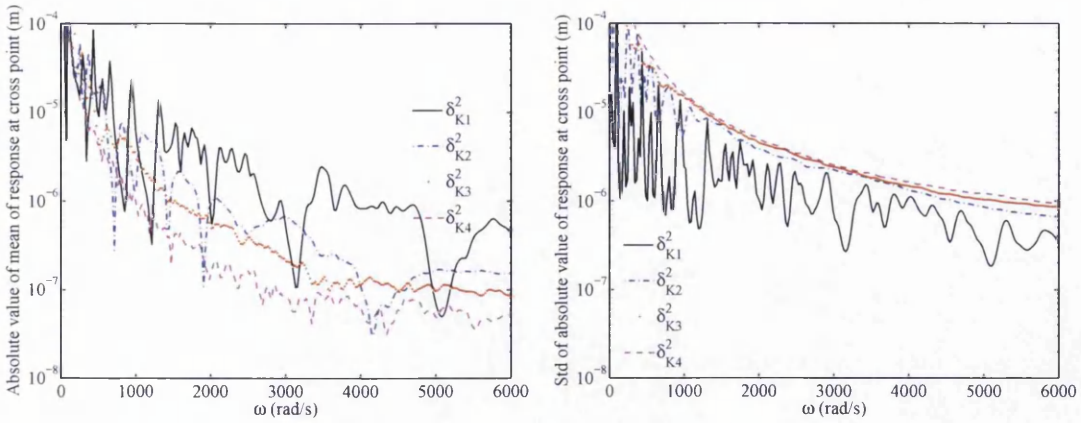

(a) Absolute value of mean. (b) Standard deviation.

Figure 5.2: Mean and standard deviation of the absolute value of the transfer function for $\delta_M = 0.0028^2$ and different δ^2_K.

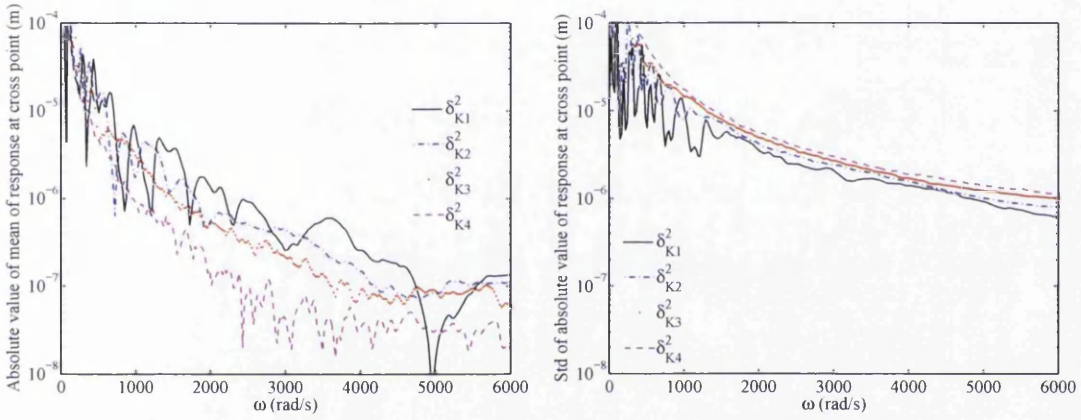

(a) Absolute value of mean. (b) Standard deviation.

Figure 5.3: Mean and standard deviation of the absolute value of the transfer function for $\delta^2_M = 0.0964$ and different δ^2_K.

of uncertainty in the mass matrix increases, i.e. comparing the previous two figures to Subfigure 5.4(a) and Subfigure 5.5(a), all plots are of the same order of magnitude.

When comparing the standard deviation of the absolute value, it is observed that for all the plots, i.e. Subfigure 5.2(b), Subfigure 5.3(b), Subfigure 5.4(b) and Subfigure 5.5(b), larger amounts of uncertainty in the stiffness matrix leads to higher variance.

The same observations would be drawn for plots with different dispersion of mass matrix and fixed dispersion parameter of the stiffness matrix.

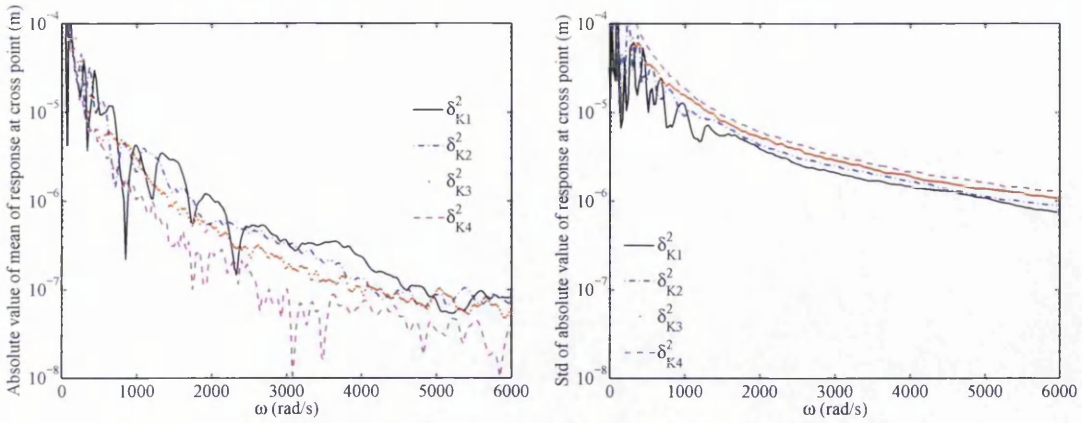

(a) Absolute value of mean. (b) Standard deviation.

Figure 5.4: Mean and standard deviation of the absolute value of the transfer function for $\delta^2_M = 0.1901$ and different δ^2_K.

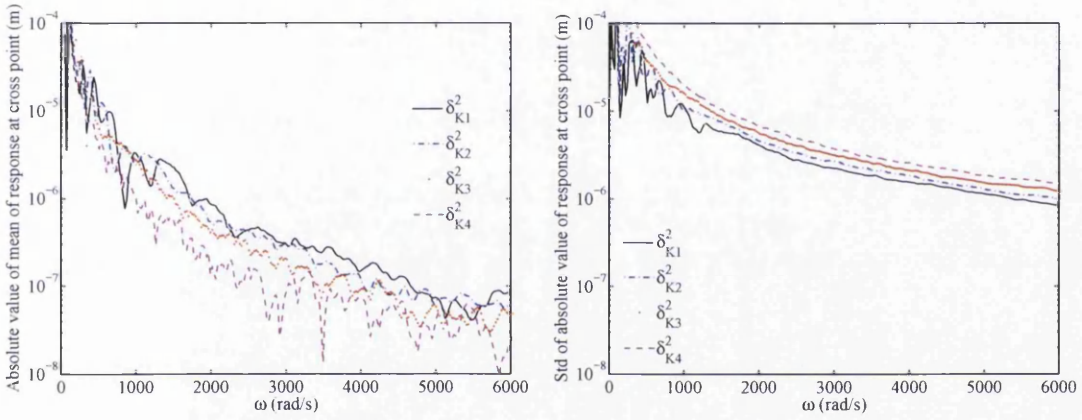

(a) Absolute value of mean. (b) Standard deviation.

Figure 5.5: Mean and standard deviation of the absolute value of the transfer function for $\delta^2_M = 0.2837$ and different δ^2_K.

5.5.2 Modelling with different White Wishart parameters

The system matrices are independent Wishart matrices such that $\delta^2_K = 0.0538$ and $\delta^2_M = 0.0568$. The vertical displacement of the system using White Wishart is calculated with MCS using 5000 samples. The mean of the absolute value of the response is shown in Subfigure 5.6(a). The standard deviation of the response at the same location is given at Subfigure 5.6(b). When considering only the mean of the system, i.e. Subfigure 5.6(a), both approaches are equally close to the system where both system matrices are Wishart matrices. From the covariance Subfigure 5.6(b), it is observed that the approach that models the White Wishart matrix using only information from the deterministic system is the closest to the system where both matrices are Wishart. Therefore, in the next

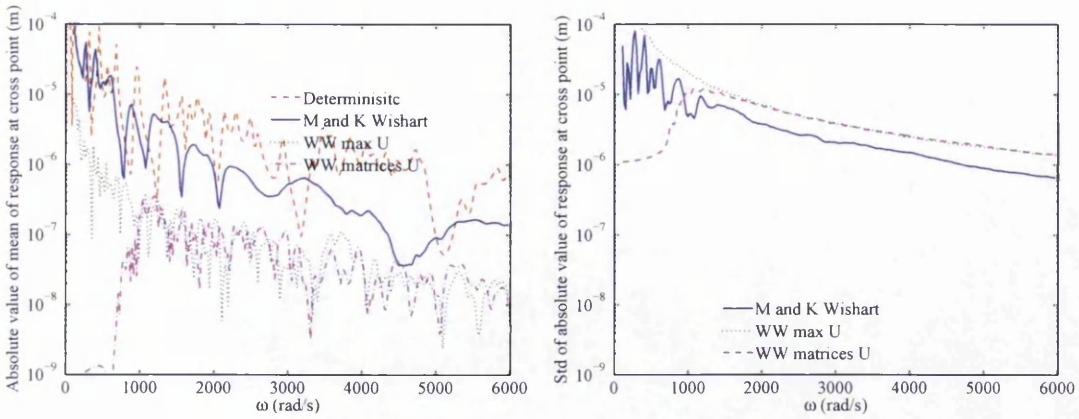

(a) Absolute value of mean.

(b) Standard deviation.

Figure 5.6: Absolute value of mean of response and standard deviation of absolute value of response. The results are obtained using MCS. The different FRFs are obtained using (1) the deterministic system, (2) system matrices modelled with Wishart matrices, denoted by "M and K Wishart", (3) a White Wishart matrix whose parameters are calculated using the maximum uncertainty modelling approach from subsection 5.3.1, denoted by "WW max U", (4) a White Wishart matrix whose parameters are calculated from the dispersion parameters of $\mathbf{M}$ and $\mathbf{K}$ as explained in subsection 5.3.2, denoted by "WW matrices U".

subsection, the analytical expressions for the mean and variance of a system using the eigenvalues and eigenvectors of a White Wishart matrix are compared against MCS of the system whose uncertainty is modelled using a White Wishart matrix.

5.5.3 Accuracy of White Wishart analytical expressions

The vertical displacement of the system using a White Wishart multivariate distribution with parameters calculated as indicated in subsection 5.3.1 is calculated both with MCS using 5000 samples and using the analytical expressions from section 5.4. The absolute value of the mean and the standard deviation of the absolute value of the mean are shown respectively in Subfigure 5.7(a) and Subfigure 5.7(b). It is observed in Subfigure 5.7(b) that the standard deviation plots agree perfectly. That is, neglecting the effect of Var [Trace($\mathbf{H}$)] in Equation (5.60) has no noticeable effect. On the other side, the analytical expressions for the absolute value of the mean of the response do not follow the results from MCS as closely, as can be observed from Subfigure 5.7(a). This is likely to be due to, in part, to a slow convergence of results from MCS with the number of samples, and also, to the small values of the mean. These values are, as can be observed, two orders of magnitude smaller than the results from the standard deviation.

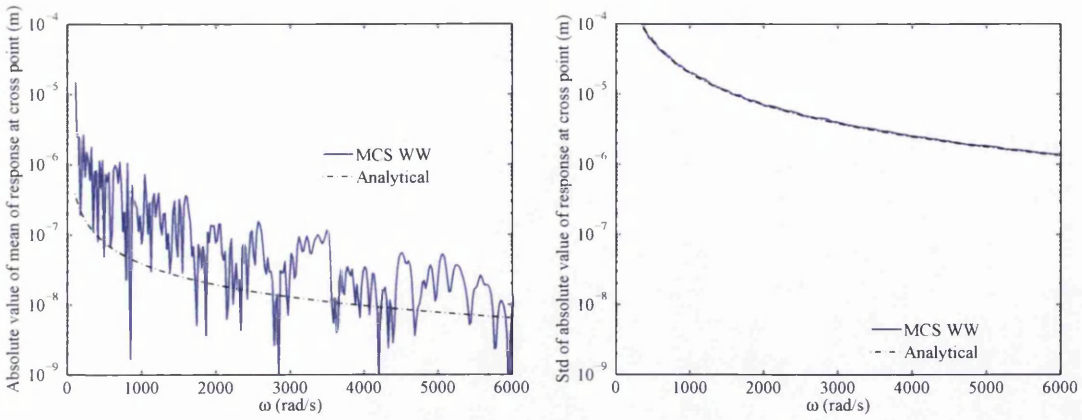

(a) Absolute value of mean.

(b) Standard deviation.

Figure 5.7: Absolute value of mean of response and standard deviation of absolute value of response. The system approximates the eigenvalues matrix with a White Wishart using information from the deterministic eigenvalues and eigenvectors. Analytical expressions and results from MCS are compared.

5.6 Conclusions

The Chapter considers the propagation of nonparametric uncertainty in linear dynamic systems. Three aspects of the problem are considered. Firstly, The system mass and stiffness matrices are modelled with Wishart matrices with different dispersion parameters, and the effect of these dispersion parameters on the response mean and variance is compared. Secondly, The effect of these two Wishart matrices is approximated using a single White Wishart matrix, and two methods to obtain the parameters of the White Wishart matrix are developed and compared. The two methods are based, respectively, on using information from the deterministic eigenvalues, on using information on the randomness of the system matrices. A method to obtain the parameters of mass and stiffness matrices from the first two moments of eigenvalues is also studied. Finally, analytical expressions for the mean and variance of the absolute value of the response are derived, based on results on the asymptotic distribution of eigenvalues of a White Wishart matrix. The numerical example of a rectangular thin plate clamped in one edge is used to illustrate the procedure. It is observed that the method that calculates the White Wishart distribution parameters using information from the deterministic eigenvalues is closer to the case where both matrices are modelled with Wishart matrices. The analytical expressions are applied to this case and compared to MCS.

Until now, parametric and nonparametric uncertainties have been considered to af-

fect the system separately, in the next Chapter, both kinds of uncertainties are considered together.

Chapter 6

Combined parametric-nonparametric uncertainty quantification

6.1 Introduction

Previously, new propagation methods for systems affected by parametric uncertainty were discussed in Chapter 2 and Chapter 3, and maximum entropy principles affecting dynamic systems were considered in Chapter 4 and Chapter 5, but both kinds of uncertainties can affect real life structures. Both uncertainties can affect the same domain of a structure, as, for example, the case of a flow through porous media problem, where permeability is modelled with a random field, but the mapping of this random field into the system operator is not completely known. Also, structures may be composed of several parts, where the parametric uncertainties affecting each part is known, but the modelling of the joints is subjected to errors or simplifications. That is why both kinds of uncertainties should be considered.

The system considered is modelled with a linear partial differential equation (e.g. stationary elliptic PDE) and this equation can be discretized with the finite element method (FEM) (e.g. Zienkiewicz and Taylor (1991)). Then, if n is the number of degrees of freedom of the system, a vector of nodal response $\mathbf{u} \in \mathbb{R}^n$, a linear operator or stiffness matrix $\mathbf{K} \in \mathbb{R}^{n \times n}$ and a forcing term $\mathbf{f} \in \mathbb{R}^n$ are related through the equation

$$\mathbf{K}\mathbf{u} = \mathbf{f} \tag{6.1}$$

The uncertainty appearing as random forces applied to the structure is included in the random forcing term $\mathbf{f}$. For data/aleatoric uncertainties, statistics of the system param-

eters (Young's modulus, etc) can be described through their joint probability density function (pdf) or as functions of known random variables. Then, the uncertainty of the parameters is propagated to the stiffness matrix, that becomes a random matrix as a consequence. Both parametric (aleatoric) and non-parametric (epistemic) uncertainties in system (6.1) can be completely characterised by the joint pdf of $\mathbf{K}$ and $\mathbf{f}$. The method for obtaining this joint pdf will depend on the nature of uncertainties.

In this Chapter, methods to deal with two types of combined uncertainty are proposed. The first type of combined uncertainty considers that both parametric and non-parametric uncertainty affect the whole domain of the system while the second type of combined uncertainty considers that each type of uncertainty affects a different subdomain of the system. The first and second moments of the response are obtained by combining results from polynomial chaos to deal with parametric uncertainty and from analytical expressions of moments of the inverted Wishart matrix to deal with nonparametric uncertainty. The case where both kinds of uncertainties appear on overlapped domains is dealt with in section 6.2. The case of uncertainties appearing over non-overlapping domains is considered in section 6.3. Two methods are proposed based on substructuring techniques to obtain mean and standard deviation of the response. Each method uses a different technique to ensure positive definiteness of the system operator. The proposed combined approaches are applied to an Euler-Bernoulli beam problem and a flow through porous media problem.

6.2 Combined uncertainty over the entire domain

6.2.1 Problem description

Combined uncertainty over the same domain arises, for example, in flow through porous media, where the permeability can be described by a random field but at the same time the model used is not well known. That is, there are cases where the mean model of the non-parametric uncertainty can be affected by parametric uncertainty. This approach to uncertainty was adopted by Soize (2010) for a dynamic system. There, the reduced system matrices taken as the mean matrices of the nonparametric model were affected by parametric uncertainty. The response of the dynamic system was obtained through MCS. In Figure 6.1 a domain affected by both parametric and nonparamet-

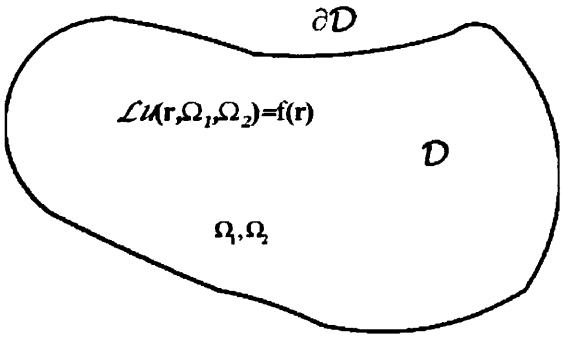

Figure 6.1: Combined uncertainty over the entire domain.

ric uncertainty is considered, where parametric uncertainty is represented by $\omega_1 \in \Omega_1$ and nonparametric uncertainty is represented by $\omega_2 \in \Omega_2$. The elliptic partial differential equation representing the mean system of nonparametric uncertainty is affected by parametric uncertainty defined on the probability space $(\Omega_1, \mathcal{F}_1, P_1)$ with $\omega_1 \in \Omega_1$ such that

$$-\nabla.\left[a(\mathbf{r},\omega_1)\nabla u(\mathbf{r},\omega_1)\right] = f(\mathbf{r}); \quad \mathbf{r} \text{ in } \mathcal{D}; \quad u(\mathbf{r},\omega_1) = 0 \text{ on } \partial\mathcal{D}. \tag{6.2}$$

where $\mathbf{r}$ denotes a point of the geometry, a is a parameter depending on the material, f is the source variable and u is the primary variable. The solution procedure to this case using PC has already been discussed in section 1.7.3, where the solution of Equation (1.88) gives the coefficients of the PC expansion. When considering nonparametric uncertainty, defined on $(\Omega_2, \mathcal{F}_2, P_2)$, the assumed knowledge of the system are the mean matrix and the dispersion parameter. If a system is known to have parametric uncertainty, the mean matrix of the combined model with respect to non-parametric uncertainty is given by the random matrix of the parametric uncertainty, that is

$$\mathrm{E}_2\left[\mathbf{K}_C\right] = \mathbf{K}_{Par} = p\boldsymbol{\Sigma} = \mathbf{K}_0 + \sum_{i=1}^{M} \xi_i \mathbf{K}_i. \tag{6.3}$$

where $\mathrm{E}_2[\,]$ denotes the mean taken with respect to Ω_2, $\mathbf{K}_{Par}$ is the random matrix model only affected by parametric uncertainty, ξ_i are independent identically distributed random variables defined on $(\Omega_1, \mathcal{F}_1, P_1)$. Parameter p is defined in Equation (1.45) where $\overline{\mathbf{G}} = \mathbf{K}_0$, that is, it is calculated as in the case where only nonparametric un-

certainty affects the system so that $p = p(\Omega_2)$. The stiffness matrix considering combined uncertainty is then modelled by $\mathbf{K}_C \backsim W_n(p, (\mathbf{K}_0 + \sum \xi_i \mathbf{K}_i)/p)$. It is observed that, to perform MCS, firstly the parametric probabilistic space $(\Omega_1, \mathcal{F}_1, P_1)$ is sampled, and based on a particular sample of this space, the nonparametric probabilistic space $(\Omega_2, \mathcal{F}_2, P_2)$ is sampled. That is, when both spaces $(\Omega_1, \mathcal{F}_1, P_1)$ and $(\Omega_2, \mathcal{F}_2, P_2)$ are independent, the sample space is given by $\Omega_1 \times \Omega_2$.

6.2.2 Analytical solution

The solution of the problem is such that $\mathbf{u} = \mathbf{K}_C^{-1}\mathbf{f}$ with matrix $\mathbf{K}$ modelled by a Wishart matrix whose mean depends on a set of independent identically distributed random variables, that is, $\mathbf{K}_C \backsim W_n(p, (\mathbf{K}_0 + \sum \xi_i \mathbf{K}_i)/p)$. It is known from the theory of random matrices that the first and second moments of the inverse of a Wishart matrix $W_p(n, \mathbf{\Sigma})$, called inverted Wishart matrix, are given by Gupta and Nagar (2000) as

$$\mathrm{E}\left[\mathbf{W}^{-1}\right] = \frac{\mathbf{\Sigma}^{-1}}{p-n-1} \tag{6.4}$$

$$\mathrm{E}\left[\mathbf{W}^{-1}\mathbf{A}\mathbf{W}^{-1}\right] = c_1\mathbf{\Sigma}^{-1}\mathbf{A}\mathbf{\Sigma}^{-1} + c_2\left[\mathbf{\Sigma}^{-1}\mathbf{A}^T\mathbf{\Sigma}^{-1} + \mathrm{Trace}\left(\mathbf{A}\mathbf{\Sigma}^{-1}\right)\mathbf{\Sigma}^{-1}\right] \tag{6.5}$$

with

$$c_1 = (p-n-2)c_2, \quad c_2 = 1/\left((p-n)(p-n-1)(p-n-3)\right) \tag{6.6}$$

Parametric and non-parametric uncertainties are assumed to be uncorrelated that is, the mean and the second moment of the response are given by

$$\mathrm{E}\left[\mathbf{u}\right] = \mathrm{E}_1\left[\mathrm{E}_2\left[\mathbf{u}\right]\right] = \frac{\mathrm{E}_1\left[\mathbf{K}_{Par}^{-1}\mathbf{f}\right]p}{p-n-1} \tag{6.7}$$

$$\mathrm{E}\left[\mathbf{u}\mathbf{u}^T\right] = \mathrm{E}_1\left[\mathrm{E}_2\left[\mathbf{u}\mathbf{u}^T\right]\right] = (c_1+c_2)p^2\mathrm{E}_1\left[\mathbf{K}_{Par}^{-1}\mathbf{F}\mathbf{K}_{Par}^{-1}\right] + c_2p^2\mathrm{E}_1\left[\mathrm{Trace}\left(\mathbf{F}\mathbf{K}_{Par}^{-1}\right)\mathbf{K}_{Par}^{-1}\right] \tag{6.8}$$

with $\mathbf{F} = \mathbf{f}\mathbf{f}^T$, and where $\mathrm{E}_1[\ ]$ is the mean taken with respect to parametric uncertainty defined on Ω_1. Means $\mathrm{E}_1\left[\mathbf{K}_{Par}^{-1}\right]$, $\mathrm{E}_1\left[\mathbf{K}_{Par}^{-1}\mathbf{F}\mathbf{K}_{Par}^{-1}\right]$ and $\mathrm{E}_1\left[\mathrm{Trace}\left(\mathbf{F}\mathbf{K}_{Par}^{-1}\right)\mathbf{K}_{Par}^{-1}\right]$ will be expressed using the polynomial chaos expansion of the response obtained from the parametric uncertainty analysis using the Galerkin method. It is noted that non-intrussive methods could also be used to approximate the means, by using a collocation method.

Denote by $\mathbf{u}^{(\mathrm{PC})}$, $\mathbf{K}_{Par}^{-1(\mathrm{PC})}$ and $\mathbf{f}^{(\mathrm{PC})}$ the PC expansion of the system response, inverse

of the parametric stiffness matrix and forcing term where only parametric uncertainty is considered. Then, the coefficients of the three PC expansions can be related through

$$\mathbf{u}^{(\mathrm{PC})} = \mathbf{K}_{Par}^{-1^{(\mathrm{PC})}} \mathbf{f}^{(\mathrm{PC})} \tag{6.9}$$

$$\mathbf{u}_k \mathrm{E}\left[\Gamma_k^2\right] = \sum_{i=1}^{P}\sum_{j=1}^{P} \mathbf{K}_i^{-1^{(\mathrm{PC})}} \mathbf{f}_j \mathrm{E}\left[\Gamma_i \Gamma_j \Gamma_k\right] \tag{6.10}$$

For $k = 1$, $\mathbf{u}_1 = \sum_i \mathbf{K}_i^{-1^{(\mathrm{PC})}} \mathbf{f}_i \mathrm{E}\left[\Gamma_i^2\right]$ is the first term of PC expansion of the response. Then the PC expansion of $\mathbf{K}_{Par}^{-1^{(\mathrm{PC})}} = \sum_{i=1}^{P} \mathbf{K}_i^{-1^{(\mathrm{PC})}} \Gamma_i$ can be retrieved from the inverse of $\mathbf{A}^{(\mathrm{PC})}$, that is $(\mathbf{A}^{(\mathrm{PC})})^{-1}$, where $\mathbf{A}^{(\mathrm{PC})}$ is defined in Equation (1.88). Denote by $\mathbf{A}^{(\mathbf{K}^{-1})}$ the matrix formed by the first n rows of matrix $(\mathbf{A}^{(\mathrm{PC})})^{-1}$. Then $\mathbf{K}_i^{-1^{(\mathrm{PC})}} = \mathbf{A}_i^{(\mathbf{K}^{-1})}$ where $\mathbf{A}_i^{(\mathbf{K}^{-1})}$ is the i-th block of n columns of $\mathbf{A}^{(\mathbf{K}^{-1})}$. Finally, the means appearing in Equations (6.7) and (6.8) are given by

$$\mathrm{E}_1\left[\mathbf{K}_{Par}^{-1}\mathbf{f}\right] = \mathrm{E}_1\left[\mathbf{u}^{(\mathrm{PC})}\right] = \mathbf{u}_1^{(\mathrm{PC})} \tag{6.11}$$

$$\mathrm{E}_1\left[\mathbf{K}_{Par}^{-1}\mathbf{F}\mathbf{K}_{Par}^{-1}\right] = \mathrm{E}_1\left[\mathbf{u}^{(\mathrm{PC})}(\mathbf{u}^{(\mathrm{PC})})^T\right] = \sum_{i=1}^{P} \mathbf{u}_i (\mathbf{u}_i)^T \mathrm{E}\left[\Gamma_i^2\right] \tag{6.12}$$

$$\begin{aligned}\mathrm{E}_1\left[\mathrm{Trace}\left(\mathbf{F}\mathbf{K}_{Par}^{-1}\right)\mathbf{K}_{Par}^{-1}\right] &= \mathrm{E}_1\left[\mathrm{Trace}\left(\mathbf{f}(\mathbf{u}^{(\mathrm{PC})})^T\right)\mathbf{K}_{Par}^{-1}\right] \\ &= \sum_{i=1}^{P}\sum_{j=1}^{P}\sum_{k=1}^{P} (\mathbf{u}_i)^T \mathbf{f}_j \mathbf{K}_k^{-1^{(\mathrm{PC})}} \mathrm{E}\left[\Gamma_i \Gamma_j \Gamma_k\right]\end{aligned} \tag{6.13}$$

The first and second moment of the response can then be approximated by

$$\mathrm{E}\left[\mathbf{u}\right] = \frac{\mathbf{u}_1^{(\mathrm{PC})} p}{(p-n-1)} \tag{6.14}$$

$$\begin{aligned}\mathrm{E}\left[\mathbf{u}\mathbf{u}^T\right] &= (c_1 + c_2)p^2 \sum_{i=1}^{P} \mathbf{u}_i (\mathbf{u}_i)^T \mathrm{E}\left[\Gamma_i^2\right] + \\ &\quad c_2 p^2 \sum_{i=1}^{P}\sum_{j=1}^{P}\sum_{k=1}^{P} (\mathbf{u}_i)^T \mathbf{f}_j \mathbf{K}_k^{-1^{(\mathrm{PC})}} \mathrm{E}\left[\Gamma_i \Gamma_j \Gamma_k\right]\end{aligned} \tag{6.15}$$

The expressions obtaining the nonparametric moments are exact, and therefore the source of error is the PC approximation. The propagation of parametric uncertainty is an ongoing research topic, and improvements to the PC methods have been introduced by reducing the size of the matrices (Sachdeva et al., 2006b, Maute et al., 2009). Also, other methods are available by projecting the stochastic partial differential equation in a different basis (Nouy, 2009, Maître and Knio, 2010), or through the use of

non-intrussive methods (Xiu, 2009, Maître and Knio, 2010).

6.2.3 Numerical example: Euler-Bernoulli beam

We first consider a simple 1-D example from structural mechanics to illustrate the proposed method. The case of a clamped-free beam of length $L = 1.65$ m subjected to uniform distributed force $f = 1$ N/m is considered, as shown in Figure 6.2. The system is

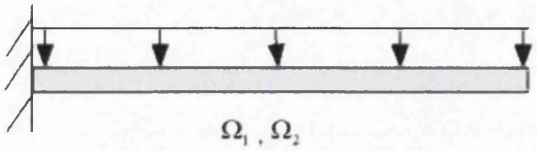

Figure 6.2: Euler-Bernoulli beam with spatially varying random bending rigidity $w(x, \theta)$ and nonparametric uncertainty affecting the whole domain. The length of the beam is $L = 1.65$ m, the section area is $A = 8.2123 \times 10^{-5}$ m^2, the density is $\rho = 7800$ kg/m^3 and the mean of the bending rigidity homogeneous random field is $\mu = 5.7520$ kg.m^2.

modelled applying the Finite Element method to the Euler-Bernoulli equation using 50 elements, details on the method can be found, for example, in Dawe (1984). Parametric uncertainty is introduced in the system by a Gaussian random field $w(x, \theta) = EI_z$, and its mean is $\mu = \mathrm{E}[EI_z] = 5.7520$ N.m^2. The discretization of $w(x, \theta)$ is done with the KL expansion of the exponential autocorrelation function $C(x_1, x_2) = e^{-|x_1 - x_2|/L}$, described in subsection 1.4.4. The KL expansion is truncated at $M = 2$, so that the corresponding KL expansion of the stiffness matrix is $\mathbf{K} = \mathbf{K}_0 + \mathbf{K}_1\xi_1 + \mathbf{K}_2\xi_2$, where the standard deviation of the random field is included in the $\mathbf{K}_i$ matrices. The maximum order of the Hermite polynomial used is 4, so that $P = 15$ polynomials are used as basis functions.

The analytical expressions for mean and standard deviation can be obtained respectively from Equations (6.14) and (1.90) where the mean and second moment of the response can be obtained from Equations (6.14) and (6.15) respectively. The result of applying these expressions can be compared with Monte Carlo Simulation (MCS) results for different combinations of normalised standard deviations σ/μ of the random field and dispersion parameters δ of the Wishart matrix. The mean and standard deviation of the displacement for the case of $\delta = 0.05$ and $\sigma = 0.1\mu$ is given in Figure 6.3. The mean and standard deviation of the tip displacement for different combinations of δ and σ obtained with the proposed method are displayed in Figure 6.4. The accuracy

of the method is evaluated, through the error of the mean and standard deviation of tip displacement between the analytical expressions and MCS, in Figure 6.5. MCS is performed both in Wishart matrix and parametric uncertainty, using 500 samples for Wishart matrices and 1000 samples for PC, resulting in 500000 samples in total.

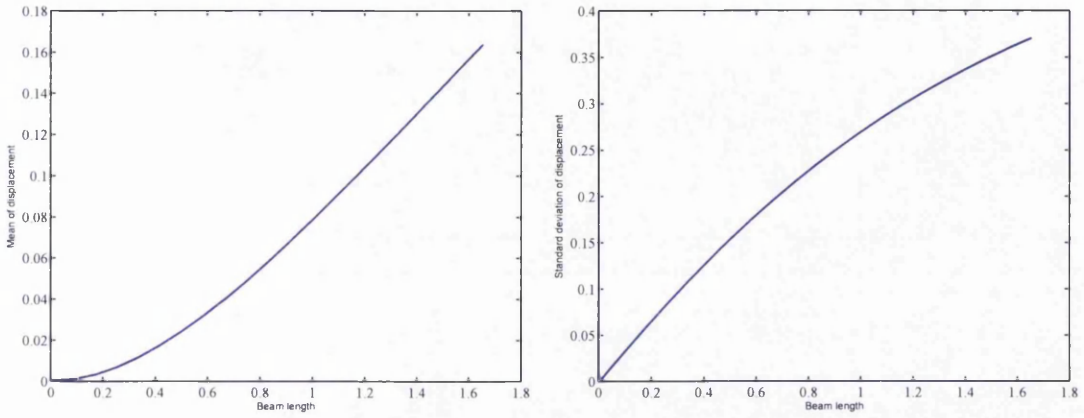

(a) Mean. (b) Standard deviation.

Figure 6.3: Mean and standard deviation of the vertical displacement obtained using the proposed analytical expressions for $\delta = 0.05$ and $\sigma = 0.1\mu$.

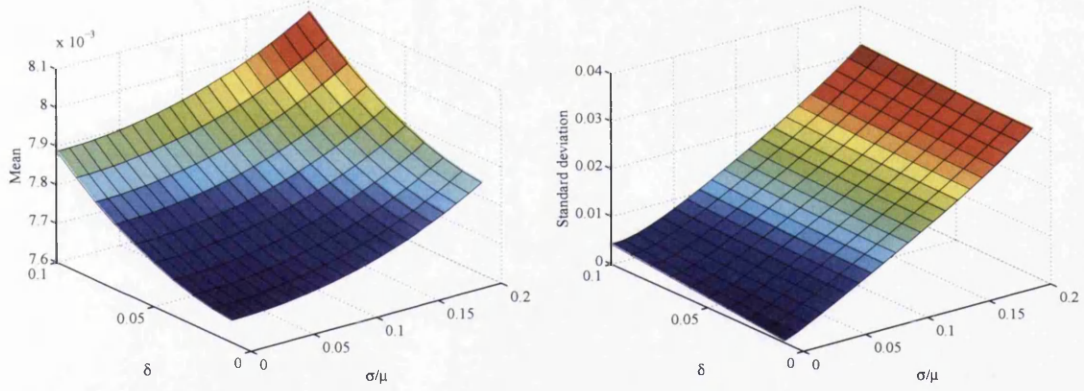

(a) Mean. (b) Standard deviation.

Figure 6.4: Mean and standard deviation of the tip vertical displacement obtained using the proposed analytical expressions.

It is observed in Subfigure 6.4(a) that the mean of the tip displacement varies both with the standard deviation of the random field and the dispersion parameter of the random matrix. This observation can be extended to the standard deviation in Subfigure 6.4(b), where the effect of σ/μ is more important than the one of δ in comparison to the results obtained for mean. With respect to the error of both quantities, it is observed that the error does not depend strongly on δ, as it is almost constant for each normalised

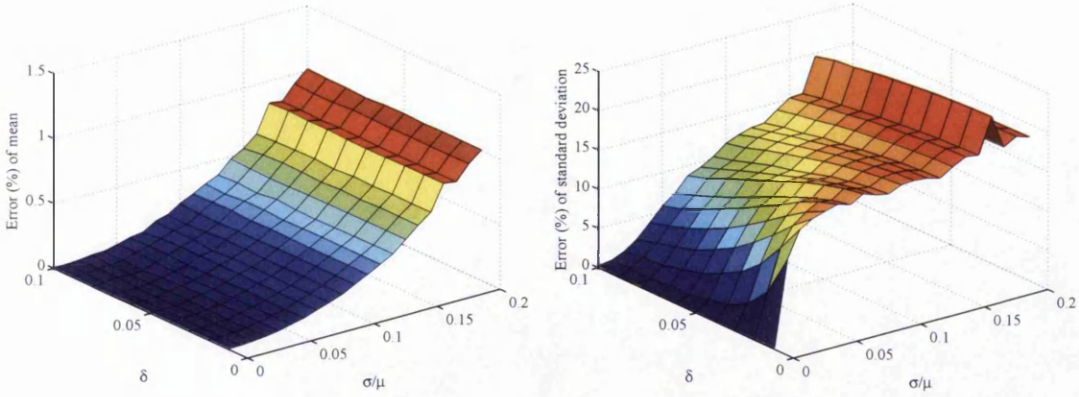

(a) Percentage error of mean.

(b) Percentage error of standard deviation.

Figure 6.5: Percentage error of mean and standard deviation of the tip vertical displacement between the analytical expressions and Monte Carlo Simulation (MCS) using 500000 samples.

standard deviation of the random field. It is also observed in Subfigure 6.5(a) that the error of mean grows approximately in a quadratic way as a function of σ/μ. The percentage error for standard deviation, on the contrary, firstly grows very rapidly to then remain close to a constant around 10% error.

6.2.4 Numerical example: flow through porous media

In the previous subsection, a 1-D example was given, now the efficiency of the method for a 2-D example is perused. A numerical example of flow through porous media is now considered to show the efficiency of the proposed method. The two-dimensional domain considered is a rectangle of length L=0.998 m and width W=0.59 m, as shown in Figure 6.6. The domain is divided with a uniform mesh of 25×15 rectangular elements. The porous medium within the domain is subjected to a constant flux $q_b = 1$ cm/s along the portion of its boundary where $y = -0.2950$ m and $x \in [0.2994\,, 0.4990]$ m. The head is fixed at value $h_b = 0$ cm along the portion of the boundary such that $x = -0.4990$ m, $y \in [0.1770\,,\, 0.2950]$ m. The deterministic system has $n = 412$ degrees of freedom. A Gaussian hydraulic conductivity (k) with 2D exponential covariance function is considered. The 2D covariance function is obtained as the product of two 1D exponential covariance functions, the first one depending on x, with correlation length $b_x = L$; and the second one depending on y, with correlation length $b_y = W$. Two terms of the KL expansion in each direction are kept, that is, the KL expansion has four matrices for the whole system. The mean value of the hydraulic conductivity is

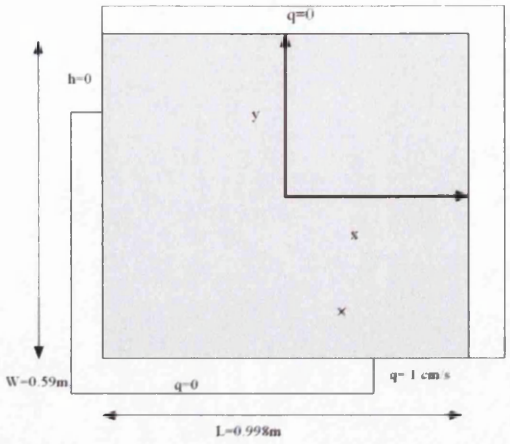

Figure 6.6: Flow through a rectangular porous media. The porous media is assumed to have stochastically inhomogeneous hydraulic conductivity.

given by $\overline{k} = 1$ cm/s. The stiffness element matrices are given by Equations (2.41) and (2.42) and the stiffness matrix of the system is obtained as in section 2.6. $(\varphi(x)\varphi(y))_i$ means that two eigenfunctions of the KL expansion are multiplied, knowing that only two eigenfunctions are kept in each direction. The eigenvalues and eigenfunctions of the KL expansion used to obtain the deterministic stiffness matrix are respectively $\sqrt{\nu} = \overline{k}$ and $\varphi(x, y) = 1$. The eigenvalues and eigenfunctions depend on the autocorrelation function of the random field when considering the remaining terms of the KL expansion of the stiffness matrix. Parametric uncertainty is dealt with using a fourth-order polynomial chaos, so that the total number of polynomials is 70.

The analytical expressions for the mean, given by Equation (6.14), and standard deviation, given by Equation (1.90) where the mean and second moment of the response can be obtained from Equations (6.14) and (6.15) respectively, are applied and compared with MCS results for different combinations of normalised standard deviations σ/μ of the random field and dispersion parameters δ of the Wishart matrix. The mean and standard deviation of the head obtained with the proposed method for $\sigma = 0.1$ and $\delta = 0.05$ are displayed in Figure 6.7. The same results for the point situated at $(x, y) = (0.6786,\ 0.0393)$ and different combinations of σ/μ and δ are shown in Figure 6.8. The choice of this point is for illustration only, the method proposed here is applicable to all points of the domain. The accuracy of the method is evaluated through the error of the mean and standard deviation of the head at this point, in Figure 6.9. MCS is performed both in Wishart matrix and parametric uncertainty, using 100 samples for Wishart matrices and 1000 samples for the random field, so that the total number of

samples used is 100000. It is observed in Subfigure 6.8(a) that the mean of the tip

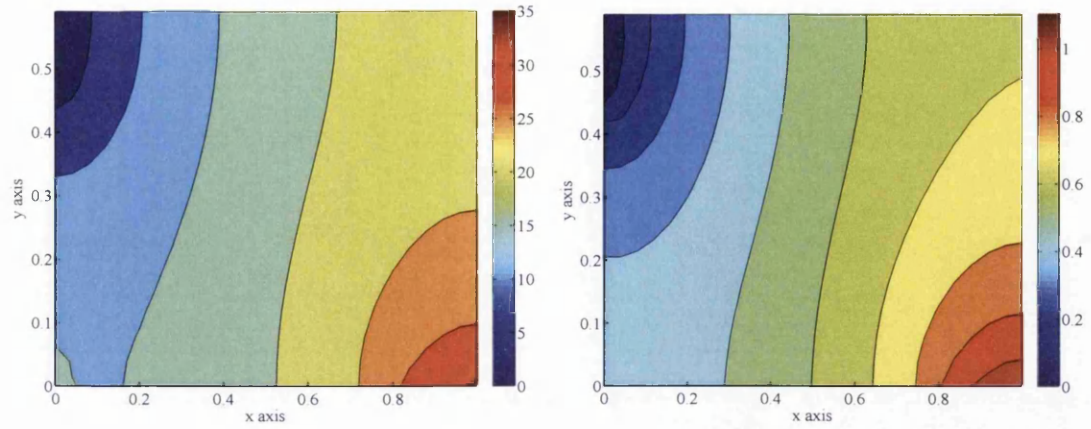

(a) Mean. (b) Standard deviation.

Figure 6.7: Mean and standard deviation of the head obtained using the proposed analytical expressions for $\sigma = 0.1$ and $\delta = 0.05$.

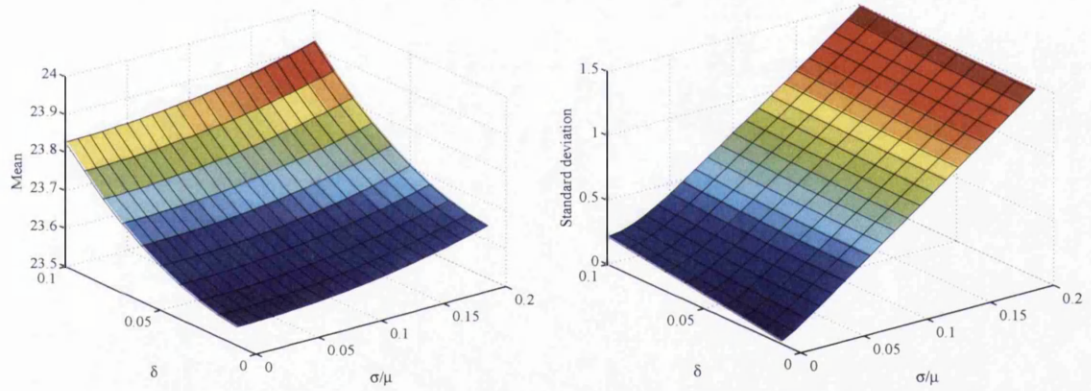

(a) Mean. (b) Standard deviation.

Figure 6.8: Mean and standard deviation of the head at $(x, y) = (0.6786, 0.0393)$ obtained using the proposed analytical expressions.

displacement increases both with the standard deviation of the random field and the dispersion parameter of the random matrix, where the effect of the dispersion parameter is more important than the effect of the normalised standard deviation. The standard deviation displayed in Subfigure 6.8(b) also increases with both parameters, but the effect of σ/μ is more important than the one of δ. With respect to the error of both quantities, it is observed that the error does not depend on δ, as it is maintained almost constant for each normalised standard deviation of the random field. It is also observed in Subfigure 6.5(a) that the error of is also close to constant with respect to σ/μ. The percentage

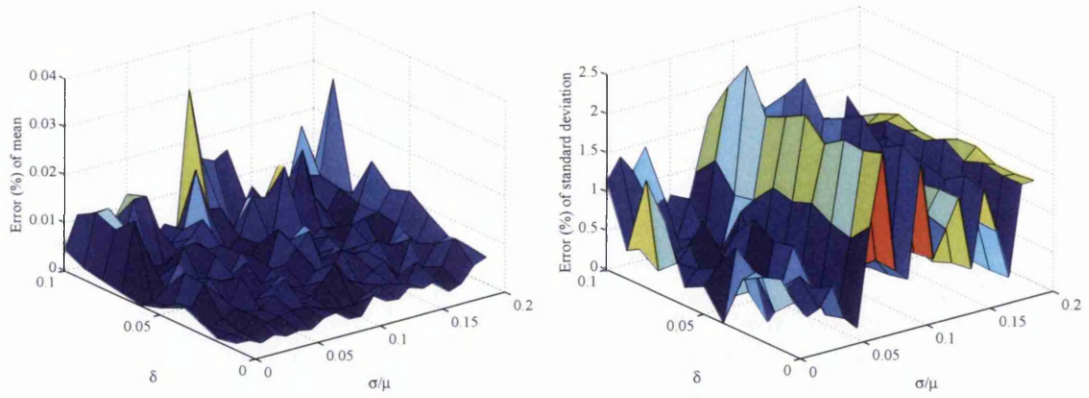

(a) Percentage error of mean.

(b) Percentage error of standard deviation.

Figure 6.9: Percentage error of mean and standard deviation of the head at $(x, y) = (0.6786, 0.0393)$ between the analytical expressions and Monte Carlo Simulation (MCS) using 100000 samples.

error for standard deviation seems to increase with σ/μ. Both errors are of lower order than the ones obtained for the beam problem.

6.3 Combined uncertainty over non-overlapping subdomains

6.3.1 Problem description

Combined uncertainty over different domains arises, for example, when a structure is constituted of several parts where some of them are accurately modelled through parametric uncertainty and the behavior of the remaining substructures is not well understood and therefore can be modelled with nonparametric uncertainty. This situation arises, for example, in the wing of a plane with engines attached to it, where the wing could be modelled with parametric uncertainty and the engines with nonparametric uncertainty due to complexity. Several substructuring techniques are available in the literature (Smith et al., 1996). Domain decomposition and FETI-based methods have been applied for the case of parametric uncertainty affecting the whole domain (Sarkar et al., 2009, Ghosh et al., 2009). Craig-Bampton method has already been applied when nonparametric uncertainty affects a dynamic system (Soize and Chebli, 2003, Arnst et al., 2006). In these studies, the substructures were deterministic or had nonparametric uncertainty and the mean system was a reduced matrix derived from each substructure

deterministic matrix. In this section, the case where each kind of uncertainty (parametric and non-parametric) affects a different subdomain of the structure is considered.

6.3.2 Proposed solution procedure

In Figure 6.10, two probability spaces are considered, $(\Omega_j, \mathcal{F}_j, P_j)$ for $j = 1, 2$, each one affecting the system on the subdomain $\mathcal{D}_j$ of $\mathcal{D}$, such that $\mathcal{D}_1 \bigcup \mathcal{D}_2 = \mathcal{D}$, $\mathcal{D}_1 \bigcap \mathcal{D}_2 = \varnothing$ and Γ is the boundary between the two subdomains. The case of an elliptic partial dif-

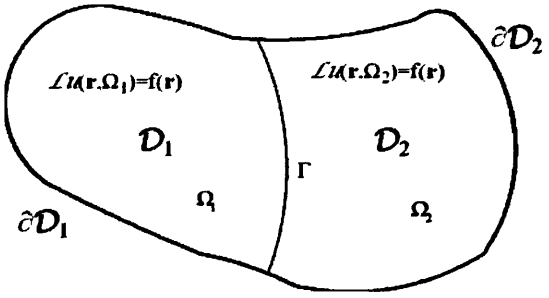

Figure 6.10: Combined uncertainty over non-overlapping domain.

ferential equation with a Dirichlet boundary condition is considered, where the equation is affected by parametric uncertainty defined on $(\Omega_1, \mathcal{F}_1, P_1)$ and by nonparametric uncertainty defined on $(\Omega_2, \mathcal{F}_2, P_2)$. The parametric uncertainty is firstly introduced in the elliptic partial differential equation

$$-\nabla.\left[a(\mathbf{r},\omega_1)\nabla u(\mathbf{r},\omega_1)\right] = f(\mathbf{r}); \quad \mathbf{r} \text{ in } \mathcal{D}; \quad u(\mathbf{r},\omega_1) = 0 \text{ on } \partial\mathcal{D} \tag{6.16}$$

First consider domain $\mathcal{D}_2$ is deterministic. The finite element method can be applied, where the random field used to model the parameter $a(\mathbf{r},\omega_1)$ is expanded with the KL expansion. The elliptic partial differential equation with parametric uncertainty in subdomain $\mathcal{D}_1$ leads to the algebraic equation

$$\begin{bmatrix} [\mathbf{K}_{11_0} + \sum_{i=1}^{M} \xi_i(\theta)\mathbf{K}_{11_i}] & [\mathbf{K}_{12}] \\ [\mathbf{K}_{21}] & [\mathbf{K}_{22}] \end{bmatrix} \begin{bmatrix} \mathbf{u}_I(\Omega_1) \\ \mathbf{u}_{II}(\Omega_1) \end{bmatrix} = \begin{bmatrix} \mathbf{f}_I(\Omega_1) \\ \mathbf{f}_{II}(\Omega_1) \end{bmatrix}. \tag{6.17}$$

Here, response and forcing vectors can be expanded with PC such that the response and force for nodes in $\mathcal{D}_1$ are given by $\mathbf{u}_I = \sum_{j=1}^{P} \mathbf{u}_{Ij}\Gamma_j(\Omega_1)$ and $\mathbf{f}_I = \sum_{j=1}^{P} \mathbf{f}_{Ij}\Gamma_j(\Omega_1)$, and the response and force for nodes in $\mathcal{D}_2$ are $\mathbf{u}_{II} = \sum_{j=1}^{P} \mathbf{u}_{IIj}\Gamma_j(\Omega_1)$ and $\mathbf{f}_{II} = \sum_{j=1}^{P} \mathbf{f}_{IIj}\Gamma_j(\Omega_1)$. The vectors $\mathbf{u}_{Ij}$ and $\mathbf{u}_{IIj}$ can be retrieved by applying Galerkin method to Equation (6.17) or through numerical integration. The vectors $\mathbf{u}_{1j}$ result-

ing from applying Galerkin method, that is, multiplying Equation (6.17) by each basis function Γ_p and taking mean, are obtained from the solution of the deterministic linear system

$$\hat{\mathbf{K}} \begin{bmatrix} \mathbf{u}_{I1} \\ \vdots \\ \mathbf{u}_{IIP} \end{bmatrix} = \begin{bmatrix} \mathbf{f}_{I1} - \mathbf{K}_{12}\mathbf{K}_{22}^{-1}\mathbf{f}_{II1} \\ \vdots \\ \mathbf{f}_{IP} - \mathbf{K}_{12}\mathbf{K}_{22}^{-1}\mathbf{f}_{IIP} \end{bmatrix} \tag{6.18}$$

where

$$\hat{\mathbf{K}} = \mathbf{d} \otimes (\mathbf{K}_{11_0} - \mathbf{K}_{12}\mathbf{K}_{22}^{-1}\mathbf{K}_{21}) + \sum_{i=1}^{M} \mathbf{c}_i \otimes \mathbf{K}_{11_i} \tag{6.19}$$

and vector of coefficients $[\mathbf{u}_{II1}; \ldots; \mathbf{u}_{IIP}]$ can be related to coefficients $[\mathbf{u}_{I1}; \ldots; \mathbf{u}_{IP}]$ through

$$\begin{bmatrix} \mathbf{u}_{II1} \\ \vdots \\ \mathbf{u}_{IIP} \end{bmatrix} = \begin{bmatrix} \mathbf{K}_{22}^{-1}(\mathrm{E}\left[\Gamma_1, \mathbf{f}_{II}\right] - \mathbf{K}_{12}\mathbf{u}_{I1}) \\ \vdots \\ \mathbf{K}_{22}^{-1}(\mathrm{E}\left[\Gamma_P, \mathbf{f}_{II}\right] - \mathbf{K}_{12}\mathbf{u}_{IP}) \end{bmatrix} \tag{6.20}$$

Alternatively, vectors $\mathbf{u}_{Ij}$ can be obtained using Equation (1.66), where each response $\mathbf{u}_{Ij}(\xi_{1j_1} \ldots \xi_{Mj_M})$ used for the quadrature is obtained through

$$\mathbf{u}_{Ij}(\xi_{1j_1} \ldots \xi_{Mj_M}) = \left(\mathbf{K}_{11_0} - \mathbf{K}_{12}\mathbf{K}_{22}^{-1}\mathbf{K}_{21} + \sum_{i=1}^{M} \xi_{ij_i}\mathbf{K}_{11_i} \right)^{-1} \left(\mathbf{f}_I - \mathbf{K}_{12}\mathbf{K}_{22}^{-1}\mathbf{f}_{II} \right) \tag{6.21}$$

The vector of coefficients $[\mathbf{u}_{II1}; \ldots; \mathbf{u}_{IIP}]$ can be related to coefficients $[\mathbf{u}_{I1}; \ldots; \mathbf{u}_{IP}]$ through Equation (6.20). Model uncertainty, represented by $(\Omega_2, \mathcal{F}_2, P_2)$ affects the subdomain $\mathcal{D}_2$ and can be included in the algebraic equation (6.17) through submatrix $\mathbf{K}_{22}(\Omega_2)$. This type of uncertainty can only be considered after calculating the system matrix, as it is part of the information used to find the matrix pdf

$$\begin{bmatrix} [\mathbf{K}_{11_0} + \sum_{i=1}^{M} \xi_i(\theta)\mathbf{K}_{11_i}] & [\mathbf{K}_{12}] \\ [\mathbf{K}_{21}] & [\mathbf{K}_{22}(\Omega_2)] \end{bmatrix} \begin{bmatrix} \sum_{j=1}^{P} \mathbf{u}_{Ij}(\Omega_2)\Gamma_j(\Omega_1) \\ \sum_{j=1}^{P} \mathbf{u}_{IIj}(\Omega_2)\Gamma_j(\Omega_1) \end{bmatrix} = \begin{bmatrix} \sum_{j=1}^{P} \mathbf{f}_{Ij}\Gamma_j(\Omega_1) \\ \sum_{j=1}^{P} \mathbf{f}_{IIj}\Gamma_j(\Omega_1) \end{bmatrix} \tag{6.22}$$

The global matrix has to remain positive definite. This is not satisfied for any positive definite matrix $\mathbf{K}_{22}(\Omega_2)$. Two methods are proposed in the next two subsections to model $\mathbf{K}_{22}$ using Wishart random matrix such that positive definiteness of the global matrix is satisfied. Once the samples $\mathbf{K}_{22}(\Omega_2)$ are obtained, vectors $\mathbf{u}_{Ij}$, $\mathbf{u}_{IIj}$ are obtained from Equations (6.22) and (6.20). The mean and second moments of the response

are then retrieved

$$\mathrm{E}\left[\mathbf{u}_I\right] = \mathrm{E}_2\left[\mathrm{E}_1\left[\mathbf{u}_I\right]\right] = \mathrm{E}_2\left[\mathbf{u}_{I1}\right] \tag{6.23}$$

$$\mathrm{E}\left[\mathbf{u}_I\mathbf{u}_I^T\right] = \mathrm{E}_2\left[\mathrm{E}_1\left[\mathbf{u}_I\mathbf{u}_I^T\right]\right] = \mathrm{E}_2\left[\sum_{j=1}^{P}\mathbf{u}_{Ij}\mathbf{u}_{Ij}^T\mathrm{E}\left[\Gamma_j^2\right]\right]$$

$$= \sum_{j=1}^{P}\mathrm{E}_2\left[\mathbf{u}_{Ij}\mathbf{u}_{Ij}^T\right]\mathrm{E}\left[\Gamma_j^2\right] \tag{6.24}$$

The same expressions are valid to retrieve the moments of $\mathbf{u}_{II}$ by changing the subindex I to II.

Ensuring positive definiteness through sample selection

Submatrix $\mathbf{K}_{22}(\Omega_2)$ is modelled using the maximum entropy principle exposed in subsection 1.6.1, leading to the distribution of a Wishart random matrix. This distribution is conditional on the global matrix being positive definite, that is, for every sample of $\mathbf{K}_{22}(\Omega_2)$, the matrix $[\mathbf{K}_{11_0} + \sum_{i=1}^{M}\xi_i(\Omega_1)\mathbf{K}_{11_i}\,\mathbf{K}_{12};\mathbf{K}_{21}\mathbf{K}_{22}(\Omega_2)]$ has to be positive definite. It is assumed that this is satisfied for a particular sample of $\mathbf{K}_{22}(\Omega_2)$ and for all samples of ξ_i if the matrix

$$\begin{bmatrix}\mathbf{K}_{11_0} - C\sum_{i=1}^{M}\mathbf{K}_{11_i} & \mathbf{K}_{12}\\ \mathbf{K}_{21} & \mathbf{K}_{22}(\Omega_2)\end{bmatrix} \tag{6.25}$$

is positive definite. This assumption implies that the upper diagonal block matrix is positive definite $\mathbf{K}_{11_0} - C\sum_{i=1}^{M}\mathbf{K}_{11_i} > 0$. Heuristically, we can observe that, if matrices $\mathbf{K}_{11_0}$ and $\mathbf{K}_{11_i}$ are scalar, $\mathbf{K}_{11_0} + \sum_{i=1}^{M}\xi_i\mathbf{K}_{11_i}$ reduces to a gaussian random variable, so that $\xi_i = -4\sqrt{\left(\sum_{i=1}^{M}\mathbf{K}_{11_i}^2\right)}$ implies that 99.99% of the samples of this random variable lead to larger values than $\mathbf{K}_{11_0} - 4\sum_{i=1}^{M}\mathbf{K}_{11_i}$. That is, if we want $\mathbf{K}_{11_0} + \sum_{i=1}^{M}\xi_i\mathbf{K}_{11_i} > 0$, introducing $C = 4$ in Equation (6.25) is likely to lead to a positive definite upper diagonal submatrix. In other words, we can consider the global matrix $[\mathbf{K}_{11_0} + \sum_{i=1}^{M}\xi_i(\Omega_1)\mathbf{K}_{11_i}\,\mathbf{K}_{12};\mathbf{K}_{21}\mathbf{K}_{22}(\Omega_2)]$ as the sum of a positive definite matrix $[\mathbf{K}_{11_0} - C\sum_{i=1}^{M}\mathbf{K}_{11_i}\,\mathbf{K}_{12};\mathbf{K}_{21}\mathbf{K}_{22}(\Omega_2)]$ and the non-negative definite matrices $[\sum_{i=1}^{M}(\xi_i + C)\mathbf{K}_{11_i}\,0;00]$, so that the global matrix is positive definite.

Both uncertainties are assumed independent and propagation of the parametric uncertainty is solved with PC. The equations related to the PC chosen method, i.e. Equations (6.18) and (6.20) for Galerkin method and Equations (1.66), (6.21) and (6.20) for

numerical integration, are solved for each sample of the random matrix $\mathbf{K}_{22}(\Omega_2)$. First and second moments of $\mathbf{u}$ are obtained through MCS, where $\mathbf{K}_{22} \backsim W_n(p, \mathrm{E}[\mathbf{K}_{22}]/p)$ is simulated and the only samples used are the ones leading to a positive definite matrix in Equation (6.25).

It is noted that with this method $\mathbf{K}_{22}$ does not have a Wishart distribution as some samples of the Wishart distribution will be rejected, namely the ones leading to a non-positive definite matrix in Equation (6.25).

Ensuring positive definiteness through matrix correction

The system matrix from Equation (6.22) has to be positive definite. As formerly, it is assumed that if the sample $[\mathbf{K}_{11_0} - C\sum_{i=1}^{M}\mathbf{K}_{11_i}]$ of the KL expansion leads to a positive definite matrix upper diagonal matrix, other samples of ξ_i will lead to matrix $\mathbf{K}_{11_0} + \sum_{i=1}^{M}\xi_i(\Omega_1)\mathbf{K}_{11_i}$ being positive definite. The global matrix considering only nonparametric uncertainty, i.e. substituting parametric uncertainty by the proposed sample $\mathbf{K}_{11}^{(s)} = \mathbf{K}_{11_0} - C\sum_{i=1}^{M}\mathbf{K}_{11_i}$, can be obtained through

$$\begin{bmatrix}[\mathbf{K}_{11}^{(s)}] & [\mathbf{K}_{12}]\\ [\mathbf{K}_{21}] & [\mathbf{K}_{22}(\Omega_2)]\end{bmatrix} = \begin{bmatrix}[\mathbf{I}] & [\mathbf{O}]\\ [\mathbf{A}] & [\mathbf{I}]\end{bmatrix}\begin{bmatrix}[\mathbf{K}_{11}^{(s)}] & [\mathbf{O}]\\ [\mathbf{O}] & [\mathbf{W}(\Omega_2)]\end{bmatrix}\begin{bmatrix}[\mathbf{I}] & [\mathbf{A}^T]\\ [\mathbf{O}] & [\mathbf{I}]\end{bmatrix} \tag{6.26}$$

with $\mathbf{W}$ a Wishart matrix. Matrices $[\mathbf{K}_{11_0} - C\sum_{i=1}^{M}\mathbf{K}_{11_i}]$ and $\mathbf{W}$ are positive definite, so that the resulting matrix will be positive definite. Identifying terms we obtain

$$\mathbf{A} = \mathbf{K}_{21}\left(\mathbf{K}_{11_0} - C\sum_{i=1}^{M}\mathbf{K}_{11_i}\right)^{-1}, \quad \mathbf{W} = \mathbf{K}_{22} - \mathbf{K}_{21}\left(\mathbf{K}_{11_0} - C\sum_{i=1}^{M}\mathbf{K}_{11_i}\right)^{-1}\mathbf{K}_{12} \tag{6.27}$$

where $\mathbf{W}$ is modelled as a Wishart matrix. Therefore, matrix $\mathbf{W}$ is such that $\mathrm{E}[\mathbf{W}] = \mathrm{E}[\mathbf{K}_{22}] - \mathbf{K}_{21}\left(\mathbf{K}_{11_0} - C\sum_{i=1}^{M}\mathbf{K}_{11_i}\right)^{-1}\mathbf{K}_{12}$. To calculate the dispersion parameter of matrix $\mathbf{W}$, we notice that matrix $\mathbf{K}_{21}\left(\mathbf{K}_{11_0} - C\sum_{i=1}^{M}\mathbf{K}_{11_i}\right)^{-1}\mathbf{K}_{12}$ is constant and does not introduce uncertainty in submatrix $\mathbf{K}_{22}$. Then, the dispersion parameter of $\mathbf{W}$ can be related to the one of $\mathbf{K}_{22}$ by noting that $\mathrm{E}\left[\|\mathbf{W} - \mathrm{E}[\mathbf{W}]\|_{\mathrm{F}}^2\right] = \mathrm{E}\left[\|\mathbf{K}_{22} - \mathrm{E}[\mathbf{K}_{22}]\|_{\mathrm{F}}^2\right]$, and the relationship is given by the equation

$$\delta_W^2 = \frac{\mathrm{E}\left[\|\mathbf{W} - \mathrm{E}[\mathbf{W}]\|_{\mathrm{F}}^2\right]}{\|\mathrm{E}[\mathbf{W}]\|_{\mathrm{F}}^2} = \frac{\mathrm{E}\left[\|\mathbf{K}_{22} - \mathrm{E}[\mathbf{K}_{22}]\|_{\mathrm{F}}^2\right]}{\|\mathrm{E}[\mathbf{K}_{22}]\|_{\mathrm{F}}^2}\frac{\|\mathrm{E}[\mathbf{K}_{22}]\|_{\mathrm{F}}^2}{\|\mathrm{E}[\mathbf{W}]\|_{\mathrm{F}}^2} \tag{6.28}$$

$$\delta_W^2 = \delta_{k_{22}}^2 \frac{\|\mathrm{E}[\mathbf{K}_{22}]\|_\mathrm{F}^2}{\|\mathrm{E}[\mathbf{W}]\|_\mathrm{F}^2} \tag{6.29}$$

where $\delta_{k_{22}}$ is the dispersion parameter of matrix $\mathbf{K}_{22}$. The PC expansion of the response can now be calculated as in the previous subsection, from Equations (6.18) and (6.20) for Galerkin method and Equations (1.66), (6.21) and (6.20) for numerical integration, where $\mathbf{K}_{22}(\Omega_2)$ is now simulated as the sum of a Wishart matrix $\mathbf{W}(\Omega_2)$ and a constant matrix $\mathbf{K}_{21}\left(\mathbf{K}_{11_0} - C\sum_{i=1}^{M}\mathbf{K}_{11_i}\right)^{-1}\mathbf{K}_{12}$. As in the previous subsection, $C = 4$ is assumed.

6.3.3 Numerical example: Euler-Bernoulli beam

The proposed method is firstly illustrated with a $1D$ problem. The case of a clamped-free beam of length $L = 1.65$ m subjected to uniform distributed force $f = 1$ N/m is considered, as described in Figure 6.11. The system is modelled applying the Fi-

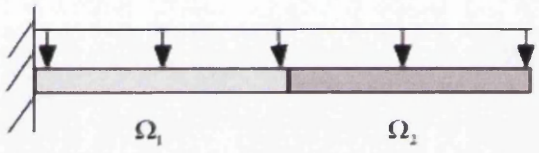

Figure 6.11: Euler-Bernoulli beam with spatially varying random bending rigidity $w(x,\theta)$ and nonparametric uncertainty affecting the different subdomains. The length of the beam is $L = 1.65$ m, the section area is $A = 8.2123 \times 10^{-5}$ m^2, the density is $\rho = 7800$ kg/m^3 and the mean of the bending rigidity random field is $\mu = \mathrm{E}[w(\theta,x)] = 5.7520$ kg.m^2. The length of the domain affected by parametric uncertainty (Ω_1) is $L_r = 0.792$ m.

nite Element method to the Euler-Bernoulli equation using $n = 50$ elements, details on the method can be found, for example, in Dawe (1984). Parametric uncertainty is introduced in the system by a Gaussian random field $w(\theta,x) = EI_z$ of mean $\mu = \mathrm{E}[EI_z] = 5.7520$ N.m^2. This uncertainty affects the submatrix corresponding to the length of the beam $L_r = 0.792$ m closer to the clamped boundary. The discretization of $w(x,\theta)$ is done with the KL expansion of the exponential autocorrelation function $C(x_1,x_2) = e^{-|x_1-x_2|/L_r}$. The KL expansion is truncated at $M = 2$, so that the corresponding KL expansion of the stiffness matrix is $\mathbf{K} = \mathbf{K}_0 + \sum_{i=1}^{2}\mathbf{K}_i\xi_i$, where the standard deviation of the random field is included in the $\mathbf{K}_i$ matrices. The maximum order of the Hermite polynomial used is 4, so that $P = 15$ polynomials are used as basis functions. The accuracy of the methods is evaluated through the error of the mean and

standard deviation of tip displacement for different standard deviations of the random field ($\sigma/\mu \in (0, 0.15)$) and dispersion parameters of the matrix $\mathbf{k}_{22}$ ($\delta_{k_{22}} \in (0, 0.1)$).

Sample selection

The beam problem is solved using the method proposed in section 6.3.2. Figure 6.12 shows the error between results from Equations (6.18) and (6.20), where Wishart matrices are simulated with MCS using 500 samples, and MCS both in Wishart matrix and parametric uncertainty, using 500 samples for Wishart matrix results and 2000 samples for PC results within each Wishart sample. In Subfigure 6.12(a) and Subfigure 6.12(b)

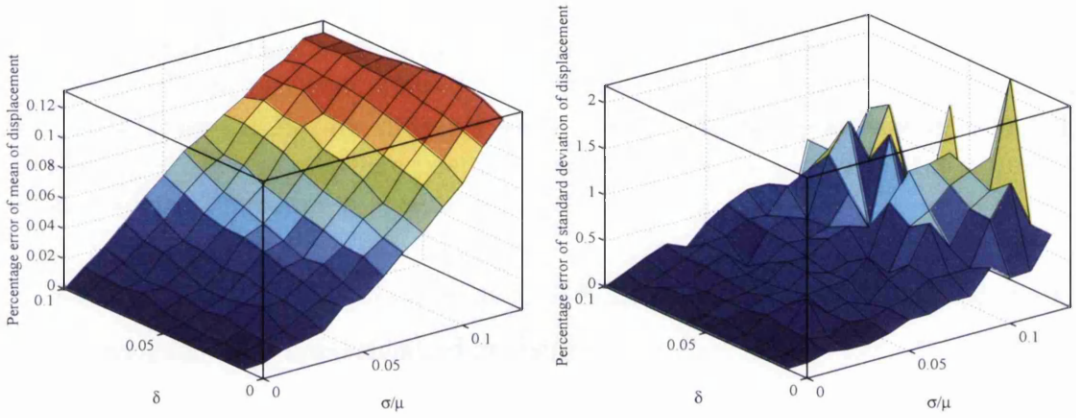

(a) Percentage error of mean. (b) Percentage error of standard deviation.

Figure 6.12: Percentage error of mean and standard deviation of the tip vertical displacement between the analytical expressions for parametric uncertainty and Monte Carlo Simulation (MCS), for different values of the dispersion parameter $\delta_{k_{22}}$ and the normalised variance σ/μ, where positive definiteness of the global matrix is ensured through a sample selection procedure.

it is observed that both errors in mean and standard deviation increase with the normalised standard deviation. It is also observed that, compared to the case of both kinds of uncertainty over the same domain, the errors obtained for this example are around one tenth of the previous ones.

Matrix correction

The beam problem is solved using the method exposed in section 6.3.2. Figure 6.13 shows the error between results from Equations (6.18) and (6.20), where Wishart matrices are simulated with MCS using 500 samples, and MCS both in Wishart matrix and parametric uncertainty, using 500 samples for Wishart matrix results and 2000 samples

for PC results within each Wishart sample. In Subfigure 6.13(a) and Subfigure 6.13(b)

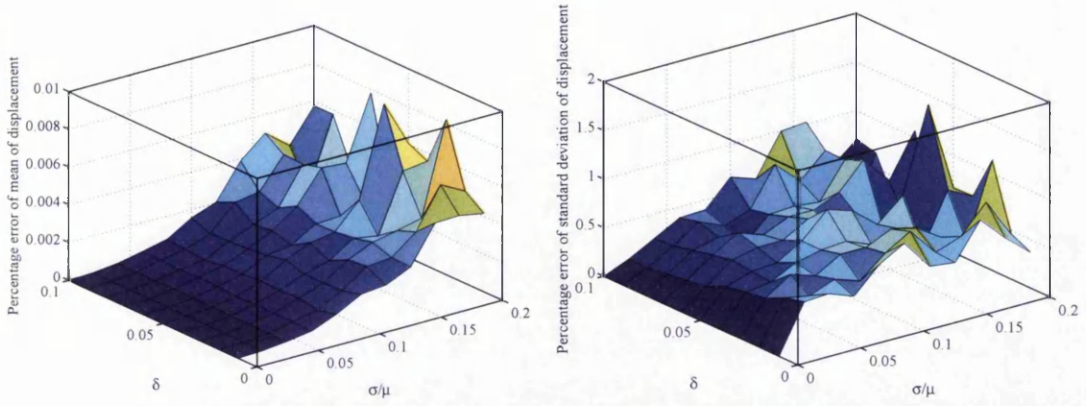

(a) Percentage error of mean.

(b) Percentage error of standard deviation.

Figure 6.13: Percentage error of mean and standard deviation of the tip vertical displacement between the analytical expressions for parametric uncertainty and Monte Carlo Simulation (MCS), for different values of the dispersion parameter δ and the normalised variance σ/μ, where positive definiteness of the global matrix is ensured through a matrix correction procedure.

it is observed that, as in the previous case, both errors in mean and standard deviation increase with the normalised standard deviation.

6.3.4 Numerical example: flow through porous media

The proposed methods are now applied to a 2 D problem. An example of flow through a porous media is considered to show the efficiency of the proposed method. The two-dimensional domain is a rectangle of length L=0.998 m and width W=0.59 m, where the top half of the domain is affected by nonparametric uncertainty and the top bottom by parametric uncertainty, as shown in Figure 6.14.

The domain is divided with a uniform mesh of 25×15 rectangular elements and is subjected to a constant flux $q_b = 1$ cm/s along the portion of its boundary comprising the last 0.1996 m in x direction. The head is fixed at value $h_b = 0$ cm along the portion of the boundary comprising the last 0.118 m in y direction. The deterministic system has $n = 412$ degrees of freedom. A Gaussian hydraulic conductivity (k) with 2D exponential covariance function is considered for the rectangular domain affecting the bottom 7 elements in y direction. The 2D covariance function is obtained as the product of two 1D exponential covariance functions, the first one depending on x, with correlation length $b_x = L$; and the second one depending on y, with correlation length

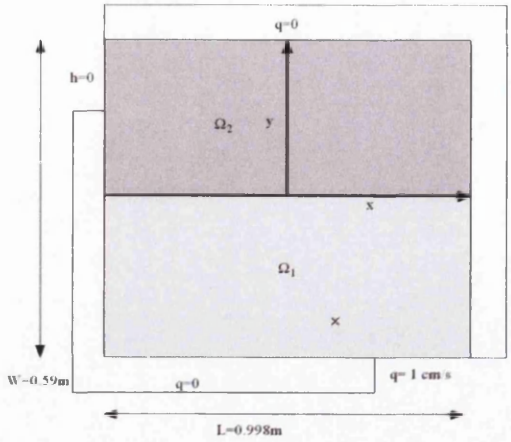

Figure 6.14: Flow through a rectangular porous media. The porous media is assumed to have stochastically inhomogeneous hydraulic conductivity.

$b_y = W8/15$. Two terms of the KL expansion in each direction are kept, that is, the KL expansion has four matrices for the subdomain affected by parametric uncertainty. The mean value of the hydraulic conductivity is given by $\overline{k} = 1$ cm/s. The stiffness element matrices are given by Equations (2.41) and (2.42), where $\mathbf{K} = \mathbf{K}_{11} + \mathbf{K}_{22}$. The eigenvalue and eigenfunction are respectively $\sqrt{\nu} = k$ and $\varphi(x, y) = 1$ in that equation for the deterministic case and depends on the autocorrelation function when considering a KL expansion of the stiffness matrix. Parametric uncertainty is dealt with using a fourth-order polynomial chaos, so that the total number of polynomials is 70.

Sample selection

The flow problem is solved using the method proposed in section 6.3.2. Figure 6.15 shows the mean and standard deviation of the head for $\sigma = 0.1$ of the underlying random field and $\delta = 0.05$ for the nonparametric uncertainty, using PC to solve parametric uncertainty and MCS with 100 samples to solve nonparametric uncertainty. Figure 6.16 shows the mean and standard deviation obtained from Equations (6.18) and (6.20), where Wishart matrices are simulated with MCS using 100 samples. Figure 6.17 shows the error between results from Equations (6.18) and (6.20), where Wishart matrices are simulated with MCS using 100 samples, and MCS both in Wishart matrix and parametric uncertainty, using 100 samples for Wishart matrix results and 100 samples for PC results within each Wishart sample. These mean, standard deviation and errors are given for the head at coordinate $(x, y) = (0.6923,\ 0.0400)$.

In Subfigure 6.16(a) and Subfigure 6.16(b) it is observed that both the mean and

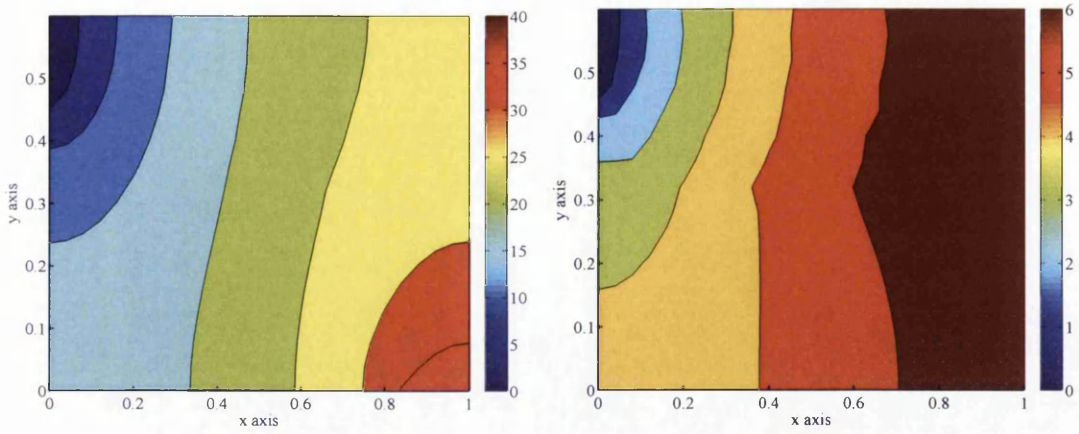

(a) Mean. (b) Standard deviation.

Figure 6.15: Mean and standard deviation of the head obtained using the analytical expressions for parametric uncertainty with $\sigma = 0.1$ and Monte Carlo Simulation (MCS) for nonparametric uncertainty with $\delta = 0.05$, where positive definiteness of the global matrix is ensured through a sample selection procedure.

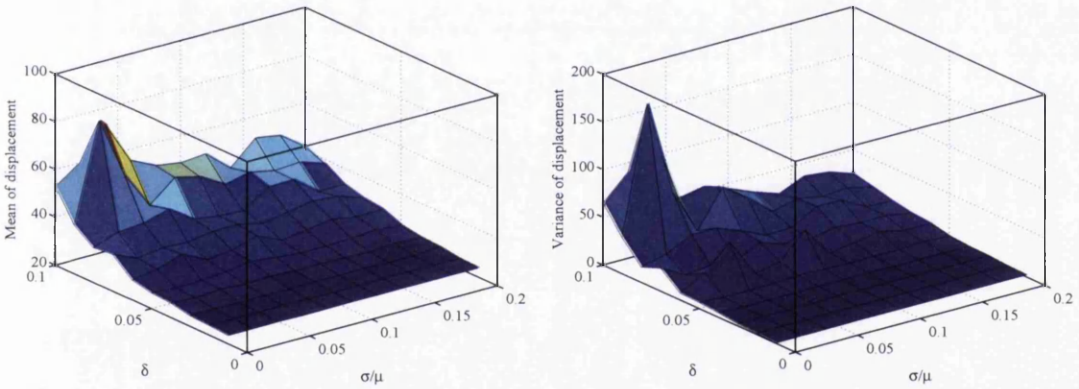

(a) Mean. (b) Standard deviation.

Figure 6.16: Mean and standard deviation of the head at $(x, y) = (0.6923, 0.0400)$ obtained from the analytical expressions for parametric uncertainty and Monte Carlo Simulation (MCS) for nonparametric uncertainty, where positive definiteness of the global matrix is ensured through a sample selection procedure.

standard deviation increase drastically with δ, so that the variation with σ/μ seems negligible in comparison. In Subfigure 6.17(a) and Subfigure 6.17(b) it is observed that the error in mean and standard deviation vary mostly with σ/μ, as the dependance with nonparametric uncertainty has been calculated with MCS. The errors are small in comparison with the ones obtained for the beam problem.

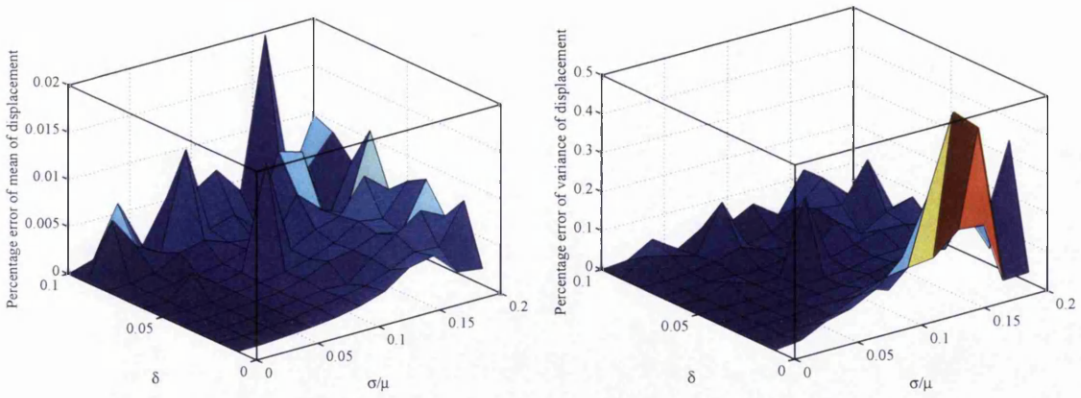

(a) Percentage error of mean.

(b) Percentage error of standard deviation.

Figure 6.17: Percentage error of mean and standard deviation of the head at $(x, y) = (0.6923, 0.0400)$ between the analytical expressions for parametric uncertainty and Monte Carlo Simulation (MCS), where positive definiteness of the global matrix is ensured through a sample selection procedure.

Matrix correction

The flow problem is solved using the method proposed in section 6.3.2. Figure 6.18 shows the mean and standard deviation of the head for $\sigma = 0.1$ of the underlying random field and $\delta = 0.05$ for the nonparametric uncertainty, using PC to solve parametric uncertainty and MCS with 100 samples to solve nonparametric uncertainty. Figure 6.19 shows the results from Equations (6.18) and (6.20), where Wishart matrices are simulated with MCS using 500 samples. Figure 6.20 shows the error between results from Equations (6.18) and (6.20), where Wishart matrices are simulated with MCS using 500 samples, and MCS both in Wishart matrix and parametric uncertainty, using 500 samples for Wishart matrix results and 2000 samples for PC results within each Wishart sample.

In Subfigure 6.19(a) it is observed that the mean increases with both δ and σ/μ, while in Subfigure 6.19(b) the standard deviation is almost constant in δ and increases linearly with σ . In Subfigure 6.20(a) and Subfigure 6.20(b) it is observed that the error in mean and standard deviation vary mostly with σ/μ, as the dependance with nonparametric uncertainty has been calculated with MCS. The errors are small in comparison with the ones obtained for the beam problem. The error in mean is of the order of the one obtained from ensuring positive definiteness of the global matrix with sample selection, but the errors in standard deviation with this method doubles the ones obtained with the previous method.

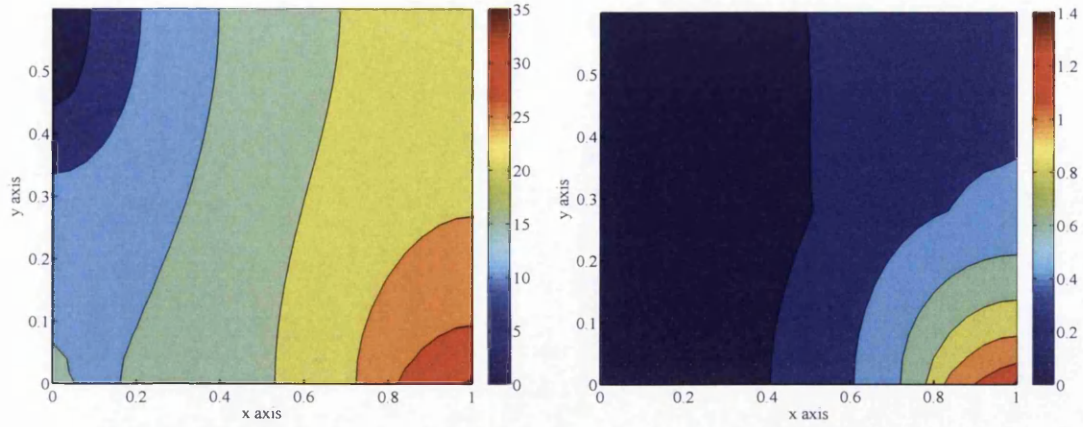

(a) Mean. (b) Standard deviation.

Figure 6.18: Mean and standard deviation of the head obtained using the analytical expressions for parametric uncertainty with $\sigma = 0.1$ and Monte Carlo Simulation (MCS) for nonparametric uncertainty with $\delta = 0.05$, where positive definiteness of the global matrix is ensured through a matrix correction procedure.

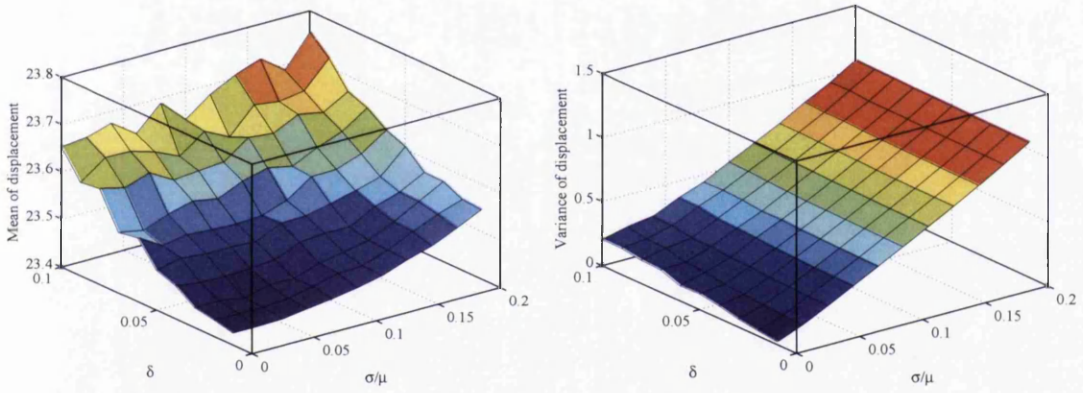

(a) Mean. (b) Standard deviation.

Figure 6.19: Mean and standard deviation of the head at $(x, y) = (0.6923, 0.0400)$ obtained from the analytical expressions for parametric uncertainty and Monte Carlo Simulation (MCS) for nonparametric uncertainty, where positive definiteness of the global matrix is ensured through a matrix correction procedure.

6.4 Conclusions

A stationary linear system is considered to be affected by two different types of uncertainties, namely, parametric uncertainty and non-parametric uncertainty. Parametric uncertainty is introduced through a Karhunen Loève expansion of a random field representing a parameter of the structure, while non-parametric uncertainty is dealt with through a random matrix theory-based method. The two different types of uncertainties are considered to affect the system in two different ways: both uncertainties influence

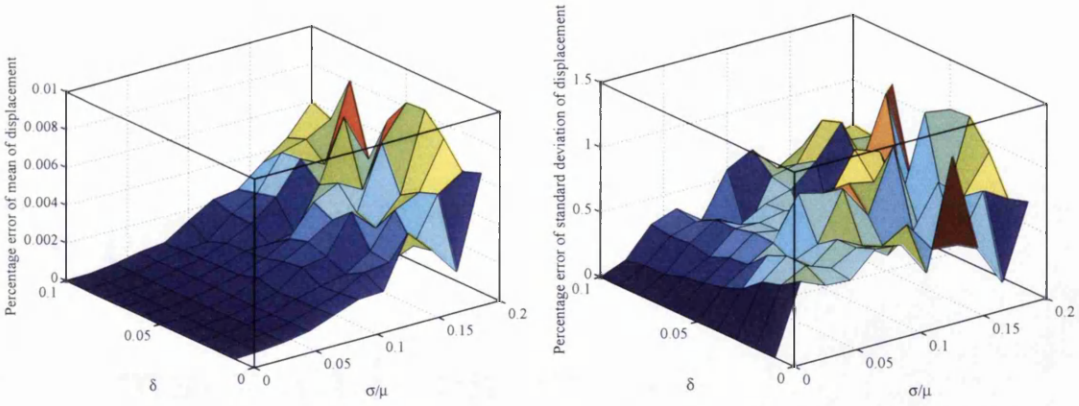

(a) Percentage error of mean.

(b) Percentage error of standard deviation.

Figure 6.20: Percentage error of mean and standard deviation of the head at $(x, y) = (0.6923, 0.0400)$ between the analytical expressions for parametric uncertainty and Monte Carlo Simulation (MCS), where positive definiteness of the global matrix is ensured through a matrix correction procedure.

the system over the entire domain or each one affects a different domain and these domains are non-overlapping.

When both uncertainties affect the whole domain, the non-parametric uncertainty is modelled with a Wishart distribution. The mean of the Wishart distribution is then modelled with the KL expansion of the system affected only by parametric uncertainty. Analytical results based on random matrix theory and polynomial chaos are then obtained for the mean and second moment of the response. The numerical results show that the error introduced in the solution is due to the error in the polynomial chaos (PC) solution, as the analytical expressions for Wishart matrices are exact.

When each uncertainty affects a different substructure, each block diagonal matrix is modelled by a different kind of matrix, that is, one block diagonal matrix is affected only by parametric uncertainty and is modelled with a KL expansion and the other block diagonal matrix is modelled with a Wishart matrix subjected to different conditions. These conditions are imposed by the positive definiteness of the global matrix, such that the non-parametric matrix can be obtained in two ways, namely, by ensuring positive definiteness through matrix selection or through a matrix decomposition-based method. The solution method proposed for this type of combined uncertainty combines PC and Monte Carlo Simulation.

Chapter 7

Summary and conclusions

The work carried out in this dissertation addresses problems arising in the propagation of parametric and nonparametric uncertainty in both dynamic and static problems. In Chapter 1 a detailed review of existing methodologies for uncertainty quantification in static and dynamic problems was conducted. Based on that, some open problems, like the need of efficient propagation techniques for parametric uncertainties in both linear problems and random eigenvalue problems, were identified. A summary of the contributions was given at the end of each Chapter.

In Chapter 2 a reduced polynomial chaos method based on the spectral decomposition of the deterministic problem was proposed. The method reduces the computational time of the classical polynomial chaos approach without decreasing significantly its accuracy. However, the basis functions used in the expansion are selected as in the classical approach, and no work has been carried out with the objective of efficiently selecting the polynomials used in the expansion or finding more suitable basis for the expansion. In Chapter 3 several methods to obtain polynomial expansion of eigenvalues and eigenvectors of a symmetric matrix were derived. The proposed methods were not able to deal with mode crossing, veering or coalescence, and no research was carried out for the case of repeated eigenvalues. The case of nonsymmetric matrices was not studied.

The dynamic response of a system has been studied, where the pdfs of eigenvalues and eigenvectors were derived from considering different information in the maximum entropy principle. In Chapter 4, vibrations in the low frequency domain were studied. Eigenvalues and eigenvectors were assumed independent and different pdfs of eigenvalues were derived applying the maximum entropy principle. The Laplace's integral

method was used to obtain the first and second moments of the response. This method did not perform as expected for some of the frequencies at which the moments were calculated. In Chapter 5, the maximum entropy principle was applied to the system matrices, and several approximations to the case where both mass and stiffness matrices are Wishart were derived. The method is expected to be accurate for high frequencies, following the lead of statistical energy analysis. Numerical integration to obtain the first two moments could be carried out for some of the approximations. Unfortunately, no close form expression could be derived for the general case of independent Wishart system matrices. In none of these studies correlation of eigenvalues and eigenvectors was dealt with in an analytical way.

Combined uncertainty was considered in Chapter 6 for the elliptic case, where both parametric and nonparametric uncertainties either affected the same domain either affected different subdomains of a structure. The combined uncertainty case was not perused for the dynamic case.

7.1 Summary of contributions made

A summary of the main contributions of this dissertation is given below:

- **Propagation method of parametric uncertainty in static problems:** SSFEM are accurate methods to propagate uncertainty, but their implementation is computationally intensive. A reduction in the system size through the use of the deterministic eigenvectors corresponding to the smallest eigenvalues was performed in Chapter 2. The application of SSFEM to the reduced system leads to results of similar accuracy compared with the classical SSFEM. This method can be applied with more general basis functions (e.g. gPC, multi-elements), not only PC.

- **Random eigenvalue problems:** The most widely used methods to calculate the dependence of eigenvalues and eigenvectors with system random variables are based on the perturbation method. Four methods to obtain a spectral expansion of eigenvectors have been proposed in Chapter 3, namely, reduced spectral power method (RSPM), reduced spectral inverse power method (RSIPM), reduced spectral constrained coefficients method (RSCCM) and spectral constrained coefficients method (SCCM). These methods have been combined with the Rayleigh

quotient to obtain a spectral representation of eigenvalues.

- **Moments of response of dynamic systems with parametric uncertainty:** Even though methods to obtain eigenvalues statistics are available, only MCS has been used to obtain the statistics of a dynamic system. In the proposed method, the first two moments of the response are calculated using Laplace's integral and numerical integration in Chapter 4. The pdfs of eigenvalues are approximated using the maximum entropy method and the first two moments. Eigenvalues and eigenvectors are assumed to be independent, which is expected in low frequency vibration problems where resonance peaks are well separated. This method is less computationally extensive than MCS.

- **Moments of response of dynamic systems with non-parametric uncertainty:** The maximum entropy principle is applied to the eigenvalues matrix. The first two moments of the response are generally calculated with MCS, which is computationally expensive. To avoid MCS, the Wishart matrix modelling the matrix of eigenvalues is approximated with a White Wishart matrix. The first two moments of the response are obtained using numerical integration and results from eigenvalues and eigenvectors statistics of random matrix theory in Chapter 5.

- **Propagation of combined parametric-nonparametric uncertainty:** Two cases have been studied. In the first one, both uncertainties affect the same domain. The system with parametric uncertainty is discretized as in SFEM. The resulting matrix is considered the mean of a non-parametric uncertain system, and a Wishart distribution with covariance matrix depending on parametric uncertainty is obtained. The first two moments of this system are obtained based on moments of the inverse Wishart matrix and SSFEM in Chapter 6. In a second case, each kind of uncertainty affects a domain. The system is divided in two subdomains, where parametric uncertainty affects one of the subdomains. A KL expansion is obtained where the random variables only affect a block diagonal submatrix of the system matrix. The maximum entropy principle is applied to the other block diagonal submatrix so as to consider the non-parametric uncertainty of a second subdomain of the structure. The first two moments of the response are obtained in Chapter 6 using MCS for the Wishart submatrix, and domain decomposition

results and SSFEM for the submatrix with parametric uncertainty.

7.2 Future research

The work carried out in this dissertation can be continued into several research topics:

- The theoretical work carried out in the reduced polynomial chaos method from Chapter 2 could be extended to nonlinear problems and time domain problems, where other size reduction methods are available from the deterministic cases (e.g. POD, snapshots, and other methods described, for example, by Meyer and Matthies (2003)).

- The reduced polynomial chaos method was applied in Chapter 2 using Hermite polynomials as basis functions, but similar studies could be carried out with other basis functions (gPC, multielements, wavelets), and using the collocation method instead of Galerkin method to obtain the coefficients of the expansion.

- Padé-Legendre approximations, i.e. ratio of two polynomials, to the response of a system with parametric uncertainty have been researched (e.g. Falsone and Ferro (2007), Chantrasmi et al. (2009)). It is noted that the results on random eigenvalues and eigenvectors from Chapter 3 could be used, together with the spectral decomposition of the operator, to obtain a Padé-Legendre approximation to the response.

- The methods developed in Chapter 3 to obtain a spectral representation of eigenvalues and eigenvectors cannot deal with mode crossing, mode veering and coalescence, described, for example, in Gallina et al. (2011). Spectral methods directed to these problems should be researched.

- Combined parametric and non-parametric uncertainty was considered, for the elliptic PDE, in Chapter 6. If both uncertainties affect the same domain, this line of research could be extended to the dynamic case, either by combining results of Chapter 3, on propagation of parametric uncertainty to the eigensolution, with results from Chapter 5, on non-parametric uncertainty in dynamic system. For the case where each type of uncertainty affects a subdomain of the structure, results

on domain decomposition for dynamics (Component Mode Synthesis) could be applied.

- In subsection 5.3.3, a method to obtain parameters of the mass and stiffness matrices modelled using Wishart matrix was derived. This method used information from system eigenvalues. Experiments could be carried out to verify the performance of modelling system matrices using the maximum entropy principle.

7.3 Published works

7.3.1 Book chapters

1. Pascual, B. and Adhikari, S., Frequency response of stochastic dynamic systems: A modal approach, in the Proceedings of the Tenth International Conference on Computational Structures Technology, Edited by B.H.V. Topping, J.M. Adam, F.J. Pallares, R. Bru and M.L. Romero, published by Civil-Comp Press, Stirlingshire, UK, 2010. ISBN 9781905088386.

7.3.2 Journal papers

1. Pascual, B., Adhikari, S., Hybrid perturbation-polynomial chaos approaches to the random algebraic eigenvalue problem, Computer Methods in Applied Mechanics and Engineering, in press.

2. Pascual, B. and Adhikari, S., A reduced polynomial chaos approach for stochastic finite element analysis, Sa-dhana- - Proceedings of the Indian Academy of Engineering Sciences, in press.

7.3.3 Conference papers

1. Pascual, B. and Adhikari, S., "Hybrid perturbation-polynomial chaos approximate solution to the algebraic random eigenvalue problem", Third International Conference on Computational Methods in Structural Dynamics and Earthquake Engineering (COMPDYN 2011), Corfu, Greece, May 2011.

2. Pascual, B. and Adhikari, S., "Frequency response of stochastic dynamic systems: A modal approach", The Tenth International Conference on Computational

Structures Technology (CST2010), Valencia, Spain, September 2010.

3. Pascual, B. and Adhikari, S., "Beyond the stochastic finite element method: hybrid uncertainty quantification using random PDEs", Fourth European Congress on Computational Mechanics (ECCM 2010), Paris, France, May 2010.

7.3.4 Work under review

1. Hybrid parametric-nonparametric uncertainty propagation using random matrix theory and polynomial chaos expansion, Computer and Structures.

2. Pascual, B. and Adhikari, S., Frequency response of stochastic dynamic systems: A modal approach, Journal of Vibration and Acoustics, ASME.

3. Pascual, B. Adhikari, S. Pastur, L. Response moments of dynamic systems affected by non-parametric uncertainty, Under preparation.

Bibliography

S. Acharjee and N. Zabaras. A concurrent model reduction approach on spatial and random domains for the solution of stochastic pdes. *International Journal for Numerical Methods in Engineering*, 12(6-7):1934 –1954, 2006.

S. Adhikari. Calculation of derivative of complex modes using classical normal modes. *Computer and Structures*, 77(6):625–633, August 2000.

S. Adhikari. Random eigenvalue problems revisited. *Sādhanā - Proceedings of the Indian Academy of Engineering Sciences*, 31(4):293–314, August 2006. (Special Issue on Probabilistic Structural Dynamics and Earthquake Engineering).

S. Adhikari. Joint statistics of natural frequencies of stochastic dynamic systems. *Computational Mechanics*, 40(4):739–752, September 2007.

S. Adhikari. Wishart random matrices in probabilistic structural mechanics. *ASCE Journal of Engineering Mechanics*, 134(12):1029–1044, December 2008.

S. Adhikari. Generalized wishart distribution for probabilistic structural dynamics. *Computational Mechanics*, 45(5):495–511, May 2010.

S. Adhikari. Stochastic finite element analysis using a reduced orthonormal vector basis. *Computer Methods in Applied Mechanics and Engineering*, 200(21-22):1804–1821, 2011.

S. Adhikari and M. I. Friswell. Random matrix eigenvalue problems in structural dynamics. *International Journal for Numerical Methods in Engineering*, 69(3):562–591, 2007.

G. Alefeld and J. Herzberger. *Introduction to interval computations.* Academic Press, New York, 1983.

U. Alibrandi, N. Impollonia, and G. Ricciardi. Probabilistic eigenvalue buckling analysis solved through the ratio of polynomial response surface. *Computer Methods in Applied Mechanics and Engineering*, 199(9-12):450 – 464, 2010.

E. Arnoult, P. Lardeur, and L. Martini. The modal stability procedure for dynamic and linear finite element analysis with variability. *Finite Elements in Analysis and Design*, 47(1):30 – 45, 2011.

M. Arnst, D. Clouteau, H. Chebli, R. Othman, and G. Degrande. A non-parametric probabilistic model for ground-borne vibrations in buildings. *Probabilistic Engineering Mechanics*, 21(1):18–34, 2006.

I Babuska, R Tempone, and GE Zouraris. Galerkin finite element approximations of stochastic elliptic partial differential equations. *Siam Journal on Numerical Analysis*, 42(2):800–825, 2004.

I Babuska, R Tempone, and GE Zouraris. Solving elliptic boundary value problems with uncertain coefficients by the finite element method: the stochastic formulation. *Computer Methods in Applied Mechanics and Engineering*, 194(12-16):1251–1294, 2005.

K. J. Badcock, S. Timme, S. Marques, H. Khodaparast, M. Prandina, J. E. Mottershead, A. Swift, A. Da Ronch, and M. A. Woodgate. Transonic aeroelastic simulation for instability searches and uncertainty analysis. *Progress in aerospace sciences*, 47(5): 392 –423, 2011.

G. B. Baecher and T. S. Ingra. Stochastic Finite Element method in settlement predictions. *Journal of Geotechnical Engineering, ASCE*, 107(4):449–463, 1981.

M. T. Bah, P. B. Nair, A. Bhaskar, and A. J. Keane. Forced response statistics of mistuned bladed disks: a stochastic reduced basis approach. *Journal of Sound and Vibration*, 263(2):377–397, 2003.

Zhidong Bai and Jack W. Silverstein. *Spectral Analysis of Large Dimensional Random Matrices*. Springer, New York, 2010.

Heinz Bauer. *Probability theory*. Walter de Gruyter & Co., Berlin, 1996.

V. Bayer and C. G. Bucher. Importance sampling for first passage problems of nonlinear structures. *Probabilistic Engineering Mechanics*, 14:27–32, 1999.

Richard Bellman. *Introduction to Matrix Analysis*. McGraw-Hill, New York, USA, 1960.

M. Berveiller, B. Sudret, and M. Lemaire. Stochastic finite elements: A non intrusive approach by regression. *European Journal of Computational Mechanics*, 15(1-3): 81–92, 2006.

Graud Blatman and Bruno Sudret. An adaptive algorithm to build up sparse polynomial chaos expansions for stochastic finite element analysis. *Probabilistic Engineering Mechanics*, 25(2):183 – 197, 2010.

W. E. Boyce. *Random Eigenvalue Problems*. Probabilistic methods in applied mathematics. Academic Press, New York, 1968.

P. Bressolette, M. Fogli, and C. Chauvière. A stochastic collocation method for large classes of mechanical problems with uncertain parameters. *Probabilistic Engineering Mechanics*, 25(2):255–270, 2010.

H. J. Bungartz and T. Dornseifer. Sparse grids: Recent developments for elliptic partial differential equations. In *Multigrid Methods V, Lecture Notes in Computational Science and Engineering*, pages 45–70. Springer, 1997.

P. D. Cha and K. A. Solberg. Applying eigenvalue perturbation theory to solve problems in structural dynamics. *International Journal of Mechanical Engineering Education*, 36:160–175, 2008.

T. Chantrasmi, A. Doostan, and G. Iaccarino. Pad-legendre approximants for uncertainty analysis with discontinuous response surfaces. *Journal of Computational Physics*, 228(19):7159 – 7180, 2009.

C. Chen, D. Duhamel, and C. Soize. Probabilistic approach for model and data uncertainties and its experimental identification in structural dynamics: Case of composite sandwich panels. *Journal of Sound and Vibration*, 294(1-2):64–81, 2006.

Guanrong Chen and Trung Tat Pham. *Introduction to Fuzzy Sets, Fuzzy Logic, and Fuzzy Control Systems*. CRC Press, Boca Raton, 2000.

S.-H. Chen, D.-T. Song, and A.-J. Ma. Eigensolution reanalysis of modified structures using perturbations and rayleigh quotients. *Communications in Numerical Methods in Engineering*, 10(2):111–119, 1994.

S. H. Chen, X. W. Yang, and H. D. Lian. Comparison of several eigenvalue reanalysis methods for modified structures. *Structural and Multidisciplinary Optimization*, 20 (4):253–259, 2000.

S.-A. Chentouf, N. Bouhaddi, and C. Laitem. Robustness analysis by a probabilistic approach for propagation of uncertainties in a component mode synthesis context. *Mechanical Systems and Signal Processing*, 25(7):2426 – 2443, 2011.

J. D. Collins and W. T. Thomson. The eigenvalue problem for structural systems with statistical properties. *AIAA Journal*, 7(4):642–648, April 1969.

Vincent Cotoni, Phil Shorter, and R. S. Langley. Numerical and experimental validation of a hybrid finite element-statistical energy analysis method. *Journal of the Acoustical Society of America*, 122(1):259–270, 2007.

Bernard Dacorogna. *Introduction to the calculus of variations*. Imperial College Press, London, 2004.

D. Dawe. *Matrix and Finite Element Displacement Analysis of Structures*. Oxford University Press, Oxford, UK, 1984.

Benoit Van den Nieuwenhof and Jean-Pierre Coyette. Modal approaches for the stochastic finite element analysis of structures with material and geometric uncertainties. *Computer Methods in Applied Mechanics and Engineering*, 192(33-34): 3705–3729, 2003.

Jian Deng, Cristina Anton, and Yau Shu Wong. Stochastic collocation method for secondary bifurcation of a nonlinear aeroelastic system. *Journal of Sound and Vibration*, 330(13):3006 – 3023, 2011.

G. Deodatis. Bounds on response variability of stochastic finite element systems. *Journal of Engineering Mechanics, ASCE*, 116(3):565–585, 1990.

G. Deodatis. Weighted integral method i: stochastic stiffness. *Journal of Engineering Mechanics, ASCE*, 117(8):1851–1864, 1991.

G. Deodatis. The weighted integral method I: stochastic stiffness matrix. *Journal of Engineering Mechanics, ASCE*, 117(8):1851–1864, 1991.

G. Deodatis and M. Shinozuka. The weighted integral method II: response variability and reliability. *Journal of Engineering Mechanics, ASCE*, 117(8):1865–1877, 1991.

A. Der-Kiureghian and J. B. Ke. The stochastic finite element in structural reliability. *Journal of Engineering Mechanics*, 3:83–91, 1987.

Armen Der-Kiureghian and Ove Ditlevsen. Aleatory or epistemic? does it matter? *Structural Safety*, 31:105–112, 2009.

C. Desceliers, C. Soize, and S. Cambier. Non-parametric-parametric model for random uncertainties in non-linear structural dynamics: Application to earthquake engineering. *Earthquake Engineering & Structural Dynamics*, 33(3):315–327, 2004.

O. Ditlevsen and H. O. Madsen. *Structural Reliability Methods*. John Wiley and Sons Ltd, Chichester, West Sussex, England, January 1996.

A. Doostan, R. G. Ghanem, and J. Red-Horse. Stochastic model reduction for chaos representations. *Computer Methods in Applied Mechanics and Engineering*, 196(37-40):39513966, 2007.

S. Du, B. R. Ellingwood, and J. V. Cox. Initialization strategies in simulation-based sfe eigenvalue analysis. *Computer-Aided Civil and Infrastructure Engineering*, 20(5): 304–315, 2005.

J. L. du Bois, S. Adhikari, and N. A. J. Lieven. On the quantification of eigenvalue curve veering: A veering index. *Transactions of ASME, Journal of Applied Mechanics*, 78 (4):041007:1–8, 2011.

M. S. Eldred. Higher order eigenpair perturbations. *AIAA Journal*, 30(7):1870–1876, 1992.

M. S. Eldred and J. Burkardt. Comparison of non-intrusive polynomial chaos and stochastic collocation methods for uncertainty quantification. 47th AIAA Aerospace Sciences Meeting including The New Horizons Forum and Aerospace Exposition, Orlando, Florida, Jan. 5-8, 2009.

H. Engels. *Numerical quadrature and cubature*. Academic Press, London, 1980.

A. Erdèlyi. *Asymptotic expansions*. Dover Publications, California Institute of Technology, 1956.

G. Falsone and G. Ferro. An exact solution for the static and dynamic analysis of fe discretized uncertain structures. *Computer Methods in Applied Mechanics and Engineering*, 196(21-24):2390 – 2400, 2007.

G. Falsone and N. Impollonia. A new approach for the stochastic analysis of finite element modelled structures with uncertain parameters. *Computer Methods in Applied Mechanics and Engineering*, 191(44):5067–5085, 2002.

A. Filiatrault. *Elements of earthquake engineering and structural dynamics*. Polytechnic International Press, Canada, 2002.

Jasmine Foo and George Em Karniadakis. Multi-element probabilistic collocation method in high dimensions. *Journal of Computational Physics*, 229(5):1536–1557, 2010.

Alexander I. J. Forrester, Andrs Sbester, and Andy J. Keane. *Engineering Design via Surrogate Modelling: A Practical Guide*. Wiley, Chichester, 2008.

R. L. Fox and M. P. Kapoor. Rates of change of eigenvalues and eigenvectors. *AIAA Journal*, 6(12):2426–2429, December 1968.

M. I. Friswell. The derivatives of repeated eigenvalues and their associated eigenvectors. *ASME Journal of Vibration and Acoustics*, 18:390–397, July 1996.

M. I. Friswell and J. E. Mottershead. *Finite Element Model Updating in Structural Dynamics*. Kluwer Academic Publishers, The Netherlands, 1995.

A. Gallina, L. Pichler, and T. Uhl. Enhanced meta-modelling technique for analysis of mode crossing, mode veering and mode coalescence in structural dynamics. *Mechanical Systems and Signal Processing*, 25(7):2297 – 2312, 2011.

W. Gautschi. On generating orthogonal polynomials. *Society for Industrial and Applied Mathematics*, 3(3):345–383, 1982.

James E. Gentle. *Random Number Generation and Monte Carlo Methods, Second Edition*. Springer, New York, 2003.

M. Géradin and D. Rixen. *Mechanical Vibrations*. John Wiely & Sons, New York, NY, second edition, 1997. Translation of: Théorie des Vibrations.

Thomas Gerstner and Michael Griebel. Numerical integration using sparse grids. *Numerical Algorithms*, 18(3-4):209–232, 1998.

R. Ghanem and A. Sarkar. Reduced models for the medium-frequency dynamics of stochastic systems. *Journal of the Acoustical Society of America*, 113(2):834–846, 2003.

R. Ghanem and P.D. Spanos. *Stochastic Finite Elements: A Spectral Approach*. Springer-Verlag, New York, USA, 1991.

R. G. Ghanem and D. Ghosh. Efficient characterization of the random eigenvalue problem in a polynomial chaos decomposition. *international journal for numerical methods in engineering*, 72:486–504, 2007.

R.G. Ghanem and S. Dham. Stochastic finite element analysis for multiphase flow in heterogeneous porous media. *Transport in Porous Media*, (32):239–262, 1998.

Roger G. Ghanem and Sonjoy Das. Hybrid representations of coupled nonparametric and parametric models for dynamic systems. *AIAA Journal*, 47(4):1035–1044, 2009.

D. Ghosh and R. G. Ghanem. Stochastic convergence acceleration through basis enrichment of polynomial chaos expansions. *International Journal for Numerical Methods in Engineering*, 73(2):162–184, 2008.

Debraj Ghosh, Roger G. Ghanem, and John Red-Horse. Analysis of eigenvalues and modal interaction of stochastic systems. *AIAA Journal*, 43(10):2196–2201, 2005.

Debraj Ghosh, Philip Avery, and Charbel Farhat. An FETI-preconditioned conjuerate gradient method for large-scale stochastic finite element problems. *International Journal for Numerical Methods in Engineering*, 80(6-7, Sp. Iss. SI):914–931, NOV 5 2009.

Paul Glasserman. *Monte Carlo Methods in Financial Engineering*. Springer, New York, 2004.

D. V. Gokhale. Maximum entropy characterizations of some distributions. *Statistical Distributions in Scientific Work*, 3:299–304, 1975.

B. Goller, H. J. Pradlwarter, and G. I. Schuëller. An interpolation scheme for the approximation of dynamical systems. *Computer Methods in Applied Mechanics and Engineering*, 200(1-4):414 – 423, 2011.

G. H. Golub and C. F. Van Loan. *Matrix Computations*. Johns Hopkins Studies in the Mathematical Sciences, Baltimore, 2010.

Michael Griebel. Adaptive sparse grid multilevel methods for elliptic pdes based on finite differences. *Computing*, 61:151–179, 1998.

M. Grigoriu. A solution of random eigenvalue problem by crossing theory. *Journal of Sound and Vibration*, 158(1):69–80, 1992.

M. Grigoriu. *Stochastic Calculus: Applications in Science and Engineering*. Birkhauser, Boston, USA, 2002.

M. Grigoriu. Galerkin solution for linear stochastic algebraic equations. *Journal of Engineering Mechanics-Asce*, 132(12):1277–1289, 2006.

M. Guedri, N. Bouhaddi, and R. Majed. Reduction of the stochastic finite element models using a robust dynamic condensation method. *Journal of Sound and Vibration*, 297(1-2):123–145, 2006.

Johann Guilleminot and Christian Soize. Probabilistic modeling of apparent tensors in elastostatics: A maxent approach under material symmetry and stochastic boundedness constraints. *Probabilistic Engineering Mechanics*, In Press, Accepted Manuscript, 2011.

A.K. Gupta and D.K. Nagar. *Matrix Variate Distributions*. Monographs & Surveys in Pure & Applied Mathematics. Chapman & Hall/CRC, London, 2000.

M. Hála. Method of ritz for random eigenvalue problems. *Kybernetika*, 30(3):263–269, 1994.

G. C. Hart. Eigenvalue uncertainties in stressed structure. *Journal of Engineering Mechanics, ASCE*, 99(EM3):481–494, June 1973.

T. K. Hasselman and G. C. Hart. Modal analysis of random structural system. *Journal of Engineering Mechanics, ASCE*, 98(EM3):561–579, June 1972.

I. C. Helton, J. D. Johnson, W. L. Oberkampf, and C. B. Storlie. A sampling-based computational strategy for the representation of epistemic uncertainty in model predictions with evidence theory. Technical Report 5557, Sandia National Laboratories, 2006.

L. Hinke, F. Dohnal, B.R. Mace, T.P. Waters, and N.S. Ferguson. Component mode synthesis as a framework for uncertainty analysis. *Journal of Sound and Vibration*, 324(12):161 – 178, 2009.

R. Jin, W. Chen, and T. W. Simpson. Comparative studies of metamodeling techniques under multiple modeling criteria. *Structural and Multidisciplinary Optimization*, 23: 1–13, 2000.

Donald R. Jones. A taxonomy of global optimization methods based on response surfaces. *Journal of Global Optimization*, 21:345–383, 2001.

J. N. Kapur. *Maximum-entropy models in science and engineering*. Wiley Eastern Limited, New Delhi, 1989.

K. Karhunen. ber lineare methoden in der wahrscheinlichkeitsrechnung. *Annales Academiae Scientiarum Fennicae*, Ser. A137, 1947.

A. J. Keane and W. G. Price. *Statistical Energy Analysis: An Overview With Applications in Structural Dynamics*. Cambridge University Press, Cambridge, UK, 1997. First published in Philosophical Transactions of the Royal Society of London, series A, vol 346, pp. 429-554, 1994.

A. Keese and H. G. Matthies. Numerical methods and smolyak quadrature for nonlinear stochastic partial differential equations. *Siam Journal on Scientific Computing*, 2003.

H. H. Khodaparast, J. E. Mottershead, and M. I. Friswell. Perturbation methods for the estimation of parameter variability in stochastic model updating. *Mechanical systems and signal processing*, 22(8):1751 –1773, 2008.

H. H. Khodaparast, J. E. Mottershead, and K. J. Badcock. Propagation of structural uncertainty to linear aeroelastic stability. *Computers and Structures*, 88(3-4):223–236, 2010.

H.H. Khodaparast, J. E. Mottershead, and K. J. Badcock. Interval model updating with irreducible uncertainty using the Kriging predictor. *Mechanical Systems and Signal Processing*, 25(4):1204–1226, 2011.

M. Kleiber and T. D. Hien. *The Stochastic Finite Element Method.* John Wiley, Chichester, 1992.

O. P. Le Maître, O. M. Knio, H. N. Najm, and R. G. Ghanem. Uncertainty propagation using WienerHaar expansions. *Journal of Computational Physics*, 197(1):28–57, 2004.

C. Lee and R. Singh. Analysis of discrete vibratory systems with parameter uncertainties, part I: Eigensolution. *Journal of Sound and Vibration*, 174(3):379–394, 1994.

Christiane Lemieux. *Monte Carlo and Quasi-Monte Carlo Sampling*. Springer, New York, 2009.

V. Lenaerts, G. Kerschen, and J. C. Golinval. Physical interpretation of the proper orthogonal modes using the singular value decomposition. *Journal of Sound and Vibration*, 249(5):849–865, January 2002.

G. Letac and H. Massam. All Invariant Moments of the Wishart Distribution. *Scandinavian Journal of Statistics*, 31:295318, 2004.

C. C. Li and A. Der-Kiureghian. Optimal discretization of random fields. *Journal of Engineering Mechanics-ASCE*, 119(6):1136–1154, 1993a.

C. C. Li and A. Der-Kiureghian. Optimal discretization of random fields. *Journal of Engineering Mechanics, ASCE*, 119(6):1136–1154, 1993b.

C. F. Li, Y. T. Feng, and D. R. J. Owen. Explicit solution to the stochastic system of linear algebraic equations $(\alpha_1 A_1 + \alpha_2 A_2 + \cdots + \alpha_m A_m)x = b$. *Computer Methods in Applied Mechanics and Engineering*, 195(44-47):6560–6576, 2006.

J. Lim. Reservoir properties determination using fuzzy logic and neural networks from well data in offshore Korea. *Journal of Petroleum Science and Engineering*, 49: 182192, 2005.

Y. K. Lin. *Probabilistic Thoery of Strcutural Dynamics*. McGraw-Hill Inc, Ny, USA, 1967.

W. K. Liu, T. Belytschko, and A. Mani. Random field finite-elements. *International Journal for Numerical Methods in Engineering*, 23(10):1831–1845, 1986.

W. K. Liu, T. Belytschko, and A. Mani. Probabilistic Finite Elements for non linear structural dynamics. *Computer Methods in Applied Mechanics and Engineering*, 56 (4):61–86, 1986a.

W. K. Liu, T. Belytschko, and A. Mani. Random field Finite Elements. *International Journal for Numerical Methods in Engineering*, 23(10):1831–1845, 1986b.

W. K. Liu, T. Belytschko, and A. Mani. Random field finite elements. *International Journal for Numerical Methods in Engineering*, 23:1831–1845, 1986c.

X. L. Liu and C. S. Oliveira. Iterative modal perturbation and reanalysis of eigenvalue problem. *Communications in Numerical Methods in Engineering*, 19(4):263–274, 2003.

M. Loève. *Fonctions aleatoires du second ordre. Supplement to P. Levy, Processus Stochastic et Mouvement Brownien*. Gauthier Villars, Paris, 1948.

R. H. Lyon and R. G. Dejong. *Theory and Application of Statistical Energy Analysis*. Butterworth-Heinmann, Boston, second edition, 1995.

Xiang Ma and Nicholas Zabaras. An adaptive hierarchical sparse grid collocation algorithm for the solution of stochastic differential equations. *Journal of Computational Physics*, 228(8):3084–3113, 2009.

Xiang Ma and Nicholas Zabaras. An adaptive hierarchical sparse grid collocation algorithm for the solution of stochastic differential equations. *Journal of Computational Physics*, 228:3084–3113, May 2009. ISSN 0021-9991.

B. R. Mace and P. J. Shorter. A local modal/perturbational method for estimating frequency response statistics of built-up structures with uncertain properties. *Journal of Sound and Vibration*, 242(5):793–811, 2001.

O. P. Le Maître and O. M. Knio. *Spectral Methods for Uncertainty Quantification: With Applications to Computational Fluid Dynamics*. Springer, Berlin, Germany, 2010.

V. Marčenko and L. Pastur. The eigenvalue distribution in some ensembles of random matrices. *Math. USSR Sbornik*, 1:457–483, 1967.

H. G. Matthies and A. Keese. Galerkin methods for linear and nonlinear elliptic stochastic partial differential equations. *Computer Methods in Applied Mechanics and Engineering*, 194(12-16):1295–1331, 2005.

H. G. Matthies, C. E. Brenner, C. G. Bucher, and C. G. Soares. Uncertainties in probabilistic numerical analysis of structures and solids - stochastic finite elements. *Structural Safety*, 19(3):283–336, 1997.

Kurt Maute, Gary Weickum, and Mike Eldred. A reduced-order stochastic finite element approach for design optimization under uncertainty. *Structural Safety*, 31(6): 450–450, 2009.

S. Mehlhose, J. vom Scheidt, and R. Wunderlich. Random eigenvalue problems for bending vibrations of beams. *Zeitschrift Fur Angewandte Mathematik Und Mechanik*, 79(10):693–702, 1999.

L. Meirovitch. *Analytical Methods in Vibrations*. Macmillan Publishing Co., Inc., New York, 1967.

M. Meyer and H. G. Matthies. Efficient model reduction in non-linear dynamics using the karhunen-love expansion and dual-weighted-residual methods. *Computational Mechanics*, 31:179–191, 2003.

M. P. Mignolet and C. Soize. Nonparametric stochastic modeling of linear systems with prescribed variance of several natural frequencies. *Probabilistic Engineering Mechanics*, 23(2-3):267–278, 2008a.

M. P. Mignolet and C. Soize. Stochastic reduced order models for uncertain geometrically nonlinear dynamical systems. *Computer Methods in Applied Mechanics and Engineering*, 197(45-48):3951–3963, 2008b.

W. C. Mills-Curran. Calculation of eigenvector derivatives for structures with repeated eigenvalues. *AIAA Journal*, 26(7):867–871, JUL 1988.

D. Moens and D. Vandepitte. A fuzzy finite element procedure for the calculation of uncertain frequency-response functions of damped structures: Part 1-procedure. *Journal of Sound and Vibration*, 288:431–462, 2005.

David Moens and Michael Hanss. Non-probabilistic finite element analysis for parametric uncertainty treatment in applied mechanics: Recent advances. *Finite Elements in Analysis and Design*, 47(1):4 – 16, 2011.

P. S. Mohan, P. B. Nair, and A. J. Keane. Multi-element stochastic reduced basis methods. *Computer Methods in Applied Mechanics and Engineering*, 197:1495–1506, 2008.

J. E. Mottershead, M. G. Tehrani, and Y. M. Ram. Assignment of eigenvalue sensitivities from receptance measurements. *Mechanical Systems and Signal Processing*, 23 (6):1931–1939, 2009.

R. J. Muirhead. *Aspects of Multivariate Statistical Theory*. John Wiely and Sons, New York, USA, 1982.

P. B. Nair. On the theoretical foundations of stochastic reduced basis methods. *AIAA Journal*, pages 2001–2677, 2001.

P. B. Nair and A. J. Keane. Stochastic reduced basis methods. *AIAA Journal*, 40(8): 1653–1664, 2002.

P. B. Nair and A. J. Keane. An approximate solution scheme for the algebraic random eigenvalue problem. *Journal of Sound and Vibration*, 260(1):45–65, 2003.

R. B. Nelson. Simplified calculation of eigenvector derivatives. *AIAA Journal*, 14(9): 1201–1205, September 1976.

T. G. Newman and P. L. Odell. *The generatorion of random variates.* Charles Griffin & company limited, 42 Drury Lane, London, WC2B 5RX, 1971.

A. Nouy. Recent developments in spectral stochastic methods for the numerical solution of stochastic partial differential equations. *Archives of Computational Methods in Engineering*, 16:251–285, 2009.

Anthony Nouy. A generalized spectral decomposition technique to solve a class of linear stochastic partial differential equations. *Computer Methods in Applied Mechanics and Engineering*, 196(45-48):4521–4537, 2007.

Anthony Nouy. Generalized spectral decomposition method for solving stochastic finite element equations: Invariant subspace problem and dedicated algorithms. *Computer Methods in Applied Mechanics and Engineering*, 197(51-52):4718–4736, 2008.

W. L. Oberkampf, S. M. DeLand, B. M. Rutherford, K. V. Diegert, and K. F. Alvin. Error and uncertainty in modeling and simulation. *Reliability Engineering & System Safety*, 75(3):333–357, 2002.

I. U. Ojalvo. Efficient computation of mode-shape derivatives for large dynamic-systems. *AIAA Journal*, 25(10):1386–1390, OCT 1987.

H. M. Panayirci and G. I. Schueller. On the Capabilities of the Polynomial Chaos Expansion Method within SFE Analysis-An Overview. *Archives of Computational Methods in Engineering*, 18(1):43–55, MAR 2011.

Costas Papadimitriou, James L. Beck, and L. S. Katafygiotis. Asymptotic expansions for reliability and moments of uncertain systems. *Journal of Engineering Mechanics, ASCE*, 123(12):1219–1229, December 1997.

Athanasios Papoulis and S. Unnikrishna Pillai. *Probability, Random Variables and Stochastic Processes.* McGraw-Hill, Boston, USA, fourth edition, 2002.

L. Pastur and M. Shcherbina. *Eigenvalue Distribution of Large Random Matrices.* American Mathematical Society, Providence, RI, USA, 2011.

L. Pichler, H.J. Pradlwarter, and G.I. Schuëller. A mode-based meta-model for the frequency response functions of uncertain structural systems. *Computers and Structures*, 87(5-6):332 – 341, 2009.

H. J. Pradlwarter, G. I. Schuëller, and G. S. Szekely. Random eigenvalue problems for large systems. *Computer and Structures*, 80(27-30):2415–2424, 2002.

W. H. Press, S. A. Teukolsky, W. T. Vetterling, and B. P. Flannery. *Numerical recipes: the art of scientific computing*. Cambridge University Press, New York, 2007.

Sharif Rahman. A solution of the random eigenvalue problem by a dimensional decomposition method. *International Journal for Numerical Methods in Engineering*, 67 (9):1318–1340, 2006.

Sharif Rahman. Stochastic dynamic systems with complex-valued eigensolutions. *International Journal for Numerical Methods in Engineering*, 71(8):963–986, 2007.

Sharif Rahman. Probability distributions of natural frequencies of uncertain dynamic systems. *AIAA Journal*, 47(6):1579–1589, 2009.

M. Rausand and A. Hoyland. *System reliability theory. Models, statistical methods, and applications, 2nd edition.* Wiley series in probabiity and statistics, New Jersey, 2004.

J. R. Red-Horse and R. G. Ghanem. Elements of a function analytic approach to probability. *International Journal for Numerical Methods in Engineering*, 80:689–716, 2009.

J. N. Reddy. *An introduction to the finite element models.* Mc Graw Hill, Inc., 1984.

J. N. Reddy. *An introduction to the finite element method.* McGraw-Hill, Inc., 1993.

S. K. Sachdeva. *Subspace Projection Schemes for Stochastic Finite Element Analysis.* PhD thesis, University of Southampton Department of Mechanical Engineering, Southampton, UK, 2006.

S. K. Sachdeva, P. B. Nair, and A. J. Keane. Comparative study of projection schemes for stochastic finite element analysis. *Computer Methods in Applied Mechanics and Engineering*, 195(19-22):2371–2392, 2006a.

S. K. Sachdeva, P. B. Nair, and A. J. Keane. Hybridization of stochastic reduced basis methods with polynomial chaos expansions. *Probabilistic Engineering Mechanics*, 21(2):182–192, 2006b.

A. Sarkar and R. Ghanem. Mid-frequency structural dynamics with parameter uncertainty. *Computer Methods in Applied Mechanics and Engineering*, 191(47-48):5499–5513, 2002.

A. Sarkar and R. Ghanem. A substructure approach for the midfrequency vibration of stochastic systems. *Journal of the Acoustical Society of America*, 113(4):1922–1934, 2003. Part 1.

Abhijit Sarkar, Nabil Benabbou, and Roger Ghanem. Domain decomposition of stochastic PDEs: Theoretical formulations. *International Journal for Numerical Methods in Engineering*, 77(5):689–701, 2009.

C. E. Shannon. A mathematical theory of communication. *Bell System Tech. Journal*, 27:379–423,623–659, 1948.

M. Shinozuka and G. Deodatis. Simulation of stochastic processes by spectral representation. *Applied Mechanics Reviews, ASME*, 44(3):499–519, 1991.

M. Shinozuka and T. Nomoto. Response variability due to spatial randomness of material properties. *Technical Report, Dept. of Civil Engineering, Columnbia University, New York*, 1980.

B. F. Smith, P. E. Bjorstad, and W. D. Gropp. *Domain decomposition: parallel multilevel methods for elliptic partial differential equations*. Cambridge University press, Cambridge, UK, 1996.

C. Soize. A nonparametric model of random uncertainties for reduced matrix models in structural dynamics. *Probabilistic Engineering Mechanics*, 15(3):277–294, 2000.

C. Soize. Maximum entropy approach for modeling random uncertainties in transient elastodynamics. *Journal of the Acoustical Society of America*, 109(5):1979–1996, May 2001. Part 1.

C. Soize. A comprehensive overview of a non-parametric probabilistic approach of model uncertainties for predictive models in structural dynamics. *Journal of Sound and Vibration*, 288(3):623–652, 2005.

C. Soize. Non-gaussian positive-definite matrix-valued random fields for elliptic stochastic partial differential operators. *Computer Methods in Applied Mechanics and Engineering*, 195(1-3):26–64, 2006.

C. Soize. Nonparametric probabilistic approach of uncertainties for elliptic boundary value problem . *International Journal for Numerical Methods in Engineering*, 80 (6-7):673–688, 2009.

C. Soize. Generalized probabilistic approach of uncertainties in computational dynamics using random matrices and polynomial chaos decompositions. *International Journal for Numerical Methods in Engineering*, 81(8):939–970, 2010.

C. Soize and H. Chebli. Random uncertainties model in dynamic substructuring using a nonparametric probabilistic model. *Journal of Engineering Mechanics, ASCE*, 129 (4):449–457, 2003.

Datong Song, Suhuan Chen, and Zhipin Qiu. Stochastic sensitivity analysis of eigenvalues and eigenvectors. *Computer and Structures*, 54(5):891–896, 1995.

George Stefanou. The stochastic finite element method: Past, present and future. *Computer Methods in Applied Mechanics and Engineering*, 198(9-12):1031 – 1051, 2009.

Bruno Sudret and Armen Der-Kiureghian. Stochastic finite element methods and reliability. Technical Report UCB/SEMM-2000/08, Department of Civil & Environmental Engineering, University Of California, Berkeley, November 2000.

G. S. Szekely and G. I. Schuëller. Computational procedure for a fast calculation of eigenvectors and eigenvalues of structures with random properties. *Computer Methods in Applied Mechanics and Engineering*, 191(8-10):799–816, 2001.

F. E. Udwadia. Response of uncertain dynamic-systems .1. *Applied Mathematics and Computation*, 22(2-3):115–150, 1987a.

F. E. Udwadia. Response of uncertain dynamic-systems .2. *Applied Mathematics and Computation*, 22(2-3):151–187, 1987b.

E. Vanmarcke and M. Grigoriu. Stochastic finite element analysis of simple beams. *Journal of Engineering Mechanics, ASCE*, 109(5):1203–1214, 1983.

E. H. Vanmarcke. *Random fields*. MIT press, Cambridge Mass., 1983.

C. V. Verhoosel, M. A. Gutiérrez, and S. J. Hulshoff. Iterative solution of the random eigenvalue problem with application to spectral stochastic finite element systems. *International Journal for Numerical Methods in Engineering*, 68(4):401–424, 2006.

X. Wan and G. E. Karniadakis. An adaptive multi-element generalized polynomial chaos method for stochastic differential equations. *Journal of Computational Physics*, 209:616–642, 2005.

X. L. Wan and G. E. Karniadakis. Beyond wiener-askey expansions: Handling arbitrary pdfs. *Journal of Scientific Computing*, 27((-3):455–464, 2006.

R. L. Weaver. Spectral statistics in elastodynamics. *Journal of the Acoustical Society of America*, 85(3):1005–1013, 1989.

J. H. Wilkinson. *The algebraic eigenvalue problem*. Oxford University Press, Amen House, London E.C.4, 1965.

J. H. Wilkinson. *The Algebraic Eigenvalue Problem*. Oxford University Press, Oxford, UK, 1988.

M. M. R. Williams. A method for solving stochastic eigenvalue problems. *Applied Mathematics and Computation*, 215(11):3906–3928, 2010.

D. Xiu. Efficient collocational approach for parametric uncertainty analysis. *Communications in Computational Physics*, 2(2):293–309, 2007.

D. Xiu. Fast numerical methods for stochastic computations: A review. *Communications in Computational Physics*, 5(2-4):242–272, 2009.

D. Xiu. *Numerical Methods for Stochastic Computations: A Spectral Method Approach*. Princeton University Press, New Jersey, 2010.

D. B. Xiu and G. E. Karniadakis. The wiener-askey polynomial chaos for stochastic differential equations. *Siam Journal on Scientific Computing*, 24(2):619–644, 2002.

Dongbin Xiu and Jan S. Hesthaven. High-order collocation methods for differential equations with random inputs. *SIAM Journal on Scientific Computing*, 27(3), 2005.

F. Yamazaki, M. Shinozuka, and G. Dasgupta. Neumann expansion for stochastic finite element analysis. *Journal of Engineering Mechanics, ASCE*, 114(8):1335–1354, 1988.

Fuzhen Zhang. *The Schur complement and its applications.* Springer Science + Business Media, Inc., New York, USA, 2005.

J. Zhang and B. Ellingwood. Orthogonal series expansion of random fields in reliability analysis. *Journal of Engineering Mechanics*, 120(12):2660–2677, 1993.

D. Zhao and D. Xue. A comparative study of metamodeling methods considering sample quality merits. *Structural and Multidisciplinary Optimization*, 42(6):923–938, 2010.

O. C. Zienkiewicz and R. L. Taylor. *The Finite Element Method.* McGraw-Hill, London, fourth edition, 1991.